



Exploring Phage Therapy as a Novel Therapeutic for *Staphylococcus pseudintermedius* Infections in Canines

Stephanie A Lynch

Bachelor of Animal and Veterinary Bioscience (Honours)

A thesis submitted in total fulfilment of the requirements for the degree of
Doctor of Philosophy

Department of Physiology, Anatomy and Microbiology
College of Science, Health and Engineering
La Trobe University, Victoria, Australia

August, 2021

© Copyright by Stephanie A Lynch (2021)

All Rights Reserved.

Except as provided in the Copyright Act 1968, this thesis may not be reproduced in any form without the written permission of the author.

I certify that I have made all reasonable efforts to secure copyright permissions for third-party content included in this thesis and have not knowingly added copyright content to my work without the owner's permission.

Table of contents

Table of contents.....	iii
List of Figures.....	vii
List of Tables.....	ix
Abstract.....	x
Statement of Authorship.....	xi
Acknowledgments.....	xii
Acknowledgment of Country.....	xv
Science engagement.....	xvi
Publications arising from this PhD.....	xvi
Conference presentations.....	xvi
Funding obtained throughout this PhD.....	xvii
Abbreviations.....	xviii
COVID statement.....	xx
Chapter 1	21
1.1 Abstract.....	22
1.2 Introduction.....	23
1.3 <i>Staphylococcus pseudintermedius</i> : A Pathogenic Bacterium of Veterinary Concern ...	23
1.3.1 Canine pyoderma.....	24
1.3.2 Otitis externa.....	25
1.3.3 Urinary Tract Infections (UTI).....	26
1.3.4 Respiratory Tract Infections.....	26
1.3.5 Reproductive Tract Infections.....	28
1.4 Current and Future Treatment Options for <i>Staphylococcus pseudintermedius</i> in Canines.....	29
1.4.1 Human Antibiotics.....	30
1.4.2 Topical therapies.....	31
1.4.3 Vaccines.....	31
1.4.3.1 Bacterins.....	32
1.3.4.2 Subunit.....	33
1.4.4 Phage therapy.....	34
1.5 Conclusions.....	37
1.6 Literature review references.....	38
Chapter 2	48
2.1 Media sterilisation.....	49
2.2 Bacterial culture.....	49
2.2.1 Collection of bacterial strains.....	49
2.2.2 Culture and storage of bacterial strains.....	53
2.2.3 Gram stain of bacterial cultures.....	53

2.2.4 Growth curve of <i>Staphylococcus pseudintermedius</i>	54
2.2.4.1 Manual growth curve	54
2.3 Bacteriophage screening	55
2.3.1 Collection and processing of samples used for phage screening	55
2.3.1.1 Collection and processing of soil and water samples for phage screening	55
2.3.1.2 Collection and processing of animal-associated samples for phage screening	56
2.3.2 Sample enrichment for phage screening	57
2.3.3 Plating for phage plaque isolation	58
2.3.4 Isolation of phages	58
2.3.5 Propagation of phages	58
2.3.6 Titration of phages	59
2.4 Characterisation of isolated phages	59
2.4.1 Genomic DNA extraction and quantification from isolated phages	59
2.4.2 Next generation sequencing (NGS) of phage DNA	60
2.4.2.1 Tagmentation of genomic DNA	60
2.4.2.2 Tagmented DNA amplification	60
2.4.2.3 Clean-up of DNA libraries	60
2.4.2.4 DNA library check	61
2.4.2.5 Pooling of DNA library	61
2.4.2.6 Normalisation of DNA libraries	61
2.4.2.7 Assembly and annotation of phage contigs	61
2.4.3 Host range analysis	61
2.4.4 Growth kinetics of phage	62
2.4.5 Turbidity reduction assay	62
2.4.6 Transmission Electron Microscopy (TEM) of phage particles	63
2.4.7 Induction of temperate phages from <i>Staphylococcus pseudintermedius</i> using Mitomycin-C	63
2.6 Bioinformatic analysis of <i>Staphylococcus pseudintermedius</i> endolysins	63
2.6.1 Computational screening of endolysins within <i>S. pseudintermedius</i> phage genomes ...	63
2.7 Expression and purification of endolysins	64
2.8 Characterisation of selected endolysins	65
2.8.1 Analysis of domain architecture	65
2.8.2 Host range analysis of selected endolysins	65
2.8.3 <i>In silico</i> analysis of 3D protein modelling	65
2.8.4 Turbidity reduction assay of candidate endolysin	66
2.9 Development of silkworm larvae model	66
2.9.1 Housing of silkworm larvae	66
2.9.2 Injection methods	66
2.9.3 Haemolymph collection	67
2.10 Effect of silkworm haemolymph on phage lytic ability and bacterial growth	67
2.11 <i>Staphylococcus pseudintermedius</i> infection trials in silkworm larvae	67

2.12 Phage therapy trials in silkworm larvae.....	68
2.13 Standard Statistical Analysis.....	68
Chapter 3	70
3.1 Summary.....	71
3.2 Introduction.....	72
3.3 Results	74
3.3.1 Collection of <i>Staphylococcus pseudintermedius</i> isolates as a host for phage screening.	74
3.3.2 Isolation of <i>Staphylococcus pseudintermedius</i> phages from environmental and dog samples.	77
3.3.3 Characterisation of isolated bacteriophages	80
3.3.3.1 Identification of four novel phages through Whole Genome Sequencing (WGS)..	80
3.3.3.2 Host range characterisation of four novel phages	83
3.3.3.3 Growth kinetics of candidate phage, Phage SP_10s	87
3.3.3.4 Secondary WGS analysis of four novel phages	90
3.3.3.5 Morphological characterisation using Transmission Electron Microscopy (TEM)	94
3.3.4 Prophages are highly prevalent in <i>Staphylococcus pseudintermedius</i> genomes	94
3.4 Discussion.....	97
3.5 Conclusions.....	101
3.6 Appendix.....	102
Chapter 4	150
4.1 Summary.....	151
4.2 Introduction.....	152
.....	152
4.3 Results	154
4.3.1 Identification of putative endolysin genes in <i>Staphylococcus pseudintermedius</i> phages	154
4.3.2 Protein alignment of identified putative endolysins	159
4.3.3 Selection and characterisation of candidate putative endolysins.....	163
4.4 Discussion.....	178
4.5 Conclusions.....	182
4.6 Appendix.....	183
Chapter 5	188
5.1 Summary.....	189
5.2 Introduction.....	190
5.3 Results	193
5.3.1 Development of silkworm larvae (<i>Bombyx mori</i>) model	193
5.3.2 Suitability assessment of silkworm model for phage and <i>S. pseudintermedius</i> administration	197
5.3.3 Safety trials of selected phage and endolysins	200
5.3.4 Infection trials of <i>S. pseudintermedius</i> in silkworm larvae	201
5.4.5 Efficacy trials of phage and/or endolysins in silkworm larvae.....	203

5.4 Discussion.....	206
5.5 Conclusions.....	209
5.6 Appendix.....	211
Chapter 6	212
6.1 Introduction.....	213
6.2 Phage therapy as a novel therapeutic for antibiotic-resistant infections.....	214
6.3 The need for ethical animal models for the progression of phage therapy	218
6.4 Final reflections and conclusions	220
Chapter 7	223
7.1 Reference list	224

List of Figures

Figure 1.1 Isolation rates of <i>S. pseudintermedius</i> and MRSP from various disease states in canines.....	29
Figure 1.2 The lytic life cycle.	34
Figure 2.1 Gram stain protocol for bacteria.	53
Figure 2.2 List of environmental samples collected for phage screening.	56
Figure 3.1 The lytic and lysogenic life cycle of bacteriophages.....	73
Figure 3.2 Isolation sources of 60 <i>Staphylococcus pseudintermedius</i> clinical isolates from infected canines.	75
Figure 3.3 Growth of <i>Staphylococcus pseudintermedius</i> representative strain CM16-689.....	76
Figure 3.4 Antibiotic resistance patterns of <i>Staphylococcus pseudintermedius</i> clinical isolates.	76
Figure 3.5 Phage enrichment and isolation workflow.....	77
Figure 3.6 Plaque forming ability of isolated <i>S. pseudintermedius</i> phages.	79
Figure 3.7 Genome maps of four novel <i>S. pseudintermedius</i> phages.....	82
Figure 3.8 Growth kinetics of candidate phage, Phage SP_10s.	89
Figure 3.9 Absorbance curve of <i>S. pseudintermedius</i> CM16-069 with the addition of Phage SP_10s using ClarioStar microplate reader.	90
Figure 3.10 Genome map of prophage extracted from <i>S. pseudintermedius</i> strain 15788 that matched dominant phage from second sequencing run.....	93
Figure 3.11 Morphological analysis of Phage SP_157588.	94
Figure 3.12 Characterisation of prophages in 59 <i>S. pseudintermedius</i> clinical isolates.....	96
Figure 3.13 Frequency of complete prophages in 59 <i>S. pseudintermedius</i> genomes.....	97
Figure 3.14 Presence of plaques following mitomycin-c induction of <i>S. pseudintermedius</i> CM16-0689 (phage propagation strain).	100
Figure 4.1 Endolysin-induced bacterial cell lysis.	152
Figure 4.2 Workflow of endolysin identification, alignment, and selection from <i>S. pseudintermedius</i> phages.....	155
Figure 4.3 Amino acid length of 26 identified endolysins from <i>S. pseudintermedius</i> phages.	159
Figure 4.4 Protein sequence alignment of putative endolysin proteins from three amino acid groups.....	163
Figure 4.5 Domain organisation of six <i>S. pseudintermedius</i> endolysins.	165
Figure 4.6 Workflow for cloning, transformation, expression, and purification of endolysins for therapeutic testing.....	166
Figure 4.7 SDS-PAGE images of six purified endolysins.	167
Figure 4.8 Scoring of endolysin lytic ability on <i>S. pseudintermedius</i> clinical isolates.....	168
Figure 4.9 Lytic spectrum of three endolysins.	174
Figure 4.10 Structural analysis of CHAP domain and catalytic residues in Lys_SN13 and LysGH15.	176
Figure 4.11 The effect of EDTA in elution buffer on the lytic ability of Lys_SN13.	177
Figure 4.12 Turbidity reduction assay of Lys_SN13 at various concentrations against <i>S. pseudintermedius</i> CM16-0689.....	178
Figure 4.13 Protein sequence alignment of putative endolysin proteins from three amino acid groups.....	186
Figure 4.14 Representative SDS-PAGE images of protein purification optimisation.....	187
Figure 5.1 Benefits of silkworm (<i>Bombyx mori</i>) larvae as a model organism for research ..	191
Figure 5.2 Life Cycle of Silkworm (<i>Bombyx mori</i>) larvae.	192

Figure 5.3 Silkworm husbandry conditions.	194
Figure 5.4 Silkworm growth over five consecutive days.	195
Figure 5.5 Diagram of silkworm larvae with injection and extraction points labelled.	196
Figure 5.6 Phage lytic ability is not inhibited by silkworm larvae hemolymph.	198
Figure 5.7 Cell viability of <i>S. pseudintermedius</i> is not inhibited by silkworm larvae hemolymph.	199
Figure 5.8 Proliferation of <i>S. pseudintermedius</i> CM16-0689 in the haemolymph.	200
Figure 5.9 Visual representation of silkworm survival following <i>S. pseudintermedius</i> infection.	203
Figure 5.10 Workflow of phage or endolysin efficacy trials in silkworm larvae.	204
Figure 5.11 Temperate variation of 28 °C constant temperature room.	211
Figure 6.1 Global transmission of antibiotic resistance.	221

List of Tables

Table 2.1 Sixty clinical isolates of <i>S. pseudintermedius</i> collected from canine infections.....	50
Table 2.2 De-identified samples collected from privately-owned animals for phage screening.	57
Table 2.3 Thermocycle conditions for amplification of tagged DNA.	60
Table 3.1 Overview of phage screening success.....	78
Table 3.2 De novo assembly of the four novel <i>S. pseudintermedius</i> phage genomes.....	81
Table 3.3 Host range analysis of four <i>S. pseudintermedius</i> phages on 60 <i>S. pseudintermedius</i> clinical strains.....	84
Table 3.4 Overview of host range ability of four novel phages.	87
Table 3.5 De novo assembly of prophage extracted from <i>S. pseudintermedius</i> strain 157588 and four phage samples.	92
Table 3.6 Bacterial biochemical characterisation to confirm <i>Staphylococcus pseudintermedius</i> identification.....	102
Table 3.7 Genome annotations of Phage SP_157588.....	104
Table 3.8 Genome annotations of Phage SP_10L.....	106
Table 3.9 Genome annotations of Phage SP_22L.....	109
Table 3.10 Genome annotations of Phage SP_22s.....	111
Table 3.11 Genome annotations of Phage SP_10s.	113
Table 3.12 Genome annotations of prophage from <i>S. pseudintermedius</i> strain 157588.	116
Table 3.13 Prophages identified from 59 <i>S. pseudintermedius</i> genome sequences.....	124
Table 3.14 Overview of prophages identified in 59 <i>S. pseudintermedius</i> isolates.....	140
Table 4.1 Identification of 26 endolysin genes through genome mining of <i>S. pseudintermedius</i> phages.....	156
Table 4.2 Pairwise (%) identity of six endolysins selected.	163
Table 4.3 Six novel candidate endolysin selected for characterisation.	164
Table 4.4 Host range analysis of six purified endolysin on 60 <i>S. pseudintermedius</i> clinical strains.	170
Table 4.5 Pairwise (%) identity of nine putative endolysins from the 251 amino acid group.	183
Table 4.6 Pairwise (%) identity of nine putative endolysins from the 486 amino acid group.	183
Table 4.7 Pairwise (%) identity of nine putative endolysins from the 629 amino acid group.	184
Table 5.1 Silkworm larvae haemolymph extraction methods.....	196
Table 5.2 Survival of silkworms following injection of control solutions or <i>S. pseudintermedius</i> phages and endolysins.....	201
Table 5.3 Silkworm survival following <i>S. pseudintermedius</i> infection.	202
Table 5.4 Efficacy of phage or endolysin following <i>S. pseudintermedius</i> infection.....	205

Abstract

Phage therapy is the therapeutic application of bacteriophages and their derived products and is recognised as a novel antimicrobial agent against antibiotic resistant bacterial pathogens. Methicillin-resistant *Staphylococcus pseudintermedius* is a significant threat to the veterinary sector as a multi-drug resistant (MDR) bacterial pathogen involved in canine infections and there is currently an unmet need for novel treatment options. Therefore, this thesis aimed to explore the potential of phage therapy against *S. pseudintermedius* infections. Throughout this thesis, four novel phages were isolated which lysed up to 53% of *S. pseudintermedius* clinical isolates and candidate phage, SP_10s significantly reduced bacterial counts within 30 minutes of application *in vitro*. The four phage preps were dominated by a single temperate phage, matching a prophage within an isolate of *S. pseudintermedius*. This may be explained by the high prevalence of prophages within *S. pseudintermedius* genomes, where we identified that 60.9% of the *S. pseudintermedius* isolates contained at least one complete prophage within their genome. As temperate phages are unsuitable for phage therapy, we next identified six novel endolysins from the genome of *S. pseudintermedius* phages. Three of the endolysins were able to lyse up to 60% of the *S. pseudintermedius* clinical isolates, with complete bacterial clearance achieved 10 hours post-application of the candidate endolysin; Lys_SN13. While candidate phage (SP_10s) and endolysin (Lys_SN13) showed promising results *in vitro*, to further progress their use, their safety and efficacy should be evaluated in animals' models. Therefore, we developed a silkworm larvae model that showed to be an appropriate model for *S. pseudintermedius*, however, phage therapy results require further validation in higher order models. Overall, this body of work provides insights into the use of phage and/or endolysins as a novel therapeutic for *S. pseudintermedius* infections in canines.

Statement of Authorship

Except where reference is made in the text of the thesis, this thesis contains no material published elsewhere or extracted in whole or in part from a thesis accepted for the award of any other degree or diploma. No other persons' work has been used without due acknowledgement in the main text of the thesis. This thesis has not been submitted for the award of any degree or diploma in any other tertiary institution.

All research procedures reported in this thesis were carried out with the approval of the La Trobe University animal ethics committees (AEC19043). This work was supported by an Australian Government Research Training Program Scholarship.

Stephanie Lynch

13th of August, 2021

Acknowledgments

As I start to write these acknowledgments, I can't help but feel extremely grateful for all of the wonderful people that have supported me throughout my PhD and life. Two perfect quotes to express how I feel are; 1) "Anything is possible when you have the right people there to support you" – Misty Copeland, and 2) "It takes a village to raise a PhD student" – Vivian Tran.

First and foremost, to my supervisor Karla Helbig, there are no words to thank you for all the support you have given me over the years. From the first day of Honours, you provided me with endless support, advice, and guidance. You gave me the tools to persevere, even when it felt easier to give up, and I sure am thankful I never gave up! I will always appreciate how you always made time for me, whether it be reading through my thesis, listening to my presentations or just to have a chat, I don't know how you juggle it all. Thank you for creating a workplace environment filled with amazing researchers, where I was genuinely happy to come to work every day. Thank you to all of the past and present members of the Helbig Lab

I would also like to thank my two co-supervisors, Travis Beddoe and Steve Petrovski. Firstly, thank you Steve for taking me under your wing from the start of Honours and showing me the ropes of phage research. I will always be thankful for you letting me work in your lab and always making me feel welcomed. Travis, thank you for supporting me since undergraduate biochemistry. If it wasn't for your advice to partake in the Honours Year with Karla & Steve, I definitely wouldn't be where I am today. Thank you for letting me part of your lab and teaching me all I needed to know about the protein work!

I would also like to thank other members of my PhD panel including Subir, Brooke, Seb, and Grant for attending my RPP meetings over the last four years. Thank you for providing support and guidance when I needed it most.

Throughout my PhD I have been very fortunate to accumulate a number of wonderful mentors both informal and formal. I would like to start by thanking Paul, from the IMNIS mentoring program. Even throughout your busy schedule you always made time to meet with me, and introduced me to many great leaders, some of whom shaped my PhD project. Thank you, Paul. Next, I would like to

thank Brooke, from the PAM Mentoring Program. Brooke, from day one of our mentoring sessions, you were so enthusiastic and were always there to make me laugh. You kept me on track and gave me such great advice. Thank you, Brooke. I would also like to thank Laura, my mentor through the La Trobe Career Ready mentoring, you always made time for me after your long days at work and you were a great help with creating my CV, so thank you, Laura. Lastly, thank you to Jas, my mentor from the ASM Mentoring Program, we only met a few times, but I will always appreciate you listening to me while I was stressed about jobs and for leading me through the mock interviews.

I would like to take a moment to thank some of the wonderful researchers that showed me the ropes in the laboratory. I would like to thank Daniel, who was the first person to teach me all the basics in phage research, you were always patient and mostly kind, so thank you. I would like to extend the thanks to all members in the Petrovski lab for helping me find my feet in the lab. I would like to thank Tim and Gemma from the Beddoe lab for all of their help with the protein work, I will always be so grateful for all that you taught me in such a short amount of time. Lastly, thank you Larry for supporting me throughout the durations on my time at La Trobe.

To the team at In2science, thank you to you all for being so patient and teaching me so many skills. Thank you for all the wonderful opportunities you have given me to share my passion of STEM with the wider community. I will always remember my In2science mentees Jemma and Ruby, and I will treasure all the laughs we had over zoom. Thank you to Jessica & Jan, cofounder of Phage Directory, for taking me on as a volunteer and giving me the opportunity to meet so many amazing phage researchers. You are both the most welcoming people and I am grateful to know you both! I have also loved being part of organising PHAVES, helping write C&T blogs and all the other random projects you threw my way.

I definitely couldn't have finished this massive feat without the love and support from some truly special friends who I will always cherish. Firstly, a huge thank you Ebony for taking me under your wing in Honours. I will forever be in debt to all the times you stayed late at uni to help me, whether it was helping to fix my literature review or to streak benches full of crocodile samples. You have become a very close friend and I am glad I got to spend all of the lockdowns either on zoom or

living with you, you definitely made riding the highs and lows of a PhD more memorable! You are truly inspirational; you are a wonderful friend and an amazing research, never stop being you! To Haylo, Viv and Jordyn, I am truly grateful to have met you all. Haylo, thank you for the gym sessions, the vegan snacks, and to Jess for the times she cooked me dinner, it was honestly so appreciated. Viv, you are just one of a kind! You are always such a delight to be around and always have the best advice. I seriously can't wait to see all the wonderful things that life has waiting for you. You are a superstar! Jordyn, you are such a lovely friend. You always made time for me, and I appreciated all of our SUAW on zoom! To Jay and Jacinta, thank you to you both for all the walks around campus and for always being there for me. You are both such wonderful people and I can't wait to see all that you achieve. To Sarah and Jemma, you are two of the kindest people I have ever met. Sarah, I will honestly never forget the countless times you have made me food or left gifts on my desk, I can't thank you enough for all of your support over the year, you deserve the best. Jemma, thank you for always supporting me throughout our time of the HDR Committee and for all the zoom chats, you will do amazing things! To Aurelie, Vahee and Britt, I honestly don't think I would have made it past Honours without you all. You always knew how to cheer me up when I wanted to give up and I will always cherish all the great food we have eaten together of the years!

I am also super thankful for my beautiful friends outside of uni, the friends that were always there to distract me from my work and have supported me throughout life. Diane, you are my best friend, you have been there through thick and thin over the past 12 years, and I couldn't think of anyone else I'd rather have by my side. Thank you for opening up your home to me and letting me escape my PhD to visit you, thank you for all the zoom yoga, painting, and chat sessions, I will always appreciate your friendship. To Hannah, you are truly a one in a million friend. From the first day I met you in undergrad, I knew we would be friends for life. You are always the life of the party but also the first one there if I need support. You are the best, never change for anyone! To Nick and Pat, two of my longest friends, while we don't see each other often, your continuous support over the years has always been appreciated!

Lastly, but certainly not least, thank you to my wonderful, crazy family who I wouldn't trade for the world. I certainly wouldn't be where I am today without you all! Mum, I will never be able to

repay you for all the support you have given me over the years, from cooking me food to taking the dogs for a walk. You always put everyone before yourself and have got a lot of love to give. I will always appreciate and love you. Dad, I don't even know where to start, but I am so thankful for you every day. I will always appreciate how much interest you took in my projects and all of the phone calls on my drive home. You always pushed me to keep going and to do my best, I will always love and cherish you! To Courteney and Aaron, my favourite siblings. You are both the reason I keep going every day, I always want to be the big sister you look up to, but I more so look up to both of you. Courteney, I am so blessed to be granted with such a beautiful sister and best friend. I am so thankful we are so close and always appreciate your support. Aaron, thank you for always being there to help with my project, from painting 3D silkworms to injecting live silkworms. You are a great brother, and I am proud of all that you do. Of course, thank you to my fur babies Leah and Loki for always being there when I force cuddles upon you.

Thank you again everyone for the endless support, I am forever grateful.

Acknowledgment of Country

I acknowledge the people of the Woi wurrung and Boon wurrung language groups of the Kulin Nation, on whose unceded lands this work was produced on. I pay my respects to their Elders past and present, as well as the Traditional Custodians of the land.

I also celebrate and acknowledge First Nations people as our first scientists.

Science engagement

Publications arising from this PhD

Lynch SA*, Helbig KJ. The Complex Diseases of *Staphylococcus pseudintermedius* in Canines: Where to Next?. *Veterinary Sciences*. 2021 Jan;8(1):11.

** SA Lynch contributed significantly to the conception, design, drafting and revision (overall 95% contribution) of this manuscript as evidenced by her first authorship.*

Abdelrahman F, Easwaran M, Daramola OI, Ragab **S. Lynch*** S, Oduselu TJ, Khan FM, Ayobami A, Adnan F, Torrents E, Sanmukh S. Phage-Encoded Endolysins. *Antibiotics*. 2021 Feb;10(2):124.

** SA Lynch contributed significantly to the conception, design, drafting and revision of this manuscript as all authors contributed equally.*

Conference presentations

2021: Phage Futures Congress: Poster presentation & 5-minute spotlight presentation. “Phage therapy for *Staphylococcus pseudintermedius* infections in canines”.

2021: PHAVES, Phage Directory. A 30-minute seminar to phage researchers. ““Phage therapy: A novel therapeutic for canine infections.”

2021: La Trobe Infection & Immunity (I&I) Forum. A 30-minute seminar. “Phage therapy: A novel therapeutic for canine infections.”

2021: La Trobe Library ‘Bright Sparks’. A 30-minute seminar to engage undergraduate students in further study at La Trobe.

2020: IBRT Bacteriophage Week Webinar Series. A 45-minute seminar. “PhD Perspective: Opportunities for phage research.”

2020: PAM Research Symposium: 3-minute presentation. “Using sequencing approaches to find the solution within the ‘problem’”.

2020: MicroSeq Seminar. A 3-minute seminar. “Using sequencing approaches to find the solution within the ‘problem.’”

2020: Monash-USCD Phage Conference [cancelled due to COVID-19]: 10-minute presentation. “Phage therapy against *Staphylococcus pseudintermedius*: Towards therapeutics”.

2019: PAM Research Symposium: 10-minute presentation & poster presentation. “Isolation and Characterisation of Bacteriophages against *Staphylococcus pseudintermedius*.”

2019: Victorian Infection and Immunity Network (VIIN): Poster presentation. “Development and optimisation of a silkworm (*Bombyx mori*) infection model for phage therapy trials.”

2018: PAM Research Symposium: 3-minute presentation & poster presentation. “The Isolation and Characterisation of Bacteriophages Against Canine Pyoderma.”

2018: Australian Microbiology Society (Brisbane): Poster presentation “Isolation and Characterisation of Novel Bacteriophages Against Causative Organisms of Bovine Mastitis”.

2017: Australian Microbiology Society VIC Branch Nancy Millis Awards Night. 10-minute talk “Exploring bacteriophage as an alternative therapeutic to animal diseases; bovine mastitis.”

Funding obtained throughout this PhD

Work throughout this PhD was supported by numerous grants, funds, and scholarships

2020: Canine Research Foundation Grant; \$9,700.00 funding provided by Dogs Victoria and Canine Research Foundation to support “Phage therapy for antibiotic resistant *Staphylococcus pseudintermedius* in canines”.

2019: Recipient of Defence Science Institute’s Research Higher Degree (RHD) Student Grant; \$15,000 funding to support postgraduate research students undertaking research projects consistent with the Institute’s technology themes.

2019: Intellectual climate fund for graduate researchers; \$600 awarded to graduate researcher to lead a range of academic, social, and cultural activities that will seed or enhance a stimulating intellectual climate and supportive network within their local graduate research community.

2018: Intellectual climate fund for graduate researchers; \$500 awarded to graduate researcher to lead a range of academic, social, and cultural activities that will seed or enhance a stimulating intellectual climate and supportive network within their local graduate research community.

2017: Recipient of the Student Travel Scholarship at the ASM Nancy Millis Student Award (VIC); Was awarded a travel scholarship of \$1,000 to assist in conference, travel, and accommodation fees to attend the ASM AGM in Brisbane.

2017: Present: Australian government’s research training program scholarship (RTP); Fully funded by the Australian Government and awarded to students of exceptional research potential undertaking a Higher Degree by Research (HDR) to assist with tuition and general living costs.

Abbreviations

%	Percent
°C	Degrees Celsius
µg	Micrograms
µL	Microlitres
µm	Micrometre
AEC	Animal Ethics Committee
Amc	Augmentin
BLAST	Basic Local Alignment Search Tool
bp	Base Pairs
CFU	Colony Forming Units
CHAP	Cysteine, Histidine-Dependent Amidohydrolases/Peptidases
CI	Containing Integrase
CIRDC	Canine Infectious Respiratory Disease Complex
CIV	Canine Influenza Virus
CL	Cephalexin
cm	Centimetre
CoNS	Coagulase Negative <i>Staphylococcal</i>
Cro	Repressor
CWA	Cell Wall Anchored
CWB	Cell Wall Binding
dH2O	Deionised Water
DNA	Deoxyribonucleic Acid
e.g.	Exempli Gratia
EM	Electron Microscopy
Enr	Enrofloxacin
EDTA	Ethylenediaminetetraacetic acid
g	Grams
HBA	Horse Blood Agar
hrs	Hours
IgG	Immunoglobulin G
kb	Kilobase
kDa	Kilodaltons
kPa	Kilopascal
L	Litre
mA	Milliamps
MDR	Multidrug Resistant
MIC	Minimum Inhibitory Concentration
min	Minutes
mL	Millilitres
mm	Millimetres
mM	Millimolar
mmol	Millimole
MOI	Multiplicity Of Infection
MRSA	Methicillin Resistant <i>Staphylococcus Aureus</i>
MRSP	Methicillin Resistant <i>Staphylococcus Pseudintermedius</i>
NA	Nutrient Agar
NCBI	National Center For Biotechnology Information
NGS	Next Generation Sequencing
nm	Nanometres

OD	Optical Density
OE	Otitis Externa
ORF	Open Reading Frame
PCR	Polymerase Chain Reaction
PDB	Protein Data Base
PEN	Penicillin
PFU	Plaque Forming Units
Phages	Bacteriophages
pM	Picomole
R	Resistant
RFLP	Restriction Fragment Length Polymorphism
rpm	Rates Per Minute
RT	Room Temperature
RTI	Respiratory Tract Infections
S	Sensitive
SDS-PAGE	Sodium Dodecyl Sulfate Polyacrylamide Gel Electrophoresis
sec	Seconds
SF	Sulfafurazole
SIG	<i>Staphylococcus Intermedius</i> Group
spA	<i>Staphylococcal</i> Protein A
SPL	Staphage Lysate
Te	Tertacycline
TSB	Tryptic Soya Broth
UTI	Urinary Tract Infections
UV	Ultraviolet
v/v	Volume Per Volume
W	Trimethoprim
w/v	Weight Per Volume
WGS	Whole Genome Sequencing
x g	Times Gravity
β	Beta
φ	Phi

COVID statement

Dear Thesis Examiner,

The COVID-19 pandemic has no doubt affected everyone to various degrees. I would like to preface this thesis by highlighting the alterations made to this PhD project due to COVID lockdowns. I would also like to note that from March 2020 – December 2020 I did not have laboratory access.

The specific impact on COVID lockdowns on this thesis are as follows:

- **Chapter 3** – We were unable to isolate DNA or perform subsequent experiments on prophages induced from *S. pseudintermedius* bacterial isolates. These prophages were successfully induced in March 2020; however, laboratory access was revoked.
- **Chapter 4** – At the beginning of March 2020, I had not yet started working on my second results chapter. Therefore, we had to significantly alter the direction of my second chapter to suit working from home. The majority of this chapter was performed during the 2020 lockdown by computational analysis. The hands-on laboratory work was performed during the short laboratory access in Jan 2021 - March 2021 prior to further lockdowns in Melbourne.
- **Chapter 5** – Due to the extensive lockdowns in 2020 and 2021, there were extreme delays in postage deliveries. Currently, our silkworm supplies (larvae and food) are sent from QLD to Melbourne, and during peak lockdown would take 5-7 days to arrive. This delay in shipping meant that many silkworms did not survive in transit, and those that did survive were often too sick to include in experiments. There were no other feasible silkworm suppliers within an appropriate distance, therefore, silkworm experiments were significantly hampered.

Chapter 1

This chapter provides an introduction to this thesis in the form of a published literature review.

Citation:

Lynch, S.A.; Helbig, K.J. The Complex Diseases of *Staphylococcus pseudintermedius* in Canines: Where to Next? *Vet. Sci.* **2021**, *8*, 11. <https://doi.org/10.3390/vetsci8010011>

The Complex Diseases of *Staphylococcus pseudintermedius* in Canines: Where to Next?

Stephanie A. Lynch and Karla J. Helbig *

Department of Physiology, Anatomy and Microbiology, La Trobe University, Melbourne, VIC 3086, Australia; Stephanie.Lynch@latrobe.edu.au

* Correspondence: K.Helbig@latrobe.edu.au; Tel.: +61-3-9479-6650

1.1 Abstract

Staphylococcus pseudintermedius is a pathogenic bacterium of concern within the veterinary sector and is involved in numerous infections in canines, including topical infections such as canine pyoderma and otitis externa, as well as systemic infections within the urinary, respiratory, and reproductive tract. The high prevalence of methicillin-resistant *Staphylococcus pseudintermedius* (MRSP) within such infections is a growing concern. Therefore, it is crucial to understand the involvement of *S. pseudintermedius* in canine disease pathology to gain better insight into novel treatment avenues. Here, we review the literature focused on *S. pseudintermedius* infection in multiple anatomic locations in dogs and the role of MRSP in treatment outcomes at these niches. Multiple novel treatment avenues for MRSP have been pioneered in recent years and these are discussed with a specific focus on vaccines and phage therapy as potential therapeutic options. Whilst both undertakings are in their infancy, phage therapy is versatile and has shown high success in both animal and human medical use. It is clear that further research is required to combat the growing problems associated with MRSP in canines.

Keywords: *Staphylococcus pseudintermedius*; methicillin resistance; antimicrobial resistance; canines

1.2 Introduction

Over the last decade, *Staphylococcus pseudintermedius* has been identified as a bacterial species of concern within the veterinary sector. *S. pseudintermedius* is an opportunistic pathogen frequently isolated from healthy canines and, more importantly, associated with numerous infections in animals [1]. Dogs are the most common animal species infected with *S. pseudintermedius*, with 84.7% of all *S. pseudintermedius* isolates originating from canine diseases including skin, ear, and urinary tract infections [2]. It has been reported that up to 97.8% of methicillin-resistant *S. pseudintermedius* (MRSP) isolates show multidrug resistance (MDR) to three or more antibiotics routinely used in veterinary medicine [2–4]. *S. pseudintermedius* was first isolated in 1976; however, it was formerly identified as *Staphylococcus intermedius* due to the morphological similarities between the two species [5]. In 2005, using a DNA–DNA hybridisation technique on *S. intermedius* isolates collected from animals, *S. pseudintermedius* was revealed as a novel species [6]. It is now known that *S. pseudintermedius* belongs to a collective known as the *Staphylococcus intermedius* group (SIG) which encompasses three distinct species, *S. pseudintermedius*, *S. intermedius* and *S. delphini* [7]. While all members within the SIG group have been shown to colonise numerous animal species, *S. pseudintermedius* is said to be the most common SIG species associated with animals—particularly, the most prevalent commensal bacterium in dogs [7–11]. Therefore, for the purpose of this review, all literature describing canine isolates formerly identified as *S. intermedius* will be referred to as *S. pseudintermedius*, unless otherwise shown by genomic investigation. This current review aims to discuss the various infections that *S. pseudintermedius* is associated with to corroborate the significant impact that the bacterium has on the veterinary sector, followed by a discussion on current and future treatment options against *S. pseudintermedius* infections in dogs.

1.3 *Staphylococcus pseudintermedius*: A Pathogenic Bacterium of Veterinary Concern

Although *S. pseudintermedius* is primarily known for its pathogenic potential in canine infections, it is important to understand that *S. pseudintermedius* is also a significant member of the normal flora in canines [12–14]. Several studies have isolated *S. pseudintermedius* from 46–92% of healthy dogs, with the highest prevalence at the perineum (the skin between the anus and vulva/scrotum), followed by either the nasal or oral mucosa [12–14]. One study found that 0–4.5% of healthy dogs are colonised with MRSP as part of their normal flora [15]. Methicillin resistance in *Staphylococcal* spp. is known to alter the affinity to all β -lactam antibiotics. MRSP is a growing concern, with a recent study finding that 63% of *S. pseudintermedius* strains isolated from sick dogs were methicillin-resistant, with 78% of these isolates also described as MDR, being resistant to three or more antibiotic classes [16]. Additionally, MRSP can be transferred from sick dogs to otherwise healthy canines via direct transmission or indirect environmental transmission [17]. *S. pseudintermedius* transmission and subsequent colonisation may be associated with numerous infections, with skin infections being the most common (see Figure 1). However, *S. pseudintermedius* is also present as a pathogen in multiple other canine disease pathologies [17–20]. This highlights the fact that antibiotic resistance is a real concern moving forward in the veterinary space, especially for the treatment of *S. pseudintermedius* in canines, and adds perspective about whether antibiotics are a viable treatment option for the future of veterinary medicine.

1.3.1 Canine pyoderma

Canine pyoderma is one of the most common bacterial skin infections diagnosed in small veterinary medicine and is associated with redness, lesions, pain, and inflammation [21]. Canine pyoderma can vary from moderate infections to severe infections and is triggered by underlying factors such as allergic skin disease, ectoparasites and endocrinopathies. This initiates the colonisation of pathogenic *S. pseudintermedius*, which is the most common pathogen associated with cutaneous infections, isolated as the predominant pathogen in up to 92% of canine pyoderma cases (see Figure 1) [22–25]. While it is evident that *S. pseudintermedius* is the predominant pathogen associated with canine pyoderma, it is also the most common commensal species in dogs, and there is currently a lack of clear evidence as to whether commensal species cause infection or if external isolates initiate infection.

To assess this knowledge gap, multiple studies have compared the sequence diversity between commensal and pathogenic *S. pseudintermedius* isolates from the same canines; however, the collective evidence from these studies has not been able to conclusively answer this question. A handful of studies have shown no distinguishable differences between *S. pseudintermedius* isolates from healthy or atopic dogs using molecular techniques, therefore indicating that no specific strains or clusters of strains are associated with canine pyoderma [26–28]. More specifically, *S. pseudintermedius* isolates collected from the mucosa, a colonisation site for commensal species, and lesion sites from infected dogs in one study were either indistinguishable or closely related, perhaps indicating that the commensal *S. pseudintermedius* isolates may also be the causative agent in these pyoderma cases [26]. In contrast, isolates from canine pyoderma lesions have also been shown to be completely unrelated to mucosal isolates, suggesting either the commensal species mutate to become pathogenic or external isolates of *S. pseudintermedius* colonise to cause infection [26]. It is clear that longitudinal studies are required to truly assess genetic relatedness between commensal isolates and those involved in pyoderma cases, despite the fact that these studies will undoubtedly be difficult to perform given the inability to predict the onset of canine pyoderma, which would in turn require very large cohorts of animals to give meaningful study outcomes.

The rise in MRSP may explain the discordance between *S. pseudintermedius* species isolated from canine pyoderma. MRSP is isolated in up to 59% of canine pyoderma cases (see **Figure 1.1**), perhaps indicating that *S. pseudintermedius* isolates involved in infections may acquire genes required for methicillin resistance and appear unrelated to the commensal species [22–25,29]. Additionally, the acquisition of external strains that may lead to disease may be supported by two independent studies which have shown that MRSP from infected dogs can transmit to healthy contact dogs and the environment (e.g., sleeping and eating areas) [17,19]. In the majority of cases, the healthy dogs were only MRSP-positive when the infected dog was MRSP-positive, implying contamination rather than colonisation in healthy dogs [17]. However, there was one case where the healthy dog remained MRSP-positive, resulting in an ear infection, even after the infected dog recovered [17]. This implies that *S. pseudintermedius* isolates recovered from canine infections that are unrelated to the dog's commensal species may be caused by external species acquired from contact with infected dogs. However, this still leaves room for research into the factors that may contribute to the difference between acquired infection versus no infection upon contact of a healthy dog with an MRSP-infected dog

showing disease pathology. However, these findings suggest that MRSP may have the ability to spread further within the dog community, which may affect the availability of treatment options to treat MRSP infections [17,19]. Additionally, MRSP isolates are often also multidrug-resistant, demonstrating high levels of antibiotic resistance against multiple antibiotic classes [30]. One study showed that the number and variety of antibacterial drug classes previously prescribed to dogs resulted in higher cases of MRSP, particularly those that received beta-lactam drugs and concurrent immunomodulatory therapy [30,31]. The evidence of high antibacterial resistance in pyoderma isolates is concerning from a treatment perspective, especially as *S. pseudintermedius* causes various other diseases throughout dogs.

1.3.2 Otitis externa

Otitis externa (OE), or inflammation of the outer ear, is a disease routinely diagnosed in small veterinary practices [32–35]. Primary causes of OE are factors that initiate inflammation, including foreign bodies, such as grass awns, endocrinopathies including hypothyroidism as well as the presence of parasites [35–37]. However, the most frequent primary cause of OE highlighted across multiple studies is allergies, including adverse food reactions or atopic dermatitis [35–37], with studies showing that up to 75% of those diagnosed with OE were also diagnosed with atopic dermatitis [35–38]. Bacteria and yeasts, particularly *S. pseudintermedius* and *Malassezia spp.*, respectively, two commensal species of the skin, are listed as secondary causes of otitis externa [34]. *S. pseudintermedius* is a predominant pathogen associated with OE, isolated from 20–94.3% of OE cases in canines (see Figure 1) [32,34,36,38–43]. The variation surrounding the prevalence of *S. pseudintermedius* in OE is still under investigation; however, geographical location has been suggested as a potential strong contributor, but with no influence on seasonal trend [40].

While dog breeds such as spaniels, German Shepherd and Shar-Pei are represented significantly more in OE cases [36,37,40], the breed and the age of the dog may also influence the type of pathogen present [36]. Interestingly, breed as a predisposing factor to OE may be explained by ear confirmation, particularly in spaniel breeds, with two independent studies identifying a significant increase in diagnosis frequency in dogs with pendulous ears, likely due to the moist, warm conditions facilitating secondary bacterial and fungal growth [37,40]. This is not surprising as the outer ear has a similar structure to the epidermis of the skin and, therefore, species that affect the skin, such as *S. pseudintermedius*, can also affect the external ear canal [35]. This is important for veterinarians to consider, as dogs with canine pyoderma are therefore at a higher risk of developing a secondary infection of *S. pseudintermedius* within the ear canal, which should be considered when prescribing treatment options for OE. Importantly, MRSP strains have been isolated in 10–48.1% of canine OE cases (see Figure 1) [2,39,41,42], with one study showing that all MRSP isolates were also multidrug-resistant, being resistant to two or more antibiotic classes [39]. This study also found that recent administration of beta-lactam antimicrobials significantly increased the frequency of methicillin and fluoroquinolone resistance [39], with the number and duration of prior exposures significantly increasing resistance to particular antimicrobial classes and the prevalence of methicillin resistance, respectively [39]. These studies highlight that antibiotic treatment of OE moving forward is likely to be plagued with difficulties and that novel treatment options to reduce antimicrobial resistance should be considered.

1.3.3 Urinary Tract Infections (UTI)

Urinary tract infections (UTIs), particularly those caused by bacteria, are another common diagnosis within small veterinary practices, with approximately 14% of dogs contracting a UTI within their lifetime [44,45]. Numerous bacteria species have been isolated previously from canine UTI cases, including *Enterococcus* spp., *Proteus* spp., *Staphylococcus* spp. and *Streptococcus* spp., with *Escherichia coli* identified as the most common uropathogen, isolated from up to 51% of canine UTIs [44–49]. More recently, *S. pseudintermedius* has been shown as the most common *Staphylococcal* spp. present in canine UTIs, with studies reporting a variable frequency of *S. pseudintermedius* isolation in 6.3–94.7% of UTIs in canines (see Figure 1) [45,46,48–53]. The large variation in *S. pseudintermedius* isolation has in part been explained in a recent multicenter study over a 6-year period across 14 European countries [53]. This study found that the bacterial species isolated from canine UTI cases varied based on geographical location, as did the antimicrobial resistance of the respective bacteria isolated [53]. Within this study, *S. pseudintermedius* was the most frequently isolated pathogen from UTI cases in most countries; however, this varied from 0% *S. pseudintermedius* isolation rate in Spain to as high as 94.7% in Italy; similarly, the isolation of MRSP varied from as low as 1.15% in Sweden to as high as 50% in Italy [53]. Within this study, the variation in antimicrobial resistance, particularly MRSP, was potentially attributed to countries, such as Sweden, following tighter regulations in regard to antimicrobial regulation and use, therefore resulting in lower resistance rates. However, differences in methods used to identify antimicrobial resistance were also reported across countries, which may have impacted the prevalence rates. In addition, the differences in methods used for urine sampling and bacterial isolation may have also affected the *S. pseudintermedius* prevalence rates [45]. This highlights the importance of unifying the methods of isolation and antimicrobial resistance characterisation for more accurate representations of *S. pseudintermedius* prevalence and resistance. Alarming, despite the variation in sampling and detection methods across the sector, multiple studies have reported high rates of MRSP and MDR *S. pseudintermedius* from UTIs in canines [45,46,52,54], with a significant increase in methicillin and gentamicin resistance in *S. pseudintermedius* isolates over a 16-year period, and a significant increase in fluoroquinolone resistance over the last 7-year period [45,46,52,54]. Additionally, there has been a temporal increase in MDR resistance in MRSP isolates, with all MRSP isolates in the study by Marques and colleagues displaying resistance to all antibiotics tested [52]. This is concerning as *S. pseudintermedius* has been isolated in up to 33% of recurrent UTI in canines [55], therefore alluding to the fact that antimicrobial resistance in *S. pseudintermedius* is impacting the resolution of UTI, resulting in major therapeutic limitations.

1.3.4 Respiratory Tract Infections

Respiratory tract infections (RTI) in canines are relatively common and encompass various diseases including bacterial pneumonia, canine infectious respiratory disease complex (CIRDC) and viral infections; additionally, they are readily passed between dogs in social settings such as dog parks and boarding kennels [56]. There are numerous bacterial and viral pathogens that cause RTI in dogs, resulting in clinical symptoms such as coughing, sneezing or excess discharge [57]. Based on these symptoms, in addition to the medical history and physical examination of the patient, a presumptive diagnosis is

generally made. However, to identify the causative agents or perform antibiotic susceptibility testing, samples of the airway lavage are generally used to culture the bacterial species [58,59]. As a result, studies have reported several bacterial species associated with RTI, particularly *Staphylococcus spp.*, including *S. pseudintermedius*, which is isolated in 9.3–60% of RTI in canines (see Figure 1) [50,56–64]. There are many factors influencing the prevalence of *S. pseudintermedius* in canine RTI, including the type of RTI diagnosed, which has been shown to affect the bacterial species isolated [58]. Interestingly, *Staphylococcus spp.* is more likely to be isolated from canines with aspiration pneumonia, usually caused by fluid from the stomach or mouth entering the lungs, compared to dogs that have community-acquired pneumonia [58]. The heightened prevalence of *S. pseudintermedius* in cases of aspiration pneumonia is likely due to the presence of *S. pseudintermedius* in the mouths of healthy canines, therefore entering the lungs and causing infection. This variation in dominant species present in different RTI was confirmed by a recent study which also found differences in bacterial communities between community-acquired pneumonia and secondary-bacterial pneumonia [59]. In particular, dogs with community-acquired pneumonia showed a loss of bacterial diversity and a dominant taxon [59]. Meanwhile, dogs with secondary-bacterial pneumonia also had a dominant species; however, usually those derived from the upper respiratory tract—for example, *S. pseudintermedius* from the mouth—thus indicating that bacterial symbiosis is a common phenomenon in canine bacterial pneumonia [59].

In addition to the type of RTI influencing the prevalence of *S. pseudintermedius* isolation, studies aiming to monitor the antimicrobial resistance patterns of canine isolates throughout Europe found a higher proportion of *S. pseudintermedius* isolates from RTI in Poland from 2008 to 2014, therefore suggesting that geographical location may contribute to variation in *S. pseudintermedius* isolation from canine RTI [56,60]. This variation due to geographical location was in agreement with a recent study which additionally found a potential association between RTI and the season or the age of the dog, albeit not statistically significant [62].

As mentioned, both bacterial and viral pathogens are associated with canine RTI; therefore, previous research has explored the potential interaction between bacterial and viral pathogens involved in respiratory infections. Preliminary results performed in a mouse model showed that mice co-infected with *S. pseudintermedius* and canine influenza virus (CIV) showed significant increases in bacterial and viral load in various organs compared to mice infected with *S. pseudintermedius* or CIV alone and, subsequently, a significant increase in lesion scores in the tissues of co-infected mice [61]. This indicates that the control or treatment of viral infections in addition to *S. pseudintermedius* infections in canine RTI are equally as important for a successful outcome [61]. However, this phenomenon would need to be looked at in dogs to see if these data are translatable to actual clinical data.

In regard to treatment, bacterial RTI in canines are currently prescribed antibiotics such as trimethoprim, amoxicillin-clavulanic acid or enrofloxacin, either as monotherapy or dual therapy, depending on the severity of the infection [64,65]. A recent study found that 99.4% of all isolates recovered from canine RTI were resistant to at least one antibiotic, with 64.7% of isolates listed as MDR, with *Staphylococcus spp.* making up 7.1% of the MDR isolates [62]. Importantly, there is a significant association between the sex of the dog or the geographical season and the presence of MDR isolates, which is important to take into account when prescribing treatment options [62]. This high rate of resistance was

confirmed in a similar study, as an alarming 57.4% of dogs had a bacterial isolate that was resistant to the antibiotics that were previously or currently prescribed to that dog [58]. Therefore, confirming previous antibiotic administration can increase the resistance profiles of respiratory bacterial isolates [58]. With increasing trends of antibiotic resistance in respiratory isolates, studies suggest minimising this using broad-spectrum antibiotic use and to avoid using previously prescribed antibiotics, which may limit the treatment availability for bacterial RTI in canines in the future [56].

1.3.5 Reproductive Tract Infections

Previous research has identified an increase in the frequency of *S. pseudintermedius* in healthy dams isolated from vaginal samples, the placenta as well as colostrum and milk samples around the time of parturition [66–70]. However, the presence of *S. pseudintermedius* within the reproductive tract, such as the uterus and the mammary glands, has been associated with diseases in canines including pyometra and mastitis, respectively, which may result in complications including neonatal mortality [66,69–73]. Canine pyometra is an infection within the uterus of breeding female dogs, with *E. coli* and *Staphylococcus* spp., predominantly isolated from pyometra cases [74]. To date, two studies have isolated *S. pseudintermedius* in 10.5–18% of pyometra cases; however, these two studies had relatively small sample sizes and therefore may not accurately represent the prevalence of *S. pseudintermedius* in canine pyometra cases (see Figure 1) [73,75]. There have been no additional studies to explain the role of *S. pseudintermedius* in pyometra cases; therefore, further work is required to determine the pathogenicity of *S. pseudintermedius* in canine pyometra cases. Additionally, *S. pseudintermedius* has also been isolated from canines with clinical mastitis; however, the prevalence of *S. pseudintermedius* in mastitis cases has not been well researched [66,69–72]. Despite the lack of research into prevalence, it has been shown that all dogs experimentally inoculated with *S. pseudintermedius* develop clinical mastitis, resulting in symptoms including painful, hot and inflamed mammary glands [72], thus indicating that *S. pseudintermedius* can be pathogenic in the mammary gland and may be responsible for many canine mastitis cases [72]. It has been shown that in limited cases, *S. pseudintermedius* is the causative agent of mastitis in cows; therefore, further research is required to determine how often *S. pseudintermedius* is present in canine mastitis and whether it is the causative agent in dogs also [76]. While the presence of *S. pseudintermedius* in the reproductive tract may cause infection in the female canines, it has also been shown that identical or closely related *S. pseudintermedius* strains have been isolated from the mother's milk and vaginal tract and the puppies' skin and placental samples, indicating that *S. pseudintermedius* may be transmitted by intrauterine or vertical transmission [67,77,78]. While, in many cases, such transmission results in the healthy colonisation of commensal *S. pseudintermedius*, in the puppies, it has been shown that the transmission of *S. pseudintermedius*, specifically MRSP, has been associated with premature death within the first 2–3 weeks of life, also known as neonatal mortality [66,79–81]. Multiple studies have reported outbreaks of neonatal mortality due to septicemia, with *S. pseudintermedius* or MRSP isolated from the blood or organs of all deceased puppies [66,79,82]. Interestingly, it was found that *S. pseudintermedius* strains collected from the organs of puppies were found to be linked to isolates from the mother's milk and vaginal samples, therefore indicating that the vertical transmission of pathogenic

S. pseudintermedius can result in fatal sepsis in puppies [79,82]. However, the cause of neonatal mortality is multifactorial and, in addition to infections, congenital defects and low birth weight may also contribute to neonatal mortality [83]. Interestingly, puppies born with no detectable microbiota (including *S. pseudintermedius*) have a slower growth rate compared to those born with a microbiota within placental and meconium samples [67]. While this was not directly attributed to neonatal mortality, the lack of commensal species including *S. pseudintermedius* may be a contributing factor. Considering that the transmission of pathogenic *S. pseudintermedius* from the mother to her puppies may result in fatal sepsis, however, the lack of microbiota, including *S. pseudintermedius* may contribute to low birth weight and thus may lead to neonatal mortality. Therefore, there is a fine line between commensal *S. pseudintermedius* colonisation and pathogenic infection, with some studies suggesting that commensal colonisation of *S. pseudintermedius* may protect against pathogenic *S. pseudintermedius*, by bacterial interference [78]. Similarly, to respiratory tract infections, it appears that symbiosis of commensal species is important and should be taken into consideration when developing treatment options.

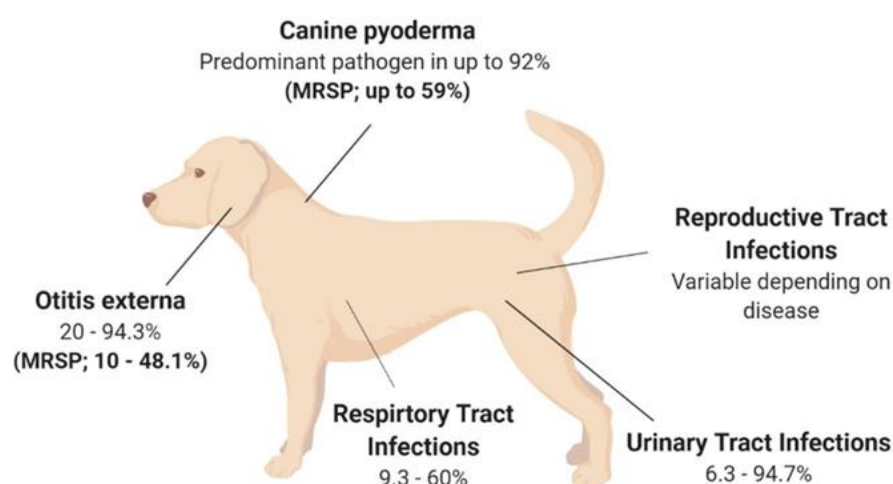


Figure 1.1 Isolation rates of *S. pseudintermedius* and MRSP from various disease states in canines. The isolation rates are presented as a range due to the variation described between studies; variation is described in detail in the main text. Canine pyoderma [22–25,29]; Otitis externa [2,32,34,36,38–43]. Urinary Tract Infections [45,46,48–53]; Respiratory Tract Infections [50,56–64]; Reproductive Tract Infections [66,69–73,76].

1.4 Current and Future Treatment Options for *Staphylococcus pseudintermedius* in Canines

S. pseudintermedius has the potential to cause or associate with a range of moderate to severe infections, of which, those left untreated, may have devastating outcomes. Therefore, future treatment options against such infections, especially in light of increasing antibiotic resistance, are a significant area of focus. It is important to note that the majority of studies on treatment options against *S. pseudintermedius* are in the context of canine pyoderma, as it is one of the primary reasons for antimicrobial prescription in the small animal veterinary sector [84]. Current guidelines created by diplomats of the American and European Colleges of Veterinary Dermatology state that canine pyoderma

caused by *S. pseudintermedius* should be treated by topical and/or systemic antimicrobial therapy, as a gold standard [84]. A recent study found that 96.5% of dogs were prescribed antimicrobials for systemic and/or topical administration upon the diagnosis of canine pyoderma, with the majority of dogs receiving antibiotics including amoxicillin-clavulanate (55.7%), followed by cephalexin (43.9%) or clindamycin (10.0%) [85]. In addition to systemic antibiotics, 27.7% of canine pyoderma cases also received topical treatments, with active ingredients including fusidic acid, chlorhexidine, and miconazole plus chlorhexidine shampoo [85]. Therefore, there is a significant need for alternative therapeutics. Two progressive areas of research for the treatment of canine pyoderma are vaccines and phage therapy, both of which have been successful in alternative animal diseases and offer promising alternative therapies for canine pyoderma and other *S. pseudintermedius* diseases moving forward. These novel therapies along with current therapies are discussed below.

1.4.1 Human Antibiotics

Antibiotics are the current frontline option against a multitude of infections in canines, due to their previously high efficacy, safety, and ease of administration [86]. However, due to the rise in antibiotic resistance, particularly of *S. pseudintermedius*, against the majority of current antibiotic classes, research has focused on the potential veterinary use of new antibiotic classes or antibiotic classes that are currently reserved for human use. One of the new antibiotics, cefovecin, is a semisynthetic cephalosporin developed for use in cats and dogs and is effective in vitro against a broad range of Gram-positive and Gram-negative clinical strains obtained from Europe and the US [87]. Cefovecin has also been shown to have a long half-life, allowing for repeated doses in 14-day intervals, therefore reducing the frequency of antimicrobial exposure, which may reduce resistance rates [87]. When used in randomised clinical trials to treat dogs with superficial or deep pyoderma, cefovecin was shown to have a high clinical efficacy similar to previously used antibiotics, with only a small percentage of dogs showing adverse symptoms [88]. Although these results indicate that cefovecin is a safe and effective newly synthesised antimicrobial for veterinary use in particular geographical locations, the use of cefovecin is restricted only to use in cats and dogs where antibiotic sensitivity testing indicated use is required; therefore, additional research has focused on repurposing multiple human antibiotics for use in animals [89–91]. Many studies have tested the efficacy of various human antibiotics including nitrofurantoin, rifampicin, doxycycline, cefazolin, and linezolid in the treatment of *S. pseudintermedius* infections in canines, mainly pyoderma, UTIs and surgical site infections [89–91]. Whilst studies did show that the use of such human antibiotics was effective in vitro against clinical isolates or was able to treat the infection of interest in clinical trials, it is important to note that some of these antibiotics resulted in adverse side effects and possessed a short half-life in serum, therefore requiring frequent and repeated doses, which is known to increase resistance [89–91]. Importantly, resistance was already noted against these tested antibiotics, either by the target strain, *S. pseudintermedius*, or associated species. For example, one study showed that rifampicin successfully treated pyoderma in 90% of dogs; however, in the 10% of dogs that failed to respond, *Proteus spp.* were isolated that were resistant to rifampicin [90]. The presence of resistance in the veterinary sector against human antibiotics is a major concern, as antibiotics such as nitrofurantoin, rifampicin, doxycycline and linezolid are essential in human medicine for

the treatment of UTIs, tuberculosis in chemotherapy patients, chronic skin infections and pneumonia in humans, respectively; therefore, resistance would significantly impact the availability of treatment options in human medicine [89–91]. While alternative antibiotics may be effective in the treatment of *S. pseudintermedius* infections in dogs, particularly pyoderma, where other treatment options have failed, moving forward, the use of antibiotics intended for the treatment of human diseases may not be appropriate in veterinary medicine.

1.4.2 Topical therapies

Recent guidelines state that topical therapy with proven activity against *Staphylococcus spp.* is the recommended treatment option against canine pyoderma and should be used in superficial cases of pyoderma where the owner can be compliant [92]. Currently, topical treatments are most likely used in combination with systemic antimicrobials, as topical treatments rapidly resolve lesions, show low rates of resistance and are shown to reduce the frequency and duration of antibiotics, which may decrease the evolution of antibiotic resistance [84]. Topical therapies are generally only sufficient for superficial canine pyoderma and include a multitude of formulations including shampoos, lotions, gels, creams, and ointments with a range of antiseptic, disinfectant, and active ingredients, as reviewed previously [93,94].

Shampoos are one of the most common topical therapies used for canine pyoderma as they are appropriate for large surface areas, act to remove both the bacteria and debris associated with the infection and are generally a cheaper option [94]. Previously, studies have shown that shampoos containing various active ingredients such as benzoyl peroxide, salicylic acid and chlorhexidine are effective in treating pyoderma by significantly improving bacterial counts and lesion scores, therefore successfully resolving canine pyoderma with no adverse side effects [95–97]. Importantly, combination treatment with a chlorhexidine shampoo and chlorhexidine digluconate spray also resolves pyoderma cases where MRSP is the causative agent and has been proven to be as effective as systemic antibiotic therapy [98]. One of the potential downfalls of shampoo formulas is the short contact time with the infected area before rinsing (~10 min); however, it has been shown that the fur collected from healthy dogs washed with the medicated shampoo shows antibacterial activity up to 17 days after the initial shampoo wash [99,100]. Therefore, in conjunction with previous results, the antibacterial activity of shampoo against pyoderma is safe, effective, and long-lasting [99,100]. However, the administration of shampoos is generally only effective against superficial pyoderma and can be time-consuming, as throughout the studies, shampoos were generally applied multiple times a week for extended timeframes. This is concerning as the effectiveness of shampoos heavily relies on the compliance of the owners. Therefore, shampoos may not be appropriate as a sole treatment option for canine pyoderma, especially in more severe or chronic cases.

1.4.3 Vaccines

Vaccines are a common and effective therapeutic used in canines as a protective mechanism against an array of viral and bacterial diseases. The majority of licensed vaccines used in veterinary medicine are either live-attenuated or inactivated vaccines

(bacterins) [101]. Such vaccines have been explored as a potential therapeutic for canine pyoderma.

1.4.3.1 Bacterins

Bacterins are inactivated vaccines consisting of lysed suspensions of bacterial strains and adjuvants such as aluminum hydroxide, which aim to elicit an immune response within the host [101]. Research surrounding bacterin vaccines in animal therapy has been well explored. An early study demonstrated that *Staphylococcal* bacterin therapy, in addition to antibiotics and corticosteroids, promoted the regression of clinical signs of *Staphylococcal blepharitis*, with no adverse side effects observed [102], proving that bacterin vaccines may be a safe and effective option for further studies [102]. This paved the way for studies to assess the efficacy of bacterins in the form of vaccines to control recurrent pyoderma. Bacterin vaccines containing suspensions of *Staphylococcal* strains, in combination with systemic antimicrobial treatments, reduced clinical scores and demonstrated improved or complete remission for the majority of canines in multiple studies [103–105]. This treatment combination showed no adverse side effects. The commercialisation of a bacterin vaccine known as Staphage Lysate (SPL)[®] has been a welcome addition to the new arsenal of treatment options for canine pyoderma. SPL is prepared by lysing cultures of *S. aureus* by *Staphylococcal* bacteriophages, followed by bacterial sterilisation [106]. One study found that SPL injections resulted in significant decreases in pruritus scores at weeks 12 and 23 of the treatment protocol [105]. Importantly, at the time of publication, no dogs from the study required follow-up antibiotics, indicating that the use of bacterins may prolong the recurrence of pyoderma and may reduce the frequency of antibiotics prescribed for recurrent pyoderma in the veterinary sector. However, this treatment may not offer a cure for recurring pyoderma infection caused by *S. pseudintermedius*.

A recent retrospective study analysed medical records from dogs that had received autogenous *Staphylococcus (pseud)intermedius* bacterin therapy for recurrent pyoderma that had not cleared in response to antibiotic therapy [107]. Bacterin therapy was administered subcutaneously to all dogs; however, the combined use of antimicrobials varied based on the veterinary surgeon's discretion. Results from this study indicated that prior to bacterin therapy, 77.3% of dogs had a diagnosed or suspected allergic skin infection, with 64.7% of these dogs prescribed glucocorticoids or antibiotics concurrently with bacterin therapy for the management of the allergic skin disease. Throughout the 24-month study period, alongside systemic antibiotics, 68% of dogs required topical antimicrobial therapy, 36% of dogs required chlorhexidine-based shampoos, and a further 27% of dogs received antibacterial wash solutions. No adverse side effects were reported throughout the bacterin therapy protocol despite the variations in combination therapies used. Importantly, following bacterin therapy, 23% of dogs did not require follow-up antibiotics, with the remainder of the dogs prescribed significantly fewer courses and shorter exposure periods of systemic antibiotic therapy. However, 59.3% of dogs did require at least one repeat dose of bacterin therapy, with 50% of dogs requiring the repeat within 13 weeks of the first treatment [107]. These results are important, as although the findings indicate that less systemic antibiotics were required following bacterin therapy, there was still a reliance on topical and wash-based antimicrobial therapy to control canine pyoderma. Another crucial point discussed in this study was whether resistance genes, particularly in the context of

MRSP strains, were destroyed during the production of bacterin therapeutics; therefore, further work is required to understand such factors [107].

It appears as though bacterin therapy is a safe and effective protocol in combination with alternative antimicrobial strategies for the management of *Staphylococcal* canine pyoderma; however, further development of this vaccine is required to release a product that will completely protect against pyoderma caused by *S. pseudintermedius*.

1.3.4.2 Subunit

Subunit vaccines generally consist of specific part(s) of the target pathogen that are highly antigenic—for example, polysaccharides or proteins—to elicit an immune response within the host [101]. Vaccines against *Staphylococcal* infections have proved hard to develop and generally do not elicit a protective immune response against *Staphylococcal* infections [108]. One of the bacterial components that contributes to virulence and has been explored in both *S. aureus* and *S. pseudintermedius* is the presence of a specific cell wall anchored (CWA) protein, *Staphylococcal protein A* (spA) [109]. The spA in *S. aureus* and the orthologue spsQ in *S. pseudintermedius* is secreted during the log phase of bacterial growth and has been shown to have an immunosuppressive role [110,111]. This is because spA binds to the Fc domain of immunoglobulin (Ig) G to block opsonophagocytic killing and interacts with the Fab domain of IgM, resulting in B-cell superantigen activity, thus allowing the *Staphylococcal* spp. to evade the host immune system [110,111]. Previous research has administered an altered form of spA of *S. aureus* in both mice and guinea pigs [112, 113]. Results show the production of antibodies that block the virulence of *S. aureus* and promote opsonophagocytic killing, therefore protecting the mice against challenge with a lethal concentration of methicillin-resistant *Staphylococcus aureus* (MRSA) [112,113]. As mentioned, *S. pseudintermedius* contains an orthologue of the spA protein, known as spsQ, and this cell wall protein is found in all clinical isolates of *S. pseudintermedius* [110]. Therefore, multiple research groups have explored the potential of protein A as a vaccine candidate for numerous *Staphylococcal* infections [110].

Currently, preliminary results show that canine IgG interacts with the cell wall protein of *S. pseudintermedius*, spsQ; however, this binding can be blocked by the presence of anti-protein A antibody, thus causing *S. pseudintermedius* to be more susceptible to phagocytosis [114]. Subsequently, when mutants of the spsQ were injected into clinically healthy dogs, there was a lowered toxic effect on canine B-cells, which resulted in a high titre of spsQ-specific antibodies which peaked 29 days after injection [115]. Therefore, the production of spsQ-specific antibodies may reduce immune suppression and establish a protective immunity against recurrent *S. pseudintermedius* infections. While results indicate that such vaccines against *S. pseudintermedius* are promising, it has been suggested that a *S. pseudintermedius* vaccine would likely contain additional virulence factor targets.

There is a lot of work still to be done on the subunit vaccine front in order to achieve a successful protective immune response against *S. pseudintermedius* infection in the canine. However, recent use of innovative approaches such as whole proteome and serological proteomic characterisation analysis on clinical isolates of *S. pseudintermedius* is yielding future potential targets for vaccine candidates.

1.4.4 Phage therapy

Phage therapy is a therapeutic application of interest due to its success in both human and animal clinical trials. Phage therapy involves the use of small viruses called bacteriophages to kill specific strains of bacteria and has potential as an alternative treatment option for canine pyoderma [116]. Bacterio(phages) were first described by Fredrick Twort in 1915 as ultra-microscopic filter-passing viruses [117]. Phages were subsequently isolated by Félix d'Hérelle in 1917, and d'Hérelle characterised the phages' ability to cease bacterial cell development, resulting in lysis of the bacterial host (on an invisible microbe antagonistic) [118]. With over 100 years of research, it is now well understood that phages are highly abundant, small viruses that infect and replicate within their bacterial host and, in some instances, cause bacterial lysis, as reviewed Gordillo Altamirano and Barr [119]. Phage therapy for clinical infections focuses on lytic phages as their life cycle results in bacterial cell lysis [120], as shown in **Figure 1.2**, and will, therefore, be the focus throughout this section of the review.

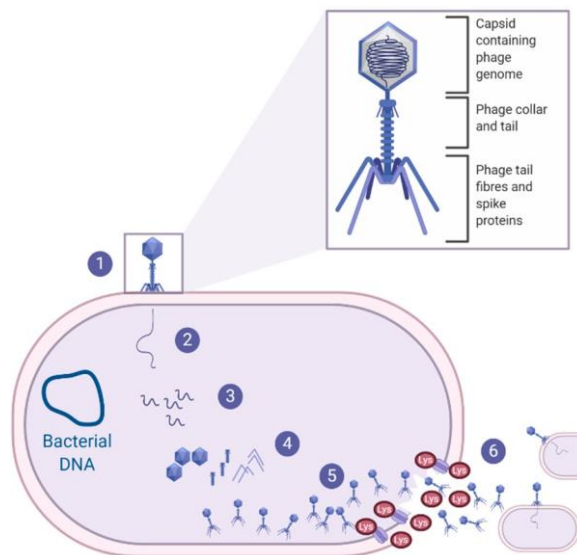


Figure 1.2 The lytic life cycle. Lytic bacteriophages undergo the lytic life cycle, which is initiated by (1) phage adsorption, in which the phage tail fibres recognise and attach to the bacterial outer membrane receptors. This results in an irreversible attachment of the phage to the bacterial surface which causes (2) the contraction of the phage tail sheaths to puncture the outer membrane and cell wall, allowing the phage genomic material to pass from the phage capsid to the bacterial cell via the phage tail. (3) The phage DNA is replicated using the bacterial host cell machinery and is subsequently (4) transcribed and translated into new viral components (e.g., capsid, tail, tail fibres). (5) Newly synthesised viral components will assemble to become mature virions which will secrete proteins known as holins and endolysins. (6) Holins will create a pore in the bacterial membrane, allowing the endolysins to pass through and degrade the peptidoglycan layer. This results in bacterial cell lysis, releasing hundreds of mature phage virions that will continue to infect and lyse neighbouring bacterial cells [119,120].

From a clinical perspective, phages are favourable as they are highly host specific. A recent in vitro study demonstrated that a phage cocktail was able to significantly reduce the levels of pathogenic *Escherichia coli* with no detectable impact on the six non-pathogenic *E. coli* species [121] compared to antibiotics that reduced all bacterial levels including

commensals [121]. This indicates that the use of phage therapy is less likely to disrupt the host's normal flora, thus reducing the likelihood of symbiosis or secondary infections, which is particularly important in the context of this review, as *S. pseudintermedius* is both a commensal bacterium and an opportunistic pathogen. In addition, phage therapy has been shown to be versatile and can be administered in the form of liquids, creams, aerosols, tablets and injections via numerous routes—for example, oral, subcutaneous and intravenous routes—depending on where the bacterial infection resides [122,123]. This is also important in the context of this review as infections caused by *S. pseudintermedius* occur in various regions of the body. Therefore, if the same phages could be used with altering formulations, this would significantly reduce barriers to the discovery and clinical development of new therapeutics for *S. pseudintermedius* canine infections.

There is significant research on phage therapy for human and animal infections with promising results; however, to the author's knowledge, there has only been one veterinary clinical trial of phage administration in dogs to date. This preliminary clinical trial explored the efficacy of a phage cocktail containing six lytic phages against OE (otitis externa) caused by *Pseudomonas aeruginosa* [124]. Treatment using the phage cocktail resulted in a 30.1% reduction in clinical scores in the 10 dogs after 48 h [124]. Importantly, there was also a 67% reduction in *P. aeruginosa* counts after 48 h, and a parallel increase in phage titres, with up to a 100-fold increase in four dogs treated with the phage cocktail [124]. This phenomenon of increasing phage titres after administration at the infection site is known as auto-dosing and is another advantageous attribute of phage therapy.

Whilst there are limited studies of phage therapy in canines specifically, there has been an increase in clinical data for phage therapy in humans. A recent review shows the versatility and success of phage therapy in humans against numerous infections at multiple niches [125]. While human data on phage therapy cannot be directly translated to animals, these data show the promising potential of phage therapy for the multiple infections caused by *S. pseudintermedius* in canines.

Given the previously mentioned benefits and promising results of phage therapy in humans and animal clinical trials, it is not surprising that research has begun exploring bacteriophages as an alternative therapy for canine infections caused by *S. pseudintermedius*. While there are 19 phages that target *S. pseudintermedius* in the National Center for Biotechnology Information (NCBI) database, as displayed in the supplementary material by Zeman and colleagues, there are currently limited studies understanding these *S. pseudintermedius* phages [126]. The first known study characterising *S. pseudintermedius*-specific phages was published by Moodley and colleagues, who isolated four phages from canine faeces that were shown to preferentially lyse MRSP [127]. This was mentioned as a favourable attribute for phage therapy as these bacteriophages showed lowered lytic activity on methicillin-sensitive *Staphylococcus pseudintermedius* (MSSP); therefore, these phages would be less likely to lyse commensal MSSP strains.

Azam and colleagues also described four phages specific against *S. pseudintermedius*, of which three of the four phages (ϕ SP120, ϕ SP197 and ϕ SP270) possessed a broad host range, as they showed strong infectivity activity against 95% of *S. pseudintermedius* strains, as well as moderate infectivity towards select coagulase-negative *Staphylococcal* (CoNS) species [128]. Whole-genome sequencing of these phages showed that there were no virulence, toxin or antibiotic-resistant genes present within the phage genomes, making them suitable candidates for phage therapy against *S. pseudintermedius* [128]. However,

one downfall of all currently isolated phages against *S. pseudintermedius* is the fact that they are all temperate phages, containing integrase (CI) and repressor (Cro) genes within their genome. These genes indicate that the phages are able to undergo the lysogenic life cycle, which is unfavorable for phage therapy due to a lack of reliable bacterial killing. As mentioned by Moodley and colleagues, to remove the lysogenic life cycle potential of the phages, *vir* mutants can be selected via spontaneous mutation or by genetic modifications [127]. Random mutagenesis protocols for *S. pseudintermedius* temperate phage have been attempted, however, with no success to date [129]. Therefore, more research is required in optimising a protocol for site-specific modifications of the temperate phage genome to remove the lysogeny module or, alternatively, the isolation of truly lytic *S. pseudintermedius* phages.

To address the issues associated with the current *S. pseudintermedius* phages, two recent independent studies have explored the potential use of lytic *Staphylococcus aureus* phages with broad host ranges against *S. pseudintermedius* isolates [128,130]. Results from both studies showed that while the *S. aureus* phages tested (ϕ SA039 and phiSA012) did possess a broad host range, able to infect *S. aureus*, *S. pseudintermedius*, *S. schleiferi* and CoNS, they both showed only weak to moderate infectivity towards *S. pseudintermedius* [128,130]. Therefore, further work is required to determine if the lytic activity of lytic *S. aureus* phages is sufficient enough to exploit their use in treating *S. pseudintermedius* canine infections. While phage therapy research has expanded, there are few clinical trials of phage therapy in companion animals, and as reviewed by Squires, there are numerous potential limitations that must be addressed to expand the use of phages as therapeutics [131]. In the context of canine pyoderma, it is important to understand the phage-resistant mechanisms and how this may impact the treatment of chronic or recurrent infections. Since it is known that pyoderma in dogs occurs due to underlying conditions, unless the underlying disease is well managed, the infection will recur, and it would be crucial to know whether the same phage formulation would be appropriate for re-treatment. Additional research is also required to assess the safety of using phages with a broad host range on the host flora and the potential infection of secondary opportunistic pathogens.

Interestingly, also within the realm of phage therapy, the use of endolysins as a novel antibacterial therapeutic has gained momentum, with studies assessing the potential of *Staphylococcal* endolysins against *S. pseudintermedius* canine pyoderma. As shown in **Figure 1.2**, endolysins are bacteriophage-encoded enzymes that are secreted and utilised by the mature phage at the end of the phage life cycle. Endolysins act to hydrolyse the peptidoglycan layer of the bacterial host from within, resulting in the destruction of the cell wall and the release of phage progeny, to infect neighboring target cells and continue the phage life cycle [132]. One study expressed and purified the lysin (Lys-phiSA012) from the previously mentioned phiSA012 phage, which had somewhat weak activity against *S. pseudintermedius*, whereas its endolysins, Lys-phiSA012, had clear lytic activity toward the *S. pseudintermedius* isolates [130]. Similarly, a secondary study also expressed and purified endolysins from another *Staphylococcal* phage (*Staphylococcus* phage K); the endolysins showed lytic activity against the various *Staphylococci* strains obtained from canine pyoderma lesions [133]. Due to the efficacy of the endolysin in vitro, preliminary clinical trials were conducted on canine pyoderma lesions that had been present for almost a year and were resistant to all antibiotics tested [133]. The selected endolysin was formulated into a hydrogel and applied directly to the canine pyoderma lesions twice a

day for 8 consecutive days. Results from the preliminary trial indicated that five out of the six dogs showed an 88–95% reduction in CFU of bacteria, with a subsequent reduction in redness and discharge from the lesion sites, and importantly, there were no allergic or adverse effects noted after 8 days of treatment [133]. This research highlights a novel contribution to an important issue of limited therapeutic availability; however, further work is necessary to characterise *S. pseudintermedius*-specific endolysins, to ensure that there are no off-target effects on the dogs' commensal flora.

1.5 Conclusions

During this review, we have shown that while *S. pseudintermedius* have been isolated from healthy canines as part of the normal flora, *S. pseudintermedius* is also associated with a multitude of moderate to severe infections in dogs, particularly canine pyoderma. While studies support that *S. pseudintermedius* is required for a healthy microbiota in dogs, there is limited research to understand whether commensal *S. pseudintermedius* prevents or contributes to infections or, if commensal strains are involved in disease, which factors result in their pathogenicity. It is important to explore the involvement of commensal strains in disease progression as this would likely influence the type of therapy required to treat *S. pseudintermedius* infections. Whilst the exact mechanisms of infection are not well defined, it is now well known that *S. pseudintermedius* infections in canines are frequent and are commonly treated with antibiotics, and the misuse and overuse of antibiotics contributes to the global increase in antibiotic resistance, particularly the rise in MRSP. Additionally, *S. pseudintermedius* can transmit between dogs, the environment and to humans, thus showing that the presence of *S. pseudintermedius* is an ever-growing problem which impacts the availability of treatment options available in both the veterinary and human sector. Importantly, although *S. pseudintermedius* can transmit from infected canines to healthy canines, in the majority of cases, *S. pseudintermedius* colonisation does not result in disease in the healthy canines; therefore, further research into the factors that are associated with *S. pseudintermedius* infections is essential in understanding how to control and treat this pathogenic bacterium. Recent research endeavors have presented the field with some promising areas for future treatment options that will hopefully address canine infections caused by antibiotic-resistant *S. pseudintermedius* moving forward.

Author Contributions: Both authors contributed to the conceptualization, writing, and reviewing of this manuscript. All authors have read and agreed to the published version of the manuscript.

Funding: This work was funded by The Canine Research Foundation.

Institutional Review Board Statement: Not applicable.

Informed Consent Statement: Not applicable.

Data Availability Statement: Not applicable.

Acknowledgments: The authors would like to acknowledge Kim Coyner, from the Dermatology Clinic for Animals, Washington, USA, for critical reading of the manuscript.

Conflicts of Interest: The authors declare no conflict of interest.

1.6 Literature review references

1. Bannoehr, J.; Guardabassi, L. *Staphylococcus pseudintermedius* in the dog: Taxonomy, diagnostics, ecology, epidemiology, and pathogenicity. *Vet. Dermatol.* **2012**, *23*, 253–266, e51-2. [[CrossRef](#)] [[PubMed](#)]
2. Ruscher, C.; Lübke-Becker, A.; Wleklinski, C.-G.; Soba, A.; Wieler, L.H.; Walther, B. Prevalence of Methicillin-resistant *Staphylococcus pseudintermedius* isolated from clinical samples of companion animals and equidae. *Vet. Microbiol.* **2009**, *136*, 197–201. [[CrossRef](#)] [[PubMed](#)]
3. Wegener, A.; Broens, E.M.; Zomer, A.; Spaninks, M.; Wagenaar, J.A.; Duim, B. Comparative genomics of phenotypic antimicrobial resistances in methicillin-resistant *Staphylococcus pseudintermedius* of canine origin. *Vet. Microbiol.* **2018**, *225*, 125–131. [[CrossRef](#)] [[PubMed](#)]
4. Worthing, K.A.; Abraham, S.; Coombs, G.W.; Pang, S.; Saputra, S.; Jordan, D.; Trott, D.J.; Norris, J.M. Clonal diversity, and geographic distribution of methicillin-resistant *Staphylococcus pseudintermedius* from Australian animals: Discovery of novel sequence types. *Vet. Microbiol.* **2018**, *213*, 58–65. [[CrossRef](#)] [[PubMed](#)]
5. Hajek, V. *Staphylococcus intermedius*, a new species isolated from animals. *Int. J. Syst. Evol. Microbiol.* **1976**, *26*, 401–408. [[CrossRef](#)]
6. Devriese, L.A.; Vancanneyt, M.; Baele, M.; Vaneechoutte, M.; De Graef, E.; Snauwaert, C.; Cleenwerck, I.; Dawyndt, P.; Swings, J.; Decostere, A. *Staphylococcus pseudintermedius* sp. nov., a coagulase-positive species from animals. *Int. J. Syst. Evol. Microbiol.* **2005**, *55*, 1569–1573. [[CrossRef](#)]
7. Sasaki, T.; Kikuchi, K.; Tanaka, Y.; Takahashi, N.; Kamata, S.; Hiramatsu, K. Reclassification of phenotypically identified *Staphylococcus intermedius* strains. *J. Clin. Microbiol.* **2007**, *45*, 2770–2778. [[CrossRef](#)]
8. Mališová, L.; Šafránková, R.; Kekláková, J.; Petráš, P.; Žemličková, H.; Jakubů, V. Correct species identification (reclassification in CNCTC) of strains of *Staphylococcus intermedius*-group can improve an insight into their evolutionary history. *Folia Microbiol.* **2019**, *64*, 231–236. [[CrossRef](#)]
9. Bannoehr, J.; Franco, A.; Iurescia, M.; Battisti, A.; Fitzgerald, J.R. Molecular diagnostic identification of *Staphylococcus pseudintermedius*. *J. Clin. Microbiol.* **2009**, *47*, 469–471. [[CrossRef](#)]
10. Sasaki, T.; Tsubakishita, S.; Tanaka, Y.; Sakusabe, A.; Ohtsuka, M.; Hirotaki, S.; Kawakami, T.; Fukata, T.; Hiramatsu, K. Multiplex-PCR method for species identification of coagulase-positive *Staphylococci*. *J. Clin. Microbiol.* **2010**, *48*, 765–769. [[CrossRef](#)]
11. Chrobak, D.; Kizerwetter-Świda, M.; Rzewuska, M.; Moodley, A.; Guardabassi, L.; Binek, M. Molecular characterization of *Staphylococcus pseudintermedius* strains isolated from clinical samples of animal origin. *Folia Microbiol.* **2011**, *56*, 415–422. [[CrossRef](#)] [[PubMed](#)]
12. Ma, G.C.; Worthing, K.A.; Ward, M.P.; Norris, J.M. Commensal *Staphylococci* Including Methicillin-Resistant *Staphylococcus aureus* from Dogs and Cats in Remote New South Wales, Australia. *Microb. Ecol.* **2020**, *79*, 164–174. [[CrossRef](#)] [[PubMed](#)]
13. Paul, N.C.; Bärghman, S.C.; Moodley, A.; Nielsen, S.S.; Guardabassi, L. *Staphylococcus pseudintermedius* colonization patterns and strain diversity in healthy

- dogs: A cross-sectional and longitudinal study. *Vet. Microbiol.* **2012**, *160*, 420–427. [[CrossRef](#)] [[PubMed](#)]
14. Iverson, S.A.; Brazil, A.M.; Ferguson, J.M.; Nelson, K.; Lautenbach, E.; Rankin, S.C.; Morris, D.O.; Davis, M.F. Anatomical patterns of colonization of pets with *Staphylococcal* species in homes of people with methicillin-resistant *Staphylococcus aureus* (MRSA) skin or soft tissue infection (SSTI). *Vet. Microbiol.* **2015**, *176*, 202–208. [[CrossRef](#)]
 15. van Duijkeren, E.; Catry, B.; Greko, C.; Moreno, M.A.; Pomba, M.C.; Pyörälä, S.; Ruzauskas, M.; Sanders, P.; Threlfall, E.J.; Torren-Edo, J.; et al. Review on methicillin-resistant *Staphylococcus pseudintermedius*. *J. Antimicrob. Chemother.* **2011**, *66*, 2705–2714. [[CrossRef](#)]
 16. Hartantyo, S.H.P.; Chau, M.L.; Fillon, L.; Ariff, A.Z.B.M.; Kang, J.S.L.; Aung, K.T.; Gutiérrez, R.A. Sick pets as potential reservoirs of antibiotic-resistant bacteria in Singapore. *Antimicrob. Resist. Infect. Control* **2018**, *7*, 106. [[CrossRef](#)]
 17. Laarhoven, L.M.; de Heus, P.; van Luijn, J.; Duim, B.; Wagenaar, J.A.; van Duijkeren, E. Longitudinal study on methicillin-resistant *Staphylococcus pseudintermedius* in households. *PLoS ONE* **2011**, *6*, e27788. [[CrossRef](#)]
 18. van Duijkeren, E.; Kamphuis, M.; van der Mije, I.C.; Laarhoven, L.M.; Duim, B.; Wagenaar, J.A.; Houwers, D.J. Transmission of methicillin-resistant *Staphylococcus pseudintermedius* between infected dogs and cats and contact pets, humans and the environment in households and veterinary clinics. *Vet. Microbiol.* **2011**, *150*, 338–343. [[CrossRef](#)]
 19. Windahl, U.; Gren, J.; Holst, B.S.; Börjesson, S. Colonization with methicillin-resistant *Staphylococcus pseudintermedius* in multi-dog households: A longitudinal study using whole genome sequencing. *Vet. Microbiol.* **2016**, *189*, 8–14. [[CrossRef](#)]
 20. Feßler, A.T.; Schuenemann, R.; Kadlec, K.; Hensel, V.; Brombach, J.; Murugaiyan, J.; Oechtering, G.; Burgener, I.A.; Schwarz, S. Methicillin-resistant *Staphylococcus aureus* (MRSA) and methicillin-resistant *Staphylococcus pseudintermedius* (MRSP) among employees and in the environment of a small animal hospital. *Vet. Microbiol.* **2018**, *221*, 153–158. [[CrossRef](#)]
 21. Loeffler, A.; Lloyd, D.H. What has changed in canine pyoderma? A narrative review. *Vet. J.* **2018**, *235*, 73–82. [[CrossRef](#)] [[PubMed](#)]
 22. Griffeth, G.C.; Morris, D.O.; Abraham, J.L.; Shofer, F.S.; Rankin, S.C. Screening for skin carriage of methicillin-resistant coagulase-positive *Staphylococci* and *Staphylococcus schleiferi* in dogs with healthy and inflamed skin. *Vet. Dermatol.* **2008**, *19*, 142–149. [[CrossRef](#)] [[PubMed](#)]
 23. Bryan, J.; Frank, L.A.; Rohrbach, B.W.; Burgette, L.J.; Cain, C.L.; Bemis, D.A. Treatment outcome of dogs with methicillin-resistant and methicillin-susceptible *Staphylococcus pseudintermedius* pyoderma. *Vet. Dermatol.* **2012**, *23*, 361–e65. [[CrossRef](#)]
 24. Huerta, B.; Maldonado, A.; Ginel, P.J.; Tarradas, C.; Gómez-Gascón, L.; Astorga, R.J.; Luque, I. Risk factors associated with the antimicrobial resistance of *Staphylococci* in canine pyoderma. *Vet. Microbiol.* **2011**, *150*, 302–308. [[CrossRef](#)] [[PubMed](#)]
 25. Yoo, J.-H.; Yoon, J.W.; Lee, S.-Y.; Park, H.-M. High prevalence of Fluoroquinolone- and Methicillin-resistant *Staphylococcus pseudintermedius* isolates from canine pyoderma and otitis externa in veterinary teaching hospital. *J. Microbiol. Biotechnol.* **2010**, *20*, 798–802.
 26. Fazakerley, J.; Williams, N.; Carter, S.; McEwan, N.; Nuttall, T. Heterogeneity of

- Staphylococcus pseudintermedius* isolates from atopic and healthy dogs. *Vet. Dermatol.* **2010**, *21*, 578–585. [[CrossRef](#)]
27. Shimizu, A.; Berkhoff, H.A.; Kloos, W.E.; George, C.G.; Ballard, D.N. Genomic DNA fingerprinting, using pulsed-field gel electrophoresis, of *Staphylococcus intermedius* isolated from dogs. *Am. J. Vet. Res.* **1996**, *57*, 1458–1462.
 28. Hesselbarth, J.; Witte, W.; Cuny, C.; Rohde, R.; Amtsberg, G. Characterization of *Staphylococcus intermedius* from healthy dogs and cases of superficial pyoderma by DNA restriction endonuclease patterns. *Vet. Microbiol.* **1994**, *41*, 259–266. [[CrossRef](#)]
 29. Wang, Y.; Yang, J.; Logue, C.M.; Liu, K.; Cao, X.; Zhang, W.; Shen, J.; Wu, C. Methicillin-resistant *Staphylococcus pseudintermedius* isolated from canine pyoderma in North China. *J. Appl. Microbiol.* **2012**, *112*, 623–630. [[CrossRef](#)]
 30. Pires Dos Santos, T.; Damborg, P.; Moodley, A.; Guardabassi, L. Systematic Review on Global Epidemiology of Methicillin- Resistant *Staphylococcus pseudintermedius*: Inference of Population Structure from Multilocus Sequence Typing Data. *Front. Microbiol.* **2016**, *7*, 1599. [[CrossRef](#)] [[PubMed](#)]
 31. Hensel, N.; Zabel, S.; Hensel, P. Prior antibacterial drug exposure in dogs with methicillin-resistant *Staphylococcus pseudintermedius* (MRSP) pyoderma. *Vet. Dermatol.* **2016**, *27*, 72-e20. [[CrossRef](#)]
 32. Dziva, F.; Wint, C.; Auguste, T.; Heeraman, C.; Dacon, C.; Yu, P.; Koma, L.M. First identification of methicillin-resistant *Staphylococcus pseudintermedius* strains among coagulase-positive staphylococci isolated from dogs with otitis externa in Trinidad, West Indies. *Infect. Ecol. Epidemiol.* **2015**, *5*, 29170. [[CrossRef](#)] [[PubMed](#)]
 33. Lyskova, P.; Vydrzalova, M.; Mazurova, J. Identification and antimicrobial susceptibility of bacteria and yeasts isolated from healthy dogs and dogs with otitis externa. *J. Vet. Med. A Physiol. Pathol. Clin. Med.* **2007**, *54*, 559–563. [[CrossRef](#)] [[PubMed](#)]
 34. Bugden, D.L. Identification, and antibiotic susceptibility of bacterial isolates from dogs with otitis externa in Australia. *Aust. Vet. J.* **2013**, *91*, 43–46. [[CrossRef](#)] [[PubMed](#)]
 35. Paterson, S. Discovering the causes of otitis externa. *Practice* **2016**, *38*, 7–11. [[CrossRef](#)]
 36. Zur, G.; Lifshitz, B.; Bdolah-Abram, T. The association between the signalment, common causes of canine otitis externa and pathogens. *J. Small Anim. Pract.* **2011**, *52*, 254–258. [[CrossRef](#)]
 37. Saridomichelakis, M.N.; Farmaki, R.; Leontides, L.S.; Koutinas, A.F. Aetiology of canine otitis externa: A retrospective study of 100 cases. *Vet. Dermatol.* **2007**, *18*, 341–347. [[CrossRef](#)]
 38. Ngo, J.; Taminiau, B.; Fall, P.A.; Daube, G.; Fontaine, J. Ear canal microbiota—A comparison between healthy dogs and atopic dogs without clinical signs of otitis externa. *Vet. Dermatol.* **2018**, *29*, 425-e140. [[CrossRef](#)]
 39. Zur, G.; Gurevich, B.; Elad, D. Prior antimicrobial use as a risk factor for resistance in selected *Staphylococcus pseudintermedius* isolates from the skin and ears of dogs. *Vet. Dermatol.* **2016**, *27*, 468-e125. [[CrossRef](#)]
 40. Perry, L.R.; MacLennan, B.; Korven, R.; Rawlings, T.A. Epidemiological study of dogs with otitis externa in Cape Breton, Nova Scotia. *Can. Vet. J.* **2017**, *58*, 168–174.
 41. Chan, W.Y.; Hickey, E.E.; Khazandi, M.; Page, S.W.; Trott, D.J.; Hill, P.B. In vitro antimicrobial activity of narasin against common clinical isolates associated with canine otitis externa. *Vet. Dermatol.* **2018**, *29*, 149-e57. [[CrossRef](#)] [[PubMed](#)]
 42. Sim, J.X.F.; Khazandi, M.; Chan, W.Y.; Trott, D.J.; Deo, P. Antimicrobial activity of

- thyme oil, oregano oil, thymol and carvacrol against sensitive and resistant microbial isolates from dogs with otitis externa. *Vet. Dermatol.* **2019**, *30*, 524-e159. [[CrossRef](#)] [[PubMed](#)]
43. Petrov, V.; Zhelev, G.; Marutsov, P.; Koev, K.; Georgieva, S.; Toneva, I.; Urumova, V. Microbiological and antibacterial resistance profile in canine otitis externa—A comparative analysis. *Bulg. J. Vet. Med.* **2019**, *22*, 447–456. [[CrossRef](#)]
 44. Roberts, M.; White, J.; Lam, A. Prevalence of bacteria and changes in trends in antimicrobial resistance of *Escherichia coli* isolated from positive canine urinary samples from an Australian referral hospital over a 5-year period (2013–2017). *Vet. Rec. Open* **2019**, *6*, e000345. [[CrossRef](#)]
 45. Windahl, U.; Holst, B.S.; Nyman, A.; Grönlund, U.; Bengtsson, B. Characterisation of bacterial growth and antimicrobial susceptibility patterns in canine urinary tract infections. *BMC Vet. Res.* **2014**, *10*, 217. [[CrossRef](#)]
 46. Penna, B.; Vargas, R.; Martins, R.; Martins, G.; Lilenbaum, W. In vitro antimicrobial resistance of *Staphylococci* isolated from canine urinary tract infection. *Can. Vet. J.* **2010**, *51*, 738–742.
 47. Ling, G.V.; Norris, C.R.; Franti, C.E.; Eisele, P.H.; Johnson, D.L.; Ruby, A.L.; Jang, S.S. Interrelations of organism prevalence, specimen collection method, and host age, sex, and breed among 8,354 canine urinary tract infections (1969–1995). *J. Vet. Intern. Med.* **2001**, *15*, 341–347.
 48. Gatoria, I.S.; Saini, N.S.; Rai, T.S.; Dwivedi, P.N. Comparison of three techniques for the diagnosis of urinary tract infections in dogs with urolithiasis. *J. Small Anim. Pract.* **2006**, *47*, 727–732. [[CrossRef](#)]
 49. Ball, K.R.; Rubin, J.E.; Chirino-Trejo, M.; Dowling, P.M. Antimicrobial resistance and prevalence of canine uropathogens at the Western College of Veterinary Medicine Veterinary Teaching Hospital, 2002–2007. *Can. Vet. J.* **2008**, *49*, 985–990.
 50. Hoekstra, K.A.; Paulton, R.J.L. Clinical prevalence and antimicrobial susceptibility of *Staphylococcus aureus* and *Staph. intermedius* in dogs. *J. Appl. Microbiol.* **2002**, *93*, 406–413. [[CrossRef](#)]
 51. Waki, M.F.; Kogika, M.M.; Wirthl, V.A.B.F.; Oyafuso, M.K.; Prosser, C.S.; Monteiro, P.R.; Coelho, B.P.; Simões, D.M.N.; Kanayama, K.K. Association of urinary tract infection with urolithiasis in dogs. *Clín. Vet.* **2009**, *14*, 130–131.
 52. Marques, C.; Belas, A.; Franco, A.; Aboim, C.; Gama, L.T.; Pomba, C. Increase in antimicrobial resistance and emergence of major international high-risk clonal lineages in dogs and cats with urinary tract infection: 16 year retrospective study. *J. Antimicrob. Chemother.* **2018**, *73*, 377–384. [[CrossRef](#)]
 53. Marques, C.; Gama, L.T.; Belas, A.; Bergström, K.; Beurlet, S.; Briend-Marchal, A.; Broens, E.M.; Costa, M.; Criel, D.; Damborg, P.; et al. European multicenter study on antimicrobial resistance in bacteria isolated from companion animal urinary tract infections. *BMC Vet. Res.* **2016**, *12*, 213. [[CrossRef](#)]
 54. Rubin, J.E.; Gaunt, M.C. Urinary tract infection caused by methicillin-resistant *Staphylococcus pseudintermedius* in a dog. *Can. Vet. J.* **2011**, *52*, 162.
 55. Hutchins, R.G.; Vaden, S.L.; Jacob, M.E.; Harris, T.L.; Bowles, K.D.; Wood, M.W.; Bailey, C.S. Vaginal microbiota of spayed dogs with or without recurrent urinary tract infections. *J. Vet. Intern. Med.* **2014**, *28*, 300–304. [[CrossRef](#)]
 56. Moyaert, H.; de Jong, A.; Simjee, S.; Rose, M.; Youala, M.; El Garch, F.; Vila, T.; Klein, U.; Rzewuska, M.; Morrissey, I. Survey of antimicrobial susceptibility of bacterial pathogens isolated from dogs and cats with respiratory tract infections in Europe:

- ComPath results. *J. Appl. Microbiol.* **2019**, *127*, 29–46. [[CrossRef](#)]
57. Kalhor, D.H.; Gao, S.; Kalhor, M.S. *Staphylococcus pseudintermedius* isolation from canine, bacterial colonization, and clinical picture in balb/c mouse model. *JAPS J. Anim. Plant Sci.* **2017**, *27*, 422–429.
 58. Proulx, A.; Hume, D.Z.; Drobatz, K.J.; Reineke, E.L. In vitro bacterial isolate susceptibility to empirically selected antimicrobials in 111 dogs with bacterial pneumonia. *J. Vet. Emerg. Crit. Care* **2014**, *24*, 194–200. [[CrossRef](#)]
 59. Vientós-Plotts, A.I.; Ericsson, A.C.; Rindt, H.; Reiner, C.R. Respiratory Dysbiosis in Canine Bacterial Pneumonia: Standard Culture vs. Microbiome Sequencing. *Front. Vet. Sci.* **2019**, *6*, 354. [[CrossRef](#)]
 60. Morrissey, I.; Moyaert, H.; de Jong, A.; El Garch, F.; Klein, U.; Ludwig, C.; Thiry, J.; Youala, M. Antimicrobial susceptibility monitoring of bacterial pathogens isolated from respiratory tract infections in dogs and cats across Europe: ComPath results. *Vet. Microbiol.* **2016**, *191*, 44–51. [[CrossRef](#)]
 61. Kalhor, D.H.; Gao, S.; Xie, X.; Liang, S.; Luo, S.; Zhao, Y.; Liu, Y. Canine influenza virus coinfection with *Staphylococcus pseudintermedius* enhances bacterial colonization, virus load and clinical presentation in mice. *BMC Vet. Res.* **2016**, *12*, 87. [[CrossRef](#)]
 62. Qekwana, D.N.; Naidoo, V.; Oguttu, J.W.; Odoi, A. Occurrence and Predictors of Bacterial Respiratory Tract Infections and Antimicrobial Resistance Among Isolates From Dogs Presented With Lower Respiratory Tract Infections at a Referral Veterinary Hospital in South Africa. *Front. Vet. Sci.* **2020**, *7*, 304. [[CrossRef](#)]
 63. Rheinwald, M.; Hartmann, K.; Hähner, M.; Wolf, G.; Straubinger, R.K.; Schulz, B. Antibiotic susceptibility of bacterial isolates from 502 dogs with respiratory signs. *Vet. Rec.* **2015**, *176*, 357. [[CrossRef](#)]
 64. Dear, J.D. Bacterial pneumonia in dogs and cats. *Vet. Clin. N. Am. Small Anim. Pract.* **2014**, *44*, 143–159.
 65. Lappin, M.R.; Blondeau, J.; Boothe, D.; Breitschwerdt, E.B.; Guardabassi, L.; Lloyd, D.H.; Papich, M.G.; Rankin, S.C.; Sykes, J.E.; Turnidge, J.; et al. Antimicrobial use Guidelines for Treatment of Respiratory Tract Disease in Dogs and Cats: Antimicrobial Guidelines Working Group of the International Society for Companion Animal Infectious Diseases. *J. Vet. Intern. Med.* **2017**, *31*, 279–294. [[CrossRef](#)]
 66. Rota, A.; Milani, C.; Drigo, I.; Drigo, M.; Corrà, M. Isolation of methicillin-resistant *Staphylococcus pseudintermedius* from breeding dogs. *Theriogenology* **2011**, *75*, 115–121. [[CrossRef](#)]
 67. Zakošek Pipan, M.; Kajdič, L.; Kalin, A.; Plavec, T.; Zdovc, I. Do newborn puppies have their own microbiota at birth? Influence of type of birth on newborn puppy microbiota. *Theriogenology* **2020**, *152*, 18–28. [[CrossRef](#)]
 68. Saijonmaa-Koulumies, L.E.; Lloyd, D.H. Colonization of neonatal puppies by *Staphylococcus intermedius*. *Vet. Dermatol.* **2002**, *13*, 123–130. [[CrossRef](#)]
 69. Rota, A.; Corrà, M.; Drigo, I.; Bortolami, A.; Börjesson, S. Isolation of coagulase-positive *Staphylococci* from bitches' colostrum and milk and genetic typing of methicillin-resistant *Staphylococcus pseudintermedius* strains. *BMC Vet. Res.* **2015**, *11*, 160. [[CrossRef](#)]
 70. Maluping, R.P.; Paul, N.C.; Moodley, A. Antimicrobial susceptibility of methicillin-resistant *Staphylococcus pseudintermedius* isolated from veterinary clinical cases in the UK. *Br. J. Biomed. Sci.* **2014**, *71*, 55–57. [[CrossRef](#)]

71. Vasiu, I.; Dąbrowski, R.; Martinez-Subiela, S.; Ceron, J.J.; Wdowiak, A.; Pop, R.A.; Brudașcă, F.G.; Pastor, J.; Tvarijonaviciute, A. Milk C-reactive protein in canine mastitis. *Vet. Immunol. Immunopathol.* **2017**, *186*, 41–44. [[CrossRef](#)]
72. Ververidis, H.N.; Mavrogianni, V.S.; Fragkou, I.A.; Orfanou, D.C.; Gougoulis, D.A.; Tzivara, A.; Gouletsou, P.G.; Athanasiou, L.; Boscos, C.M.; Fthenakis, G.C. Experimental *Staphylococcal* mastitis in bitches: Clinical, bacteriological, cytological, haematological, and pathological features. *Vet. Microbiol.* **2007**, *124*, 95–106. [[CrossRef](#)]
73. Ros, L.; Holst, B.S.; Hagman, R. A retrospective study of bitches with pyometra, medically treated with aglepristone. *Theriogenology* **2014**, *82*, 1281–1286. [[CrossRef](#)]
74. Hagman, R. Pyometra in Small Animals. *Vet. Clin. N. Am. Small Anim. Pract.* **2018**, *48*, 639–661.
75. Robaj, A.; Sylejmani, I.; Hamidi, A. Occurrence and antimicrobial susceptibility of bacterial agents of canine pyometra. *Indian J. Anim. Res.* **2018**, *52*, 394–400.
76. Pilla, R.; Bonura, C.; Malvisi, M.; Snel, G.G.M.; Piccinini, R. Methicillin-resistant *Staphylococcus pseudintermedius* as causative agent of dairy cow mastitis. *Vet. Rec.* **2013**, *173*, 19. [[CrossRef](#)]
77. Paul, N.C.; Damborg, P.; Guardabassi, L. Dam-to-offspring transmission and persistence of *Staphylococcus pseudintermedius* clones within dog families. *Vet. Dermatol.* **2014**, *25*, 3-e2. [[CrossRef](#)]
78. Saijonmaa-Koulumies, L.E.M.; Myllys, V.; Lloyd, D.H. Diversity, and stability of the *Staphylococcus intermedius* flora in three bitches and their puppies. *Epidemiol. Infect.* **2003**, *131*, 931–937. [[CrossRef](#)]
79. Latronico, F.; Moodley, A.; D'Abramo, M.; Greco, M.F.; Corrente, M.; Guardabassi, L. Outbreak of methicillin-resistant *Staphylococcus pseudintermedius* in a litter of puppies: Evidence of vertical perinatal and horizontal transmission. In Proceedings of the ASM Conference on Methicillin-Resistant *Staphylococci* in Animals, London, UK, 22–25 September 2009; Volume 76.
80. Milani, C.; Corrà, M.; Drigo, M.; Rota, A. Antimicrobial resistance in bacteria from breeding dogs housed in kennels with differing neonatal mortality and use of antibiotics. *Theriogenology* **2012**, *78*, 1321–1328. [[CrossRef](#)]
81. Meloni, T.; Martino, P.A.; Grieco, V.; Pisu, M.C.; Banco, B.; Rota, A.; Veronesi, M.C. A survey on bacterial involvement in neonatal mortality in dogs. *Vet. Ital.* **2014**, *50*, 293–299.
82. Pipan, M.Z.; Švara, T.; Zdovc, I.; Papić, B.; Avberšek, J.; Kušar, D.; Mrkun, J. *Staphylococcus pseudintermedius* septicemia in puppies after elective cesarean section: Confirmed transmission via dam's milk. *BMC Vet. Res.* **2019**, *15*, 41.
83. Ogbu, K.I.; Ochai, S.O.; Danladi, M.M.A.; Abdullateef, M.H.; Agwu, E.O.; Gyengdeng, J.G. A review of Neonatal mortality in Dogs. *Int. J. Life Sci.* **2016**, *4*, 451–460.
84. Hillier, A.; Lloyd, D.H.; Scott Weese, J.; Blondeau, J.M.; Boothe, D.; Breitschwerdt, E.; Guardabassi, L.; Papich, M.G.; Rankin, S.; Turnidge, J.D.; et al. Guidelines for the diagnosis and antimicrobial therapy of canine superficial bacterial folliculitis (Antimicrobial Guidelines Working Group of the International Society for Companion Animal Infectious Diseases). *Vet. Dermatol.* **2014**, *25*, 163-e43. [[CrossRef](#)]
85. Summers, J.F.; Hendricks, A.; Brodbelt, D.C. Prescribing practices of primary-care veterinary practitioners in dogs diagnosed with bacterial pyoderma. *BMC Vet. Res.* **2014**, *10*, 240. [[CrossRef](#)]

86. Ungemach, F.R.; Müller-Bahrddt, D.; Abraham, G. Guidelines for prudent use of antimicrobials and their implications on antibiotic usage in veterinary medicine. *Int. J. Med. Microbiol.* **2006**, 296 (Suppl. 41), 33–38. [[CrossRef](#)]
87. Stegemann, M.R.; Passmore, C.A.; Sherington, J.; Lindeman, C.J.; Papp, G.; Weigel, D.J.; Skogerboe, T.L. Antimicrobial activity and spectrum of cefovecin, a new extended-spectrum cephalosporin, against pathogens collected from dogs and cats in Europe and North America. *Antimicrob. Agents Chemother.* **2006**, 50, 2286–2292. [[CrossRef](#)]
88. Stegemann, M.R.; Coati, N.; Passmore, C.A.; Sherington, J. Clinical efficacy and safety of cefovecin in the treatment of canine pyoderma and wound infections. *J. Small Anim. Pract.* **2007**, 48, 378–386. [[CrossRef](#)]
89. Maaland, M.; Guardabassi, L. In vitro antimicrobial activity of nitrofurantoin against *Escherichia coli* and *Staphylococcus pseudintermedius* isolated from dogs and cats. *Vet. Microbiol.* **2011**, 151, 396–399. [[CrossRef](#)]
90. Şentürk, S.; Özel, E.; Şen, A. Clinical efficacy of rifampicin for treatment of canine pyoderma. *Acta Vet. Brno* **2005**, 74, 117–122. [[CrossRef](#)]
91. Blondeau, J.M.; Fitch, S.D. In vitro killing of canine strains of *Staphylococcus pseudintermedius* and *Escherichia coli* by cefazolin, cefovecin, doxycycline and pradofloxacin over a range of bacterial densities. *Vet. Dermatol.* **2020**, 31, 187. [[CrossRef](#)]
92. Morris, D.O.; Loeffler, A.; Davis, M.F.; Guardabassi, L.; Weese, J.S. Recommendations for approaches to meticillin-resistant *Staphylococcal* infections of small animals: Diagnosis, therapeutic considerations, and preventative measures. Clinical Consensus Guidelines of the World Association for Veterinary Dermatology. *Vet. Dermatol.* **2017**, 28, 304–e69. [[CrossRef](#)]
93. Mueller, R.S.; Bergvall, K.; Bensignor, E.; Bond, R. A review of topical therapy for skin infections with bacteria and yeast. *Vet. Dermatol.* **2012**, 23, 330–341.e62. [[CrossRef](#)]
94. Nuttall, T. Topical therapy in canine atopic dermatitis: New products. *Companion Anim.* **2020**, 25, 76–82. [[CrossRef](#)]
95. Fadok, V.A.; Irwin, K. Sodium Hypochlorite/Salicylic Acid Shampoo for Treatment of Canine *Staphylococcal* Pyoderma. *J. Am. Anim. Hosp. Assoc.* **2019**, 55, 117–123. [[CrossRef](#)] [[PubMed](#)]
96. Loeffler, A.; Cobb, M.A.; Bond, R. Comparison of a chlorhexidine and a benzoyl peroxide shampoo as sole treatment in canine superficial pyoderma. *Vet. Rec.* **2011**, 169, 249. [[CrossRef](#)] [[PubMed](#)]
97. Murayama, N.; Nagata, M.; Terada, Y.; Shibata, S.; Fukata, T. Efficacy of a surgical scrub including 2% chlorhexidine acetate for canine superficial pyoderma. *Vet. Dermatol.* **2010**, 21, 586–592. [[CrossRef](#)] [[PubMed](#)]
98. Borio, S.; Colombo, S.; La Rosa, G.; De Lucia, M.; Damborg, P.; Guardabassi, L. Effectiveness of a combined (4% chlorhexidine digluconate shampoo and solution) protocol in MRS and non-MRS canine superficial pyoderma: A randomized, blinded, antibiotic-controlled study. *Vet. Dermatol.* **2015**, 26, 339–344.e72. [[CrossRef](#)] [[PubMed](#)]
99. Ramos, S.J.; Woodward, M.; Hoppers, S.M.; Liu, C.-C.; Pucheu-Haston, C.M.; Mitchell, M.S. Residual antibacterial activity of canine hair treated with five mousse products against *Staphylococcus pseudintermedius* in vitro. *Vet. Dermatol.* **2019**, 30, 183–e57. [[CrossRef](#)]
100. Kloos, I.; Straubinger, R.K.; Werckenthin, C.; Mueller, R.S. Residual antibacterial

- activity of dog hairs after therapy with antimicrobial shampoos. *Vet. Dermatol.* **2013**, 24, 250–e54. [CrossRef]
101. Jorge, S.; Dellagostin, O.A. The development of veterinary vaccines: A review of traditional methods and modern biotechnology approaches. *Biotechnol. Res. Innov.* **2017**, 1, 6–13. [CrossRef]
 102. Chambers, E.D.; Severin, G.A. Staphylococcal bacterin for treatment of chronic *Staphylococcal blepharitis* in the dog. *J. Am. Vet. Med. Assoc.* **1984**, 185, 422–425.
 103. DeBoer, D.J.; Moriello, K.A.; Thomas, C.B.; Schultz, K.T. Evaluation of a commercial *Staphylococcal* bacterin for management of idiopathic recurrent superficial pyoderma in dogs. *Am. J. Vet. Res.* **1990**, 51, 636–639.
 104. Curtis, C.F.; Lamport, A.I.; Lloyd, D.H. Masked, controlled study to investigate the efficacy of a *Staphylococcus intermedius* autogenous bacterin for the control of canine idiopathic recurrent superficial pyoderma. *Vet. Dermatol.* **2006**, 17, 163–168. [CrossRef]
 105. Borku, M.K.; Ozkanlar, Y.; Hanedan, B.; Duru, S.Y. Efficacy of *Staphylococcal* bacterin for treatment of canine re-current pyoderma: An open clinical trial. *Revue de Médecine Vétérinaire* **2007**, 158, 234.
 106. Staphage Lysate (SPL). Available online: <https://www.drugs.com/vet/staphage-lysate-spl.html> (accessed on 4 January 2021).
 107. Wilson, A.; Allers, N.; Lloyd, D.H.; Bond, R.; Loeffler, A. Reduced antimicrobial prescribing during autogenous staphylococcal bacterin therapy: A retrospective study in dogs with pyoderma. *Vet. Rec.* **2019**, 184, 739. [CrossRef]
 108. Thamavongsa, V.; Kim, H.K.; Missiakas, D.; Schneewind, O. *Staphylococcal* manipulation of host immune responses. *Nat. Rev. Microbiol.* **2015**, 13, 529–543. [CrossRef]
 109. Grandolfo, E. Looking through *Staphylococcus pseudintermedius* infections: Could SpA be considered a possible vaccine target? *Virulence* **2018**, 9, 703–706. [CrossRef]
 110. Abouelkhair, M.A.; Bemis, D.A.; Kania, S.A. Characterization of recombinant wild-type and nontoxigenic protein A from *Staphylococcus pseudintermedius*. *Virulence* **2018**, 9, 1050–1061. [CrossRef]
 111. Votintseva, A.A.; Fung, R.; Miller, R.R.; Knox, K.; Godwin, H.; Wyllie, D.H.; Bowden, R.; Crook, D.W.; Walker, A.S. Prevalence of *Staphylococcus aureus* protein A (spa) mutants in the community and hospitals in Oxfordshire. *BMC Microbiol.* **2014**, 14, 63. [CrossRef]
 112. Kim, H.K.; Cheng, A.G.; Kim, H.-Y.; Missiakas, D.M.; Schneewind, O. Nontoxigenic protein A vaccine for methicillin-resistant *Staphylococcus aureus* infections in mice. *J. Exp. Med.* **2010**, 207, 1863–1870. [CrossRef]
 113. Kim, H.K.; Falugi, F.; Thomer, L.; Missiakas, D.M.; Schneewind, O. Protein A suppresses immune responses during *Staphylococcus aureus* bloodstream infection in guinea pigs. *MBio* **2015**, 6. [CrossRef]
 114. Balachandran, M.; Bemis, D.A.; Kania, S.A. Expression and function of protein A in *Staphylococcus pseudintermedius*. *Virulence* **2018**, 9, 390–401. [CrossRef]
 115. Schiebel, J.; Chang, A.; Lu, H.; Baxter, M.V.; Tonge, P.J.; Kisker, C. *Staphylococcus aureus* FabI: Inhibition, substrate recognition, and potential implications for in vivo essentiality. *Structure* **2012**, 20, 802–813. [CrossRef]
 116. El-Shibiny, A.; El-Sahhar, S. Bacteriophages: The possible solution to treat infections caused by pathogenic bacteria. *Can. J. Microbiol.* **2017**, 63, 865–879.

[CrossRef]

117. Twort, F.W. An investigation on the nature of ultra-microscopic viruses. *Lancet* **1915**, 186, 1241–1243. [CrossRef]
118. D'Herelle, M.F. On an invisible microbe antagonistic to dysentery bacilli. Note by M. F. d'Herelle, presented by M. Roux. *Comptes Rendus Academie des Sciences* **1917**; 165:373–5. *Bacteriophage* **2011**, 1, 3–5.
119. Gordillo Altamirano, F.L.; Barr, J.J. Phage Therapy in the Postantibiotic Era. *Clin. Microbiol. Rev.* **2019**, 32. [CrossRef]
120. Rakhuba, D.V.; Kolomiets, E.I.; Dey, E.S.; Novik, G.I. Bacteriophage receptors, mechanisms of phage adsorption and penetration into host cell. *Pol. J. Microbiol.* **2010**, 59, 145–155. [CrossRef]
121. Cieplak, T.; Soffer, N.; Sulakvelidze, A.; Nielsen, D.S. A bacteriophage cocktail targeting *Escherichia coli* reduces *E. coli* in simulated gut conditions, while preserving a non-targeted representative commensal normal microbiota. *Gut Microbes* **2018**, 9, 391–399.
122. Malik, D.J.; Sokolov, I.J.; Vinner, G.K.; Mancuso, F.; Cinquerrui, S.; Vladislavljivic, G.T.; Clokie, M.R.J.; Garton, N.J.; Stapley, A.G.F.; Kirpichnikova, A. Formulation, stabilisation, and encapsulation of bacteriophage for phage therapy. *Adv. Colloid Interface Sci.* **2017**, 249, 100–133. [CrossRef]
123. Ryan, E.M.; Gorman, S.P.; Donnelly, R.F.; Gilmore, B.F. Recent advances in bacteriophage therapy: How delivery routes, formulation, concentration, and timing influence the success of phage therapy. *J. Pharm. Pharmacol.* **2011**, 63, 1253–1264. [CrossRef] [PubMed]
124. Hawkins, C.; Harper, D.; Burch, D.; Anggård, E.; Soothill, J. Topical treatment of *Pseudomonas aeruginosa* otitis of dogs with a bacteriophage mixture: A before/after clinical trial. *Vet. Microbiol.* **2010**, 146, 309–313. [CrossRef] [PubMed]
125. McCallin, S.; Sacher, J.C.; Zheng, J.; Chan, B.K. Current State of Compassionate Phage Therapy. *Viruses* **2019**, 11, 343. [CrossRef] [PubMed]
126. Zeman, M.; Bárdy, P.; Vrbovska, V.; Roudnický, P.; Zdráhal, Z.; Růžicková, V.; Doškař, J.; Pantůček, R. New Genus Fibrilongavirus in Siphoviridae Phages of *Staphylococcus pseudintermedius*. *Viruses* **2019**, 11, 1143. [CrossRef]
127. Moodley, A.; Kot, W.; Nälgård, S.; Jakociune, D.; Neve, H.; Hansen, L.H.; Guardabassi, L.; Vogensen, F.K. Isolation and characterization of bacteriophages active against methicillin-resistant *Staphylococcus pseudintermedius*. *Res. Vet. Sci.* **2019**, 122, 81–85. [CrossRef]
128. Azam, A.H.; Kadoi, K.; Miyanaga, K.; Usui, M.; Tamura, Y.; Cui, L.; Tanji, Y. Analysis host-recognition mechanism of staphylococcal kayvirus ϕ SA039 reveals a novel strategy that protects *Staphylococcus aureus* against infection by *Staphylococcus pseudintermedius* Siphoviridae phages. *Appl. Microbiol. Biotechnol.* **2019**, 103, 6809–6823. [CrossRef]
129. Breteau, M. Study of *Staphylococcus pseudintermedius* Phages: Towards the Development of Phage Therapy. Ph.D. Thesis, University of Warwick, Coventry, UK, 2016.
130. Nakamura, T.; Kitana, J.; Fujiki, J.; Takase, M.; Iyori, K.; Simoike, K.; Iwano, H. Lytic Activity of Polyvalent *Staphylococcal* Bacteriophage PhiSA012 and Its Endolysin Lys-PhiSA012 Against Antibiotic-Resistant *Staphylococcal* Clinical Isolates From Canine Skin Infection Sites. *Front. Med.* **2020**, 7, 234. [CrossRef]
131. Squires, R.A. Bacteriophage therapy for management of bacterial infections in veterinary practice: What was once old is new again. *N. Z. Vet. J.* **2018**, 66, 229–235.

[[CrossRef](#)]

132. Schmelcher, M.; Donovan, D.M.; Loessner, M.J. Bacteriophage endolysins as novel antimicrobials. *Future Microbiol.* **2012**, *7*, 1147–1171. [[CrossRef](#)]
133. Junjappa, R.P.; Desai, S.N.; Roy, P.; Narasimhaswamy, N.; Raj, J.R.M.; Durgaiah, M.; Vipra, A.; Bhat, U.R.; Satyanarayana, S.K.; Shankara, N.; et al. Efficacy of anti-staphylococcal protein P128 for the treatment of canine pyoderma: Potential applications. *Vet. Res. Commun.* **2013**, *37*, 217–228. [[CrossRef](#)]

Chapter 2

This chapter provides the materials and methods used in experiments to produce this thesis

2.1 Media sterilisation

The media used throughout this study were autoclaved at 121 kPa at 120 °C for 15 min unless specified otherwise.

2.2 Bacterial culture

2.2.1 Collection of bacterial strains

Sixty *Staphylococcus pseudintermedius* strains were kindly gifted by Marc Marenda and Rhys Bushell from Melbourne University Veterinary Centre, Werribee. The isolation of the bacterial strains and the subsequent biochemical, 16s sequencing and resistance profiling of the isolates were performed at Melbourne University and are listed in **Table 2.1**. The antibiotic sensitivity profiling was performed by collaborators, as described previously ¹. The sixty isolates were provided from a larger database based on varying antibiotic resistance profiles and source of infection.

Table 2.1 Sixty clinical isolates of *S. pseudintermedius* collected from canine infections. An isolate identifier was assigned to each isolate, denoted by the year of isolation. The source and antibiotic sensitivity were recorded for each isolate, the tested antibiotics included: Penicillin (PEN), Augmentin (Amc), Cephalexin (CL), Sulfafurazole (SF), Trimethoprim (W), Tetracycline (Te), Enrofloxacin (Enr). R = Resistant, S= Sensitive, - = not tested. All isolates were kindly gifted by M. Marenda from Melbourne University Veterinary Centre.

Isolate identifier	Source	Antibiotic resistant/sensitive profiles							Owner
		Pen	Amc	CL	SF	W	Te	Enr	
CM2017-0410	Skin	R	R	R	R	R	R	R	M. Marenda
CM2016-0933	Musco-skeletal	R	R	R	S	R	R	R	M. Marenda
CM2012-0529	Musco-skeletal	R	R	R	S	R	S	R	M. Marenda
CM2012-0654	Skin	R	R	R	S	R	S	R	M. Marenda
CM2012-0745	Respiratory	R	R	R	S	R	S	R	M. Marenda
CM2013-0059	Respiratory	R	R	R	S	R	S	R	M. Marenda
CM2016-0920	Ear	R	R	R	S	R	S	R	M. Marenda
CM2017-0272	Musco-skeletal	R	R	R	S	R	S	R	M. Marenda
CM2017-0292	Skin	R	R	R	S	R	S	R	M. Marenda
CM2016-0889	Skin	R	S	-	S	-	R	R	M. Marenda
CM2016-0917	Urinary	R	S	R	S	-	R	R	M. Marenda
CM2015-0460	Urinary	R	S	R	S	R	R	S	M. Marenda
CM2016-0471	Ear	R	S	S	R	R	R	R	M. Marenda
CM2009-0471	Musco-skeletal	R	S	S	R	R	R	S	M. Marenda
CM2012-0093	Ear	R	S	S	R	R	R	S	M. Marenda
CM2017-0973	Urinary	R	S	S	R	R	R	S	M. Marenda
CM2009-0886	Urinary	R	S	S	R	S	R	S	M. Marenda
CM2015-0031	Musco-skeletal	R	S	S	R	S	R	S	M. Marenda
CM2015-0597	Ear	R	S	S	R	S	R	S	M. Marenda
CM2013-0255	Skin	R	S	S	S	R	R	S	M. Marenda
CM2013-0910	Urinary	R	S	S	S	R	R	S	M. Marenda
CM2015-0965	Urinary	R	S	S	S	R	R	S	M. Marenda
CM2015-1096	Musco-skeletal	R	S	S	S	R	R	S	M. Marenda
CM2011-0112	Urinary	S	S	S	R	R	R	S	M. Marenda

CM2013-0351	Urinary	S	S	S	R	R	R	S	M. Marenda
CM2011-0195	Respiratory	S	S	S	S	R	S	S	M. Marenda
CM2012-0247	Urinary	S	S	S	S	R	S	S	M. Marenda
CM2014-0677	Urinary	S	S	S	S	R	S	S	M. Marenda
CM2016-0937	Urinary	R	S	S	S	R	S	R	M. Marenda
CM2017-0713	Urinary	S	S	S	S	R	S	S	M. Marenda
CM2009-0754	Urinary	S	S	S	S	S	S	S	M. Marenda
CM2009-0925	Skin	S	S	S	S	S	S	S	M. Marenda
CM2011-0079	Respiratory	S	S	S	S	S	S	S	M. Marenda
CM2011-0097	Skin	S	S	S	S	S	S	S	M. Marenda
CM2011-0132	Skin	S	S	S	S	S	S	S	M. Marenda
CM2011-0460	Skin	S	S	S	S	S	S	S	M. Marenda
CM2011-0653	Skin	S	S	S	S	S	S	S	M. Marenda
CM2011-0669	Ear	S	S	S	S	S	S	S	M. Marenda
CM2011-0671	Skin	S	S	S	S	S	S	S	M. Marenda
CM2012-0111	Skin	S	S	S	S	S	S	S	M. Marenda
CM2012-0169	Urinary	S	S	S	S	S	S	S	M. Marenda
CM2012-0193	Reproductive	S	S	S	S	S	S	S	M. Marenda
CM2012-0201	Urinary	S	S	S	S	S	S	S	M. Marenda
CM2012-0405	Skin	S	S	S	S	S	S	S	M. Marenda
CM2012-0503	Skin	S	S	S	S	S	S	S	M. Marenda
CM2012-0550	Skin	S	S	S	S	S	S	S	M. Marenda
CM2013-0140	Skin	S	S	S	S	S	S	S	M. Marenda
CM2013-0320	Skin	S	S	S	S	S	S	S	M. Marenda
CM2016-0216	Skin	S	S	S	S	S	S	S	M. Marenda
CM2016-0262	Urinary	S	S	S	S	S	S	S	M. Marenda
CM2016-0568	Urinary	S	S	S	S	S	S	S	M. Marenda
CM2016-0674	Skin	S	S	S	S	S	S	S	M. Marenda
CM2016-0689	Skin	S	S	S	S	S	S	S	M. Marenda
CM2016-1113	Skin	S	S	S	S	S	S	S	M. Marenda
CM2017-0472	Ear	S	S	S	S	S	S	S	M. Marenda

CM2017-0580	Urinary	S	S	S	S	S	S	S	M. Marenda
CM2015-0358	Urinary	S	S	S	S	S	S	S	M. Marenda
CM2016-1008	Urinary	R	S	S	S	R	S	R	M. Marenda
CM2013-0596	Urinary	S	S	S	S	S	S	S	M. Marenda
CM2013-0367	Skin	S	S	S	S	S	S	S	M. Marenda

2.2.2 Culture and storage of bacterial strains

S. pseudintermedius isolates were cultivated on Nutrient Agar (NA; 3.5% (w/v) Blood Agar Base, Oxoid + 0.5% (w/v) Yeast Extract, BD Bacto™ via a streak plate method, and incubated at 37 °C overnight (~18 hrs). Broth cultures were grown by suspending one colony from NA into 5 mL Tryptic Soya Broth (TSB; 6.0% (w/v) Tryptic Soya Broth, BD™) and incubated overnight at 37 °C with shaking at 200 rpm. For short-term storage (<2 days), strains were stored on NA plates at 4 °C. For long-term preservation, isolates were stored at -80 °C in cryotubes (1 mL broth culture + 20% v/v glycerol).

2.2.3 Gram stain of bacterial cultures

Gram staining was used to determine the Gram reaction of the isolated bacteria as preliminary analysis. A bacterial colony from sample agar plates was spread across a microscope slide with dH₂O and allowed to dry. The smear was heat fixed by passing the slide through the flame 3 times. The cells were treated as per **Figure 2.1**. Following the last dH₂O rinse, slides were dried and viewed under 100 x magnification with oil immersion on a light microscope (OLYMPUS).

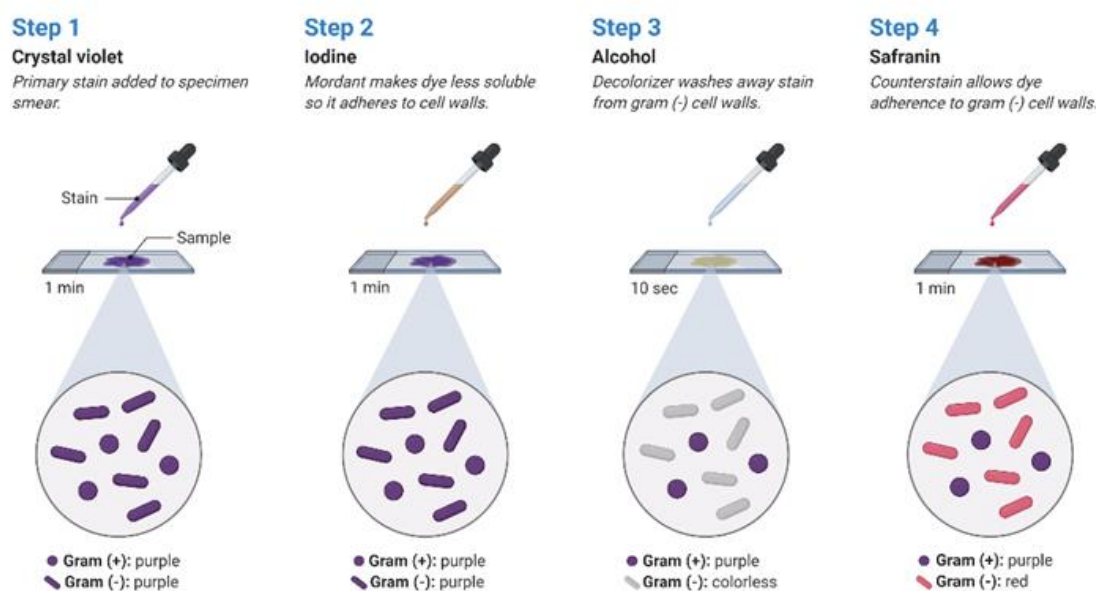


Figure 2.1 Gram stain protocol for bacteria. Downloaded from BioRender.

2.2.4 Growth curve of *Staphylococcus pseudintermedius*

2.2.4.1 Manual growth curve

An overnight culture of the *S. pseudintermedius* strain CM16-089 was created using methods described in **Section 2.2.2** Culture and storage of bacterial strains. From the overnight culture, 1 mL was suspended in 50 mL of sterile TSB within a 250 mL flask, incubated at 37 °C with shaking at 200 rpm. 1 mL aliquots were collected from the flask culture every 0.5 hrs to measure the turbidity (OD₆₀₀). The aliquot used to measure the turbidity was serially diluted (1:10), plated on sterile NA and incubated overnight. Following incubation, the colony forming units per millilitre (CFU/mL) was calculated using the following calculation:

$$CFU = \frac{\text{Colonies counted} \times \text{dilution plate the colonies were counted on}}{\text{Volume of diluted bacterial culture plated}}$$

2.2.4.2 Plate reader turbidity growth curve

An overnight culture of the *S. pseudintermedius* strain CM16-089 was created using methods described in **Section 2.2.2** Culture and storage of bacterial strains. From the overnight culture, 1 mL was suspended in 50 mL of sterile TSB within a 250 mL flask, incubated at 37 °C with shaking at 200 rpm. After 3 hrs of growth, the cell suspension was diluted to achieve 1.25 x 10⁶ CFU/50 µL. From this diluted bacterial culture (1.25 x 10⁶ CFU/50 µL), 50 µL was added to each well of a Corning™ 48- well COSTAR microplate and the plate was sealed using iQ Optical QUALTAPE. Using the CLARIOstar microplate reader (BMG LABTECH, VIC, Australia), the turbidity (OD₆₀₀) was read every 5 minutes for 12 hrs. Typical assay conditions used were as follows: discrete wavelength reading of 600 nm; orbital averaging (6 mm); 80 read cycles of 300 sec; orbital shaking at 200 rpm; at a temperature of 37 °C. Absorbance readings were transmitted from the plate reader to a computer and stored as an Excel spreadsheet. The Excel spreadsheet provided raw data values for absorbance (OD₆₀₀) vs. time (hrs), or averaged absorbance (OD₆₀₀) for a set of triplicate samples vs. time (hrs). GraphPad Prism 8.0 was used to plot absorbance vs. time to produce a growth curve.

2.3 Bacteriophage screening

2.3.1 Collection and processing of samples used for phage screening

2.3.1.1 Collection and processing of soil and water samples for phage screening

A total of nine water samples and eight soil samples were collected from different locations of Eastern Victoria as shown in **Figure 2.2**. As alluded to by Hyman, 2019, due to the nature of bacteriophages, and their reliance on their bacterial host, phages usually reside where the bacterial host resides ². Therefore, the locations below were chosen as dogs are known to frequently visit these areas and thus the soil and water may contain phages against the dog specific pathogen, *S. pseudintermedius*.

Soil and water samples were collected and processed as previously described ^{3,4}. Briefly, approximately 200 g of soil was collected and stored within a 50 mL falcon tube, at room temperature (RT) for less than 24 hrs prior to laboratory processing. 50 g of soil was suspended in 50 mL of TSB within a 250 mL flask and gently swirled at 100 rpm on an orbital shaker for 24 hrs, to dissolve the soil and release potential phage. Dissolved soil samples were then centrifuged at 4,000 x g for 20 minutes to remove large particulates, the supernatant was filtered through 0.45 µm syringe filter and stored short-term at 4 °C for subsequent phage screening. For the water samples, approximately 50 mL of water was collected and stored at room temperature (RT) for less than 24 hrs prior to laboratory processing. Water samples were centrifuged at 4,000 x g, filtered through 0.45 µm syringe filter and stored short-term at 4 °C for subsequent phage screening.

Sample location	Sample type
A	River water
A	River bank water
A	Stagnant water
A	Soil from river bank
A	Soil from walking track
B	Stagnant water near dog area
B	River water
B	Soil from river bank
B	Lake water
B	Soil from lake bank
B	Soil from dog walking track
B	Main lake water
B	Soil from main dog track
C	Pond water
C	Deeper pond water
C	Soil from pond bank
C	Soil from dog track

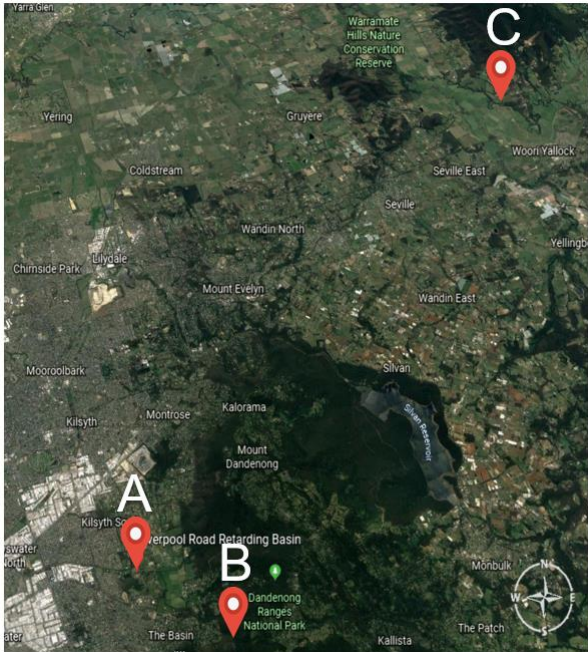


Figure 2.2 List of environmental samples collected for phage screening. Sample type and locations are listed for each collection. ((A) Liverpool Retarding Basin, Kilsyth. (B) Wicks Reserve, Doongalla. (C) Yarra River, Eltham.

2.3.1.2 Collection and processing of animal-associated samples for phage screening

A total of 32 specimens were collected from healthy privately-owned animals (**Table 2.2**), whose owners voluntarily swabbed various areas of their pet in accordance with ethics **AEC19043**. Swabs were pre-moistened in PBS prior to being run along the surface of the animal, then stored in 1 mL of PBS and sent to La Trobe University for processing. Swabs were incubated in 5 mL PBS at RT on a rotating wheel to elude the potential phages from the swab into the PBS. The PBS solution was then centrifuged at 4,000 x g for 15 mins, filtered through 0.45 µm syringe filter and stored short-term at 4 °C for subsequent phage screening.

Table 2.2 De-identified samples collected from privately-owned animals for phage screening.

De-identified sample code	Animal	Age of animal	Sample source
DK15W	Dog	15 weeks	Fur around mouth
CM2	Cat	2 years old	Fur around mouth
DJ11	Dog	11 years old	Nostrils
DJ112	Dog	11 years old	Backside
CM2	Cat	2 years old	Ear canal
CS3	Cat	3 years old	Backside
CS31	Cat	3 years old	Armpit
DJ113	Dog	11 years old	Ear canal
DS9	Dog	9 years old	Armpit
DS91	Dog	9 years old	Nostrils
CS32	Cat	3 years old	Nostrils
DS5	Dog	5 years old	Armpit
DS92	Dog	9 years old	Nostrils
DS93	Dog	9 years old	Fur around mouth
DS51	Dog	5 years old	Fur around mouth
DK15W1	Dog	15 weeks	Ear canal
CS33	Cat	3 years old	Fur around mouth
DS52	Dog	5 years old	Backside
DK15W2	Dog	15 weeks	Backside
DS94	Dog	9 years old	Fur on back
DS53	Dog	5 years old	Nostril
CM21	Cat	2 years old	Nostril
CM22	Cat	2 years old	Fur around mouth
DK15W3	Dog	15 weeks old	Nostril
DJ114	Dog	11 years old	Fur on back
DS54	Dog	5 years old	Nostril
CC3	Cat	3 years old	Ear canal
CC31	Cat	3 years old	Nostril
DL2	Dog	2 years old	Ear canal
DL21	Dog	2 years old	Nostril
CC32	Dog	3 years old	Fur on back
DL22	Dog	2 years old	Armpit

2.3.2 Sample enrichment for phage screening

Strains of *S. pseudintermedius* were grown to exponential phase using methods described in **Section**

2.2.2 Culture and storage of bacterial strains. 1 mL of each bacterial culture at exponential phase was added into a 250 mL flask which contained: 25 mL of sterile TSB, 10 mmol/L CaCl₂ and MgCl₂ and 2 mL of phage sample (soil, water, or dog-associated sample). The flask was incubated at 37 °C stationary for 1 hr to allow for the attachment of potential phage, then incubated at 37 °C, shaking at 150 rpm for 48 hrs, to allow for the enrichment of phages. Phage enrichments were then

centrifuged at 4,000 x g for 15 min, filtered through a 0.45 µm filter and stored at 4 °C for subsequent phage isolation.

2.3.3 Plating for phage plaque isolation

The 60 strains of *S. pseudintermedius* were streaked as a bacterial lawn on NA, then 10 µL of the phage enrichments from **Section 2.3.2** Sample enrichment for phage screening were spotted onto each bacterial lawn and allowed to dry. The plates were then incubated at 37 °C overnight to allow for bacterial growth and potential plaque development. After 18 hrs, the plates were examined for plaque formation, indicative of potential phage isolation.

2.3.4 Isolation of phages

If plaques were present from the spot method in **Section 2.3.3** Plating for phage plaque isolation, a single plaque was extracted from the agar using a pipette, transferred into 500 µL of TSB and vortexed to elute the bacteriophages into the broth. The phage suspensions were centrifuged at 15,000 x g for 10 min and the supernatant was serially diluted. 100 µL of phage suspension, was added to 100 µL of *S. pseudintermedius* and 4 mL of molten agar (2/3 (v/v) NA + 1/3 (v/v) TSB). The molten agar containing the phage and bacterial culture was poured over a sterile NA plate, allowed to dry, before incubating at 37 °C overnight to allow for bacterial growth and potential plaque development.

2.3.5 Propagation of phages

Phage propagation as performed as described by Kutter & Sulakvelidze, 2005, with minor adjustments ⁵. 100 µL of bacterial culture, was added to 200 µL of phage stock at appropriate titre and 4 mL of molten agar (2/3 (v/v) NA + 1/3 (v/v) TSB). The mixture was poured and spread evenly onto NA then incubated at 37 °C overnight. Plates with lacy plaque formation were scraped into 10 mL of sterile TSB, vortexed to elude the phage into the broth, centrifuged at 4,000 x g for 15 min and filtered through 0.45 µm syringe filter.

2.3.6 Titration of phages

Phage stocks were serially diluted (1:10) down to appropriate dilutions, spotted onto a bacterial lawn plate and incubated overnight. Plaques were counted the next day to determine the titre in Plaque Forming Units per mL (PFU/mL) using the following calculation:

$$PFU = \frac{\text{Plaques counted} \times \text{dilution plate the colonies were counted on}}{\text{Volume of diluted phage sample plated}}$$

2.4 Characterisation of isolated phages

2.4.1 Genomic DNA extraction and quantification from isolated phages

To extract DNA from isolated phages, 1 mL of isolated phage filtrate was digested with DNase and RNase to a final concentration of 10 µg mL⁻¹ with the addition of MgCl₂ to a concentration of 5 mM and incubated at room temperature (RT) for 30 min. 0.06 g of NaCl with 0.1 g PEG 8000 was added to the solution, mixed by inversion, then allowed to precipitate overnight at 4 °C. Following precipitation, the solution was centrifuged for 15 min at 13,000 x g and supernatant was discarded. Pellets were resuspended into 100 µL of TE buffer with the addition of; 4 µL 0.5 M EDTA, 5 µL 10% (w/v) SDS and 5 µl of 50 µg ml⁻¹ of Proteinase K. Solution was mixed by inversion, incubated at 55 °C for 1 h then left to cool to RT. 120 µL of phenol: chloroform: isoamyl alcohol (29:28:1) was added to the mixture and vortexed at 2 sec intervals until the mixture became cloudy. Mixture was centrifuged at 13,400 x g for 3 min and the top transparent aqueous solution was promptly transferred to a fresh Eppendorf tube. 110 µL of isopropanol was added, inverted, and incubated at RT for 30 min. Centrifugation at 13,400 x g for 10 min was undertaken, followed by removal of supernatant. A subsequent brief centrifugation at 16,000 x g to remove final supernatant was followed by a wash step of the pellet with 200 µl of 70% (v/v) ethanol. This solution was finally centrifuged at 16,000 x g for 5 min and supernatant was thoroughly removed. To remove any residual ethanol, tubes were placed in a Savant DNA 120 speedvac (Thermo scientific) for 5 min. Lastly, the dried pellet was resuspended into 50 µL of DH20 and stored at 4 °C.

2.4.2 Next generation sequencing (NGS) of phage DNA

2.4.2.1 Tagmentation of genomic DNA

Reagents used for tagmentation were obtained from Illumina and therefore not listed in Appendix I. These reagents were added to a PCR plate and included; 10 µL tagmented DNA buffer; 5 µL gDNA; 5 µl amplicon tagmented mix, all reagents were mixed by pipetting then subjected to an oscillating platform for 1 min. This PCR plate was placed in a thermocycler for 5 cycles at 55 °C to facilitate DNA tagmentation. To neutralise this process, 5 µL of neutralise tagmented buffer was applied to the PCR plate, mixed by pipetting, and placed on the oscillating platform for 1 min, then incubated at RT for 5 min.

2.4.2.2 Tagmented DNA amplification

5 µL of index primers were added to each well of the PCR plate, along with 15 µL of Nextera PCR mix, the contents were mixed by pipetting and placed on an oscillating platform for 1 min. Followed by thermocycler conditions listed in **Table 2.3**.

Table 2.3 Thermocycle conditions for amplification of tagmented DNA.

Temperature	Time	Cycles
72 °C	3 min	-
95 °C	30 sec	-
95 °C	10 sec	10
55 °C	30 sec	-
72 °C	30 sec	-
72 °C	5 min	∞

2.4.2.3 Clean-up of DNA libraries

The PCR plate with amplified tagmented DNA was placed on an oscillating plate for 1 min. 50 µL of the PCR product was added to a fresh PCR plate with the addition of 30 µl of AMPure XP beads and oscillated for 2 min. The PCR plate was incubated at RT for 5 min, placed on a magnetic stand until the solution turned clear (~ 2 min), then the supernatant was removed from each well. Two wash steps involved 200 µL of 80% ethanol for 30 sec, final supernatant was removed, and the plate was left to air dry for 15 min.

2.4.2.4 DNA library check

1 µl of each undiluted DNA library was quantified by Agilent Technology Tapestation to determine the concentration.

2.4.2.5 Pooling of DNA library

DNA libraries were placed on an oscillating plate for 1 min then 3 ng of each library was added to one microcentrifuge to pool the libraries.

2.4.2.6 Normalisation of DNA libraries

5 µl of the pooled DNA library was converted to a fresh microcentrifuge tube with the addition of 5 µl freshly diluted 0.2 M NaOH, which was vortexed, incubated at RT for 5 min and centrifuged for 1 min. Added to the solution was 990 µL of hybridisation buffer, then added to the denatured library to result in a concentration of 20 pM ml⁻¹. From this, 15 pM of the DNA libraries was subjected to NGS. The normalised DNA libraries were sequenced using a Miseq® V2 reagent kit (300 cycles) on an Illumina MiSeq® as 150 bp paired end reads.

2.4.2.7 Assembly and annotation of phage contigs

De novo assembly of phage genomes was undertaken using reads from WGS were used as an input into SPAdes (version 3.5.0) using default settings to assemble the reads and produce contigs⁶. The contig outputs from SPAdes were manually investigated to extract contigs of high coverage and contigs of a size expected for *S. pseudintermedius* phages. Selected contigs were compared to other genomes in the BLAST database using BLASTn⁷. Putative ORFs of the selected contigs were predicted using the GLIMMER-3 tool in Geneious 10.2.2⁸, and the protein sequence for each predicted ORF was queried by BLASTp⁷. From BLASTp search results, putative gene functions were assigned to ORFs manually. Following genome annotation, ORFs were assigned a colour based on gene function using SnapGene software (from Insightful Science; available at snapgene.com), to visualise the annotated phage genomes.

2.4.3 Host range analysis

The host range of isolated phages were initially tested using a plate spot method, similarly, described to **Section 2.3.3** Plating for phage plaque isolation. Briefly, all four phages were diluted

to the same titre (1×10^7) prior to host range testing. A bacterial lawn was created for all 60 *S. pseudintermedius* isolates and 10 µl of filtered phage enrichment was spotted onto the bacterial lawn and allowed to dry. Plates were then incubated at 37 °C overnight to allow for bacterial growth and potential plaque development. Plates were examined for plaque formation, indicative of phage lysis. Lytic activity was scored from -, +, ++, +++, based on spectrum of lysis.

2.4.4 Growth kinetics of phage

A sub-culture of *S. pseudintermedius* was grown by suspending 150 µL of overnight culture into 15 mL of sterile TSB, as specified in **Section 2.2.2** Culture and storage of bacterial strains. Following 1 hr of bacterial growth, 500 µL of phage was added, to achieve an MOI 1.0 ($\sim 1.25 \times 10^6$ CFU/mL of bacteria and $\sim 1.25 \times 10^6$ PFU/mL of phage). The bacteria and phage co-culture were incubated at 37 °C (static) for 10 mins, to allow phage absorption. Following absorption, 1 mL aliquots were taken every 30 minutes, which were first measured for turbidity (OD_{600}). From the 1 mL aliquot used to measure turbidity, 100 µL was serially diluted and plated on NA to quantify the CFU/mL. Another 100 µL from the 1 mL aliquot was centrifuged at 1,000 x g for 5 mins, serially diluted, and plated onto a bacterial lawn of *S. pseudintermedius* to quantify the PFU/mL. Lastly, a final 100 µL from the 1 mL aliquot was pipetted onto a glass microscope slide, covered with a cover slip, and imaged using a Nikon TiE inverted fluorescence microscope to calculate bacterial cell counts. The PFU/mL and CFU/mL was calculated after incubating the plates overnight at 37 °C and counting the phage plaques or bacterial colonies, respectively.

2.4.5 Turbidity reduction assay

Sample preparation of the microplate was set up according to protocols listed in **Section**

2.2.4.2 Plate reader turbidity growth *curve*. Briefly, 50 µL of *S. pseudintermedius* was added to all wells (except blank and negative control), and 50 µL of the phage preps were added to designated

wells at a MOI of 0.1, 1 or 10. The wells were topped up to 500 μ L using sterile TSB. Each condition was performed in triplicate. Turbidity (OD₆₀₀) was read every 5 mins for a total of 12 hrs.

2.4.6 Transmission Electron Microscopy (TEM) of phage particles

Prior to deposition of isolated phage on the EM grids, formvar-carbon coated EM grids were placed into the Emitech K950X Glow Discharge unit, with a 20 mA current applied, to create a hydrophilic surface on the carbon grid. 5 μ l of phage sample was deposited onto the carbon grid for 30 seconds to allow absorption, excess phage was removed by absorption onto 3 MM filter paper and rinsed with 5 μ l of MilliQ water. Subsequently, 3 μ l of 2% uranyl acetate (UA) was pipetted onto the EM grid, and excess UA was removed by absorption onto 3 MM filter paper, this was repeated a total of three times. EM grids were air dried for 15 mins prior to loading into Jeol JEM 2100 transmission electron microscope. Samples were imaged at 40, 000 – 50, 000 x magnification.

2.4.7 Induction of temperate phages from *Staphylococcus pseudintermedius* using Mitomycin-C

To induce prophage from the phage host propagation strain to explore the prophage contamination of our phage preps, 100 μ L of the host strain (CM16-0689) was added to 5 mL of TSB and incubated for 1.5 hrs at 37 °C, shaking at 180 rpm. After 1.5 hrs of growth, 0.5 μ g/mL of Mitomycin-C was added to the culture and the culture was incubated for 3 hrs at 37 °C, shaking at 180 rpm. The culture was then centrifuged for 10 mins at 5,000 x g and the supernatant was filtered through 0.45 μ m syringe filter and spotted on a bacterial host lawn to determine the presence of induced temperate phages.

2.6 Bioinformatic analysis of *Staphylococcus pseudintermedius* endolysins

2.6.1 Computational screening of endolysins within *S. pseudintermedius* phage genomes

From NCBI and our local library of phage genomes sequenced during this thesis, the whole genome sequence of all known *S. pseudintermedius* phage genomes were identified, and their genome was imported into Geneious. The whole genome sequence of all 25 *S. pseudintermedius* phages were

uploaded onto the Geneious bioinformatic platform, and their genomes were screened for the presence of endolysin genes, by searching key gene terms; lysin, autolysin, amidase, lys, and aminidase. If any genes matched the key search terms, their protein sequence was extracted and protein homology was performed by aligning the amino acid sequences of all identified endolysin genes using [Clustal Omega](https://www.geneious.com)⁹ and the Mauve tool on Geneious Prime 2021.10.2.2 (<https://www.geneious.com>). Following alignment, unique endolysin-like genes were selected and submitted to Bioneer Pacific (South Korea) for cloning into the expression vector pET-28a. The recombinant plasmids were transformed into competent *E. coli* (BL21 derivative) cells for subsequent protein expression, according to manufacturer's instructions.

2.7 Expression and purification of endolysins

E. coli cells containing the endolysin encoding plasmid were cultured in LB medium containing 50 µg/mL of kanamycin to exponential phase (0.4 - 0.6 OD₆₀₀). Protein expression was induced by the addition of isopropyl-beta-D-thiogalactopyranoside (IPTG) to a final concentration of 0.5 mM, then incubated overnight at 21 °C shaking at 200 rpm. Cells were harvested by centrifugation at 4,000 x g for 20 mins, and supernatant was discarded. The cell pellets were resuspended in lysis buffer (50 mM NaH₂PO₄, 300 mM NaCl, 10 mM imidazole) and stored at -20 °C overnight. The thawed bacterial cells were disrupted by sonication and centrifuged at 20,000 x g for 20 mins. For Ni-affinity purification of the recombinant proteins, 1.5 mL of Ni-NTA beads were added to the column and equilibrated with 10 mL lysis buffer (50mM NaH₂PO₄, 300mM NaCl, 10mM imidazole). Following equilibration, the protein suspension was run over the Ni-NTA beads at a flow rate of 1 mL/min, and the flowthrough was collected (labelled "flow through"). The column and Ni-NTA beads were then washed with 50 mL wash buffer (50mM NaH₂PO₄, 300mM NaCl, 30mM imidazole) and the flowthrough was collected (labelled "wash"). Finally, the column and Ni-NTA beads were washed with 5 mL elution buffer (50mM NaH₂PO₄, 300mM NaCl, 300mM imidazole) and flowthrough was collected (labelled "elution"). The eluted proteins were dialysed against Phosphate Buffer Solution (PBS) via Amicon Ultra-15 10K Centrifugal Filter Unit (10 kDa

molecular weight cut off; Merck Millipore). Purity and concentration were determined via SDS-PAGE and Qubit™ Protein Assay Kit (Invitrogen, Australia).

2.8 Characterisation of selected endolysins

2.8.1 Analysis of domain architecture

The amino acid sequence of the six selected endolysins was uploaded in FASTA format to InterPro 86.0¹⁰. The InterPro Search results were used to determine the predicted domains and the overall molecular function of each of the six endolysin genes selected.

2.8.2 Host range analysis of selected endolysins

The lytic ability and spectrum of the six purified endolysins was initially tested similarly to the plate spotting method in **Section 2.4.3** Host range analysis. Briefly, a bacterial lawn was created for all 60 *S. pseudintermedius* isolates and 10 µl of the six purified endolysins (2 µg/µL) was spotted onto the bacterial lawn and allowed to dry. Plates were then incubated at 37 °C overnight to allow for bacterial lysis. Plates were examined for zones of clearing, indicative of potential bacterial lysis attributed to endolysin enzymatic activity. Lytic activity was scored from -, +, ++, +++, based on spectrum of lysis.

2.8.3 *In silico* analysis of 3D protein modelling

The amino acid sequences of the six selected endolysins were run through Phyre2 to obtain PDB files¹¹. PDB files were run through PyMOL2 (Version 2.5, open-source foundation: <https://pymol.org/2/>) to visualise and analyse the protein model¹². The 3D modelling was based on proteins of similar structure, and further analysis was conducted by looking specifically at the conserved residues between our protein of interest and the closest homolog to our protein.

2.8.4 Turbidity reduction assay of candidate endolysin

Sample preparation of the microplate was set up according to protocols listed in **Section**

2.2.4.2 Plate reader turbidity growth *curve*. Briefly, 50 μL of *S. pseudintermedius* was added to all wells (except blank and negative control), and 50 μL of the endolysin prep was added to designated wells at concentrations of 1.25 μg , 2.5 μg , 5 μg , 10 μg , 20 μg , 50 μg and 100 μg . The wells were topped up to 500 μL using sterile TSB. Each condition was performed in triplicate. Turbidity (OD_{600}) was read every 5 mins for a total of 12 hrs.

2.9 Development of silkworm larvae model

Silkworm larvae (4th instar larvae) (*Bombyx mori*) were purchased from Livefoods Unlimited (Tinbeerwah, QLD). Upon receiving the silkworms, all silkworms were weighed and separated into groups to allow for an even distribution of worm weights across all experimental groups.

2.9.1 Housing of silkworm larvae

Silkworms were housed within their experimental groups (~10 silkworms) at 28 °C in plastic containers (6 x 8 cm), lined with paper towel, with 6 air holes per container. Silkworms were fed mulberry chow up until the first day of experimental procedures and were moved to fresh containers every 24 hrs for the duration of the experiment.

2.9.2 Injection methods

Experimental groups consisted of; handling control (no injection), control (sterile TSB only), bacterial control (bacteria only), phage control (phage only), bacteria and phage (bacteria followed by phage or vice versa). Silkworm larvae were injected with 50 μL of sterile TSB, phage, or bacteria at various concentrations into the 3rd segment on the dorsal side of the larvae using a 25-gauge needle and a 1 mL syringe. Pressure was applied to the injection site to reduce the loss of haemolymph.

2.9.3 Haemolymph collection

Various haemolymph collection methods were trialled based on previous literature (see **Table 5.1**). Two of the methods involved placing the silkworm larvae on ice for 5-10 mins to sedate the larvae prior to either cutting off the two front legs or the head of the silkworm with dissection scissors, allowing the released haemolymph to collect in an Eppendorf tube. The following two methods involved either using a 20-gauge syringe needle to pierce the larvae skin and draw haemolymph straight from the open circulatory system or using the 20-gauge needle to create a puncture wound, allowing the haemolymph to pool, then use a 200 μ L pipette to collect the pooled haemolymph. All haemolymph was stored on ice directly after collection and used immediately for subsequent experiments.

2.10 Effect of silkworm haemolymph on phage lytic ability and bacterial growth

To test the effect of the silkworm larvae haemolymph on the phage lytic ability or the growth of *S. pseudintermedius*, haemolymph was collected from larvae as described in **Section 2.9.3** Haemolymph collection. Fresh haemolymph was mixed with known concentrations of *S. pseudintermedius*, the co-culture was then diluted and plated on NA to count the CFU. Similarly, fresh haemolymph was mixed with a known titre of phage, the co-culture was diluted and plated on a bacterial lawn on *S. pseudintermedius* to determine the PFU. The CFU or PFU was compared to low concentrations or no haemolymph.

2.11 *Staphylococcus pseudintermedius* infection trials in silkworm larvae

Upon receiving the silkworm larvae from QLD, larvae were acclimatised to the laboratory conditions by housing them in the 28 °C incubator, with free access to food. The paper towel and food were changed daily, to avoid any mould growth. On the day of the infection trials, silkworm larvae were weighed, separated into weight groups, and then distributed evenly across the various infection groups (e.g., Bacterial control, placebo control, handling only) to obtain an even distribution of larvae weights. The injection point on the silkworm larvae was located on the second dorsal segment of the larvae, and was used to administer control solutions (PBS, TSB) or bacteria.

Each group of silkworms (n=10) were assigned as either control or bacterial groups, and each of the bacterial groups received a different concentrations of *S. pseudintermedius* (3.12×10^5 - 2×10^7 CFU). The control groups either received sterile TSB (injection control) or no injection (handling control). Following injection of bacteria or control solutions, the silkworms were placed on fresh paper towel, with each group housed in separate plastic container, which was kept in the 28 °C incubator. The silkworms were checked every 24 hrs, to count the number of live larvae, and to change the paper towel to avoid mould. Silkworm were not fed following injection, to avoid food consumption as a confounding factor. The silkworm survival was measured until 72 hrs.

2.12 Phage therapy trials in silkworm larvae

Following methods outlined in **Section 2.9.2** Injection methods, silkworm larvae were injected with either the lethal dose 50 (LD50) of *S. pseudintermedius* (1.25×10^6 CFU) or sterile TSB on the right side of the dorsal segment. 10 mins after the bacterial or control injection, a group of silkworms received either phage (MOI 1 or 10), endolysin (50 µg or 100 µg) or placebo (sterile PBS) via injection into the left side of the dorsal segment. Following injection of bacteria or control solutions, the silkworms were placed on fresh paper towel, with each group housed in separate plastic container, which was kept in the 28 °C incubator. The silkworms were checked every 24 hrs, to count the number of live larvae, and to change the paper towel to avoid mould. Silkworm were not fed following injection, to avoid food consumption as a confounding factor. The silkworm survival was measured until 72 hrs.

2.13 Standard Statistical Analysis

All results from this thesis are expressed as mean \pm SEM. Student's *t*-tests were used for statistical analysis between 2 groups, with a *P* value less than 0.05 considered to be significant. * *P*<0.05, ** *P*<0.01, *** *P*<0.001, **** *P*<0.0001. Experiments with 2 or more experimental groups were statistically analysed using either an ordinary one-way multiple comparison ANOVA or multiple *t*-tests using the Dunnett method for corrections for multiple comparisons. All statistical analysis was

performed using Prism Version 9.0 software (GraphPad, La Jolla, United States). All experiments were performed in biological triplicate (unless otherwise stated).

Chapter 3

Isolation and characterisation of novel bacteriophages that target *Staphylococcus pseudintermedius*

3.1 Summary

Methicillin-resistant *Staphylococcus pseudintermedius* (MRSP) is a significant veterinary pathogen, involved in numerous infections in canines. Due to the antibiotic-resistant and zoonotic nature of *S. pseudintermedius*, there is an urgent need for alternative therapeutics. In this work, we aimed to isolate and characterise bacteriophages against clinical isolates of *S. pseudintermedius*. Four novel phages were isolated from soil and canine fur samples, which were classified as novel by Whole Genome Sequencing (WGS). The four phages: SP_10s, SP_10L, SP_22s and SP_22L had relatively narrow host ranges, able to lyse 53%, 10%, 15% and 13% of *S. pseudintermedius* clinical isolates, respectively. Lytic growth kinetics of candidate Phage SP_10s show that the phage can significantly reduce *S. pseudintermedius* counts within 30 minutes of application. A secondary WGS of the four phage samples revealed that all phages were now dominated by a single *Siphoviridae* phage, which shows 100% similarity to a prophage from *S. pseudintermedius* strain 157588. Prophages are highly prevalent in *S. pseudintermedius* genomes, with a total of 221 prophages identified. Of the total prophages identified, 70 of the prophages were listed as complete, with the majority of these prophages being 40-60 kb in size. Importantly, 32.2% of the strains only contained 1 complete prophage, with 28.7% possessing 2-6 complete prophages. This chapter provides insights into the future use of phage therapy for *S. pseudintermedius* infections in canines.

3.2 Introduction

Methicillin-resistant *Staphylococcus pseudintermedius* (MRSP) is an opportunistic pathogen, recognised for its involvement in numerous disease states in canines (see **Section 1.3** *Staphylococcus pseudintermedius*: A Pathogenic Bacterium of Veterinary Concern **Figure 1.1**)¹³. MRSP isolates are often resistant to multiple antibiotic classes, and typically described as multidrug-resistant (MDR); therefore, novel therapeutics are essential¹⁴. One avenue of significant interest is phage therapy; the application of bacterio(phages) and their components as an alternative antimicrobial¹⁵. Phage therapy relies on the isolation of lytic phages, as they result in bacterial lysis as shown in **Figure 3.1**. Therefore, this work set out to isolate lytic phages against *S. pseudintermedius*, as there was no literature describing this work previously. However, whilst undertaking this work, three groups described the isolation of *S. pseudintermedius* phages^{16–18}. It has been shown that all of the isolated phages previously published and uploaded to the NCBI database are temperate phages as they contain genes associated with lysogeny. Temperate phages undergo the lysogenic lifecycle, which means they recognise and infect specific bacteria, however, following infection, lysogenic phage DNA incorporates within the bacterial genome to become a prophage. Prophages are then passed through daughter cells via bacterial replication (**Figure 3.1**)¹⁹. Through cell stressors such as UV light and chemical exposure, prophages can be induced to undergo the lytic life cycle, however, this is unpredictable, thus lysogenic phages are unfavourable for phage therapy (**Figure 3.1**)^{20,21}. Therefore, this chapter focused on the isolation of lytic phages against *S. pseudintermedius* as a novel therapeutic.

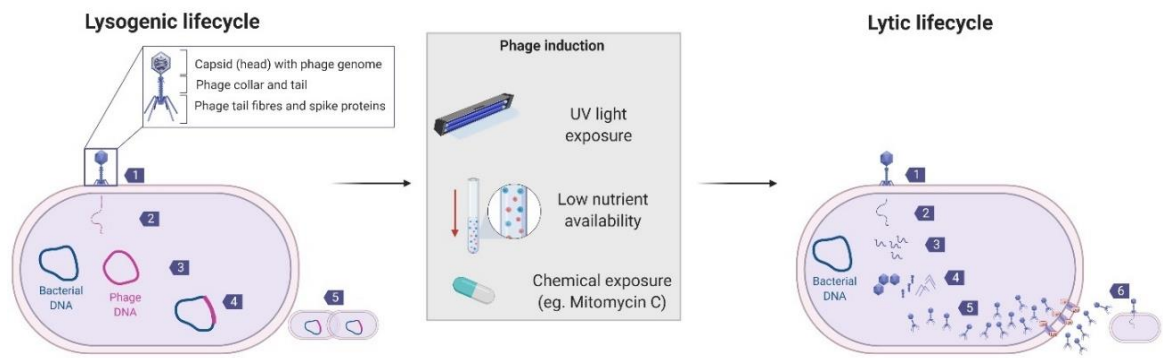


Figure 3.1 The lytic and lysogenic life cycle of bacteriophages. The lysogenic life cycle begins with (1) phage adsorption, in which the phage tail fibres recognise and attach to the bacterial outer membrane receptors. This results in an irreversible attachment of the phage to the bacterial surface which causes (2) the contraction of the phage tail sheaths to puncture the outer membrane and cell wall, allowing the phage genomic material to pass from the phage capsid to the bacterial cell via the phage tail. (3,4) The phage DNA incorporates within the bacterial genome, (5) as the bacterial cells divide, the prophage DNA is passed onto the daughter cells. Under stressful conditions, such as UV or chemical exposure or low nutrient availability, the prophages enter the lytic life cycle. The lytic life cycle (1,2) begins similarly to the lysogenic life cycle, with phage attachment and the injection of phage DNA into the bacterial host. The lytic life cycle differs with (3) the phage DNA (3) The phage DNA is replicated using the bacterial host cell machinery and is subsequently (4) transcribed and translated into new viral components (e.g., capsid, tail, tail fibres). (5) Newly synthesised viral components will assemble to become mature virions which will secrete proteins known as holins and endolysins. (6) Holins will create a pore in the bacterial membrane, allowing the endolysins to pass through and degrade the peptidoglycan layer. This results in bacterial cell lysis, releasing hundreds of mature phage virions that will continue to infect and lyse neighbouring bacterial cells ^{20,21}.

The isolation of lytic phages and their subsequent therapeutic use pre-dates antibiotics, first described in 1915 ²². However, due to the global antibiotic resistance (AR) crisis, phage therapy has resurfaced, with thousands of phages being isolated and trialled against numerous bacterial pathogens ²³. In order to begin phage isolation, it is first crucial to obtain the target bacterial strain ²⁴. The bacterial strains may be obtained as clinical isolates from human or animal patients, laboratory strains from a repository that have been well characterised or isolated from the environment. Phages are highly abundant in the environment, typically found in areas where their bacterial host may thrive ², therefore, it is also essential to know the general ecology of the bacteria such as where the bacteria resides to isolate phages. For example, phages were isolated from a fish pond, against *Flavobacterium psychrophilum* which is a bacterial pathogen affecting fish within the pond environment ²⁵. The samples used for phage screening are diverse, and range from environmental samples such as water, soil and sewage, to patient samples, including swabs and body fluids ²⁴.

The phage isolation protocol has been well described, with the successful isolation of phages from a diverse range of biological samples ^{26–32}. To begin with, environmental samples such as soil or water are centrifuged and filtered to remove any debris, and the most direct method for phage

isolation involves spotting the phage sample directly onto a bacterial lawn, to observe the presence of plaques, indicative of phage isolation ². However, in the instance that there are too few phages present in the sample to be observed, phage enrichment is required ³³. Phage enrichment involves culturing one or more bacterial strains, with the addition of the phage sample. This method aims to propagate the small population of present phages to a concentration that would be easily detectable in subsequent plating ³³. While it is routine to use only one bacterial host in the phage enrichment, this generally results in ‘narrow host range’ phages, therefore, studies have used multiple hosts in the one enrichment to broaden the host range of selected phages ^{34,35}. Following enrichment, the presence of ‘plaques’ or zones of clearing on the bacterial lawn indicates potential phage isolation. Once the phage has been isolated, subsequent characterisation of each individual phage is crucial to understand their properties for further use. While it is best to characterise isolated phages to a great extent, previous literature has listed key characterisation steps required for phages intended for phage therapy ^{2,36,37}. As described previously, the typical characterisation includes cultural lysis assays, host range testing, Transmission Electron Microscopy (TEM), and genomic analysis, all of which will be described in detail throughout this chapter ³⁸⁻⁴¹. This chapter aimed to isolate and characterise novel bacteriophages against *S. pseudintermedius*, to contribute towards the development of alternative therapeutics.

3.3 Results

3.3.1 Collection of *Staphylococcus pseudintermedius* isolates as a host for phage screening.

To screen for phages, it is first essential to isolate the host bacterium of interest. *Staphylococcus pseudintermedius* was the focal bacterium throughout this study, as it is involved in numerous canine infections, including skin and ear infections, as well as respiratory, urinary, and reproductive tract infections ¹³. In order to isolate *S. pseudintermedius*, collaborators from Melbourne University collected swabs from various disease states in canines at Werribee Veterinary Centre from 2009 – 2017 (**Figure 3.2**). A total of 60 clinical isolates of *S. pseudintermedius* were gifted to us, as bacterial hosts for phage screening.

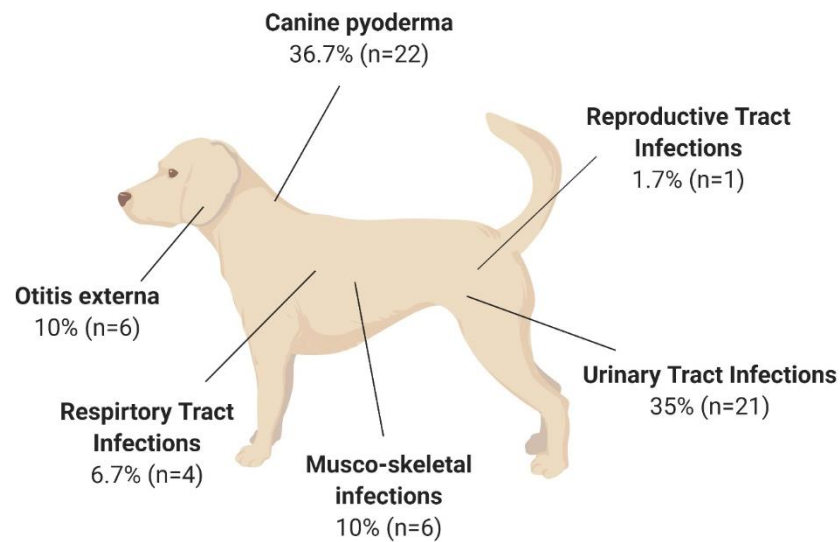


Figure 3.2 Isolation sources of 60 *Staphylococcus pseudintermedius* clinical isolates from infected canines. Isolates were collected between 2009-2017 from University of Melbourne Veterinary Centre, Werribee.

Although *S. pseudintermedius* isolates have been extensively studied, it was first essential to perform both solid and liquid medium growth analysis of a representative isolate, as all clinical isolates may vary in growth characteristics within the laboratory. *S. pseudintermedius* strain CM16-0689 was isolated from a canine skin infection and was chosen as a representative isolate. When grown on Horse Blood Agar (HBA), *S. pseudintermedius* CM16-0689, displayed expected colony morphology, as shown by the small white opaque colonies with a double haemolysis on blood agar (**Figure 3.3A**). The representative strain presents Gram positive cocci arranged in clusters following Gram staining, which is consistent with previous reports ⁴² (**Figure 3.3B**). Alongside these common characteristics, isolates were further confirmed as *S. pseudintermedius* following biochemical analysis performed by our collaborators (**Table 3.6**), with any isolates exhibiting unexpected biochemical reactions being 16s sequenced to confirm true species identification prior to inclusion in this study.

Growth curve analysis of the bacterial isolates provides a rapid way to calculate the number of cells in a given volume, based on time of incubation and the bacterial turbidity (OD_{600nm}). The growth curves in **Figure 3.3C** were obtained at mid-exponential phase following 3 hrs of incubation, which correlated to an OD_{600nm} value of 1.2. These growth curves will be used for subsequent experiments, including our phage screening protocol in **Section 2.3 Bacteriophage screening**.

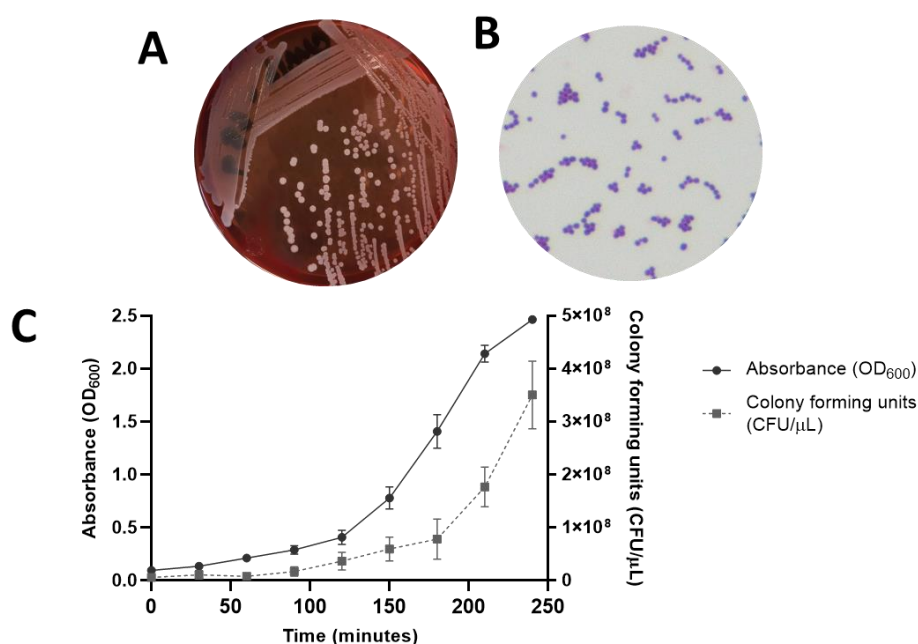


Figure 3.3 Growth of *Staphylococcus pseudintermedius* representative strain CM16-689. (A) Streak dilution of isolate CM16-0689 on Horse Blood Agar (HBA). (B) Gram stain of *S. pseudintermedius*. (C) Growth curve analysis using OD600 and CFU over a given time-course.

Previous studies have shown that a high percentage of *S. pseudintermedius* isolates are described as methicillin-resistant *S. pseudintermedius* (MRSP), as they possess genes that reduce their affinity to β -lactam antibiotics¹⁴. Additionally, a recent study found that 78% of MRSP isolates are also described as multi-drug resistant (MDR) as they show resistance to three or more antibiotic classes⁴³. Our collaborators performed antibiotic resistance analysis on the 60 *S. pseudintermedius* clinical isolates. Results in **Figure 3.4** support the high rates of antibiotic resistance to seven commonly used antibiotics. Importantly, 43% of these isolates were described as MDR, resistant to three or more of the antibiotics tested.

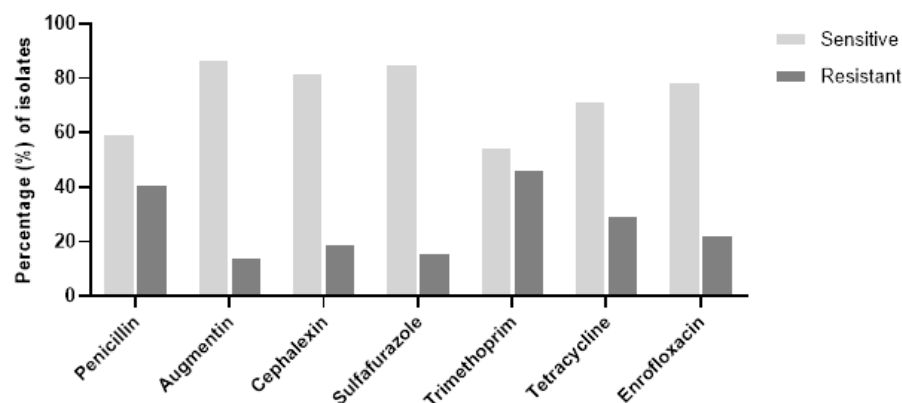


Figure 3.4 Antibiotic resistance patterns of *Staphylococcus pseudintermedius* clinical isolates. *Staphylococcus pseudintermedius* isolates were grown in broth cultures and MIC values were determined for each antibiotic listed.

3.3.2 Isolation of *Staphylococcus pseudintermedius* phages from environmental and dog samples.

When commencing the isolation of phages for this chapter, there were no published phages against *S. pseudintermedius*. Therefore, protocols used to successfully isolate phages against alternate pathogens were used, with slight modifications^{24,44-46}. Briefly, multiple *S. pseudintermedius* host strains were co-incubated with various environmental and dog-associated samples to create an enrichment and screen for lytic phages. As shown by the phage screening workflow in **Figure 3.5**, to create a phage enrichment, between three and six *S. pseudintermedius* host strains were incubated together, along with one phage sample (e.g., Fur sample from healthy dog). Several combinations of host strains and environmental samples were tested but did not result in phage isolation (**Table 3.1**). Only two combinations led to the successful isolation of phages in round 6, as highlighted in **Table 3.1**. In this case, an enrichment sample containing a fur sample with three *S. pseudintermedius* strains and an enrichment sample containing a fur sample with the same three *S. pseudintermedius* strains resulted in phage isolation (**Table 3.1**).

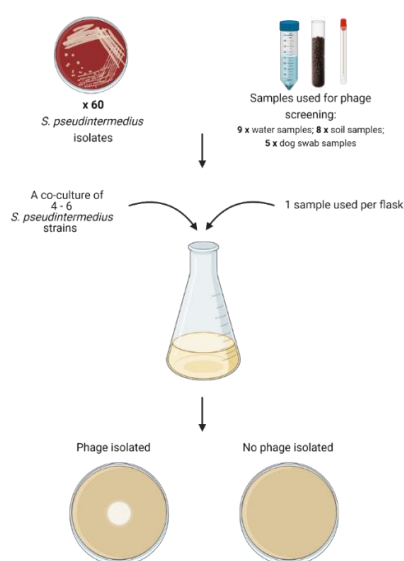


Figure 3.5 Phage enrichment and isolation workflow. A total of 60 *S. pseudintermedius* isolates and 22 phage screening samples (e.g., soil, fur, water) were used for enrichments, to screen for phages. In each individual flask, three to six *S. pseudintermedius* strains were co-incubated together, with the addition of one sample. Following incubation of the bacterial and phage sample, the enrichment was spotted onto lawns of *S. pseudintermedius* to observe the presence or absence of phage lysis.

Table 3.1 Overview of phage screening success. Bacterial strains and enviromental samples used in phage screening rounds, with an indication as to whether phages were successfully isolated. Samples used in phage screening are listed in Section 2.3.1.1 Collection and processing of soil and water samples for phage screening and 2.3.1.2 Collection and processing of animal-associated samples for phage screening; samples 1-9 = water samples, 10-17 = soil samples, 18-22 = dog-associated samples.

	Bacterial strains	Samples used for phage screening	Phage isolated?
Round 1	CM16-0937 CM16-1008 CM13-0367 CM13-0596 CM15-0965 CM15-0597	Samples 1- 22	No
Round 2	CM13-0059 CM12-0745 CM13-0320 CM13-0255 CM13-0140 CM09-0471	Samples 1- 22	No
Round 3	CM16-0262 CM12-0201 CM12-0093 CM11-0671 CM16-0920	Samples 1- 22	No
Round 4	CM09-0925 CM12-0529 CM12-0169 CM12-0111 CM11-0460 CM11-0195	Samples 1- 22	No
Round 5	CM17-0292 CM17-0272 CM15-0460 CM13-0910	Samples 1- 22	No
Round 6	CM17-0580 CM11-0132 CM16-0689	Samples 1- 22	Yes (Phage sample #10 and #22)

The successful isolation of phages was initially confirmed by the presence of plaques on *S. pseudintermedius* host strain CM16-069, produced via overlay agar (**Figure 3.6A**). Interestingly, there appeared to be two different plaque sizes that formed when the two separate phage enrichments (Phage sample 10 (soil) and Phage sample 22 (fur sample)) were spotted onto their bacterial host and the different plaque sizes remained consistent throughout subsequent propagation. Therefore, individual plaques were extracted from the phage overlay plates and treated as four separate phage samples for subsequent characterisation, named Phage Sp_10s, Phage Sp_10L, Phage Sp_22s and Phage Sp_22L (10 or 22 denotes the sample the phage originated from, and ‘s’ or ‘L’ for small or large plaques, respectively) (**Figure 3.6 B, C, D, E**).

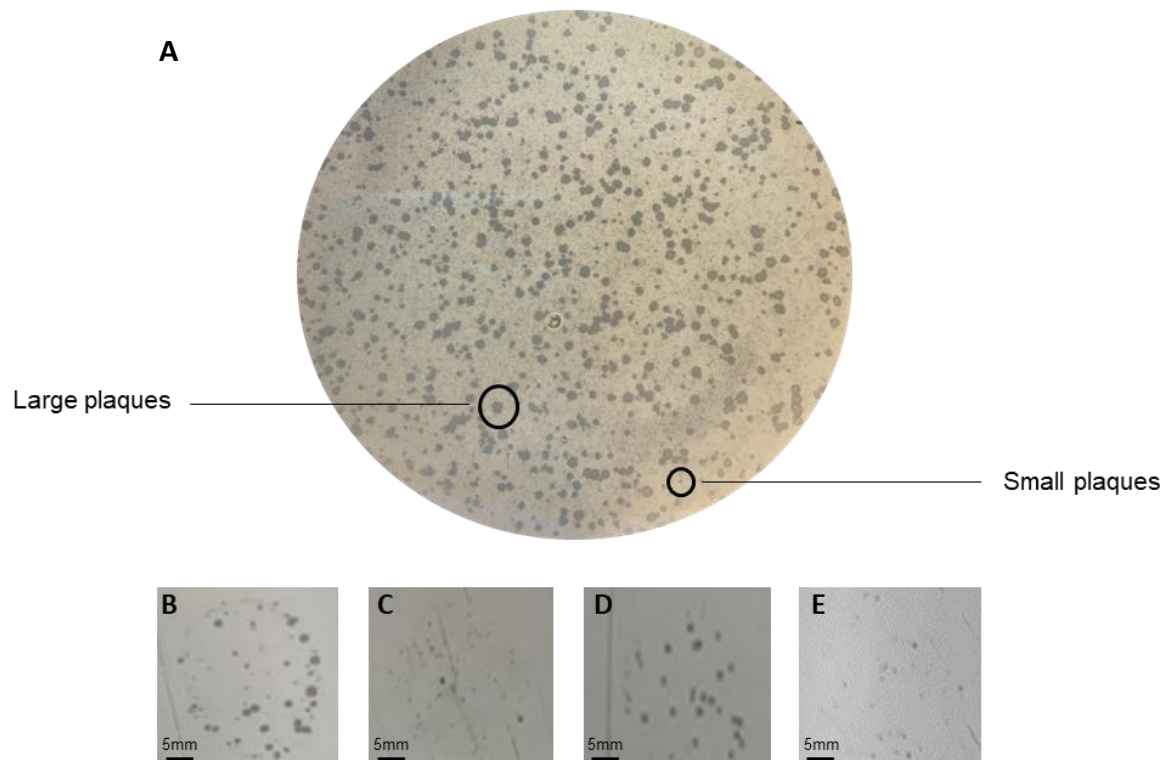


Figure 3.6 Plaque forming ability of isolated *S. pseudintermedius* phages. (A) Phage sample containing phages was mixed with *S. pseudintermedius* CM16-0689 at log phase to produce a phage overlay. Phage samples 10 and 22 produced both large and small plaques as highlighted. The differing phage morphologies were separated, treated as four individual phages and plaque morphology was subsequently analysed. (B) Plaque morphology of Phage Sp_10L, (C) Plaque morphology of Phage Sp_10s, (D) Plaque morphology of Phage Sp_22L, (E) Plaque morphology of Phage Sp_22s.

3.3.3 Characterisation of isolated bacteriophages

3.3.3.1 Identification of four novel phages through Whole Genome Sequencing (WGS)

In order to determine the genome sequence of our isolated bacteriophages, each individual phage was expanded in a bacterial broth culture using host strain *S. pseudintermedius* CM16-0689, prior to DNA extraction as outlined in **Section 2.4.1** Genomic DNA extraction and quantification from isolated phages. Extracted DNA was then subsequently sequenced using Illumina platform technology and *de novo* assembly was used to assemble the contigs (**Section 2.4.2.7** Assembly and annotation of phage contigs). As shown in **Table 3.2**, the four phages had genomes with sizes ranging from 9,507bp to 21,661 bp, encoding 17- 26 putative ORFs. The four phages had a relatively similar G + C% content between 34.0% to 37.6%. To compare the genetic similarity of the four phages, their genomes were aligned using the Geneious plug-in program, Mauve. Following alignment, the phages were not highly similar to one another, with Phage SP_22s and Phage SP_10s showing the highest nucleotide pairwise similarity of just 50.6% (**Table 3.2**). Followed by a nucleotide pairwise similarity of 49.5% between Phage SP_22L and Phage 10L, and a nucleotide pairwise similarity of 45.5% between Phage SP_22s and Phage SP_22L (**Table 3.2**).

Subsequent to genome assembly, genes were predicted using the Geneious plug-in, Glimmer. Putative protein annotations were assigned for each ORF by performing a protein BLASTp search of the amino acid sequence (**Table 3.8, Table 3.9, Table 3.10, Table 3.11**). From this, genome maps of all four phages were constructed in SnapGene, as shown in **Figure 3.7**. This figure highlights the module architecture of the four phages, with each colour representing the predicted gene function: structural, DNA replication and packaging, unknown function, hypothetical protein, or host-virulence.

The genome annotation identified many phage proteins that were expected (e.g., Tail tape measure protein, major capsid proteins) (**Figure 3.7**). However, particular genes expected in a full-length bacteriophage sequence (e.g., lysis or lysogenic modules) were missing. Therefore, it was clear that we had not sequenced the entire genome of the isolated phages, and subsequent sequencing was required. The genomes also contained many hypothetical proteins, and it is unknown what role these hypothetical proteins play on the phage or the host bacterium.

Table 3.2 *De novo* assembly of the four novel *S. pseudintermedius* phage genomes. Size (bp), GC (%) content, number of ORF's and the nucleotide pairwise identity was explored for the four phage samples using bioinformatic software, Geneious.

<i>Staphylococcus</i> <i>pseudintermedius</i> phage	Size (bp)	GC	Number of	Nucleotide Pairwise Identity (%)			
		Content	putative	Phage SP_10s	Phage SP_22s	Phage SP_10L	Phage SP_22L
		(%)	ORFs				
Phage SP_10s	20,952	35.6	20	-	50.6	19.0	0.0
Phage SP_22s	9,507	37.6	21	50.6	-	0.0	45.5
Phage SP_10L	21,661	36.7	26	19.0	0.0	-	49.5
Phage SP_22L	13,367	34.0	17	0.0	45.5	49.5	-

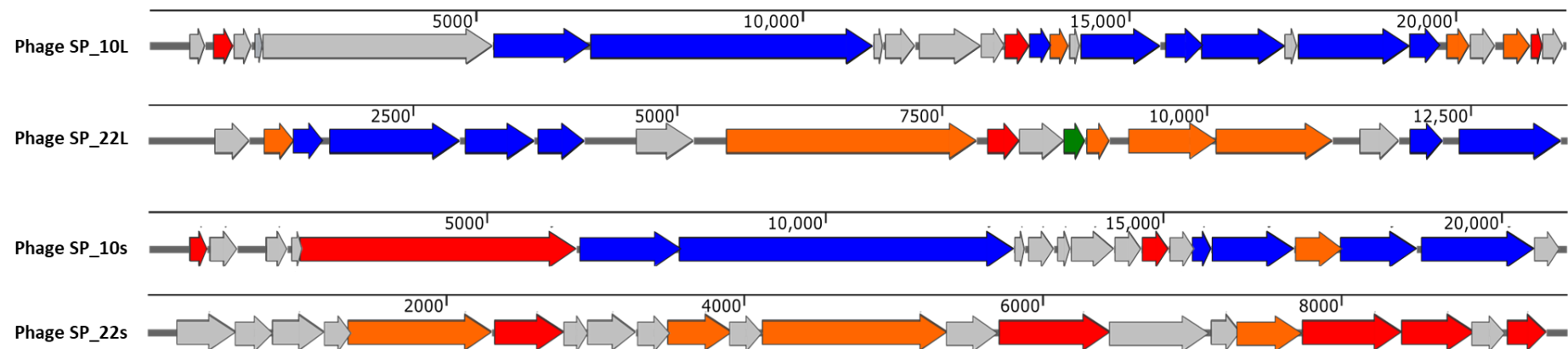


Figure 3.7 Genome maps of four novel *S. pseudintermedius* phages. The putative function for each phage gene was assigned based on a BLASTp search; hypothetical protein, unknown function, structural, DNA packaging & replication, or host virulence genes. Visualisation of the phage genome architecture was achieved using SnapGene.

3.3.3.2 Host range characterisation of four novel phages

In order to examine the host range ability of the four isolated phages, each phage was spotted onto a bacterial lawn. The bacterial strains tested for host range were selected from a library of 60 *S. pseudintermedius* clinical strains, which were isolated from various infection sites in dogs. Each phage was diluted to equal titres (1×10^6 PFU/mL) and tested 3 times on each individual strain. Lysis was scored; '-' = no lysis, '+' = plaques formed, '++' = turbid lysis and '+++' = clear lysis. Based on the lysis patterns shown in **Table 3.3**, all four phages showed differing phage patterns, however, three were described as having a narrow host range, only able to lyse select strains of *S. pseudintermedius*. Whereas Phage SP_10s was described to have a moderate-broad host range, able to lyse a range of strains from various canine infection sites.

Table 3.3 Host range analysis of four *S. pseudintermedius* phages on 60 *S. pseudintermedius* clinical strains. Antibiotics tested included Pen = Penicillin, Amc = Ampicillin, CL = Cephalexin, SF = Sulfafurazole, W = Trimethoprim, Te = Tetracycline, Enr = Enrofloxacin, with the resistance profiles (R: Resistant, S: Sensitive) tested at Melbourne University. Lysis scoring of the phages were as follows; ; ‘-‘ = no lysis, ‘+’ = plaques formed, ‘++’ = turbid lysis and ‘+++’ = clear lysis. Spot testing was performed in triplicate.

	Antibiotics tested								Phages tested				
Strain	Pen	Amc	CL	SF	W	Te	Enr	Source	Phage SP_10s	Phage Sp_10L	Phage SP_22s	Phage Sp_22L	combination of all 4
CM2017-0410	R	R	R	R	R	R	R	Skin	+++	-	-	-	+++
CM2016-0933	R	R	R	S	R	R	R	Musco-skeletal	+++	-	-	-	+++
CM2012-0529	R	R	R	S	R	S	R	Musco-skeletal	+++	-	-	-	-
CM2012-0654	R	R	R	S	R	S	R	Skin	-	-	-	-	+++
CM2012-0745	R	R	R	S	R	S	R	Respiratory	-	-	-	-	-
CM2013-0059	R	R	R	S	R	S	R	Respiratory	+++	-	-	-	-
CM2016-0920	R	R	R	S	R	S	R	Ear	-	-	-	-	.
CM2017-0272	R	R	R	S	R	S	R	Musco-skeletal	-	-	-	-	-
CM2017-0292	R	R	R	S	R	S	R	Skin	-	-	-	-	-
CM2016-0889	R	S	R	S	R	R	R	Skin	+++	-	-	-	+++
CM2016-0917	R	S	R	S	R	R	R	Urinary	-	-	-	-	-
CM2015-0460	R	S	R	S	R	R	S	Urinary	++	-	-	-	-
CM2016-0471	R	S	S	R	R	R	R	Ear	+++	+	++	+	-
CM2009-0471	R	S	S	R	R	R	S	Musco-skeletal	++	+++	+	++	+
CM2012-0093	R	S	S	R	R	R	S	Ear	+++	-	-	-	+++
CM2017-0973	R	S	S	R	R	R	S	Urinary	+++	-	-	-	+

CM2009-0886	R	S	S	R	S	R	S	Urinary	+	-	-	-	-
CM2015-0031	R	S	S	R	S	R	S	Musco-skeletal	-	-	-	-	-
CM2015-0597	R	S	S	R	S	R	S	Ear	-	-	-	-	-
CM2013-0255	R	S	S	S	R	R	S	Skin	+++	-	-	-	-
CM2013-0910	R	S	S	S	R	R	S	Urinary	-	-	-	-	-
CM2015-0965	R	S	S	S	R	R	S	Urinary	-	-	-	-	-
CM2015-1096	R	S	S	S	R	R	S	Musco-skeletal	-	++	++	++	+
CM2016-0937	R	S	S	S	R	S	R	Urinary	+++	-	-	-	+
CM2016-1008	R	S	S	S	R	S	R	Urinary	+++	-	-	-	-
CM2011-0112	S	S	S	R	R	R	S	Urinary	-	-	-	-	-
CM2013-0351	S	S	S	R	R	R	S	Urinary	-	-	-	-	-
CM2011-0195	S	S	S	S	R	S	S	Respiratory	+	++	+	++	+
CM2012-0247	S	S	S	S	R	S	S	Urinary	-	-	-	-	-
CM2014-0677	S	S	S	S	R	S	S	Urinary	+++	-	-	-	-
CM2017-0713	S	S	S	S	R	S	S	Urinary	-	-	-	-	-
CM2009-0754	S	S	S	S	S	S	S	Urinary	-	-	-	-	-
CM2009-0925	S	S	S	S	S	S	S	Skin	-	-	-	-	-
CM2011-0079	S	S	S	S	S	S	S	Respiratory	-	-	-	-	-
CM2011-0097	S	S	S	S	S	S	S	Skin	-	-	-	-	+++
CM2011-0132	S	S	S	S	S	S	S	Skin	-	-	-	-	-
CM2011-0460	S	S	S	S	S	S	S	Skin	+++	-	-	-	-
CM2011-0653	S	S	S	S	S	S	S	Skin	+++	-	-	-	+++
CM2011-0669	S	S	S	S	S	S	S	Ear	+++	-	-	-	-

CM2011-0671	S	S	S	S	S	S	S	Skin	+++	-	-	-	-
CM2012-0111	S	S	S	S	S	S	S	Skin	+++	-	-	-	-
CM2012-0169	S	S	S	S	S	S	S	Urinary	+++	-	-	-	-
CM2012-0193	S	S	S	S	S	S	S	Reproductive	-	-	-	-	-
CM2012-0201	S	S	S	S	S	S	S	Urinary	+++	-	+	+	-
CM2012-0405	S	S	S	S	S	S	S	Skin	++	-	+	+	-
CM2012-0503	S	S	S	S	S	S	S	Skin	-	-	-	-	++
CM2012-0550	S	S	S	S	S	S	S	Skin	-	-	-	-	+++
CM2013-0140	S	S	S	S	S	S	S	Skin	+++	-	-	-	-
CM2013-0320	S	S	S	S	S	S	S	Skin	-	-	-	-	-
CM2013-0367	S	S	S	S	S	S	S	Skin	+++	-	-	-	+++
CM2013-0596	S	S	S	S	S	S	S	Urinary	-	-	-	-	+
CM2015-0358	S	S	S	S	S	S	S	Urinary	-	-	-	-	-
CM2016-0216	S	S	S	S	S	S	S	Skin	+++	+++	+++	+++	+++
CM2016-0262	S	S	S	S	S	S	S	Urinary	+++	-	-	-	-
CM2016-0568	S	S	S	S	S	S	S	Urinary	+++	-	-	-	-
CM2016-0674	S	S	S	S	S	S	S	Skin	-	-	-	-	-
CM2016-0689	S	S	S	S	S	S	S	Skin	+++	+++	+++	+++	+++
CM2016-1113	S	S	S	S	S	S	S	Skin	+++	-	-	-	-
CM2017-0472	S	S	S	S	S	S	S	Ear	+++	-	+	-	+++
CM2017-0580	S	S	S	S	S	S	S	Urinary	-	-	-	-	-

Information extrapolated from **Table 3.3** was summarised in **Table 3.4**, which shows that Phage Sp_10s had the largest host range ability, able to lyse 53% of *S. pseudintermedius* clinical strains. Followed by Phage Sp_22s, Phage Sp_22L and Phage Sp_10L that lysed 15, 13 and 10% of *S. pseudintermedius* strains, respectively. Bacterial strains originating from various sources were lysed by at least one phage, with the exception of the strain isolated from a canine reproductive infection, where no phage was able to lyse this strain.

Table 3.4 Overview of host range ability of four novel phages. Four *S. pseudintermedius* phages were tested on sixty clinical isolates of *S. pseudintermedius* strains from various infection sites.

Phage	Source						Total
	Skin	Musco-skeletal	Respiratory	Urinary	Ear	Reproductive	
Phage Sp_10L	9% [2/22]	33% [2/6]	25% [1/4]	0% [0/21]	16% [1/6]	0% [0/1]	10%
Phage Sp_10s	59% [13/22]	50% [3/6]	50% [2/4]	48% [10/21]	67% [4/6]	0% [0/1]	53%
Phage Sp_22L	14% [3/22]	33% [2/6]	25% [1/4]	5% [1/21]	17% [1/6]	0% [0/1]	13%
Phage Sp_22s	14% [3/22]	33% [2/6]	25% [1/4]	5% [1/21]	33% [2/6]	0% [0/1]	15%

3.3.3.3 Growth kinetics of candidate phage, Phage SP_10s

Phage SP_10s was initially selected as the candidate for phage growth kinetics, due to its broad host range and ease of passage. Phage SP_10s was added to the host strain, *S. pseudintermedius* CM16-0689, at a phage-host ratio of 1.0, and subsequently, bacterial and phage parameters were measured every 15 minutes (**Figure 3.8**).

The phage number (in PFU) began to rise within 15 minutes of application to the bacterial suspension, with a peak PFU at 45 mins, as shown in **Figure 3.8A**. This rise in phage titre may have attributed to the decrease in *S. pseudintermedius* CFU within 15 minutes of phage application, compared to no phage added **Figure 3.8B**. The phenomenon of reduction in bacterial CFU was

supported by **Figure 3.8C**, where there was a difference in OD between the sample with phage added, compared to sample with no phage added, with the OD reaching 0.0 by 75 mins of phage application. The aliquots that were used to measure CFU and OD were also imaged and analysed from bacterial density, in which there was a significant decline of bacterial density following phage addition, within just 30 minutes **Figure 3.8D**. Representative images used to create **Figure 3.8D** are displayed in **Figure 3.8E, F**, where we can see no bacterial cells on the slide after 180 mins when Phage SP_10s was added, compared to the bacterial density when no phage was added.

The growth kinetics of Phage SP_10s were also explored by an automated turbidity reduction assay using the ClarioStar Microplate reader (**Figure 3.9**). Phage SP_10s was added at different ratios (MOI 0.1 and 0.01) to *S. pseudintermedius* CM16-0689, and OD₆₀₀ was measured every 5 mins. As can be shown in **Figure 3.9**, Phage SP_10s at a MOI 0.01 had no significant effect on the bacterial growth curve, however, Phage SP_10s at a MOI 0.1 showed to inhibit the growth of *S. pseudintermedius*.

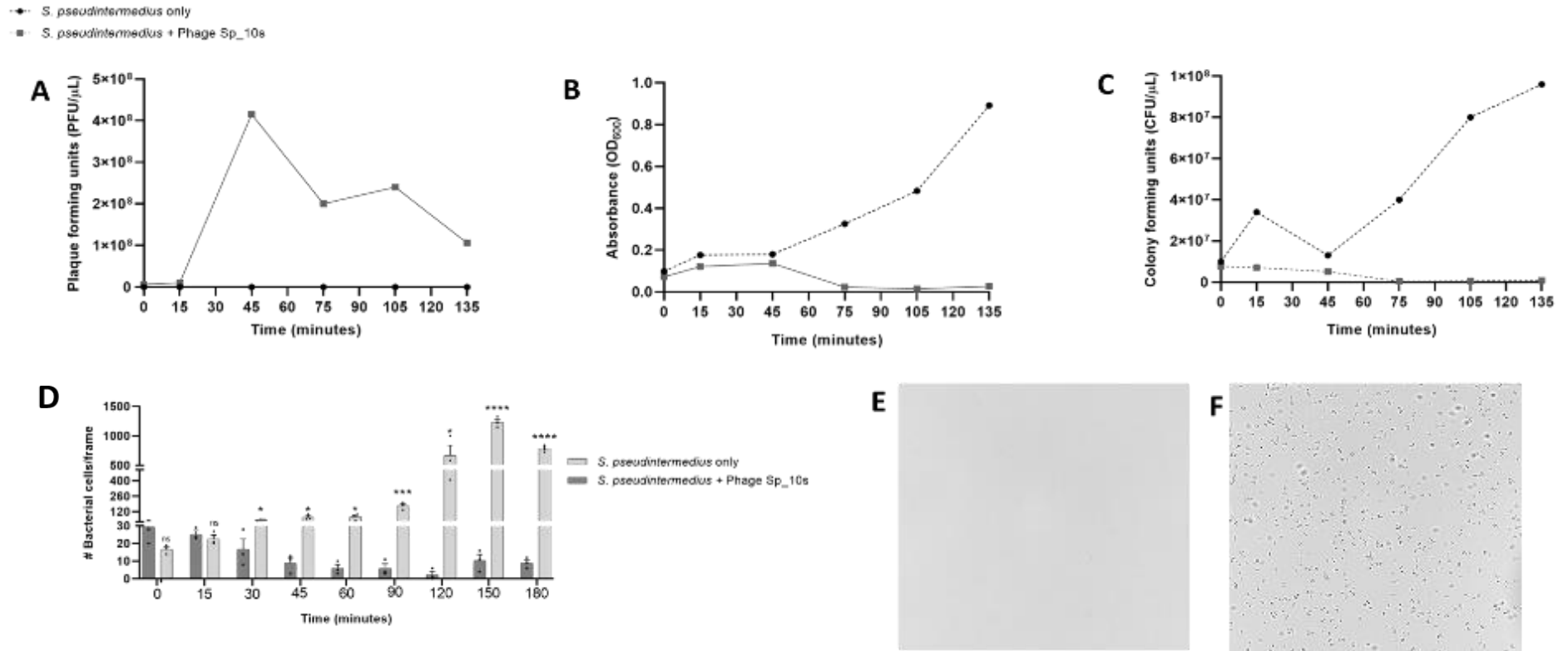


Figure 3.8 Growth kinetics of candidate phage, Phage SP_10s. For graphs A-C Black closed circles (●) indicate *S. pseudintermedius* only, grey closed squares (■) indicate *S. pseudintermedius* + Phage SP_10s. (A) Plaque forming ability of Phage SP_10s over a 2 hr time course. (B) Absorbance of CM16-689 culture compared with CM16-689 + phage SP_10s. (C) Colony forming ability of CM16-689 culture compared with CM16-689 + phage SP_10s. (D) Analysis of microscopy images over a 2 hr time-course. (E) Microscopy image of CM16-689 + Phage Sp_10s at 180 mins culture (F) Microscopy image of CM16-689 only at 180 mins.

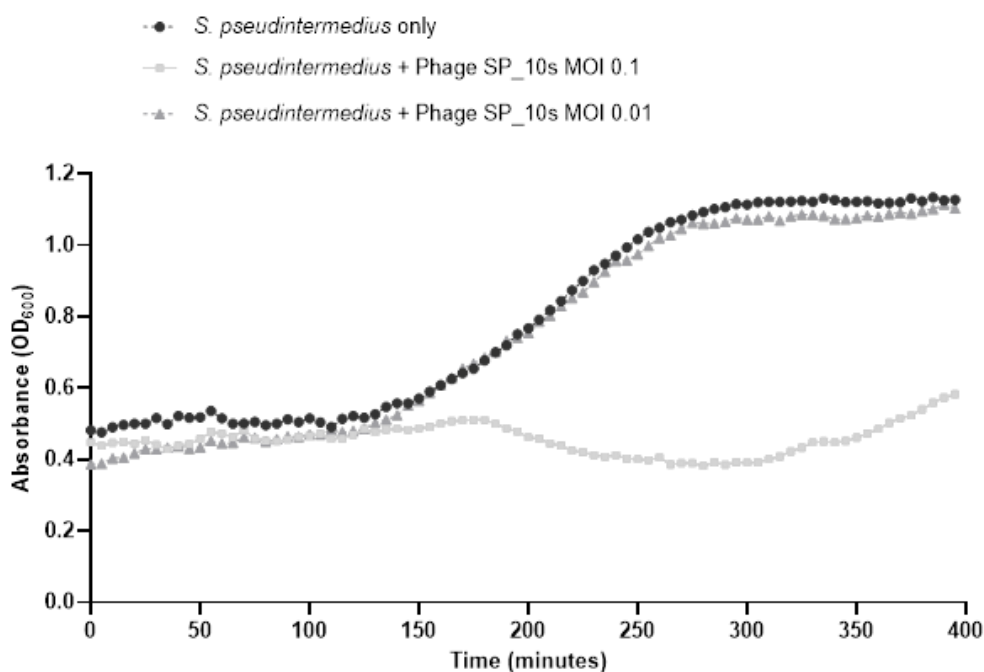


Figure 3.9 Absorbance curve of *S. pseudintermedius* CM16-069 with the addition of Phage SP_10s using ClarioStar microplate reader. *S. pseudintermedius* CM16-069 was grown in a 48-well plate with the addition of either MOI 1 phage SP_10s or MOI 0.01 phage SP_10s and absorbance (OD₆₀₀) was measured every 5 minutes for a total of 6 hrs (400 minutes).

3.3.3.4 Secondary WGS analysis of four novel phages

As initial sequencing runs did not reveal the full genome sequences of our candidate phages, an additional sequence run was performed on newly isolated DNA from each bacteriophage aliquot. All phages had been maintained over time by serial passaging on the host bacterial strain, *S. pseudintermedius* CM16-0689. As shown in **Table 3.5**, the four phage samples in the sequencing run all had a genome size of 21,866 bp, encoding 22 putative ORFs and a G + C% of 35.6%. The 21,866bp phage genome was run through PHASTER to detect prophage-like elements and showed 100% nucleotide pairwise identity to a prophage from *S. pseudintermedius* strain 157588.

Similarly, to the first sequencing run, the genomes were compared using Mauve program. This showed that all four phages were now 100% identical. Genes were predicted using Glimmer and putative protein annotations were assigned for each ORF by searching the amino acid sequence in NCBI BLASTp database (**Table 3.7**). From this, genome maps of all four phage samples were constructed in SnapGene, as shown in **Figure 3.10** This figure highlights the module architecture of the four phages are identical to one another and shows highly similar architecture to prophage

from *S. pseudintermedius* strain 157588. Therefore, the new dominant phage was named 'Phage SP_157588'. Phage SP_157588 shows 100% identity with Phage SP_10s from the first run, highlighting that one of the four phages originally isolated was likely a prophage from the host bacterial strain within the enrichment screening culture. The similarity in module architecture between the prophage from *S. pseudintermedius* strain 157588 and our dominant Phage SP_157588' is derived from the high similarity in annotated genes as shown in **Table 3.7** and **Table 3.12**.

Table 3.5 *De novo* assembly of prophage extracted from *S. pseudintermedius* strain 157588 and four phage samples.

<i>Staphylococcus</i> <i>pseudintermedius</i> phage	Size (bp)	GC Content (%)	Number of putative ORFs	Nucleotide Pairwise Identity (%)				
				Phage	Phage	Phage	Phage	<i>S. pseudintermedius</i>
				SP_10s	SP_22s	SP_10L	SP_22L	strain 157588
Prophage from <i>S. pseudintermedius</i> strain 157588	48,558	35.1%	75	100	100	100	100	-
Phage SP_10s	21,886	35.6	22	-	100	100	100	100
Phage SP_22s	21,866	35.6	22	100	-	100	100	100
Phage SP_10L	21,866	35.6	22	100	100	-	100	100
Phage SP_22L	21,866	35.6	22	100	100	100	-	100

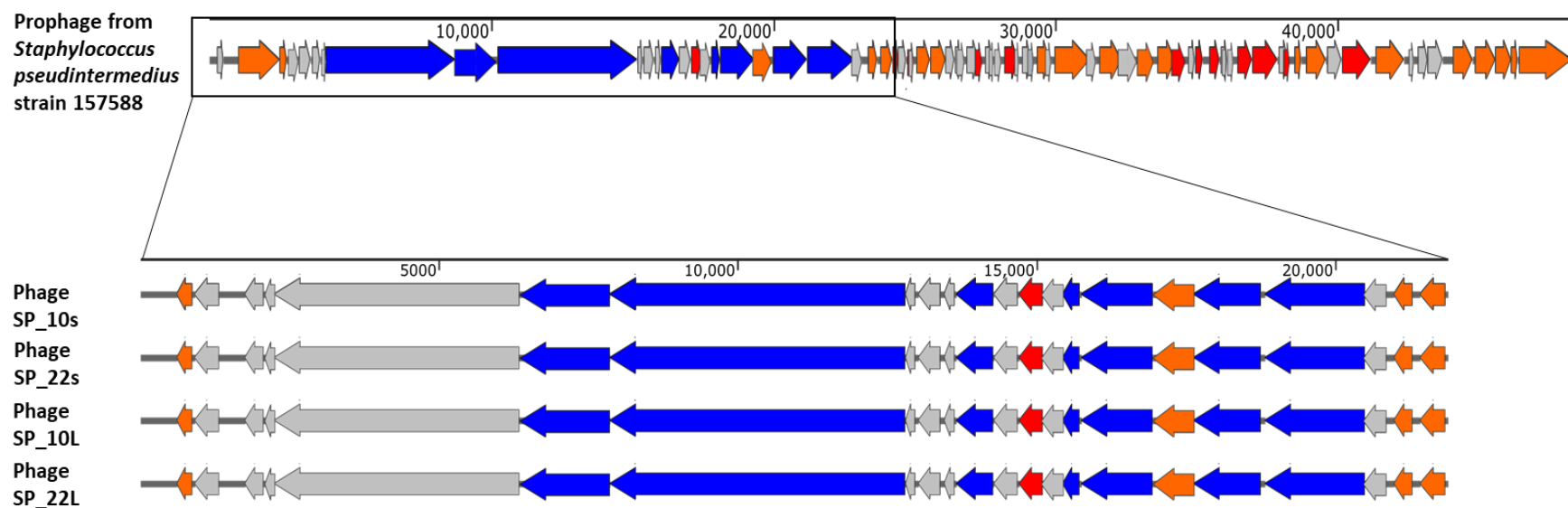


Figure 3.10 Genome map of prophage extracted from *S. pseudintermedius* strain 15788 that matched dominant phage from second sequencing run. The putative function for each phage gene was assigned based on a BLASTp search, hypothetical protein, unknown function, structural, DNA packaging & replication, or host virulence genes. Visualisation of the phage genome architecture was achieved using SnapGene.

3.3.3.5 Morphological characterisation using Transmission Electron Microscopy (TEM)

As the second sequencing run determined that all four phage samples were now dominated by one phage, Transmission Electron Microscopy (TEM) was used to determine the morphology of the dominant phage, Phage SP_157588. This technique was performed with the help of Dr. Peter Lock and Dr. Subir Sarker at La Trobe BioImaging Platform. Phage SP_157588 had an icosahedral head and long tail as depicted in **Figure 3.11A**. Using the scale bar as reference (200 nm), the phage capsid diameter and tail were measured (**Figure 3.11B**). From this, it was concluded that the capsid diameter was ~82.15 nm and the tail length was ~460.84 nm, as summarised in **Figure 3.11C**. Based on these morphological features, Phage SP_157588 can be classified within the phage family *Siphoviridae*.

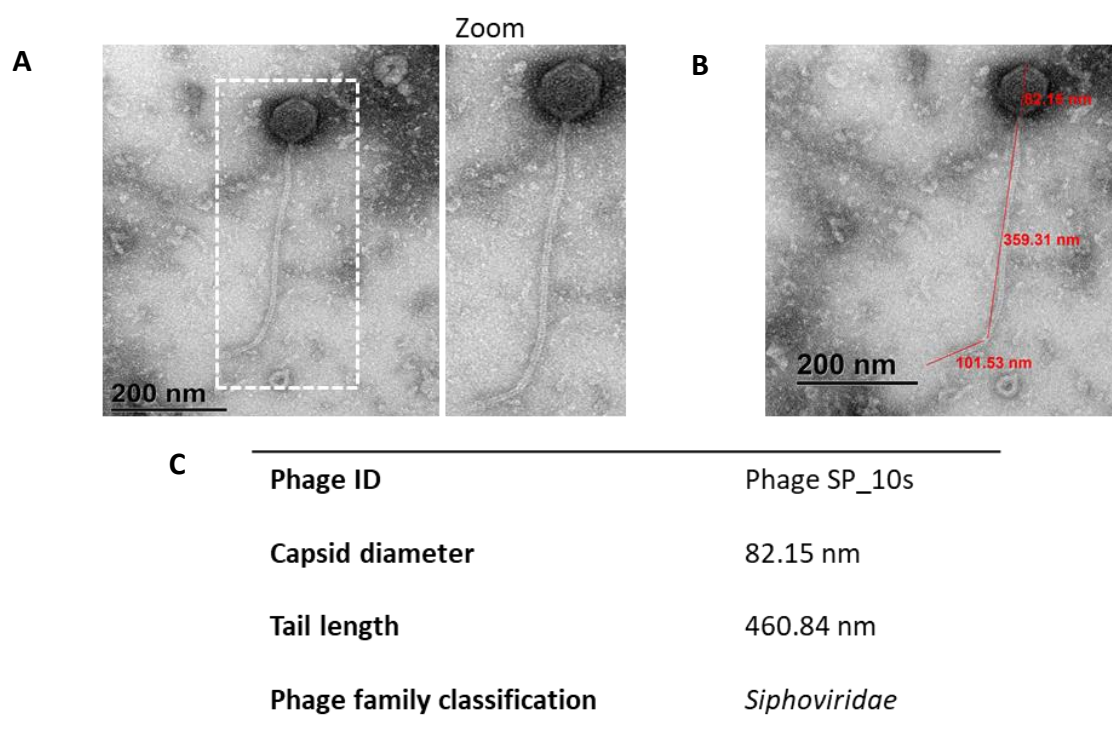


Figure 3.11 Morphological analysis of Phage SP_157588. (A) TEM image of Phage SP_10s shows icosahedral head and long contractile tail. (B) TEM measurement tool analysis on Phage SP_10s. (C) Summary of capsid and tail measurements of Phage SP_10s.

3.3.4 Prophages are highly prevalent in *Staphylococcus pseudintermedius* genomes

Phage SP_157588 was the main phage isolated within this thesis, as it dominated all phages in the phage preps studied. Phage SP_157588 appeared to be a temperate phage excised from the bacterial genome (prophage) as it contained lysogeny modules within its genome and matched a

S. pseudintermedius bacterial strain prophage. Therefore, we next examined *S. pseudintermedius* genomes from the NCBI database to determine the prevalence of prophages within their genome. By determining the prevalence of prophages within *S. pseudintermedius* genomes, this may give insight into how many novel phages can be induced from the *S. pseudintermedius* genome, and how this may affect phage therapy moving forward.

Computational identification of all prophages was achieved by running 59 *S. pseudintermedius* whole-genome sequences through the PHASTER program. Although we had 60 *S. pseudintermedius* isolates within our database, none had undergone full genome sequencing, therefore could not be used to mine for prophages. Instead, 59 *S. pseudintermedius* WGS available on the NCBI database were used. PHASTER identified a total of 221 prophage elements within the 59 genomes, as shown in **Figure 3.12A** and **Table 3.13**. Of the 221 prophages, the majority of these (n=133) were identified as incomplete prophages, 70 of the prophages were identified as complete, and 18 were identified as questionable. Of the complete, incomplete, or questionable prophages identified, the number of prophages per strain varied from 1-9 prophages, with 22% of strains harbouring 5 prophage-like elements, as shown in **Figure 3.12B** and **Table 3.14**. The size of the total prophages varied from 4.7 kb to 130 kb in size, with the majority of incomplete phages falling within the 5-10kb range, and the majority of the complete phages falling within the 40-60kb range, as depicted in **Figure 3.12C**.

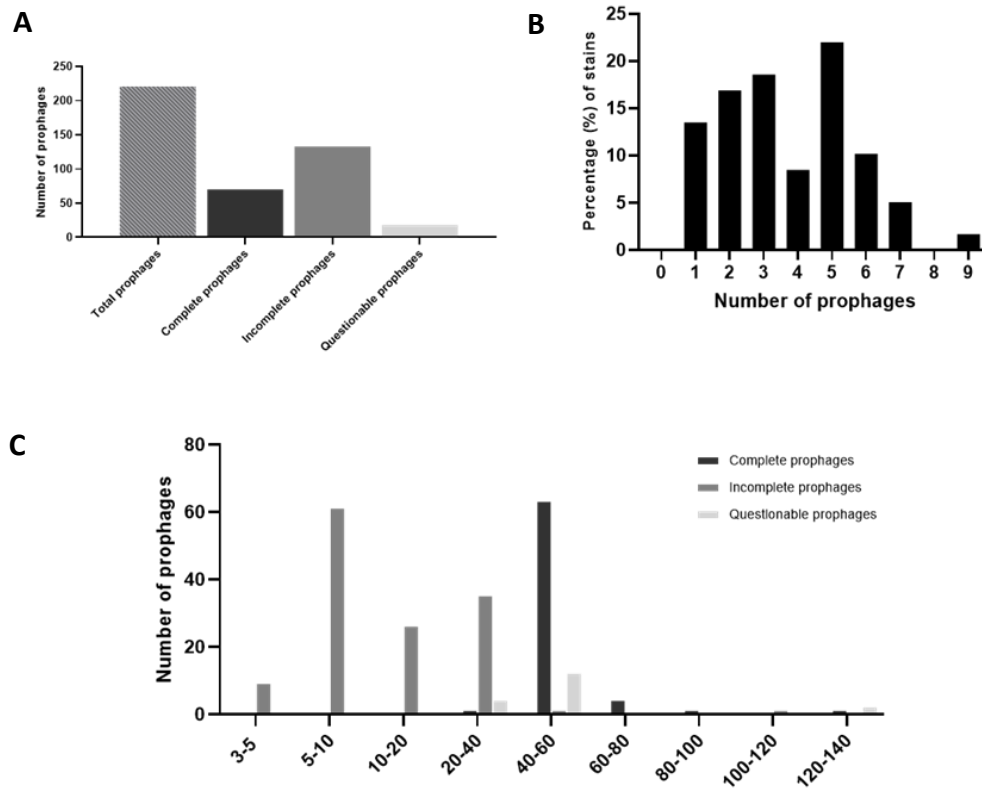


Figure 3.12 Characterisation of prophages in 59 *S. pseudintermedius* clinical isolates. (A) Distribution of total prophages identified into each classification: complete, incomplete, or questionable. (B) Frequency of prophages in 59 *S. pseudintermedius* genomes. (C) The size range of the prophages identified.

Across the 59 *S. pseudintermedius* strains, 221 total prophages were identified, with 70 of these prophages classified as complete prophages. Of the 59 host strains, 37.3% of the genomes contain no complete prophages, followed by 32.2% of strains harbouring 1 complete prophage (**Figure 3.13**). A further 28.7% of host strains contained between 2 and 4 complete prophages. Interestingly, PHASTER identified 1 strain with a total of 6 complete prophages in its genome.

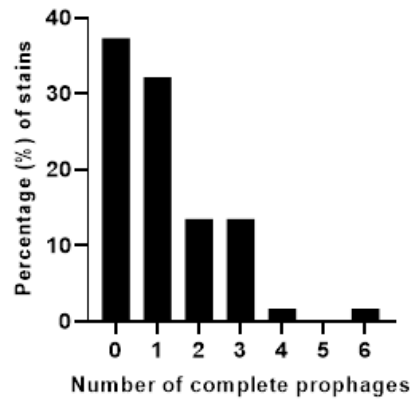


Figure 3.13 Frequency of complete prophages in 59 *S. pseudintermedius* genomes.

3.4 Discussion

Staphylococcus pseudintermedius is a pathogenic bacterium of concern within the veterinary sector, as it causes a wide range of diseases and multidrug resistant (MDR) *S. pseudintermedius* strains are becoming increasingly prevalent^{47,48}. Bacteriophage therapy has emerged in recent years as a potential solution for antibiotic resistant bacterial infections, and this chapter sought to detect novel bacteriophages that may be of clinical use against this emerging problem in canines.

Throughout this chapter, 60 *S. pseudintermedius* clinical isolates were collected from numerous canine infections, with varying degrees of antibiotic resistance, which were used for phage screening (**Figure 3.2, Figure 3.3, Figure 3.4**). At the commencement of this work, there were no publications describing the isolation of *S. pseudintermedius* phages, therefore, we optimised a phage screening protocol based on previous work⁴⁹, as shown in **Figure 3.5**. Contrary to older phage screening studies, our protocol added multiple bacterial hosts together within the same phage enrichment, as recent literature suggests that the addition of multiple hosts can result in phages with broader host ranges, in a more controlled manner³⁵. We also utilised various environmental and dog-associated samples to screen for phages, as previous studies have successfully isolated phages from soil, water, and animal samples^{26–32}. Using this optimised protocol, 6 rounds of phage screening were performed, with the isolation of phages from an enrichment containing soil and an enrichment containing a fur sample from healthy dogs (**Table 3.1**). Interestingly, phages from the two enrichments (soil and fur samples) each displayed two different plaque morphologies (**Figure**

3.6). There are many biological explanations that may explain variations in plaque size from the same phage, but generally difference in plaque size indicates distinct phages, therefore, unique plaques were extracted and treated as four individual phages (**Figure 3.6**)^{50,51}.

Whole Genome Sequencing revealed that the four phages isolated in this study appeared to vary in size and were unique in their genome sequence (**Table 3.2**). Whole genome analysis further revealed low nucleotide pairwise identity (0 - 50.6% nucleotide identity) between each of the four phages (**Table 3.2**). A nucleotide BLAST analysis demonstrated that 3 of the 4 phages matched *Staphylococcal* strains and matched regions of the bacterial genome that are likely prophages, which have not previously been isolated. Genome annotation maps of the four phages, revealed that the isolated phages contain some classical phage structural and functional genes, however, no lysis modules (e.g., holin, lysin, β -N-acetylglucosaminidase) were identified in any of the four phages, and no lysogeny modules were annotated, with the exception of one phage (**Figure 3.7**). As our phages were missing key phage gene modules, including endolysins and holins, it was likely that we did not have the full genome of the phages, therefore, a subsequent sequencing run would be required to obtain the full sequence. Although we had not yet obtained the full genome sequence of the phages, we continued with subsequent characterisation of the four phages.

Initial characterisation showed that the four phages all displayed a moderate-narrow host range of different host spectra, with Phage SP_10s displaying the broadest host range, able to lyse 53% of the *S. pseudintermedius* clinical isolates (**Table 3.3**). The remaining three phages were only able to lyse between 10 - 15% of the strains. Due to its broader host range and ease of passage, Phage SP_10s was chosen as the candidate phage for growth kinetics analysis. When Phage SP_10s was applied to the bacterial suspension of *S. pseudintermedius* CM16-0689, there was a significant amplification of PFU at 45 mins (**Figure 3.8A**), which correlated with the decline in bacterial OD, CFU, and cell-density (**Figure 3.8B, C, (D)**). These growth kinetics of Phage SP_10s are supported by the phenomenon known as ‘auto-dosing’, as phage titres increase when they come into contact with the bacterial infection site and taper off once the bacterial counts have diminished⁵². This can be beneficial for phage therapy as it can lower the initial dose or dose frequency required. As shown

in **Figure 3.9**, one application of Phage SP_10s at a MOI as low as 0.1 can reduce the bacterial growth, potentially due to the auto-dosing properties of the phage.

With the promising lytic abilities of the four phages observed during characterisation, a secondary sequencing run was performed to obtain the full genome sequence and to identify whether the phages contained lysogeny modules, as this would impact the future use of these phages. From the second WGS assembly of the four phage samples, it was observed that all samples were now dominated by the same 21.8 kb contig (**Table 3.5**). The contig had a G + C% of 35.6% and encoded 22 putative ORFs. A nucleotide BLAST search revealed this contig matched to *Staphylococcus pseudintermedius* strain 157588. When we ran the bacterial genome of this strain through PHASTER, we identified one complete prophage which was 48.5 kb in size, with a G + C% of 35.1%, encoding 75 putative ORFs. Using Mauve alignment, the newly dominant phage in our four phage samples showed a 100% pairwise nucleotide identity to the prophage from *S. pseudintermedius* strain 157588 (**Table 3.5**), with it also sharing an identical genome map (**Figure 3.10**). Importantly, the 21.8 kb phage that is now dominant in all four phage samples, was present at low levels in all four phage samples in the first sequencing run and showed 100% nucleotide identity to Phage SP_10s from the first sequencing run. Therefore, we hypothesise that the now dominant phage is a prophage from the host bacterial strain used to propagate our phages. We base this hypothesis on previous research which has shown the presence of integrase genes (genes essential for lysogeny), both in the isolated phage DNA and the bacterial host DNA, implying that the isolated phages were induced through the phage screening protocol, rather than isolated from the environmental samples ⁴⁹.

Previously it has been demonstrated that prophages can be induced through host cell stress (low nutrients or chemical exposure ^{49,53–58}, as shown in **Figure 3.1**. Therefore, we attempted to induce prophages from our host propagating strain, extract DNA for subsequent WGS and RFLP analysis, to determine whether the dominant phage in our preps was a prophage induced from our propagating strain. Prophages were successfully induced from the host propagating strain (*S. pseudintermedius* CM16-0689) by exposure to mitomycin-C, as shown by the appearance of plaques in **Figure 3.14**. However, given the time constraints due to COVID-19, we were unable to complete DNA

extraction or subsequent WGS and RFLP analysis. However, this work supports previous findings that future bacteriophage isolation protocols should include the use of bacterial strains that do not contain prophages within their genome, to avoid prophage contamination and domination within isolated phage preps⁵⁹.



Figure 3.14 Presence of plaques following mitomycin-c induction of *S. pseudintermedius* CM16-0689 (phage propagation strain).

TEM analysis of the dominant phage revealed that Phage SP_157588 displayed characteristics that resemble phages from the *Siphoviridae* family, notably, the presence of a long contractile tail (**Figure 3.11**). Although at the commencement of this work, no *S. pseudintermedius* phages had been described previously, during this study, three papers were published describing the isolation, characterisation and genomic analysis of *S. pseudintermedius* phages^{16–18}. One of these studies highlighted that due to the lack of *S. pseudintermedius* phages, they are rarely described morphologically, however, the majority of *S. pseudintermedius* phages belong to the *Siphoviridae* family, similarly to our Phage SP_157588¹⁷. Despite the morphological similarity with published *S. pseudintermedius* phages, the four phages we initially isolated had smaller genomes than previously published phages, and showed no preferential lysis towards antibiotic resistant strains or strains from particular infection sites, unlike phages described by Moodley and colleagues which showed preferential lysis towards MRSP strains^{16,18}.

More recently, based on the morphological, phylogenetic, and genomic analysis of all known non-*S. aureus* (*S. pseudintermedius*) phages, a novel genus within the *Siphoviridae* family was described, known as *Fibralongavirus*¹⁷. Importantly, the phages used to create a new genus were also temperate phages (prophages), as they contained lysogeny modules^{16,17}.

The presence of prophages within *S. pseudintermedius* genomes has been reported in several papers, however, the prevalence of such prophages has yet to be elucidated^{60–62}. Although we had 60

S. pseudintermedius isolates within our possession, none of the isolates have been sequenced, therefore, could not be used to screen for prophages. Instead, 59 *S. pseudintermedius* genomes extracted from the NCBI database were analysed for the presence of phage genes. Using computational techniques, a total of 221 prophages were identified, which varied from complete, incomplete, and questionable prophages, as shown in **Figure 3.12A**. The number of identified prophages per strain varied, as did the size of the prophages (**Figure 3.12B,C**), which has been previously shown in alternative bacterial species^{63–65}. Of the total prophages identified, the 70 prophages classified as ‘complete’ were of significant interest, as they have the ability to excise from the genome, transfer antibiotic resistance or virulence genes and enter the lytic lifecycle, as has been shown previously^{66–69}. Our findings in **Figure 3.13** show that 32.2% of the *S. pseudintermedius* strains had at least one complete phage within their genomes, with 28.7% of strains harbouring between 2–6 prophages. This is an important finding, especially in reference to phage isolation, where it is advised that only bacterial strains containing no inducible prophages should be used, to avoid prophage contaminating phage samples. This is also interesting as previous literature suggests that the insertion of prophages in ST71 *S. pseudintermedius* isolates may result in disruption to bacterial competence^{60,70}.

3.5 Conclusions

Despite isolating four novel phages throughout this study, the passaging of the four phages resulted in a dominating phage, likely a prophage induced from the host propagating strain, *S. pseudintermedius* CM16-0689. Morphological characterisation of the dominating phage revealed that Phage SP_157588 belonged to the *Siphoviridae* family. However, genomic analysis revealed that Phage SP_157588 possessed lysogeny modules, therefore, was not suitable for phage therapy moving forward. Within this chapter we also revealed the high prevalence of prophages within the genomes of clinical isolates of *S. pseudintermedius*, and the implications this may have on phage therapy moving forward. The findings throughout this chapter provide insights into the direction of phage therapy as a novel therapeutic against *S. pseudintermedius* infections in veterinary medicine.

3.6 Appendix

Table 3.6 Bacterial biochemical characterisation to confirm *Staphylococcus pseudintermedius* identification.

Biochemical analysis				
Strain	Clumping (CF)	VP	PYR	16s PCR ID
CM2009-0471	-	+	+	NT
CM2009-0754	-	+	+	NT
CM2009-0886	+	+	+	S. <i>pseudintermedius</i>
CM2009-0925	-	-	+	NT
CM2011-0079	-	+	+	NT
CM2011-0097	-	+	+	NT
CM2011-0112	-	+	+	NT
CM2011-0132	-	+	+	NT
CM2011-0195	-	+	+	NT
CM2011-0460	-	+	+	NT
CM2011-0653	-	+	+	NT
CM2011-0669	-	+	+	NT
CM2011-0671	-	+	+	S. <i>pseudintermedius</i>
CM2012-0093	-	+	+	NT
CM2012-0111	-	+	+	NT
CM2012-0169	-	+	+	NT
CM2012-0193	-	+	+	NT
CM2012-0201	-	+	+	NT
CM2012-0247	-	+	+	NT
CM2012-0405	-	-	+	S. <i>pseudintermedius</i>
CM2012-0503	-	+	+	S. <i>pseudintermedius</i>
CM2012-0529	-	+	+	NT
CM2012-0550	-	+	+	S. <i>pseudintermedius</i>
CM2012-0654	-	+	+	NT
CM2012-0745	-	+	+	NT

CM2013-0059 / 0	-	+	+	NT
CM2013-0140 / 0	-	+	+	NT
CM2013-0255 / 0	-	+	+	NT
CM2013-0320 / 1	-	+	+	NT
CM2013-0351 / 0	-	+	+	NT
CM2013-0367 / 0	-	+	+	NT
CM2013-0596 / 0	-	+	+	NT
CM2013-0910 / 1	-	+	+	NT
CM2014-0677 / 2	-	+	+	NT
				NT
CM2015-0358 / 0	-	+	+	NT
CM2015-0460 / 2	-	+	+	NT
CM2015-0597 / 2	-	-	+	NT
CM2015-0965 / 0	-	+	+	NT
CM2015-1096 / 0	-	-	+	S. <i>pseudintermedius</i>
CM2016-0216 / 2	-	+	+	NT
CM2016-0262 / 0	+	+	+	S. <i>pseudintermedius</i>
CM2016-0471 / 1	-	+	+	NT
CM2016-0568 / 2	+	+	+	NT
CM2016-0674 / 0	-	+	+	NT
CM2016-0689 / 0	-	+	+	NT
CM2016-0889 / 0	-	+	+	NT
CM2016-0917 / 2	-	+	+	NT
CM2016-0920 / 0	-	+	+	NT
CM2016-0933 / 0	-	+	+	NT
CM2016-0937 / 0	+	+	+	NT
CM2016-1008 / 0	+	+	+	NT
CM2016-1113 / 0	-	+	+	S. <i>pseudintermedius</i>
CM2017-0272 / 0	-	+	+	NT
CM2017-0292 / 0	-	+	+	S. <i>pseudintermedius</i>
CM2017-0410 / 0	-	+	+	NT

CM2017-0472 / 0	-	+	+	NT
CM2017-0580 / 1	-	-	+	NT
CM2017-0713 / 0	-	-	+	NT

Table 3.7 Genome annotations of Phage SP_157588.

Name	Minimum	Maximum	Length (bp)	Putative protein name from BLASTp	Match identity	NCBI accession	E-value
orf00001	20	442	423	transcriptional regulator [Staphylococcus pseudintermedius]	140/140(100%)	WP_105503558.1	2.00E-99
orf00002	569	874	306	MULTISPECIES: HNH endonuclease [Staphylococcus]	101/101(100%)	WP_100008560.1	5.00E-68
orf00003	1000	1383	384	hypothetical protein [Staphylococcus pseudintermedius]	127/127(100%)	WP_140232678.1	9.00E-86
orf00004	1370	3037	1668	MULTISPECIES: terminase large subunit [Staphylococcus]	555/555(100%)	WP_101485395.1	0
orf00005	3105	4235	1131	MULTISPECIES: phage portal protein [Staphylococcus]	376/376(100%)	WP_115903434.1	0
orf00006	4219	4911	693	Clp protease-like protein [Staphylococcus phage phiSP15-1]	229/230(99%)	AZB66525.1	6.00E-163
orf00007	4924	6123	1200	MULTISPECIES: phage major capsid protein [Staphylococcus]	399/399(100%)	WP_096586310.1	0
orf00008	6141	6428	288	MULTISPECIES: phage gp6-like head-tail	95/95(100%)	WP_101485386.1	6.00E-63

				connector protein [Staphylococcus]			
orf00009	6412	6780	369	MULTISPECIES: hypothetical protein [Staphylococcus]	122/122(100%)	WP_115898112.1	2.00E-84
orf00010	6770	7159	390	MULTISPECIES: HK97 gp10 family phage protein [Staphylococcus]	129/129(100%)	WP_110158924.1	2.00E-87
orf00011	7180	7575	396	hypothetical protein [Staphylococcus pseudintermedius]	131/131(100%)	EGQ0317854.1	2.00E-90
orf00012	7588	8211	624	MULTISPECIES: phage tail protein [Staphylococcus]	207/207(100%)	WP_101485382.1	4.00E-148
orf00013	8233	8412	180	MULTISPECIES: hypothetical protein [Staphylococcus]	59/59(100%)	WP_101485381.1	3.00E-33
orf00014	8472	8843	372	MULTISPECIES: hypothetical protein [Staphylococcus]	123/123(100%)	WP_101485380.1	2.00E-84
orf00015	8903	9046	144	MULTISPECIES: hypothetical protein [Staphylococcus]	47/47(100%)	WP_168250651.1	4.00E-24
orf00017	9063	14009	4947	phage tail tape measure protein [Staphylococcus pseudintermedius]	1648/1648(100%)	WP_129950955.1	0
orf00018	14006	15514	1509	phage tail family protein [Staphylococcus pseudintermedius]	502/502(100%)	WP_129950954.1	0
orf00019	15530	19627	4098	hypothetical protein [Staphylococcus pseudintermedius]	1358/1365(99%)	EGQ1793636.1	0

orf00020	19617	19775	159	hypothetical protein [Staphylococcus pseudintermedius]	52/52(100%)	WP_020219680.1	4.00E-27
orf00021	19816	20118	303	hypothetical protein [Staphylococcus pseudintermedius]	100/100(100%)	WP_129950953.1	7.00E-66
orf00023	20560	20955	396	MULTISPECIES: hypothetical protein [Staphylococcus intermedius group]	131/131(100%)	WP_020219677.1	7.00E-90
orf00024	21002	21250	249	MULTISPECIES: PTS mannose transporter subunit IID [Staphylococcus intermedius group]	82/82(100%)	WP_086429242.1	4.00E-51

Table 3.8 Genome annotations of Phage SP_10L.

Name	Minimum	Maximum	Length	Putative protein name from BLASTp	match identity	NCBI accession	E-value
orf00001	617	865	249	MULTISPECIES: hypothetical protein [Staphylococcus]	82/82(100%)	WP_015978015.1	5.00E-51
orf00002	992	1291	300	DUF2951 family protein [Staphylococcus pseudintermedius]	99/99(100%)	WP_037542783.1	1.00E-63
orf00003	1300	1575	276	hypothetical protein [Staphylococcus pseudintermedius]	91/91(100%)	WP_020220196.1	4.00E-60

orf00004	1622	1759	138	MULTISPECIES: hypothetical protein [Staphylococcus intermedius group]	45/45(100%)	WP_020220195.1	2.00E-22
orf00005	1740	5261	3522	hypothetical protein [Staphylococcus pseudintermedius]	1172/1173(99%)	EGQ3800392.1	0.00E+00
orf00006	5277	6767	1491	tail protein [Staphylococcus phage SpT99F3]	496/496(100%)	APD20008.1	0.00E+00
orf00008	6767	11077	4311	phage tail tape measure protein [Staphylococcus pseudintermedius]	1435/1436(99%)	EGQ3800390.1	0.00E+00
orf00009	11094	11234	141	hypothetical protein [Staphylococcus pseudintermedius]	46/46(100%)	WP_096533186.1	4.00E-24
orf00010	11276	11722	447	hypothetical protein [Staphylococcus pseudintermedius]	148/148(100%)	WP_065354471.1	2.00E-98
orf00011	11789	12733	945	hypothetical protein [Staphylococcus pseudintermedius]	313/314(99%)	EGQ3800387.1	0
orf00012	12745	13107	363	hypothetical protein [Staphylococcus pseudintermedius]	120/120(100%)	EGQ1650254.1	5.00E-82
orf00013	13104	13481	378	HK97 gp10 family phage protein [Staphylococcus pseudintermedius]	125/125(100%)	EGQ3800385.1	1.00E-87
orf00014	13481	13813	333	head-tail adaptor protein [Staphylococcus pseudintermedius]	110/110(100%)	WP_103926969.1	1.00E-74

orf00015	13794	14084	291	DNA packaging protein [Staphylococcus phage phiSP38-1]	96/96(100%)	AZB66599.1	4.00E-64
orf00016	14094	14252	159	MULTISPECIES: hypothetical protein [Staphylococcus intermedius group]	52/52(100%)	WP_020220186.1	5.00E-27
orf00017	14269	15489	1221	phage major capsid protein [Staphylococcus pseudintermedius]	406/406(100%)	WP_105503562.1	0
orf00018	15568	16140	573	HK97 family phage prohead protease [Staphylococcus pseudintermedius]	190/190(100%)	WP_037542765.1	5.00E-138
orf00019	16115	17386	1272	phage portal protein [Staphylococcus pseudintermedius]	422/423(99%)	WP_180291811.1	0
orf00020	17392	17589	198	hypothetical protein [Staphylococcus pseudintermedius]	65/65(100%)	WP_037542762.1	8.00E-35
orf00021	17601	19301	1701	terminase [Staphylococcus pseudintermedius]	566/566(100%)	EGQ3800378.1	0
orf00022	19301	19771	471	phage terminase small subunit P27 family [Staphylococcus pseudintermedius]	156/156(100%)	WP_037542759.1	3.00E-110
orf00023	19866	20222	357	HNH endonuclease [Staphylococcus pseudintermedius]	118/118(100%)	WP_065354480.1	3.00E-82
orf00024	20228	20605	378	hypothetical protein [Staphylococcus pseudintermedius]	125/125(100%)	EGQ3367133.1	8.00E-82

orf00025	20732	21154	423	transcriptional regulator [Staphylococcus pseudintermedius]	140/140(100%)	EGQ3800374.1	6.00E-100
orf00026	21166	21342	177	MULTISPECIES: DUF1514 family protein [Staphylococcus]	58/58(100%)	WP_075773683.1	1.00E-31
orf00027	21345	21647	303	hypothetical protein [Staphylococcus pseudintermedius]	100/100(100%)	EGQ4530661.1	1.00E-67

Table 3.9 Genome annotations of Phage SP_22L.

Name	Minimum	Maximum	Length	Putative protein name from BLASTp	Match identity	NCBI accession	E-value
orf00001	636	956	321	hypothetical protein [Staphylococcus felis]	106/106(100%)	WP_115902526.1	1.00E-78
orf00002	1094	1384	291	MULTISPECIES: HNH endonuclease [Staphylococcus]	96/96(100%)	WP_099987251.1	2.00E-66
orf00003	1377	1658	282	MULTISPECIES: head- tail connector protein [Staphylococcus]	93/93(100%)	WP_099987253.1	5.00E-60
orf00004	1717	2946	1230	phage major capsid protein [Staphylococcus pseudintermedius]	409/409(100%)	WP_129924562.1	0
orf00005	2948	3514	567	HK97 family phage prohead protease [Staphylococcus pseudintermedius]	188/188(100%)	WP_096636614.1	1.00E-136
orf00006	3501	4745	1245	HK97 family phage portal protein	402/414(97%)	EZW77330.1	0

				[Staphylococcus aureus 7-B-1]			
orf00007	4816	5157	342	MULTISPECIES: hypothetical protein [Staphylococcus]	113/113(100%)	WP_015728774.1	2.00E-77
orf00008	5465	7837	2373	DNA primase [Staphylococcus pseudintermedius]	789/790(99%)	WP_140230449.1	0
orf00009	7935	8237	303	DUF1474 family protein [Staphylococcus pseudintermedius]	100/100(100%)	WP_110168747.1	4.00E-68
orf00010	8241	8657	417	hypothetical protein [Staphylococcus pseudintermedius]	138/138(100%)	WP_096636609.1	1.00E-92
orf00011	8659	8862	204	pathogenicity island protein [Staphylococcus pseudintermedius]	67/67(100%)	WP_096636608.1	4.00E-40
orf00012	8874	9092	219	helix-turn-helix transcriptional regulator [Staphylococcus pseudintermedius]	72/72(100%)	WP_129955394.1	3.00E-45
orf00013	9272	10105	834	MULTISPECIES: helix-turn-helix transcriptional regulator [Staphylococcus]	276/277(99%)	WP_099987271.1	0
orf00014	10095	11201	1107	site-specific integrase [Staphylococcus pseudintermedius]	368/368(100%)	WP_110168746.1	0
orf00015	11456	11824	369	MULTISPECIES: hypothetical protein [Staphylococcus]	122/122(100%)	WP_015728782.1	3.00E-81

orf00016	11931	12239	309	MULTISPECIES: phage head closure protein [Staphylococcus]	102/102(100%)	WP_096636618.1	1.00E-68
orf00017	12397	13362	966	terminase large subunit [Staphylococcus pseudintermedius]	321/321(100%)	WP_096636617.1	0

Table 3.10 Genome annotations of Phage SP_22s

Name	Minimum	Maximum	Length	Putative protein name from BLASTp	match identity	NCBI accession	E-value
orf00001	197	595	399	hypothetical protein [Staphylococcus pseudintermedius]	131/131(100%)	EGQ1603774.1	5.00E-90
orf00002	592	843	252	hypothetical protein [Staphylococcus pseudintermedius]	83/83(100%)	HAR6210913.1	2.00E-54
orf00003	840	1190	351	hypothetical protein [Staphylococcus pseudintermedius]	116/116(100%)	WP_203152605.1	4.00E-76
orf00004	1187	1372	186	hypothetical protein [Staphylococcus pseudintermedius]	61/61(100%)	WP_203152604.1	8.00E-36
orf00005	1350	2309	960	DNA (cytosine-5-)-methyltransferase [Staphylococcus pseudintermedius]	319/319(100%)	WP_203152603.1	0
orf00006	2333	2794	462	DUF3310 domain-containing protein [Staphylococcus pseudintermedius]	153/153(100%)	WP_110160704.1	8.00E-107

orf00007	2794	2958	165	hypothetical protein [Staphylococcus phage phiSP38-1]	54/54(100%)	AZB66617.1	4.00E-31
orf00008	2955	3275	321	hypothetical protein [Staphylococcus pseudintermedius]	106/106(100%)	WP_103926857.1	2.00E-70
orf00009	3288	3506	219	hypothetical protein [Staphylococcus pseudintermedius]	72/72(100%)	WP_103926858.1	3.00E-44
orf00010	3490	3921	432	RusA family crossover junction endodeoxyribonuclease [Staphylococcus pseudintermedius]	142/143(99%)	WP_103926859.1	9.00E-100
orf00011	3905	4126	222	hypothetical protein [Staphylococcus pseudintermedius]	73/73(100%)	WP_096536666.1	8.00E-46
orf00012	4123	5367	1245	AAA family ATPase [Staphylococcus pseudintermedius]	414/414(100%)	WP_203157255.1	0
orf00013	5360	5707	348	MULTISPECIES: hypothetical protein [Staphylococcus intermedius group]	115/115(100%)	WP_065354055.1	5.00E-77
orf00014	5712	6458	747	DnaD domain protein [Staphylococcus pseudintermedius]	248/248(100%)	WP_203157257.1	0
orf00015	6451	7125	675	hypothetical protein [Staphylococcus pseudintermedius]	223/224(99%)	EGQ3545839.1	2.00E-166
orf00016	7134	7328	195	MULTISPECIES: hypothetical protein [Staphylococcus]	64/64(100%)	WP_015728806.1	8.00E-39

orf00017	7309	7746	438	MULTISPECIES: single-stranded DNA- binding protein [Staphylococcus]	145/145(100%)	WP_015728805.1	4.00E-100
orf00018	7746	8414	669	MULTISPECIES: ERF family protein [Staphylococcus intermedius group]	222/222(100%)	WP_015728804.1	5.00E-161
orf00019	8415	8900	486	MULTISPECIES: siphovirus Gp157 family protein [Staphylococcus]	161/161(100%)	WP_060830236.1	3.00E-112
orf00020	8884	9108	225	hypothetical protein [Staphylococcus schleiferi]	74/74(100%)	WP_060830237.1	1.00E-43
orf00021	9120	9380	261	DUF1108 family protein [Staphylococcus pseudintermedius]	86/86(100%)	EGQ1274869.1	2.00E-53

Table 3.11 Genome annotations of Phage SP_10s.

Name	Minimum	Maximum	Length	Putative protein name from BLASTp	match identity	NCBI accession	E-value
orf00001	617	865	249	MULTISPECIES: PTS mannose transporter subunit IID [Staphylococcus intermedius group]	82/82(100%)	WP_086429242.1	4.00E-51
orf00002	912	1307	396	MULTISPECIES: hypothetical protein	131/131(100%)	WP_020219677.1	7.00E-90

				[Staphylococcus intermedius group]			
orf00004	1749	2051	303	hypothetical protein [Staphylococcus pseudintermedius]	100/100(100%)	WP_129950953.1	7.00E-66
orf00005	2092	2250	159	hypothetical protein [Staphylococcus pseudintermedius]	52/52(100%)	WP_020219680.1	4.00E-27
orf00006	2240	6337	4098	Phage protein [Staphylococcus pseudintermedius]	1358/1365(99%)	ANS89870.1	0
orf00007	6353	7861	1509	phage tail family protein [Staphylococcus pseudintermedius]	502/502(100%)	WP_129950954.1	0
orf00009	7858	12804	4947	phage tail tape measure protein [Staphylococcus pseudintermedius]	1648/1648(100%)	WP_129950955.1	0
orf00010	12821	12964	144	MULTISPECIES: hypothetical protein [Staphylococcus]	47/47(100%)	WP_168250651.1	4.00E-24
orf00011	13024	13395	372	MULTISPECIES: hypothetical protein [Staphylococcus]	123/123(100%)	WP_101485380.1	2.00E-84
orf00012	13455	13634	180	MULTISPECIES: hypothetical protein [Staphylococcus]	59/59(100%)	WP_101485381.1	3.00E-33
orf00013	13656	14279	624	MULTISPECIES: phage tail protein [Staphylococcus]	207/207(100%)	WP_101485382.1	4.00E-148
orf00014	14292	14687	396	hypothetical protein [Staphylococcus pseudintermedius]	131/131(100%)	EGQ0317854.1	2.00E-90

orf00015	14708	15097	390	MULTISPECIES: HK97 gp10 family phage protein [Staphylococcus]	129/129(100%)	WP_110158924.1	2.00E-87
orf00016	15087	15455	369	MULTISPECIES: hypothetical protein [Staphylococcus]	122/122(100%)	WP_115898112.1	2.00E-84
orf00017	15439	15726	288	MULTISPECIES: phage gp6-like head-tail connector protein [Staphylococcus]	95/95(100%)	WP_101485386.1	6.00E-63
orf00018	15744	16943	1200	MULTISPECIES: phage major capsid protein [Staphylococcus]	399/399(100%)	WP_096586310.1	0
orf00019	16956	17648	693	Clp protease-like protein [Staphylococcus phage phiSP15-1]	229/230(99%)	AZB66525.1	6.00E-163
orf00020	17632	18762	1131	MULTISPECIES: phage portal protein [Staphylococcus]	376/376(100%)	WP_115903434.1	0
orf00021	18830	20497	1668	MULTISPECIES: terminase large subunit [Staphylococcus]	555/555(100%)	WP_101485395.1	0
orf00022	20484	20867	384	hypothetical protein [Staphylococcus pseudintermedius]			

Table 3.12 Genome annotations of prophage from *S. pseudintermedius* strain 157588.

Name	Minimum	Maximum	Length	Putative protein name from BLASTp	match identity	NCBI accession	E-value
orf00001	299	499	201	MULTISPECIES: hypothetical protein [Staphylococcus]	66/66(100%)	WP_015728984.1	4.00E-39
orf00003	1057	2517	1461	peptidoglycan DD-metalloendopeptidase family protein [Staphylococcus pseudintermedius]	486/486(100%)	WP_129950952.1	0
orf00004	2519	2767	249	MULTISPECIES: PTS mannose transporter subunit IID [Staphylococcus intermedius group]	82/82(100%)	WP_086429242.1	4.00E-51
orf00005	2814	3209	396	MULTISPECIES: hypothetical protein [Staphylococcus intermedius group]	131/131(100%)	WP_020219677.1	7.00E-90
orf00006	3193	3615	423	MULTISPECIES: hypothetical protein [Staphylococcus intermedius group]	140/140(100%)	WP_086429241.1	2.00E-96
orf00007	3653	3955	303	hypothetical protein [Staphylococcus pseudintermedius]	100/100(100%)	WP_103891590.1	1.00E-65
orf00008	3996	4154	159	hypothetical protein [Staphylococcus pseudintermedius]	52/52(100%)	WP_020219680.1	4.00E-27

orf00009	4144	8721	4578	phage tail protein [Staphylococcus pseudintermedius]	1525/1525(100%)	WP_208664551.1	0
orf00010	8737	10245	1509	phage tail family protein [Staphylococcus pseudintermedius]	502/502(100%)	WP_129950954.1	0
orf00011	10242	15188	4947	phage tail tape measure protein [Staphylococcus pseudintermedius]	1648/1648(100%)	WP_140232677.1	0
orf00012	15205	15348	144	MULTISPECIES: hypothetical protein [Staphylococcus]	47/47(100%)	WP_168250651.1	4.00E-24
orf00013	15408	15779	372	MULTISPECIES: hypothetical protein [Staphylococcus]	123/123(100%)	WP_101485380.1	2.00E-84
orf00014	15839	16018	180	MULTISPECIES: hypothetical protein [Staphylococcus]	59/59(100%)	WP_101485381.1	3.00E-33
orf00015	16040	16663	624	phage tail protein [Staphylococcus pseudintermedius]	207/207(100%)	WP_168250653.1	4.00E-148
orf00016	16676	17071	396	hypothetical protein [Staphylococcus pseudintermedius]	131/131(100%)	EGQ0317854.1	2.00E-90
orf00017	17092	17481	390	MULTISPECIES: HK97 gp10 family phage protein [Staphylococcus]	129/129(100%)	WP_110158924.1	2.00E-87
orf00018	17471	17839	369	MULTISPECIES: hypothetical protein [Staphylococcus]	122/122(100%)	WP_115898112.1	2.00E-84
orf00019	17823	18110	288	ULTISPECIES: phage gp6-like head-tail	95/95(100%)	WP_101485386.1	6.00E-63

				connector protein [Staphylococcus]			
orf00020	18128	19327	1200	MULTISPECIES: phage major capsid protein [Staphylococcus]	399/399(100%)	WP_096586310.1	0
orf00021	19340	20032	693	Clp protease-like protein [Staphylococcus phage phiSP15-1]	229/230(99%)	AZB66525.1	6.00E-163
orf00022	20016	21194	1179	MULTISPECIES: phage portal protein [Staphylococcus]	392/392(100%)	WP_115903434.1	0
orf00023	21214	22881	1668	MULTISPECIES: terminase large subunit [Staphylococcus]	555/555(100%)	WP_101485395.1	0
orf00024	22868	23251	384	hypothetical protein [Staphylococcus pseudintermedius]	127/127(100%)	WP_140232678.1	9.00E-86
orf00025	23378	23683	306	MULTISPECIES: HNH endonuclease [Staphylococcus]	101/101(100%)	WP_100008560.1	5.00E-68
orf00026	23810	24232	423	transcriptional regulator [Staphylococcus pseudintermedius]	140/140(100%)	WP_194178515.1	5.00E-100
orf00027	24244	24420	177	MULTISPECIES: DUF1514 family protein [Staphylococcus]	58/58(100%)	WP_075773683.1	1.00E-31
orf00028	24423	24725	303	hypothetical protein [Staphylococcus pseudintermedius]	100/100(100%)	EGQ4530661.1	1.00E-67
orf00029	24725	24868	144	hypothetical protein [Staphylococcus pseudintermedius]	47/47(100%)	WP_180293829.1	1.00E-24

orf00030	24865	25083	219	DUF1381 domain-containing protein [Staphylococcus pseudintermedius]	72/72(100%)	WP_105503557.1	5.00E-44
orf00031	25080	25544	465	class I SAM-dependent methyltransferase [Staphylococcus pseudintermedius]	154/154(100%)	WP_202993536.1	2.00E-110
orf00032	25581	26111	531	dUTP diphosphatase [Staphylococcus pseudintermedius]	176/176(100%)	WP_194178516.1	6.00E-125
orf00033	26115	26438	324	hypothetical protein [Staphylococcus pseudintermedius]	107/107(100%)	WP_194178517.1	5.00E-71
orf00034	26460	26621	162	hypothetical protein [Staphylococcus pseudintermedius]	53/53(100%)	WP_194178518.1	5.00E-28
orf00035	26622	26906	285	MULTISPECIES: hypothetical protein [Staphylococcus]	85/85(100%)	WP_015728818.1	5.00E-53
orf00036	26879	27262	384	hypothetical protein [Staphylococcus pseudintermedius]	127/127(100%)	WP_194178519.1	6.00E-86
orf00037	27262	27510	249	hypothetical protein SpT5_042 [Staphylococcus phage SpT5]	82/82(100%)	APD19790.1	1.00E-53
orf00038	27510	27761	252	hypothetical protein [Staphylococcus pseudintermedius]	83/83(100%)	WP_020219706.1	4.00E-52
orf00039	27758	27943	186	hypothetical protein [Staphylococcus pseudintermedius]	61/61(100%)	WP_189722262.1	4.00E-36

orf00040	27947	28198	252	hypothetical protein [Staphylococcus pseudintermedius]	83/83(100%)	WP_015978017.1	3.00E-52
orf00041	28195	28680	486	DUF3310 domain- containing protein [Staphylococcus pseudintermedius]	161/161(100%)	WP_037543621.1	5.00E-112
orf00042	28680	28844	165	hypothetical protein [Staphylococcus pseudintermedius]	54/54(100%)	WP_180291855.1	4.00E-31
orf00043	28841	29149	309	MULTISPECIES: hypothetical protein [Staphylococcus]	102/102(100%)	WP_037543623.1	2.00E-68
orf00044	29160	29378	219	hypothetical protein [Staphylococcus pseudintermedius]	72/72(100%)	WP_037543625.1	2.00E-44
orf00045	29371	29793	423	RusA family crossover junction endodeoxyribonuclease [Staphylococcus pseudintermedius]	140/140(100%)	WP_103926859.1	7.00E-98
orf00046	29777	29998	222	hypothetical protein [Staphylococcus pseudintermedius]	73/73(100%)	WP_037543628.1	5.00E-46
orf00047	29995	31239	1245	AAA family ATPase [Staphylococcus pseudintermedius]	414/414(100%)	WP_037543631.1	0
orf00048	31232	31573	342	hypothetical protein [Staphylococcus pseudintermedius]	113/113(100%)	WP_037543633.1	5.00E-75
orf00049	31570	32367	798	phage replisome organizer N-terminal domain-containing	265/265(100%)	WP_037543635.1	0

				protein [Staphylococcus pseudintermedius]			
orf00050	32367	33035	669	hypothetical protein [Staphylococcus pseudintermedius]	222/222(100%)	WP_037543638.1	6.00E-166
orf00051	33049	33639	591	single-stranded DNA-binding protein [Staphylococcus pseudintermedius]	196/196(100%)	WP_037543641.1	2.00E-137
orf00052	33636	34265	630	ERF family protein [Staphylococcus pseudintermedius]	209/209(100%)	WP_208664552.1	3.00E-151
orf00053	34262	34747	486	siphovirus Gp157 family protein [Staphylococcus pseudintermedius]	161/161(100%)	WP_037543647.1	3.00E-112
orf00054	34731	34955	225	MULTISPECIES: hypothetical protein [Staphylococcus intermedius group]	74/74(100%)	WP_019167935.1	9.00E-44
orf00055	34967	35227	261	DUF1108 family protein [Staphylococcus pseudintermedius]	86/86(100%)	WP_140223646.1	3.00E-54
orf00057	35485	35808	324	DUF771 domain-containing protein [Staphylococcus pseudintermedius]	107/107(100%)	WP_100008589.1	6.00E-71
orf00058	35878	36087	210	hypothetical protein [Staphylococcus pseudintermedius]	69/69(100%)	WP_100008588.1	1.00E-41
orf00059	36080	36220	141	hypothetical protein [Staphylococcus pseudintermedius]	46/46(100%)	WP_100008587.1	2.00E-21

orf00060	36257	36478	222	MULTISPECIES: hypothetical protein [Staphylococcus]	73/73(100%)	WP_100008586.1	7.00E-46
orf00061	36475	36978	504	MULTISPECIES: ORF6C domain- containing protein [Staphylococcus]	167/167(100%)	WP_065520554.1	2.00E-117
orf00062	36991	37872	882	MULTISPECIES: DUF3102 domain- containing protein [Staphylococcus]	293/293(100%)	WP_065520555.1	0
orf00063	37929	38264	336	MULTISPECIES: hypothetical protein [Staphylococcus]	111/111(100%)	WP_020219728.1	1.00E-73
orf00064	38250	38483	234	DUF2829 domain- containing protein [Staphylococcus pseudintermedius]	77/77(100%)	WP_100008585.1	1.00E-49
orf00066	38495	38710	216	transcriptional regulator [Staphylococcus pseudintermedius]	71/71(100%)	WP_065354506.1	1.00E-42
orf00067	38905	39597	693	helix-turn-helix transcriptional regulator [Staphylococcus pseudintermedius]	230/230(100%)	WP_065354507.1	5.00E-166
orf00068	39653	40150	498	hypothetical protein [Staphylococcus pseudintermedius]	165/165(100%)	WP_194178521.1	2.00E-112
orf00069	40197	41180	984	DUF3644 domain- containing protein [Staphylococcus pseudintermedius]	327/327(100%)	WP_100008583.1	0

orf00070	41355	42380	1026	site-specific integrase [Staphylococcus pseudintermedius]	341/341(100%)	WP_100008582.1	0
orf00071	42711	42887	177	hypothetical protein [Staphylococcus pseudintermedius]	58/58(100%)	WP_194178560.1	1.00E-31
orf00072	42880	43209	330	MULTISPECIES: hypothetical protein [Staphylococcus]	109/109(100%)	WP_096535802.1	1.00E-69
orf00073	43225	43749	525	MULTISPECIES: hypothetical protein [Staphylococcus]	174/174(100%)	WP_015728980.1	4.00E-121
orf00074	44113	44787	675	IS6 family transposase [Staphylococcus pseudintermedius]	224/224(100%)	WP_015728979.1	6.00E-165
orf00075	44907	45599	693	MULTISPECIES: Crp/Fnr family transcriptional regulator [Staphylococcaceae]	230/230(100%)	WP_011867731.1	5.00E-170
orf00076	45616	46167	552	DNA starvation/stationary phase protection protein [Staphylococcaceae]	183/183(100%)	WP_015728978.1	8.00E-131
orf00077	46169	46405	237	MULTISPECIES: heavy-metal-associated domain-containing protein [Staphylococcus]	78/78(100%)	WP_015728977.1	3.00E-47
orf00078	46469	48319	1851	heavy metal translocating P-type ATPase [Staphylococcus pseudintermedius]	616/616(100%)	WP_065354411.1	0

Table 3.13 Prophages identified from 59 *S. pseudintermedius* genome sequences.

Prophage	Prophage length	Completeness	# Total protein	Region position (bp)	Most common phage	GC%	Phage proteins identified
1. <i>Staphylococcus pseudintermedius</i> strain MAD401 chromosome							
1	45.5Kb	intact	72	320035-365556	PHAGE_Staphy_SA7_NC_048658(18)	35.00%	transposase, integrase, lysin, recombinase, tail
2	7.9Kb	incomplete	15	1294538-1302461	PHAGE_Burkho_Bcep22_NC_005262(1)	37.10%	transposase
3	22.1Kb	incomplete	12	1333689-1355831	PHAGE_Staphy_vB_SpsS_QT1_NC_048192(4)	35.63%	head, tail
4	15.6Kb	incomplete	20	1812410-1828106	PHAGE_Staphy_187_NC_007047(3)	35.94%	head, tail
5	45.2Kb	intact	72	2014059-2059330	PHAGE_Staphy_IME_SA4_NC_029025(20)	35.29%	tail, head, capsid, portal, terminase, lysin, integrase
6	59.8Kb	incomplete	72	2108508-2168371	PHAGE_Staphy_vB_SpsS_QT1_NC_048192(11)	35.09%	capsid, tail, lysin
7	49.1Kb	intact	58	2483669-2532769	PHAGE_Staphy_187_NC_007047(12)	36.80%	protease, capsid, tail, head, portal, terminase, integrase
2. <i>Staphylococcus pseudintermedius</i> strain FDAARGOS_1073 chromosome							
1	48.7Kb	intact	68	89512-138221	PHAGE_Staphy_StauST398_2_NC_021323(11)	34.24%	integrase, tail, capsid, portal
2	15.7Kb	incomplete	20	335362-351158	PHAGE_Staphy_187_NC_007047(3)	35.76%	head, tail
3	52.3Kb	intact	67	846045-898437	PHAGE_Staphy_187_NC_007047(23)	36.19%	tail, terminase, capsid, integrase, recombinase
4	27.4Kb	incomplete	13	1743643-1771092	PHAGE_Staphy_PT1028_NC_007045(5)	36.99%	integrase
5	45.8Kb	questionable	56	2228631-2274473	PHAGE_Staphy_187_NC_007047(12)	36.57%	tail, integrase, terminase, protease
6	44.3Kb	intact	60	2578512-2622879	PHAGE_Staphy_SA7_NC_048658(17)	36.15%	lysine, tail, head
3. <i>Staphylococcus pseudintermedius</i> strain ME4692 chromosome							

1	23.2Kb	incomplete	13	102121-125359	PHAGE_Staphy_PT1028_NC_007045(5)	37.65%	integrase
2	44.5Kb	intact	55	593300-637848	PHAGE_Staphy_187_NC_007047(12)	36.72%	integrase, tail, terminase, portal, head, capsid, protease
3	30.6Kb	intact	31	651049-681728	PHAGE_Clostr_phiCDHM14_NC_048665(3)	35.11%	integrase, tail, portal, head, capsid, terminase
4	46.9Kb	questionable	59	1145052-1192023	PHAGE_Staphy_SA7_NC_048658(15)	36.23%	recombinase, tail
5	48.6Kb	intact	71	1655021-1703651	PHAGE_Staphy_vB_SpsS_QT1_NC_048192(11)	34.06%	tail, head, capsid
6	13Kb	incomplete	9	2720568-2733591	PHAGE_Staphy_SPbeta_like_NC_029119(3)	31.93%	integrase, tail
4. <i>Staphylococcus pseudintermedius</i> strain VTH737 chromosome							
1	48.8Kb	intact	66	20479-69320	PHAGE_Staphy_187_NC_007047(22)	36.11%	protease, tail, terminase, capsid, integrase, recombinase
2	35.8Kb	incomplete	13	863909-899781	PHAGE_Staphy_PT1028_NC_007045(5)	37.20%	integrase, capsid
3	22.1Kb	incomplete	12	1657284-1679424	PHAGE_Staphy_vB_SpsS_QT1_NC_048192(4)	35.64%	head, tail
4	6.4Kb	incomplete	10	1760647-1767059	PHAGE_Staphy_SPbeta_like_NC_029119(5)	34.37%	portal, head, transposase
5	49.3Kb	intact	60	1941428-1990773	PHAGE_Staphy_StauST398_2_NC_021323(11)	34.26%	integrase, capsid, tail, portal
6	14.3Kb	incomplete	20	2187562-2201923	PHAGE_Staphy_Ipla88_NC_011614(2)	35.18%	head, portal
5. <i>Staphylococcus pseudintermedius</i> strain MAD568 chromosome							
1	61.7Kb	intact	67	599275-661003	PHAGE_Staphy_187_NC_007047(23)	36.70%	integrase, tail, recombinase, capsid
2	7.9Kb	incomplete	15	1010359-1018291	PHAGE_Staphy_vB_SauM_Remus_NC_022090(1)	37.10%	transposase
3	23.2Kb	incomplete	13	2536888-2560151	PHAGE_Staphy_PT1028_NC_007045(5)	37.65%	integrase

6. <i>Staphylococcus pseudintermedius</i> strain MAD627 chromosome							
1	18.8Kb	incomplete	10	628738-647601	PHAGE_Staphy_phiPV83_NC_002486(2)	36.54%	integrase, head
2	31Kb	incomplete	19	1097861-1128929	PHAGE_Staphy_187_NC_007047(3)	35.76%	head, integrase
3	34.9Kb	questionable	35	1657209-1692178	PHAGE_Clostr_phiCDHM14_NC_048665(3)	35.09%	head, terminase, capsid, portal, integrase
7. <i>Staphylococcus pseudintermedius</i> strain DG099 chromosome							
1	7.9Kb	incomplete	15	967615-975545	PHAGE_Burkho_Bcep22_NC_005262(1)	37.06%	transposase
2	51.6Kb	intact	66	1015545-1067229	PHAGE_Staphy_StauST398_2_NC_021323(10)	34.42%	tail, recombinase, capsid, portal, head
3	22.1Kb	incomplete	11	2551546-2573687	PHAGE_Strept_315.6_NC_004589(1)	36.49%	integrase
8. <i>Staphylococcus pseudintermedius</i> strain 53_60 chromosome							
1	14.4Kb	incomplete	19	241439-255852	PHAGE_Paenib_Xenia_NC_028837(3)	32.95%	transposase
2	30.7Kb	incomplete	10	1810451-1841153	PHAGE_Staphy_phi7247PVL_NC_048624(2)	32.52%	head
3	8.9Kb	incomplete	11	2486835-2495783	PHAGE_Enterof_AA91_ss_NC_022750(2)	32.65%	tail, transposase
9. <i>Staphylococcus pseudintermedius</i> strain 51_92 chromosome							
1	30.9Kb	incomplete	18	39180-70096	PHAGE_Staphy_187_NC_007047(3)	35.66%	head, integrase
10. <i>Staphylococcus pseudintermedius</i> strain 53_88 chromosome							
1	18.1Kb	incomplete	20	93750-111880	PHAGE_Staphy_PT1028_NC_007045(2)	32.69%	integrase, terminase, tail
2	8.9Kb	incomplete	9	575392-584343	PHAGE_Staphy_phiIBB_SEP1_NC_041928(1)	32.54%	tail, transposase

3	50.5Kb	intact	60	1201841-1252408	PHAGE_Staphy_2638A_NC_007051(21)	34.91%	integrase, lysin, portal, head, tail
4	8.5Kb	incomplete	12	2300559-2309104	PHAGE_Arthro_Sonali_NC_048152(2)	37.61%	transposase, tail
11. <i>Staphylococcus pseudintermedius</i> strain 49_44 chromosome							
1	8.5Kb	incomplete	10	85805-94322	PHAGE_Halocy_JM_2012_NC_017975(1)	36.43%	transposase
2	45.3Kb	intact	64	1832211-1877536	PHAGE_Staphy_187_NC_007047(13)	35.75%	tail, head, capsid, virion, portal, terminase, recombinase
3	7.5Kb	incomplete	16	1919277-1926858	PHAGE_Lactob_Lenus_NC_047897(1)	37.19%	transposase
12. <i>Staphylococcus pseudintermedius</i> strain 157588 chromosome							
1	12.5Kb	incomplete	16	192070-204607	PHAGE_Staphy_SPbeta_like_NC_029119(3)	37.12%	protease
2	6.4Kb	incomplete	10	477931-484335	PHAGE_Staphy_StB27_NC_019914(2)	26.32%	head, portal
3	4.7Kb	incomplete	7	566717-571510	PHAGE_Staphy_phiPV83_NC_002486(2)	34.44%	head
4	11.4Kb	incomplete	13	2202993-2214463	PHAGE_Staphy_phiSal19_NC_025460(1)	34.15%	N/A
5	8.3Kb	incomplete	8	2427188-2435503	PHAGE_Prochl_P_SSM2_NC_006883(4)	40.45%	N/A
13. <i>Staphylococcus pseudintermedius</i> E140 chromosome, whole genome shotgun sequence							
1	27.4Kb	incomplete	13	25001-52450	PHAGE_Staphy_PT1028_NC_007045(5)	36.99%	integrase
2	124.7Kb	intact	178	1143785-1268499	PHAGE_Staphy_SA7_NC_048658(18)	36.21%	lysin, tail, head
3	48.7Kb	intact	67	1440855-1489564	PHAGE_Staphy_StauST398_2_NC_021323(11)	34.24%	Integrase, tail, capsid, portal
4	44.1Kb	intact	72	2203573-2247696	PHAGE_Staphy_187_NC_007047(24)	35.88%	tail, terminase, capsid, integrase

5	57.3Kb	questionable	56	2282197-2339576	PHAGE_Staphy_187_NC_007047(12)	36.91%	protease, tail, terminase, integrase
14. <i>Staphylococcus pseudintermedius</i> strain HSP132 chromosome							
1	5.5Kb	incomplete	12	936972-942518	PHAGE_Staphy_StauST398_4_NC_023499(1)	37.57%	N/A
2	4.7Kb	incomplete	7	983207-987999	PHAGE_Staphy_phiPV83_NC_002486(2)	35.03%	head
3	12.5Kb	incomplete	16	1347057-1359598	PHAGE_Staphy_SPbeta_like_NC_029119(3)	37.16%	protease
4	8.3Kb	incomplete	8	1726900-1735215	PHAGE_Prochl_P_SSM2_NC_006883(4)	40.56%	N/A
5	7.7Kb	incomplete	9	1933290-1941019	PHAGE_Staphy_P1105_NC_048636(1)	31.91%	N/A
15. <i>Staphylococcus pseudintermedius</i> strain HSP136 chromosome							
1	12.5Kb	incomplete	16	317026-329567	PHAGE_Staphy_SPbeta_like_NC_029119(3)	37.16%	protease
2	8.3Kb	incomplete	8	696869-705184	PHAGE_Prochl_P_SSM2_NC_006883(4)	40.56%	N/A
3	7.7Kb	incomplete	9	903262-910990	PHAGE_Bacill_Gamma_NC_007458(1)	31.92%	N/A
4	5.5Kb	incomplete	12	2419674-2425220	PHAGE_Bacter_Lily_NC_028841(1)	37.57%	N/A
5	4.7Kb	incomplete	8	2465908-2470699	PHAGE_Clostr_phiMMP01_NC_028883(2)	35.04%	Head
16. <i>Staphylococcus pseudintermedius</i> HKU10-03, complete sequence							
1	46.8Kb	questionable	28	529856-576683	PHAGE_Clostr_phiCD481_1_NC_028951(3)	35.71%	integrase, portal, head, capsid, terminase
2	44.1Kb	intact	72	581326-625485	PHAGE_Staphy_187_NC_007047(20)	35.77%	integrase, tail, recombinase, capsid, terminase
3	60Kb	intact	69	1305861-1365871	PHAGE_Staphy_StauST398_2_NC_021323(11)	34.52%	capsid, tail, portal, integrase, recombinase

17. <i>Staphylococcus pseudintermedius</i> strain FDAARGOS_930 chromosome, complete genome							
1	7.7Kb	incomplete	16	436698-444495	PHAGE_Strept_Str_PAP_1_NC_028666(2)	37.07%	tail, transposase
2	38.4Kb	incomplete	13	1465390-1503879	PHAGE_Strept_315.4_NC_004587(1)	35.08%	transposase, integrase
18. <i>Staphylococcus pseudintermedius</i> strain DG064 chromosome, complete genome							
1	57.9Kb	intact	66	637774-695726	PHAGE_Staphy_187_NC_007047(25)	36.14%	integrase, tail, capsid, terminase
2	44.3Kb	intact	61	1106720-1151087	PHAGE_Staphy_SA7_NC_048658(17)	36.15%	lysine, tail, head
3	6.4Kb	incomplete	9	1235330-1241743	PHAGE_Staphy_SPbeta_like_NC_029119(5)	34.36%	portal, head, transposase
4	48.7Kb	intact	71	1416282-1464994	PHAGE_Staphy_StauST398_2_NC_021323(11)	34.24%	integrase, tail, capsid, portal
5	14.3Kb	incomplete	19	1661969-1676350	PHAGE_Staphy_187_NC_007047(3)	35.17%	head
6	54.3Kb	intact	58	2010258-2064593	PHAGE_Staphy_vB_SpsS_QT1_NC_048192(42)	36.48%	tail, lysine, transposase
7	46Kb	intact	62	2215847-2261921	PHAGE_Staphy_2638A_NC_007051(35)	36.45%	tail, lysine, integrase
8	59.2Kb	intact	56	2298264-2357512	PHAGE_Staphy_187_NC_007047(12)	37.07%	protease, tail, terminase, integrase
9	27.4Kb	incomplete	13	2816933-2844382	PHAGE_Staphy_PT1028_NC_007045(5)	36.99%	Integrase
19. <i>Staphylococcus pseudintermedius</i> strain NA45, complete genome.							
1	62.5Kb	intact	71	639147-701734	PHAGE_Staphy_187_NC_007047(22)	36.76%	integrase, tail, recombinase, capsid
2	7.9Kb	incomplete	15	1045865-1053799	PHAGE_Strept_Str_PAP_1_NC_028666(2)	37.09%	transposase, tail
3	129Kb	questionable	150	1620277-1749310	PHAGE_Staphy_SPbeta_like_NC_029119(68)	32.99%	tail, recombinase, integrase

4	46.1Kb	intact	72	2208689-2254837	PHAGE_Staphy_SA7_NC_048658(15)	36.15%	protease, tail, integrase
5	49.2Kb	intact	71	2466008-2515251	PHAGE_Staphy_EW_NC_007056(20)	36.88%	tail, capsid, recombinase
6	23.2Kb	incomplete	13	2771364-2794613	PHAGE_Staphy_PT1028_NC_007045(5)	37.65%	Integrase
20. <i>Staphylococcus pseudintermedius</i> strain FDAARGOS_1072 chromosome, complete genome							
1	45.8Kb	questionable	56	7114-52956	PHAGE_Staphy_187_NC_007047(12)	36.58%	tail, integrase, terminase, protease
2	44.3Kb	intact	60	356999-401366	PHAGE_Staphy_SA7_NC_048658(17)	36.15%	lysine, tail, head
3	48.7Kb	intact	65	667100-715809	PHAGE_Staphy_StauST398_2_NC_021323(11)	34.24%	integrase, tail, capsid, portal
4	15.7Kb	incomplete	21	912950-928746	PHAGE_Staphy_187_NC_007047(3)	35.76%	head, tail
5	92.6Kb	intact	137	1423633-1516232	PHAGE_Staphy_187_NC_007047(24)	36.00%	tail, terminase, capsid, integrase, recombinase
6	27.4Kb	incomplete	13	2361457-2388906	PHAGE_Staphy_PT1028_NC_007045(5)	36.99%	Integrase
21. <i>Staphylococcus pseudintermedius</i> strain DG072 chromosome, complete genome							
1	48.1Kb	intact	63	1059995-1108095	PHAGE_Staphy_SA7_NC_048658(17)	36.44%	lysine, tail, head
2	6.4Kb	incomplete	9	1193830-1200242	PHAGE_Staphy_SPbeta_like_NC_029119(4)	34.37%	portal, head, transposase
3	48.7Kb	intact	68	1374778-1423486	PHAGE_Staphy_StauST398_2_NC_021323(11)	34.24%	integrase, tail, capsid, portal
4	24Kb	incomplete	19	1610920-1635005	PHAGE_Staphy_187_NC_007047(3)	35.10%	head, integrase
5	53.5Kb	intact	55	1968914-2022447	PHAGE_Staphy_vB_SpsS_QT1_NC_048192(45)	36.67%	tail, lysine, transposase
6	57.5Kb	intact	72	2163888-2221460	PHAGE_Staphy_187_NC_007047(26)	36.39%	tail, terminase, capsid, integrase

7	57.3Kb	questionable	55	2251252-2308632	PHAGE_Staphy_187_NC_007047(12)	36.91%	protease, tail, terminase, integrase
8	27.4Kb	incomplete	13	2760872-2788322	PHAGE_Staphy_PT1028_NC_007045(5)	36.99%	Integrase
22. <i>Staphylococcus pseudintermedius</i> strain DSP021 chromosome, complete genome							
1	44.3Kb	intact	61	1056320-1100684	PHAGE_Staphy_SA7_NC_048658(17)	36.15%	lysine, tail, head
2	6.4Kb	incomplete	9	1184926-1191338	PHAGE_Staphy_SPbeta_like_NC_029119(4)	34.37%	portal, head, transposase
3	48.7Kb	intact	67	1365767-1414476	PHAGE_Staphy_StauST398_2_NC_021323(11)	34.24%	integrase, tail, capsid, portal
4	14.3Kb	incomplete	19	1611614-1625995	PHAGE_Staphy_187_NC_007047(3)	35.18%	head
5	44.1Kb	intact	71	2124077-2168201	PHAGE_Staphy_187_NC_007047(24)	35.88%	tail, terminase, capsid, integrase
6	57.3Kb	questionable	55	2202677-2260058	PHAGE_Staphy_187_NC_007047(12)	36.91%	protease, tail, terminase, integrase
7	27.4Kb	incomplete	13	2719466-2746916	PHAGE_Staphy_PT1028_NC_007045(5)	36.99%	Integrase
23. <i>Staphylococcus pseudintermedius</i> strain DSP020 chromosome, complete genome							
1	44.3Kb	intact	61	1056336-1100699	PHAGE_Staphy_SA7_NC_048658(17)	36.15%	lysine, tail, head
2	6.4Kb	incomplete	9	1184942-1191354	PHAGE_Staphy_SPbeta_like_NC_029119(4)	34.37%	portal, head, transposase
3	48.7Kb	intact	65	1365785-1414493	PHAGE_Staphy_StauST398_2_NC_021323(11)	34.24%	integrase, tail, capsid, portal
4	14.3Kb	incomplete	19	1611633-1626014	PHAGE_Staphy_187_NC_007047(3)	35.18%	head
5	44.1Kb	intact	72	2122247-2166370	PHAGE_Staphy_187_NC_007047(24)	35.88%	tail, terminase, capsid, integrase
6	57.3Kb	questionable	55	2200845-2258225	PHAGE_Staphy_187_NC_007047(12)	36.91%	protease, tail, terminase, integrase

7	27.4Kb	incomplete	13	2717569-2745020	PHAGE_Staphy_PT1028_NC_007045(5)	37.00%	Integrase
24. <i>Staphylococcus pseudintermedius</i> strain VB16 chromosome, complete genome							
1	48.4Kb	intact	58	1295044-1343492	PHAGE_Staphy_vB_SpsS_QT1_NC_048192(35)	36.57%	lysine, tail, head
2	6.4Kb	incomplete	9	1425855-1432261	PHAGE_Staphy_SPbeta_like_NC_029119(5)	34.45%	portal, head, transposase
3	58.8Kb	intact	70	2304096-2362948	PHAGE_Staphy_187_NC_007047(19)	36.19%	tail, terminase, capsid, integrase, recombinase
4	48.3Kb	questionable	67	2598055-2646366	PHAGE_Staphy_37_NC_007055(17)	37.23%	capsid, head, terminase, recombinase
25. <i>Staphylococcus pseudintermedius</i> strain AK9 chromosome, complete genome							
1	16.6Kb	incomplete	9	482-17129	PHAGE_Staphy_SPbeta_like_NC_029119(2)	35.78%	tail
2	6.4Kb	incomplete	9	2240250-2246660	PHAGE_Staphy_SPbeta_like_NC_029119(5)	34.38%	portal, head, transposase
3	108.9Kb	incomplete	134	2678471-2787411	PHAGE_Staphy_SPbeta_like_NC_029119(65)	32.14%	plate, recombinase
26. <i>Staphylococcus pseudintermedius</i> strain AP20 chromosome, complete genome							
1	48.2Kb	intact	71	764706-812907	PHAGE_Staphy_vB_SpsS_QT1_NC_048192(21)	35.24%	integrase, lysine, tail, portal, head
2	6.4Kb	incomplete	9	895313-901725	PHAGE_Staphy_SPbeta_like_NC_029119(5)	34.38%	portal, head, transposase
3	38.2Kb	questionable	32	2304364-2342640	PHAGE_Staphy_PT1028_NC_007045(9)	35.11%	integrase, transposase, tail
27. <i>Staphylococcus pseudintermedius</i> strain 081661 isolate 20081661 chromosome, complete genome							
1	48.7Kb	intact	66	1318351-1367059	PHAGE_Staphy_StauST398_2_NC_021323(11)	34.24%	integrase, tail, capsid, portal
2	24Kb	incomplete	20	1552191-1576273	PHAGE_Staphy_187_NC_007047(3)	35.09%	head, integrase
3	56.5Kb	intact	67	2059166-2115709	PHAGE_Staphy_187_NC_007047(24)	36.65%	tail, terminase, integrase

4	57.3Kb	questionable	55	2145524-2202902	PHAGE_Staphy_187_NC_007047(12)	36.91%	protease, tail, terminase, integrase
5	27.4Kb	incomplete	14	2655097-2682542	PHAGE_Staphy_PT1028_NC_007045(5)	36.98%	integrase
28. Staphylococcus pseudintermedius strain AI14 chromosome, complete genome							
1	6.4Kb	incomplete	9	79993-86404	PHAGE_Staphy_SPbeta_like_NC_029119(5)	34.37%	portal, head, transposase
2	49.3Kb	intact	60	261102-310450	PHAGE_Staphy_StauST398_2_NC_021323(11)	34.24%	integrase, capsid, tail, portal
3	38.2Kb	incomplete	30	1530731-1568979	PHAGE_Staphy_PT1028_NC_007045(8)	35.08%	integrase, transposase
29. Staphylococcus pseudintermedius strain G3C4 chromosome, complete genome							
1	27.4Kb	incomplete	13	461305-488756	PHAGE_Staphy_PT1028_NC_007045(5)	36.98%	integrase
2	48.7Kb	intact	67	1867933-1916637	PHAGE_Staphy_StauST398_2_NC_021323(11)	34.24%	integrase, tail, capsid, portal
3	19.3Kb	incomplete	19	2110705-2130029	PHAGE_Staphy_187_NC_007047(3)	35.46%	head, integrase
4	59Kb	intact	69	2616404-2675451	PHAGE_Staphy_187_NC_007047(23)	36.51%	tail, terminase, capsid, integrase
30. Staphylococcus pseudintermedius strain VB88 chromosome, complete genome							
1	6.4Kb	incomplete	9	498044-504457	PHAGE_Staphy_SPbeta_like_NC_029119(5)	34.36%	head, transposase, portal
2	63.7Kb	intact	73	585670-649438	PHAGE_Staphy_vB_SpsS_QT1_NC_048192(17)	35.60%	tail, head, lysin
3	27.4Kb	questionable	22	1794083-1821488	PHAGE_Staphy_SPbeta_like_NC_029119(2)	35.46%	lysine, integrase, tail
4	44.2Kb	intact	71	2275553-2319788	PHAGE_Staphy_187_NC_007047(22)	35.90%	integrase, tail
31. Staphylococcus pseudintermedius strain SP_9261-1A chromosome, complete genome							

1	45.8Kb	intact	60	1034889-1080708	PHAGE_Staphy_187_NC_007047(12)	36.72%	tail, terminase, head, virion
2	8.2Kb	incomplete	11	1163081-1171364	PHAGE_Staphy_SPbeta_like_NC_029119(5)	36.02%	portal, head, transposase, tail
3	8.5Kb	incomplete	9	2178856-2187403	PHAGE_Arthro_Sonali_NC_048152(2)	37.68%	transposase, tail
4	35.5Kb	incomplete	10	2560395-2595907	PHAGE_Strept_315.4_NC_004587(1)	35.12%	integrase
5	18.1Kb	incomplete	14	2595854-2613971	PHAGE_Staphy_PT1028_NC_007045(5)	36.69%	Integrase
32. Staphylococcus pseudintermedius strain cdc 18-1182 chromosome, complete genome							
1	58.8Kb	intact	64	1056746-1115555	PHAGE_Staphy_187_NC_007047(13)	36.43%	tail, head, terminase, integrase, recombinase
33. Staphylococcus pseudintermedius strain Z0118SP0108 chromosome, complete genome							
1	58.8Kb	intact	64	71738-130547	PHAGE_Staphy_187_NC_007047(13)	36.43%	tail, head, terminase, integrase, recombinase
34. Staphylococcus pseudintermedius strain AH18 chromosome, complete genome							
1	6.6Kb	incomplete	7	1474290-1480891	PHAGE_Bacill_PfEFR_4_NC_048641(1)	35.19%	transposase, tail
2	37.5Kb	incomplete	19	1706161-1743726	PHAGE_Staphy_187_NC_007047(3)	35.88%	integrase, head
3	6.4Kb	incomplete	9	2101967-2108379	PHAGE_Staphy_SPbeta_like_NC_029119(5)	34.38%	head, transposase, portal
4	10.2Kb	incomplete	12	2192046-2202247	PHAGE_Staphy_vB_SpsS_QT1_NC_048192(4)	33.07%	tail, head
35. Staphylococcus pseudintermedius strain KCTC 43136 chromosome, complete genome							
1	58.9Kb	intact	71	1416691-1475672	PHAGE_Staphy_187_NC_007047(25)	35.97%	integrase, tail, recombinase
2	6.4Kb	incomplete	9	1981642-1988046	PHAGE_Staphy_SPbeta_like_NC_029119(5)	34.29%	portal, head, transposase

36. Staphylococcus pseudintermedius strain KCTC 43135 chromosome, complete genome							
1	6.4Kb	incomplete	9	477931-484335	PHAGE_Staphy_SPbeta_like_NC_029119(5)	34.29%	head, transposase, portal
2	58.9Kb	intact	72	990305-1049275	PHAGE_Staphy_187_NC_007047(25)	35.98%	tail, integrase, recombinase
37. Staphylococcus pseudintermedius strain DSP030 chromosome, complete genome							
1	46.6Kb	intact	62	1020234-1066872	PHAGE_Staphy_2638A_NC_007051(18)	35.18%	integrase, lysin, capsid, portal, tail, head
38. Staphylococcus pseudintermedius strain KCTC 43134 chromosome, complete genome							
1	58.9Kb	intact	71	448937-507907	PHAGE_Staphy_187_NC_007047(24)	35.98%	tail, integrase, recombinase
2	6.4Kb	incomplete	9	2547688-2554092	PHAGE_Staphy_SPbeta_like_NC_029119(5)	34.29%	head, transposase, portal
39. Staphylococcus pseudintermedius strain SP_11304-3A chromosome, complete genome							
1	55.2Kb	questionable	59	1016148-1071371	PHAGE_Staphy_187_NC_007047(13)	36.05%	recombinase, integrase, terminase, head, tail
2	54.8Kb	intact	68	1863099-1917952	PHAGE_Staphy_phiRS7_NC_022914(19)	33.30%	recombinase, tail, head, capsid, portal, terminase, lysin, integrase
3	29.8Kb	incomplete	23	2532637-2562516	PHAGE_Staphy_PT1028_NC_007045(9)	34.64%	integrase, capsid
40. Staphylococcus pseudintermedius strain SP_11304-2A chromosome, complete genome							
1	33.4Kb	incomplete	21	44811-78266	PHAGE_Escher_503458_NC_049341(2)	33.26%	tail, transposase
2	54.7Kb	intact	66	1988054-2042791	PHAGE_Staphy_187_NC_007047(23)	36.57%	tail, recombinase, integrase
41. Staphylococcus pseudintermedius strain SP_11306-1A chromosome, complete genome							
1	48Kb	intact	57	1276784-1324821	PHAGE_Staphy_StauST398_2_NC_021323(11)	34.12%	integrase, tail, portal, capsid
42. Staphylococcus pseudintermedius strain HSP079 chromosome, complete genome							
1	8Kb	incomplete	15	951394-959416	PHAGE_Lactob_Satyr_NC_047918(1)	36.87%	transposase

2	24.6Kb	incomplete	9	2497676-2522324	PHAGE_Lactoc_PLgT_1_NC_031016(1)	34.90%	integrase, transposase
43. Staphylococcus pseudintermedius strain HSP080 chromosome, complete genome							
1	8Kb	incomplete	15	951261-959283	PHAGE_Staphy_vB_SauM_Remus_NC_022090(1)	36.88%	transposase
2	24.6Kb	incomplete	8	2497484-2522128	PHAGE_Lactoc_ul36_NC_004066(1)	34.92%	integrase, transposase
44. Staphylococcus pseudintermedius ED99, complete sequence							
1	36.5Kb	incomplete	10	2471263-2507800	PHAGE_Temper_phiNIH1.1_NC_003157(1)	35.32%	integrase, transposase
45. Staphylococcus pseudintermedius strain DSP026 chromosome, complete genome							
1	9.3Kb	incomplete	11	40144-49468	PHAGE_Escher_520873_NC_049344(2)	31.21%	plate, transposase
2	8.9Kb	incomplete	10	385326-394273	PHAGE_Staphy_phiSA_BS2_NC_047948(1)	32.59%	tail, transposase
3	7.2Kb	incomplete	11	989688-996905	PHAGE_Staphy_phi7247PVL_NC_048624(2)	32.82%	transposase
4	48.6Kb	intact	73	1648382-1697037	PHAGE_Staphy_IME_SA4_NC_029025(22)	34.79%	tail, head, capsid, portal, terminase, lysin, integrase
5	34.1Kb	incomplete	20	2485662-2519831	PHAGE_Staphy_StB27_NC_019914(2)	34.79%	integrase, terminase
46. Staphylococcus pseudintermedius strain NCTC5661 chromosome 1							
1	45.7Kb	intact	57	1010412-1056185	PHAGE_Staphy_187_NC_007047(12)	36.68%	recombinase, tail, terminase, head
2	14.2Kb	incomplete	19	1515194-1529464	PHAGE_Staphy_187_NC_007047(3)	35.36%	head
47. Staphylococcus pseudintermedius strain SP_11304-1A chromosome, complete genome							
1	44.1Kb	intact	61	953107-997260	PHAGE_Staphy_187_NC_007047(20)	35.68%	integrase, lysin, capsid, tail
2	42.6Kb	intact	56	1644336-1687006	PHAGE_Staphy_187_NC_007047(12)	36.82%	capsid, tail, virion, head, portal, terminase, integrase

48. Staphylococcus pseudintermedius strain HSP125 chromosome, complete genome							
1	39.8Kb	incomplete	23	2462237-2502102	PHAGE_Staphy_PT1028_NC_007045(2)	34.67%	integrase, lysin, terminase
49. Staphylococcus pseudintermedius strain DSP034 chromosome, complete genome							
1	36.8Kb	incomplete	21	1995997-2032865	PHAGE_Staphy_StauST398_5_NC_023500(2)	36.02%	recombinase
50. Staphylococcus pseudintermedius strain SP_11306-4A chromosome, complete genome							
1	8Kb	incomplete	16	959834-967863	PHAGE_Lactob_8014_B2_NC_047739(1)	36.79%	transposase
2	6.7Kb	incomplete	7	1010442-1017146	PHAGE_Staphy_phi7247PVL_NC_048624(2)	34.84%	transposase, head
3	43.6Kb	intact	50	1662859-1706550	PHAGE_Staphy_2638A_NC_007051(39)	36.46%	tail, integrase
51. Staphylococcus pseudintermedius strain 5912 chromosome, complete genome							
1	38.9Kb	questionable	15	1820107-1859074	PHAGE_Staphy_phiRS7_NC_022914(2)	33.19%	transposase, tail, integrase
52. Staphylococcus pseudintermedius strain HSP118 chromosome, complete genome							
1	5.5Kb	incomplete	12	934612-940158	PHAGE_Staphy_phi7247PVL_NC_048624(1)	37.57%	NA
2	4.7Kb	incomplete	7	980849-985641	PHAGE_Clostr_phiMMP01_NC_028883(2)	35.03%	head
3	12.5Kb	incomplete	16	1344691-1357232	PHAGE_Staphy_SPbeta_like_NC_029119(3)	37.16%	protease
4	8.3Kb	incomplete	8	1724556-1732871	PHAGE_Prochl_P_SSM2_NC_006883(4)	40.56%	NA
5	7.7Kb	incomplete	9	1930959-1938688	PHAGE_Strept_315.5_NC_004588(1)	31.91%	NA
53. Staphylococcus pseudintermedius strain HSP138 chromosome, complete genome							
1	5.5Kb	incomplete	12	934614-940160	PHAGE_Staphy_IME_SA4_NC_029025(1)	37.57%	NA

2	4.7Kb	incomplete	8	980848-985638	PHAGE_Clostr_phiC2_NC_009231(2)	35.04%	head
3	12.5Kb	incomplete	16	1344703-1357244	PHAGE_Staphy_SPbeta_like_NC_029119(3)	37.16%	protease
4	8.3Kb	incomplete	8	1724551-1732866	PHAGE_Prochl_P_SSM2_NC_006883(4)	40.56%	NA
5	7.7Kb	incomplete	9	1930945-1938674	PHAGE_Erwini_Derbicus_NC_048173(1)	31.91%	NA
54. Staphylococcus pseudintermedius strain HSP137 chromosome, complete genome							
1	5.5Kb	incomplete	12	934591-940137	PHAGE_Enterо_IME_EFm5_NC_028826(1)	37.57%	NA
2	4.7Kb	incomplete	7	980825-985617	PHAGE_Clostr_phiMMP03_NC_028959(2)	35.03%	head
3	12.5Kb	incomplete	16	1344642-1357183	PHAGE_Staphy_SPbeta_like_NC_029119(3)	37.16%	protease
4	8.3Kb	incomplete	8	1724488-1732803	PHAGE_Prochl_P_SSM2_NC_006883(4)	40.56%	NA
5	7.7Kb	incomplete	9	1930882-1938610	PHAGE_Pseudo_OBP_NC_016571(1)	31.92%	NA
55. Staphylococcus pseudintermedius strain HSP135 chromosome, complete genome							
1	5.5Kb	incomplete	12	934536-940082	PHAGE_Staphy_phiSa2wa_st22_NC_048681(1)	37.57%	NA
2	4.7Kb	incomplete	8	980772-985562	PHAGE_Staphy_phiSa2wa_st22_NC_048681(2)	35.04%	head
3	12.5Kb	incomplete	16	1344621-1357160	PHAGE_Staphy_SPbeta_like_NC_029119(3)	37.16%	protease
4	8.3Kb	incomplete	8	1724459-1732774	PHAGE_Prochl_P_SSM2_NC_006883(4)	40.56%	NA
5	7.7Kb	incomplete	9	1930850-1938579	PHAGE_Lactob_Lj965_NC_005355(1)	31.91%	NA
56. Staphylococcus pseudintermedius strain SP79 chromosome, complete genome							

1	5.5Kb	incomplete	13	953729-959280	PHAGE_Entero_IME_EFm1_NC_024356(1)	37.64%	NA
2	4.7Kb	incomplete	7	1002280-1007075	PHAGE_Staphy_phiPV83_NC_002486(2)	35.09%	head
3	12.5Kb	incomplete	16	1365959-1378500	PHAGE_Staphy_SPbeta_like_NC_029119(3)	37.13%	protease
4	8.3Kb	incomplete	8	1744488-1752803	PHAGE_Prochl_P_SSM2_NC_006883(4)	40.44%	NA
5	11.4Kb	incomplete	11	1973783-1985249	PHAGE_Mycoba_Catera_NC_008207(1)	34.19%	NA
57. Staphylococcus pseudintermedius strain 063228, complete genome							
1	7.9Kb	incomplete	15	872749-880677	PHAGE_Staphy_Ipla5_NC_018281(1)	37.08%	transposase
2	22.1Kb	incomplete	12	911904-934043	PHAGE_Staphy_vB_SpsS_QT1_NC_048192(4)	35.62%	head, tail
3	25.2Kb	incomplete	21	1380680-1405904	PHAGE_Staphy_187_NC_007047(3)	35.57%	head, integrase, tail
4	45.2Kb	intact	66	1591185-1636454	PHAGE_Staphy_phiRS7_NC_022914(18)	35.28%	tail, head, capsid, portal, terminase, lysin, integrase
5	45.4Kb	intact	61	2007965-2053445	PHAGE_Staphy_187_NC_007047(12)	36.63%	protease, transposase, capsid, tail, head, portal, terminase, integrase
6	52.9Kb	questionable	55	2690278-2743228	PHAGE_Staphy_SA7_NC_048658(18)	34.56%	transposase, lysin, tail
58. Staphylococcus pseudintermedius strain DSP027 chromosome, complete genome							
1	60.3Kb	intact	78	997922-1058259	PHAGE_Staphy_vB_SpsS_QT1_NC_048192(19)	35.57%	lysine, recombinase, tail, head
2	130Kb	questionable	145	1574992-1705029	PHAGE_Staphy_SPbeta_like_NC_029119(68)	32.91%	plate, recombinase, portal, tail, integrase
59. Staphylococcus pseudintermedius strain HSP134 chromosome, complete genome							

1	5.5Kb	incomplete	12	936445-941991	PHAGE_Staphy_SA1014ruMSSAST7_NC_048710(1)	37.57%	NA
2	4.7Kb	incomplete	8	982680-987471	PHAGE_Staphy_phiPV83_NC_002486(2)	35.04%	head
3	12.5Kb	incomplete	16	1346526-1359066	PHAGE_Staphy_SPbeta_like_NC_029119(3)	37.17%	protease
4	8.3Kb	incomplete	8	1726322-1734637	PHAGE_Prochl_P_SSM2_NC_006883(4)	40.56%	NA
5	7.7Kb	incomplete	10	1932712-1940440	PHAGE_Mycoba_Shauna1_NC_041989(1)	31.92%	NA

Table 3.14 Overview of prophages identified in 59 *S. pseudintermedius* isolates.

Host strain	Biosample ID	Size (Mb)	GC %	Scaffolds	Isolation source	Total no. of Prophages present	No. of complete prophages	No. of incomplete prophages	No. of questionable prophages
1. Staphylococcus pseudintermedius strain MAD401 chromosome	SAMN09206883	2.88	37.5	1	Canine wound	7	3	4	0
2. Staphylococcus pseudintermedius strain FDAARGOS_1073 chromosome	SAMN16357242	2.83	37.5	1	Unknown	6	3	2	1
3. Staphylococcus pseudintermedius strain ME4692 chromosome	SAMN10389971	2.8	37.29	2	Environment	6	3	2	1
4. Staphylococcus pseudintermedius	SAMN09206896	2.71	37.5	1	Medical equipment	6	2	4	0

strain VTH737 chromosome									
5. Staphylococcus pseudintermedius strain MAD568 chromosome	SAMN09206879	2.71	37.4	1	Canine wound	3	1	2	0
6. Staphylococcus pseudintermedius strain MAD627 chromosome	SAMN10389939	2.69	37.51	2	Canine wound	3	0	2	1
7. Staphylococcus pseudintermedius strain DG099 chromosome	SAMN17102131	2.62	37.6	1	Canine skin swab	3	1	2	0
8. Staphylococcus pseudintermedius strain 53_60 chromosome	SAMN10880484	2.62	37.5	1	Human blood (Bacteraemia)	3	0	3	0
9. Staphylococcus pseudintermedius strain 51_92 chromosome	SAMN10880482	2.51	37.8	1	Canine blood (Bacteraemia)	1	0	1	0
10. Staphylococcus pseudintermedius strain 53_88 chromosome	SAMN10880486	2.59	37.7	1	Human blood (Bacteraemia)	4	1	3	0
11. Staphylococcus pseudintermedius strain 49_44 chromosome	SAMN10880480	2.58	37.7	1	Canine blood (Bacteraemia)	3	1	2	0
12. Staphylococcus pseudintermedius	SAMN15002157	2.61	38.7	1	Canine pyoderma (pus swab)	5	0	5	0

strain 157588 chromosome									
13. Staphylococcus pseudintermedius E140 chromosome, whole genome shotgun sequence	SAMN02471704	2.77	37.4	1	Wound infection (MRSP)	5	3	1	1
14. Staphylococcus pseudintermedius strain HSP132 chromosome	SAMN17102157	2.52	37.7	1	Healthy canine skin swab	5	0	5	0
15. Staphylococcus pseudintermedius strain HSP136 chromosome	SAMN17102160	2.51	37.7	1	Healthy canine skin swab	5	0	5	0
16. Staphylococcus pseudintermedius HKU10-03, complete sequence	SAMN02603958	2.62	37.5	1	Canine pyoderma skin swab	3	2	0	1
17. Staphylococcus pseudintermedius strain FDAARGOS_930 chromosome, complete genome	SAMN13450460	2.56	37.7	1	Unknown	2	0	2	0
18. Staphylococcus pseudintermedius strain DG064 chromosome, complete genome	SAMN17102118	2.9	37.5	1	Canine pyoderma skin swab	9	6	3	0
19. Staphylococcus pseudintermedius	SAMN05181828	2.84	37.3	1	Canine urinary infection	6	3	2	1

strain NA45, complete genome.									
20. Staphylococcus pseudintermedius strain FDAARGOS_1072 chromosome, complete genome	SAMN16357241	2.84	37.5	1	Unknown	6	3	2	1
21. Staphylococcus pseudintermedius strain DG072 chromosome, complete genome	SAMN17102122	2.84	37.4	1	Canine pyoderma skin swab	8	4	3	1
22. Staphylococcus pseudintermedius strain DSP021 chromosome, complete genome	SAMN17102133	2.8	37.5	1	Canine pyoderma skin swab	7	3	3	1
23. Staphylococcus pseudintermedius strain DSP020 chromosome, complete genome	SAMN17102132	2.79	37.5	1	Canine pyoderma skin swab	7	3	3	1
24. Staphylococcus pseudintermedius strain VB16 chromosome, complete genome	SAMN09519064	2.79	37.5	1	Human mixed sample	4	2	1	1
25. Staphylococcus pseudintermedius strain AK9 chromosome, complete genome	SAMN09378519	2.79	37.3	1	Canine mixed sample	3	0	3	0

26. Staphylococcus pseudintermedius strain AP20 chromosome, complete genome	SAMN09378520	2.73	37.5	1	Human mixed sample	3	1	1	1
27. Staphylococcus pseudintermedius strain 081661 isolate 20081661 chromosome, complete genome	SAMN05181827	2.73	37.5	1	Canine pyoderma skin swab	5	2	2	1
28. Staphylococcus pseudintermedius strain AI14 chromosome, complete genome	SAMN09378648	2.72	37.5	1	Canine mixed sample	3	1	2	0
29. Staphylococcus pseudintermedius strain G3C4 chromosome, complete genome	SAMN10142584	2.72	37.5	1	Canine otitis (ear swab)	4	2	2	0
30. Staphylococcus pseudintermedius strain VB88 chromosome, complete genome	SAMN09378493	2.67	37.5	1	Human mixed sample	4	2	1	1
31. Staphylococcus pseudintermedius strain SP_9261-1A chromosome, complete genome	SAMN17039292	2.67	37.5	1	Canine pyoderma skin swab	5	1	4	0
32. Staphylococcus pseudintermedius	SAMN15897749	2.66	37.5	1	Canine	1	1	0	0

strain cdc 18-1182 chromosome, complete genome									
33. Staphylococcus pseudintermedius strain Z0118SP0108 chromosome, complete genome	SAMN15950890	2.66	37.5	1	Canine	1	1	0	0
34. Staphylococcus pseudintermedius strain AH18 chromosome, complete genome	SAMN09378491	2.62	37.5	1	Canine mixed sample	4	0	4	0
35. Staphylococcus pseudintermedius strain KCTC 43136 chromosome, complete genome	SAMN12999206	2.62	37.7	1	Human skin swab	2	1	1	0
36. Staphylococcus pseudintermedius strain KCTC 43135 chromosome, complete genome	SAMN12999204	2.62	37.7	1	Residential environment	2	1	1	0
37. Staphylococcus pseudintermedius strain DSP030 chromosome, complete genome	SAMN17102140	2.61	37.6	1	Canine pyoderma skin swab	1	1	0	0
38. Staphylococcus pseudintermedius strain KCTC 43134 chromosome, complete genome	SAMN12999170	2.61	37.6	1	Canine	2	1	1	0

39. Staphylococcus pseudintermedius strain SP_11304-3A chromosome, complete genome	SAMN17039295	2.63	37.54	3	Canine pyoderma skin swab	3	1	1	1
40. Staphylococcus pseudintermedius strain SP_11304-2A chromosome, complete genome	SAMN17039294	2.61	37.7	1	Canine pyoderma skin swab	2	1	1	0
41. Staphylococcus pseudintermedius strain SP_11306-1A chromosome, complete genome	SAMN17039296	2.61	37.6	1	Canine pyoderma skin swab	1	0	1	0
42. Staphylococcus pseudintermedius strain HSP079 chromosome, complete genome	SAMN17102145	2.59	37.5	1	Healthy canine skin swab	2	0	2	0
43. Staphylococcus pseudintermedius strain HSP080 chromosome, complete genome	SAMN17102146	2.59	37.5	1	Healthy canine skin swab	2	0	2	0
44. Staphylococcus pseudintermedius ED99, complete sequence	SAMN02604167	2.57	37.6	1	Unknown	1	0	1	0
45. Staphylococcus pseudintermedius strain DSP026	SAMN17102137	2.57	37.6	1	Canine pyoderma skin swab	5	1	4	0

chromosome, complete genome									
46. Staphylococcus pseudintermedius strain NCTC5661 chromosome 1	SAMEA3504576	2.56	37.7	1	Unknown	2	1	1	0
47. Staphylococcus pseudintermedius strain SP_11304-1A chromosome, complete genome	SAMN17039293	2.56	37.7	1	Canine pyoderma skin swab	2	2	0	0
48. Staphylococcus pseudintermedius strain HSP125 chromosome, complete genome	SAMN17102155	2.55	37.6	1	Healthy canine skin swab	1	0	1	0
49. Staphylococcus pseudintermedius strain DSP034 chromosome, complete genome	SAMN17102142	2.55	37.6	1	Canine pyoderma skin swab	1	0	1	0
50. Staphylococcus pseudintermedius strain SP_11306-4A chromosome, complete genome	SAMN17039297	2.54	37.8	1	Canine pyoderma skin swab	3	1	2	0
51. Staphylococcus pseudintermedius strain 5912 chromosome, complete genome	SAMN02947195	2.53	37.69	2	Canine ear swab	1	0	0	1
52. Staphylococcus pseudintermedius	SAMN17102154	2.51	37.7	1	Healthy canine skin swab	5	0	5	0

strain HSP118 chromosome, complete genome									
53. Staphylococcus pseudintermedius strain HSP138 chromosome, complete genome	SAMN17102162	2.51	37.7	1	Healthy canine skin swab	5	0	5	0
54. Staphylococcus pseudintermedius strain HSP137 chromosome, complete genome	SAMN17102161	2.51	37.7	1	Healthy canine skin swab	5	0	5	0
55. Staphylococcus pseudintermedius strain HSP135 chromosome, complete genome	SAMN17102159	2.51	37.7	1	Healthy canine skin swab	5	0	5	0
56. Staphylococcus pseudintermedius strain SP79 chromosome, complete genome	SAMD00154384	2.51	37.8	1	Unknown	5	0	5	0
57. Staphylococcus pseudintermedius strain 063228, complete genome	SAMN04886711	2.77	37.4	1	Canine dermatitis skin swab	6	2	3	1
58. Staphylococcus pseudintermedius strain DSP027 chromosome, complete genome	SAMN17102138	2.72	37.3	1	Canine pyoderma skin swab	2	1	0	1

59. Staphylococcus pseudintermedius strain HSP134 chromosome, complete genome	SAMN17102158	2.51	37.7	1	Healthy canine skin swab	5	0	5	0
--	--------------	------	------	---	-----------------------------	---	---	---	---

Chapter 4

Endolysins as a novel therapeutic option for *Staphylococcus pseudintermedius* canine infections

4.1 Summary

The use of phages for *Staphylococcus pseudintermedius* has gained significant interest over recent years. However, the isolation of temperate phages rather than lytic phages has halted the progression of phage therapy. Phage-encoded endolysins derived from phages (both temperate and lytic) have been regarded as a novel option to overcome this barrier. Endolysins act by degrading the peptidoglycan layer of bacteria, ultimately resulting in bacterial lysis, thus are a potential treatment option for antibiotic-resistant infections. A bioinformatic search of 25 *S. pseudintermedius* phage genomes identified 26 endolysins, and following multi-protein sequence alignment, six novel endolysins were selected for subsequent characterisation. All six endolysins (Lys_SN13, Lys_119-2, Lys_38-1, Lys_22L, Lys_SPT5, and Lys_T99F3) were successfully expressed and purified in an *Escherichia coli* system. Of the six endolysins selected, three were able to lyse clinical isolates of *S. pseudintermedius*. Endolysin, Lys_SN13, had a broad host range able to lyse 60% of clinical isolates, including both antibiotic-resistant and antibiotic sensitive strains, isolated from various sites of infection. Additionally, Lys_SN13 was able to significantly reduce the growth of *S. pseudintermedius* CM16-689 within 10 hours in liquid culture. *In silico* analysis of Lys_SN13 revealed the protein domain architecture of Lys_SN13 contains a CHAP-domain, highly homologous to *S. aureus* endolysin, LysGH15. *In silico* 3D predictive modelling found that Lys_SN13 possessed conserved residues surrounding calcium-binding, which supported preliminary evidence that Lys_SN13 requires calcium for its enzymatic activity. Overall, these results aim to set the groundwork for the progression of endolysins as a novel therapeutic for *S. pseudintermedius* infections in canines.

4.2 Introduction

Methicillin-resistant *Staphylococcus pseudintermedius* (MRSP) is a pathogenic bacterium of concern within the veterinary sector, involved in numerous canine infections¹³. Existing therapeutics, such as antibiotics, are insufficient at treating MRSP infections due to the high levels of multidrug resistance⁷¹. Therefore, there is a significant focus on alternative treatment options. As mentioned in **Chapter 3**, 3.2 Introduction phage therapy is an alternative therapeutic which has received significant research interest⁷². However, the lack of isolation of temperate phages against *S. pseudintermedius*, rather than lytic phages, creates a barrier to using this therapy against *S. pseudintermedius* moving forward^{16–18}. As a result, studies have focused on using phage-encoded endolysins as a novel therapeutic option against several bacterial species^{73–78}. Phage-encoded endolysins (endolysins) are enzymes synthesised and utilised by mature phage virions⁷⁹. Endolysins degrade the peptidoglycan layer of the bacteria, resulting in the release of hundreds of new phage particles (**Figure 4.1**)⁷⁴.

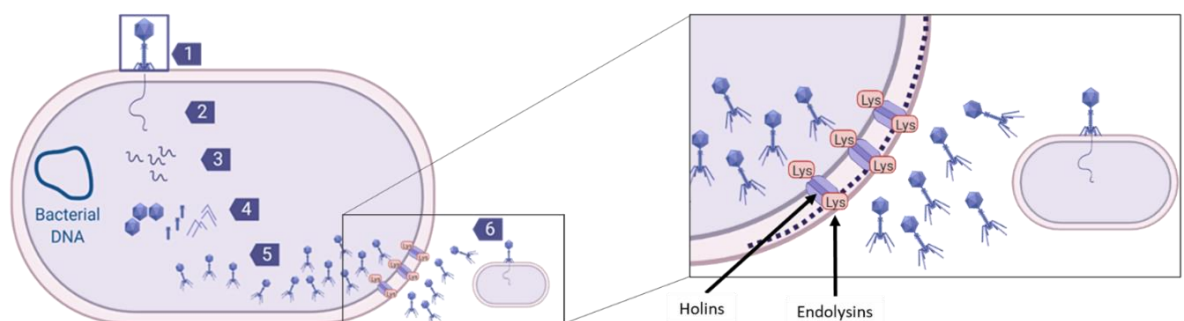


Figure 4.1 Endolysin-induced bacterial cell lysis. As part of the lytic lifecycle phages (1) recognise and attach to their bacteria host, allowing (2) the delivery of the phage genome into the host bacterial cell. (3) The phage genetic material is replicated using the host cell machinery and (4) new phage components are assembled, creating (5) hundreds of new phage progeny. (6) The mature lytic phage virions secrete two enzymes; holins and endolysins to lyse the host bacterium. Holins are small proteins which create channels within the bacterial inner membrane. These channels facilitate the access of endolysins to the bacterial peptidoglycan. The endolysins then cleave bonds within the peptidoglycan, resulting in bacterial host degradation.

Phages naturally synthesise endolysins to lyse the bacterial cell wall from within, escape the bacterial cell and continue bacterial lysis in neighbouring cells. However, numerous studies have shown that endolysins can be applied exogenously and degrade the peptidoglycan from the outside without using holins or phages, resulting in bacterial lysis and clearance^{73–78}. The exogenous

application of endolysins is particularly attractive against Gram-positive bacterium (such as *S. pseudintermedius*) as Gram-positive cells do not contain an outer membrane, therefore, allowing endolysins to access the peptidoglycan cell wall readily ⁸⁰. In addition, genomic techniques can identify endolysins from phage sequences. The identified endolysins are subsequently expressed and purified using adapted protocols from previous studies. ^{81–84}.

Purified endolysins are characterised similarly to phage, using experiments such as host range, turbidity reduction assays, and trials in animal models ⁸⁵. Through such characterisation, several studies have already shown that endolysins are safe and effective at reducing bacterial growth, both *in vitro* and within animal models, and are therefore a promising antimicrobial agent ^{78,86–93}. Additionally, compared to phage, the use of recombinant endolysins possesses several key advantages ⁸⁵. For example, studies have demonstrated that endolysins possess a broader host range and lower bacterial resistance ^{94–97}. The reduction in bacterial resistance is likely due to the enzyme's mode of action. Endolysins specifically target bonds in the bacterial peptidoglycan that are unlikely to undergo significant selective pressure, as alteration would likely result in less-fit progeny ⁸⁵. Due to gene transduction element potential, phages may also contain and spread harmful genes, including antibiotic or phage-resistant genes. However, as endolysins are small, specific enzymes, they do not harbour this concern ⁹⁸. Additionally, as shown in **Chapter 3**, phages have an auto-dosing property, and while this is advantageous in some contexts, it makes it hard to regulate the dose administered ⁹⁹. Endolysins cannot self-replicate, allowing for controlled dosing during treatment. From a regulatory point of view, a key advantage of endolysins is that they can be easily manufactured under GMP practices, making them easier to upscale from a therapeutic point of view, comparatively to phages ^{100,101}. Lastly, mentioned to previously, temperate phages are commonly isolated, especially for *S. pseudintermedius*. Temperate phages are not suitable for phage therapy due to their ability to integrate within the host genome and their unreliability to lyse their bacterial host ¹⁰². Therefore, harnessing the specific enzymes within phages (endolysin is a promising novel treatment option.

Despite the numerous benefits of endolysins, no studies have assessed the use of bacterial specific endolysins against *S. pseudintermedius*. However, one study has examined the potential of

S. aureus phage, phiSA012, and its respective endolysin, Lys-phiSA012, on isolates of *S. pseudintermedius*⁹⁷. This study found that while phage (phiSA012) showed low lytic potential against *S. pseudintermedius*, the recombinant endolysin (Lys-phiSA012) demonstrated a significant reduction in *S. pseudintermedius* growth⁹⁷. These results support findings that endolysins generally have a broader host range. A secondary study has also tested the clinical efficacy of an alternate endolysin, Protein P128, in reducing *Staphylococcal* canine pyoderma with some success¹⁰³. Protein P128 formulated into a hydrogel and applied to canine pyoderma lesions demonstrated wound healing in all canines tested (n=17). While this is a promising result, the study did not explore the reduction of *S. pseudintermedius* in the canine pyoderma cases¹⁰³. It is also important to note that Protein P128 was also derived from *S. aureus* phage K; thus, endolysins derived from *S. pseudintermedius* phages may be more effective.

There is a lack of knowledge surrounding the efficacy of endolysins against *S. pseudintermedius* and their potential use to treat canine pyoderma. Therefore, this chapter aimed to identify endolysins within *S. pseudintermedius* phages, and subsequently express and purify a selection of endolysins for therapeutic testing. Overall, this work aimed to determine the efficacy of endolysins as an alternative treatment specifically for *S. pseudintermedius* canine infections.

4.3 Results

4.3.1 Identification of putative endolysin genes in *Staphylococcus pseudintermedius* phages

Endolysins can be identified within the genomes of phages, and this study utilised a total of 25 *S. pseudintermedius* phage genomes, including those that have (i) been previously published^{16–18}; (ii) were isolated throughout this thesis experimentally (**Chapter 3**) or (iii) were retrieved using bioinformatic tools to analyse complete bacterial genomes for integrated bacteriophages. A workflow was initially established to identify candidate endolysins (**Figure 4.2**). The whole-genome sequence of all 25 *S. pseudintermedius* phages were uploaded onto the Geneious bioinformatics platform, and their genomes were screened for the presence of endolysin genes by searching key gene terms; lysin, autolysin, amidase, lys, and aminidase. This approach was necessary, as to date, no consensus protein motifs have been associated with endolysin functions of

bacteriophage genes. From this, a total of 26 endolysins were identified, aligned, and described in more detail below.

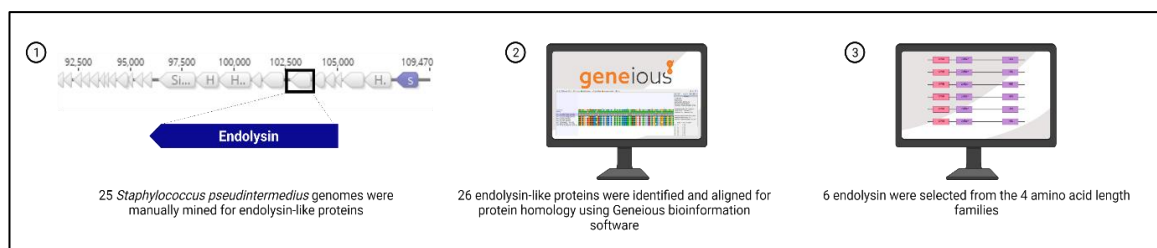


Figure 4.2 Workflow of endolysin identification, alignment, and selection from *S. pseudintermedius* phages. (A) 25 *S. pseudintermedius* whole genomes were manually mined for endolysin-like proteins. (B) 26 endolysin-like proteins were identified and aligned using the Geneious bioinformatics software. (C) Six endolysins were selected from 4 amino acid length classes based on protein alignment.

Manual gene mining identified 26 putative endolysin genes across 21 *S. pseudintermedius* phage genomes, with the remaining four phages appearing not to contain an annotated endolysin (**Table 4.1**). Following identification, the amino acid sequence of all 26 endolysins was extracted and run through BLASTp to determine whether the putative endolysins matched endolysin-like genes. As can be noted in **Table 4.1**, with only two exceptions, all of the putative endolysin genes matched either CHAP-domain containing proteins or N-acetylmuramoyl-L-alanine amidase proteins. Thus, the protein matches gave us an indication that all 26 putative endolysins were endolysin-like genes. Additionally, the presence of a holin gene in close proximity to the putative endolysin gene further confirmed the likelihood of all 26 proteins being endolysin-like proteins, as endolysins and holins are generally encoded in canonical order in a lysis cassette¹⁰⁴. Interestingly, the 26 endolysins could be divided into 4 groups based on amino acid length alone; 251 amino acids, 315 amino acids, 486 amino acids or 629 amino acids (**Figure 4.3**). The majority of the 26 putative endolysins were either 251 or 629 amino acids in length, with the remainder being 486 amino acids in length, except for one putative endolysin, which was 315 amino acids in size. Therefore, putative endolysins were grouped based on amino acid length for initial comparative analysis.

Table 4.1 Identification of 26 endolysin genes through genome mining of *S. pseudintermedius* phages. Twenty-five available *S. pseudintermedius* phage genomes were screened for the presence of endolysin genes. All 26 endolysin gene sequences were extracted for further analysis. The accession number of each endolysin-like protein is listed under the BLAST identification.

Gene annotation	Size of gene (amino acids)	Location of gene in phage genome (bp)	Holin identified in proximity to endolysin gene?	BLAST identification of gene
<i>Staphylococcus</i> Phage SP120 (AP019560 ; 40,530 kb, 35% GC)				
phage lysin CDS	251	13,576 – 14,331	Yes – downstream	CHAP domain-containing protein [Staphylococcus pseudintermedius] WP_037543567.1
N-acetylmuramoyl-L-alanine amidase CDS	629	11,402 – 13,291	Yes – upstream	N-acetylmuramoyl-L-alanine amidase [Staphylococcus phage SP120] YP_010081702.1
<i>Staphylococcus</i> Phage SP197 (AP019561 ; 41,149 kb, 35.7% GC)				
phage lysin CDS	251	30,044 – 30,799	Yes – downstream	MULTISPECIES: CHAP domain-containing protein [Staphylococcus] WP_060830200.1
N-acetylmuramoyl-L-alanine amidase CDS	629	27,870 – 29,759	Yes – upstream	N-acetylmuramoyl-L-alanine amidase [Staphylococcus phage SP197] YP_010081803.1
<i>Staphylococcus</i> Phage SP276 (AP019562 ; 40,147 kb, 35.4% GC)				
phage lysin CDS	251	10,643 – 11,398	Yes – downstream	CHAP domain-containing protein [Staphylococcus pseudintermedius] WP_099997393.1
N-acetylmuramoyl-L-alanine amidase CDS	629	8,469 – 10,358	Yes – upstream	MULTISPECIES: glucosaminidase domain-containing protein [Staphylococcus] WP_099997392.1
<i>Staphylococcus</i> Phage SpT5 (KX827368 ; 39,804 kb, 35.8% GC)				
lytN CDS	251	9,877 – 10,632	Yes – downstream	CHAP domain-containing protein [Staphylococcus pseudintermedius] WP_065354735.1
<i>Staphylococcus</i> Phage Sp152 (KX827369 ; 41,087 kb, 35.5% GC)				
lytN CDS	251	39,077 – 39,832	Yes – downstream	CHAP domain-containing protein [Staphylococcus pseudintermedius] WP_065354735.1
<i>Staphylococcus</i> Phage Sp252 (KX827370 ; 40,093 kb, 35.7% GC)				

lytN CDS	251	9,977 – 10,632	Yes – downstream	CHAP domain-containing protein [Staphylococcus pseudintermedius] WP_065354735.1
<i>Staphylococcus</i> Phage SpT99F3 (KX827371 ; 40,093 kb, 35.7% GC)				
putative lysin CDS	486	37,631 – 39,091	No	N-acetylmuramoyl-L-alanine amidase [Staphylococcus phage vB_SpsS_QT1] APD20014.1
<i>Staphylococcus</i> Phage SN13 (MF428478 ; 40,462 kb, 35.7% GC)				
bifunctional autolysin CDS	629	18,892 – 20,781	Yes – upstream	glucosaminidase domain-containing protein [Staphylococcus pseudintermedius] WP_065354737.1
<i>Staphylococcus</i> Phage SN11 (MF428479 ; 40,108 kb, 35.8% GC)				
bifunctional autolysin CDS	629	18,892 – 20,781	Yes – upstream	CHAP domain-containing protein [Staphylococcus pseudintermedius] WP_065354737.1
<i>Staphylococcus</i> Phage SN10 (MF428480 ; 39,779 kb, 35.8% GC)				
bifunctional autolysin CDS	629	18,892 – 20,781	Yes – upstream	CHAP domain-containing protein [Staphylococcus pseudintermedius] WP_065354737.1
<i>Staphylococcus</i> Phage SN8 (MF428481 ; 39,803 kb, 35.8% GC)				
bifunctional autolysin CDS	629	18,892 – 20,781	Yes – upstream	CHAP domain-containing protein [Staphylococcus pseudintermedius] WP_065354737.1
<i>Staphylococcus</i> Phage phiSp15-1 (MK075001 ; 45,164 kb, 35.5% GC)				
lysin CDS	486	41,598 – 43,058	No	SH3 domain-containing protein [Staphylococcus pseudintermedius] WP_130921486.1
<i>Staphylococcus</i> Phage phiSp38-1 (MK075002 ; 43,851 kb, 36.0% GC)				
lysin CDS	486	40,279 – 41,727	Yes – downstream	CHAP domain-containing protein [Staphylococcus pseudintermedius] WP_103926962.1
<i>Staphylococcus</i> Phage phiSp44-1 (MK075003 ; 42,565 kb, 35.9% GC)				
bifunctional autolysin Atl / N-acetylmuramoyl-L-alanine amidase / endo-beta-N-acetylglucosaminidase CDS	629	36,783 – 38,672	Yes – upstream	CHAP domain-containing protein [Staphylococcus pseudintermedius] YP_010081614.1

lysin CDS	251	38,959 – 39,714	Yes – downstream	MULTISPECIES: CHAP domain-containing protein [Staphylococcus] YP_010081616.1
<i>Staphylococcus</i> Phage phiSp119-1 (MK075004 ; 49,795 kb, 36.4% GC)				
lysin CDS	486	47,130 – 48,590	No	peptidoglycan DD-metalloendopeptidase family protein [Staphylococcus pseudintermedius] AZB66744.1
<i>Staphylococcus</i> Phage phiSp119-2 (MK075005 ; 40,011 kb, 34.1% GC)				
lysin CDS	315	39,001 – 39,948	Yes – downstream	N-acetylmuramoyl-L-alanine amidase [Staphylococcus pseudintermedius] AZB66809.1
<i>Staphylococcus</i> Phage phiSp119-3 (MK075006 ; 44,311 kb, 35.6% GC)				
bifunctional autolysin Atl / N-acetylmuramoyl-L-alanine amidase / endo-beta-N-acetylglucosaminidase CDS	629	40,169 – 42,058	Yes – upstream	CHAP domain-containing protein [Staphylococcus pseudintermedius] AZB66874.1
lysin CDS	251	42,345 – 43,100	Yes – downstream	CHAP domain-containing protein [Staphylococcus pseudintermedius] AZB66876.1
<i>Staphylococcus</i> Phage vB_SpsS_QT1 (MK450538 ; 43,029 kb, 36.9% GC)				
N-acetylmuramoyl-L-alanine amidase CDS	486	21,543 – 23,003	Yes – downstream	peptidoglycan DD-metalloendopeptidase family protein [Staphylococcus pseudintermedius] WP_203157274.1
<i>Staphylococcus</i> Phage vB_SpsM_WIS42 (MN028536 ; 40,093 kb, 35.7% GC)				
lysin CDS	251	21,226 – 21,981	Yes – downstream	CHAP domain-containing protein [Staphylococcus pseudintermedius] WP_065354735.1
<i>Staphylococcus</i> Phage SP_157588 (48,558 kb, 35.1% GC)				
Putative N-acetylmuramoyl-L-alanine amidase	486	50,453 – 51,910	No but close to endolysin chaperone	CHAP domain-containing protein [Staphylococcus pseudintermedius] EGQ1746921.1
<i>Staphylococcus</i> Phage SP_22L (48,558 kb, 35.1% GC)				
Putative N-acetylmuramoyl-L-alanine amidase	486	50,174 – 51,631	No but close to endolysin chaperone	CHAP domain-containing protein [Staphylococcus pseudintermedius] EGQ1746921.1

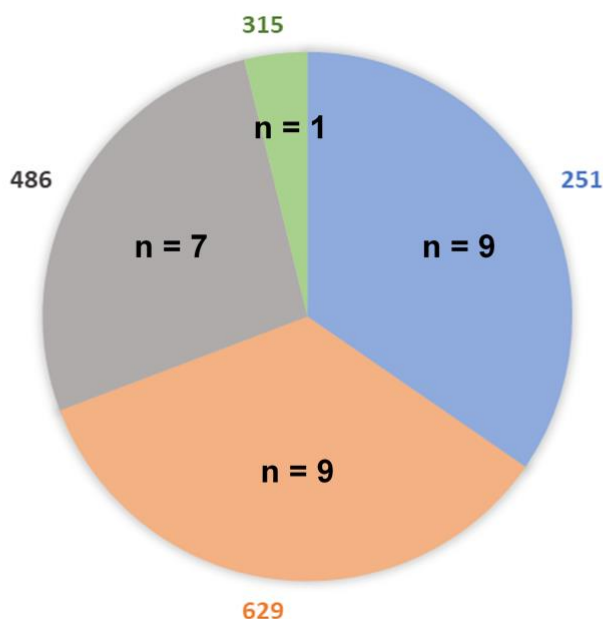


Figure 4.3 Amino acid length of 26 identified endolysins from *S. pseudintermedius* phages. The amino acid length of each gene was determined using Geneious. The 26 endolysins were grouped into four categories based on amino acid length: 9 endolysin-like proteins were 251 amino acids, 1 endolysin-like protein was 315 amino acids, 7 endolysin-like proteins were 486 amino acids, and 9 endolysin-like proteins were 629 amino acids.

4.3.2 Protein alignment of identified putative endolysins

In order to identify unique proteins, pairwise protein alignment was performed on endolysin-like genes within each of the amino acid length groups (**Figure 4.4A,B,C**). Protein alignment comparisons between the nine endolysins within the 251 amino acid group showed high identity with one another, evident by the high coverage of conserved regions in **Figure 4.4A**, denoted by the asterisk's symbols. This high conservation among the 251 amino acid endolysins is supported by the high pairwise percent identity in **Table 4.5**, demonstrating greater than 97.2% conservation of amino acids across the length of the proteins. Similarly, as shown in **Figure 4.4B**, protein alignment comparisons between the seven endolysins within the 486 amino acid group showed that four of the seven endolysins were highly similar, and two out of the seven were identical to one another but had a low sequence identity to all other endolysins. (**Table 4.6**). However, the remaining endolysins, Lys_phi38-1, showed relatively low pairwise identity to the other six endolysin proteins within the 486 amino acid group (**Table 4.6**). Lastly, protein alignment comparisons between the remaining nine endolysins within the 629 amino acid group showed high identity with one another,

evident by the high coverage of conserved regions in **Figure 4.4A**, denoted by the asterisk's symbols. This high conservation among the 629 amino acid endolysins is supported by a high pairwise percent identity in **Table 4.7**, demonstrating greater than 98.9% conservation of amino acid identity. The final endolysin, Lys_119-2, had an amino acid length of 315 amino acids and was aligned in each of the groups, however, it showed low sequence identity with all other endolysins.

A	Lys_phiSP119-3-2	MKTYSEARSRLRWYVGRYIDFDGYWAYQCMDLAVDYIYWLLDIRMWGNAKDAINNDFKNM	60
	Lys_SP120-1	MKTYSEARSRLRWYVGRYIDFDGYWAYQCMDLAVDYIYWLLDIRMWGNAKDAINNDFKNM	60
	Lys_SPT5	MKTYSEARSRLRWYVGRYIDFDGYWAYQCMDLAVDYIYWLLDIRMWGNAKDAINNDFKNM	60
	Lys_SP152	MKTYSEARSRLRWYVGRYIDFDGYWAYQCMDLAVDYIYWLLDIRMWGNAKDAINNDFKNM	60
	Lys_SP252	MKTYSEARSRLRWYVGRYIDFDGYWAYQCMDLAVDYIYWLLDIRMWGNAKDAINNDFKNM	60
	Lys_vB_SpsM	MKTYSEARSRLRWYVGRYIDFDGYWAYQCMDLAVDYIYWLLDIRMWGNAKDAINNDFKNM	60
	Lys_SP276-1	MKTYSEARSRLRWYVGRYIDFDGYWAYQCMDLAVDYIYWLLDIRMWGNAKDAINNDFKNM	60
	Lys_SP197-1	MKTYSEARSRLRWYVGRYIDFDGYWAYQCMDLAVDYIYWLLDIRMWGNAKDAINNDFKNM	60
	Lys_phiSP44-1-2	MKTYSEARSRLRWYVGRYIDFDGYWAYQCMDLAVDYIYWLLDIRMWGNAKDAINNDFKNM	60

	Lys_phiSP119-3-2	ATVYENTPSFVPQVGDAVFRSGIYKQYGHIGIVYNSGNTNQFLILEQNFQGNANTPATL	120
	Lys_SP120-1	ATIYENTPSFVPQVGDAVFRNGIYKQYGHIGIVYNSGNTNQFLILEQNFQGNANTPASL	120
	Lys_SPT5	ATIYENTPSFVPQVGDAVFRNGIYKQYGHIGIVYNSGNTNQFLILEQNFQGNANTPASL	120
	Lys_SP152	ATIYENTPSFVPQVGDAVFRNGIYKQYGHIGIVYNSGNTNQFLILEQNFQGNANTPASL	120
	Lys_SP252	ATIYENTPSFVPQVGDAVFRNGIYKQYGHIGIVYNSGNTNQFLILEQNFQGNANTPASL	120
	Lys_vB_SpsM	ATIYENTPSFVPQVGDAVFRNGIYKQYGHIGIVYNSGNTNQFLILEQNFQGNANTPASL	120
	Lys_SP276-1	ATVYENTPSFVPQVGDAVFRSGIYKQYGHIGIVYNSGNTNQFLILEQNFQGNANTPAKL	120
	Lys_SP197-1	ATIYENTLSPFVPQVGDAVFRKGIYKQYGHIGIVYNSGNTNQFLILEQNFQGNANTPAKL	120
	Lys_phiSP44-1-2	ATIYENTLSPFVPQVGDAVFRKGIYKQYGHIGIVYNSGNTNQFLILEQNFQGNANTPAKL	120
		*,****	
	Lys_phiSP119-3-2	RWDNYYGCTHFIRPHYKSENTTSKIANKISPPSHKAAGNSASKIVSGSRAPYNLKWSKGA	180
	Lys_SP120-1	RWDNYYGCTHFIRPHYKSENTTSKIANKISPPSHKAAGNSASKIISGSRAPYNLKWSKGA	180
	Lys_SPT5	RWDNYYGCTHFIRPHYKSENTTSKIANKISPPSHKAAGNAASKIVSGSRAPYNLKWSKGA	180
	Lys_SP152	RWDNYYGCTHFIRPHYKSENTTSKIANKISPPSHKAAGNAASKIVSGSRAPYNLKWSKGA	180
	Lys_SP252	RWDNYYGCTHFIRPHYKSENTTSKIANKISPPSHKAAGNAASKIVSGSRAPYNLKWSKGA	180
	Lys_vB_SpsM	RWDNYYGCTHFIRPHYKSENTTSKIANKISPPSHKAAGNAASKIVSGSRAPYNLKWSKGA	180
	Lys_SP276-1	RWDNYYGCTHFIRPHYKRENTTSKIANKISPPSHKAAGNSASKIISGSRAPYNLKWSKGA	180
	Lys_SP197-1	RWDNYYGCTHFIRPHYKRENTTSKIANKISPPSHKAAGNSASKIISGSRAPYNLKWSKGA	180
	Lys_phiSP44-1-2	RWDNYYGCTHFIRPHYKRENTTSKIANKISPPSHKAAGNSASKIISGSRAPYNLKWSKGA	180

	Lys_phiSP119-3-2	YFNAKVDGLGATSATRYGDSRANYRFQVQAEYVPGLIYVFEIIDGWCRIYNNHNNEWI	240
	Lys_SP120-1	YFNAKVDGLGATSATRYGDSRANYRFQVQAEYVPGLIYVFEIIDGWCRIYNNHNNEWI	240
	Lys_SPT5	YFNAKVDGLGATSATRYGDSRANYRFQVQAEYVPGLIYVFEIIDGWCRIYNNHNNEWI	240
	Lys_SP152	YFNAKVDGLGATSATRYGDSRANYRFQVQAEYVPGLIYVFEIIDGWCRIYNNHNNEWI	240
	Lys_SP252	YFNAKVDGLGATSATRYGDSRANYRFQVQAEYVPGLIYVFEIIDGWCRIYNNHNNEWI	240
	Lys_vB_SpsM	YFNAKVDGLGATSATRYGDSRANYRFQVQAEYVPGLIYVFEIIDGWCRIYNNHNNEWI	240
	Lys_SP276-1	YFNAKVDGLGATSATRYGDSRANYRFQVQAEYVPGLIYVFEIIDGWCRIYNNHNNEWI	240
	Lys_SP197-1	YFNAKVDGLGATSATRYGDSRANYRFQVQAEYVPGLIYVFEIINGWCRIYNNHNNEWI	240
	Lys_phiSP44-1-2	YFNAKVDGLGATSATRYGDSRANYRFQVQAEYVPGLIYVFEIINGWCRIYNNHNNEWI	240

	Lys_phiSP119-3-2	WHERLIVKEVF	251
	Lys_SP120-1	WHERLIVKEVF	251
	Lys_SPT5	WHERLIVKEVF	251
	Lys_SP152	WHERLIVKEVF	251
	Lys_SP252	WHERLIVKEVF	251
	Lys_vB_SpsM	WHERLIVKEVF	251
	Lys_SP276-1	WHERLIVKEVF	251
	Lys_SP197-1	WHERLIVKEVF	251
	Lys_phiSP44-1-2	WHERLIVKEVF	251

B

Lys_SPT99F3	MLTAIDYLTGRGKISSDPRT--YDGY---P-----KNYGYRNYIENG-----INDE	43
Lys_vB_SPs5	MLTAIDYLTGRGKISSDPRT--YDGY---P-----KNYGYRNYIENG-----INDE	43
Lys_phISP15-1	MLTAIDYLTGRGKISSDPRT--YDGY---P-----KNYGYRNYHENG-----INDE	43
Lys_phISP119-1	MLTAIDYLTGRGKISSDPRT--YDGY---P-----KNYGYRNYHENG-----INDE	43
Lys_phISP38-1	MVASLSKKEFISFLKSSGKQFNEQGWYGYQCDFANTGWLKLFGLHMLGLGAKDIPFNS	60
Lys_SP157588	MAPSKTKQEAINYALSLEGKGLDFNFAQNCQCFDANVYNNHIFGHSLKGEAKDIPNPR	60
Lys_SP22L	MAPSKTKQEAINYALSLEGKGLDFNFAQNCQCFDANVYNNHIFGHSLKGEAKDIPNPR	60
	* : * : : * : : * : : * : : *	
Lys_SPT99F3	FCG-GYHRAFDVYSNATNDVPAVTSGTVEANDYG-NFGGTF-VIR-----DANDNDWI	94
Lys_vB_SPs5	FCG-GYHRAFDVYSNATNDVPAVTSGTVEANDYG-NFGGTF-VIR-----DANDNDWI	94
Lys_phISP15-1	FCG-GYHRAFDVYSNATNDVPAVTSGTVEANDYG-NFGGTF-VIR-----DANDNDWI	94
Lys_phISP119-1	FCG-GYHRAFDVYSNATNDVPAVTSGTVEANDYG-NFGGTF-VIR-----DANDNDWI	94
Lys_phISP38-1	INKNYFKTEAKVYSNTEFLAE-AGDMVVFGENYGGYGHVAVHIEATLDYIVVLEQNL	119
Lys_SP157588	WN--DLTQEAIVPNTPEFLAE-AGDLAIFSSRFGGGYGHVGVIEATLDYIVVLEQNL	117
Lys_SP22L	WN--DLTQEAIVPNTPEFLAE-AGDLAIFSSRFGGGYGHVGVIEATLDYIVVLEQNL	117
	: * * : : : : : : : * : * : * : : : * :	
Lys_SPT99F3	YGLHQRGSMRFVVGDKVQGDIVGLQGN5NYYDNPM5AHLHIQLRPKDALKDEK5QVCSG	154
Lys_vB_SPs5	YGLHQRGSMRFVVGDKVQGDIVGLQGN5NYYDNPM5AHLHIQLRPKDALKDEK5QVCSG	154
Lys_phISP15-1	YGLHQRGSMRFVVGDKVQGDIVGLQGN5NYYDNPM5AHLHIQLRPKDALKDEK5QVCSG	154
Lys_phISP119-1	YGLHQRGSMRFVVGDKVQGDIVGLQGN5NYYDNPM5AHLHIQLRPKDALKDEK5QVCSG	154
Lys_phISP38-1	GGGTDGIEQPGSGWE-----SVTRRKHAYDFPMW-----FIRPNFK--SETLLSA-	164
Lys_SP157588	GGGITKT-----E-----VTTRKHNYEYDMI-----FVRPKYK--KEGSGRLP-	154
Lys_SP22L	GGGITKT-----E-----VTTRKHNYEYDMI-----FVRPKYK--KEGSGRLP-	154
	* : : : : * : : * : : * : : *	
Lys_SPT99F3	LAMEKYDITNLNKKQKSKNGSVKE-LKHIYSNHIKGNKITAPKPSIQGVVHNDYGSMT	213
Lys_vB_SPs5	LAMEKYDITNLNKKQKSKNGSVKE-LKHIYSNHIKGNKITAPKPSIQGVVHNDYGSMT	213
Lys_phISP15-1	LAMEKYDITNLNKKQKSKNGSVKE-LKHIYSNHIKGNKITAPKPSIQGVVHNDYGSMT	213
Lys_phISP119-1	LAMEKYDITNLNKKQKSKNGSVKE-LKHIYSNHIKGNKITAPKPSIQGVVHNDYGSMT	213
Lys_phISP38-1	---QS-----VTQKSKQPAKKPKKLNIRDEIKGYNDKRGYKPRGIVLHND--	210
Lys_SP157588	---KK-----KI-----LLVAGHGLGYWSNDS---GAAAGYNERDFIRKNIVPNVA	195
Lys_SP22L	---KK-----KI-----LLVAGHGLGYWSNDS---GAAAGYNERDFIRKNIVPNVA	195
	: , : : : : : : : : : : : : : *	
Lys_SPT99F3	PS---QYLPWLYAREN---NGTHVNGWASVYANRNEVLWYHPTDYVEWHCGNQHANAN	265
Lys_vB_SPs5	PS---QYLPWLYAREN---NGTHVNGWASVYANRNEVLWYHPTDYVEWHCGNQHANAN	265
Lys_phISP15-1	PS---QYLPWLYAREN---NGTHVNGWASVYANRNEVLWYHPTDYVEWHCGNQHANAN	265
Lys_phISP119-1	PS---QYLPWLYAREN---NGTHVNGWASVYANRNEVLWYHPTDYVEWHCGNQHANAN	265
Lys_phISP38-1	---GSAGATAEAYHKGLVNADYNRLKEGVAHSYVSGSTVYQALPEGKIAHWANRIGNRD	267
Lys_SP157588	KHLRKAGHDVHLYGGETHNQD-----LFQDTRY-----GEMVGNYS	231
Lys_SP22L	KHLRKAGHDVHLYGGETHNQD-----LFQDTRY-----GEMVGNYS	231
	* : : : : : : : : : : : : : *	
Lys_SPT99F3	LIGFEVCE5YPGRISDALFLENEEATLKVAADVMSYGLPVNRNTVRLHNEFFGT----	320
Lys_vB_SPs5	LIGFEVCE5YPGRISDALFLENEEATLKVAADVMSYGLPVNRNTVRLHNEFFGT----	320
Lys_phISP15-1	LIGFEVCE5YPGRISDALFLENEEATLKVAADVMSYGLPVNRNTVRLHNEFFGT----	320
Lys_phISP119-1	LIGFEVCE5YPGRISDALFLENEEATLKVAADVMSYGLPVNRNTVRLHNEFFGT----	320
Lys_phISP38-1	YYGIEICQSVG-ATD-KQFLANEQSAFQEAARMLKKHLPANRNTVRLHVEFYNT	320
Lys_SP157588	DYGMVWARQ6-FDSVTEFHLDAAGAQA5SGGHVIGMGLSPDTIDKAIQNTIYHFIGTIR	290
Lys_SP22L	DYGMVWARQ6-FDSVTEFHLDAAGAQA5SGGHVIGMGLSPDTIDKAIQNTIYHFIGTIR	290
	* : : : : * : : : : : : : : *	
Lys_SPT99F3	-SCPHRSWE-----LHVKGKAPY-----TTA	340
Lys_vB_SPs5	-SCPHRSWE-----LHVKGKAPY-----TTA	340
Lys_phISP15-1	-SCPHRSWE-----LHVKGKAPY-----TTA	340
Lys_phISP119-1	-SCPHRSWE-----LHVKGKAPY-----TTA	340
Lys_phISP38-1	-ACPHR-----SMLLHTGFDPYVK-----GIP-----PQA	344
Lys_SP157588	NIDPRDNLNVLNVAKNKGVNRYLAELGFIITSVKDHNNIINLESYTRGIAEDIHGGKLEP	350
Lys_SP22L	NIDPRDNLNVLNVAKNKGVNRYLAELGFIITSVKDHNNIINLESYTRGIAEDIHGGKLEP	350
	* : : : : * : : : : : : : : *	
Lys_SPT99F3	NINRMKDYFIKRIKHYDDGGKLEVSKEATIKQSDVKQEVKKQEAQVVKATDNKQNKDGI	400
Lys_vB_SPs5	NINRMKDYFIKRIKHYDDGGKLEVSKEATIKQSDVKQEVKKQEAQVVKATDNKQNKDGI	400
Lys_phISP15-1	NINRMKDYFIKRIKHYDDGGKLEVSKEATIKQSDVKQEVKKQEAQVVKATDNKQNKDGI	400
Lys_phISP119-1	NINRMKDYFIKRIKHYDDGGKLEVSKEATIKQSDVKQEVKKQEAQVVKATDNKQNKDGI	400
Lys_phISP38-1	MQLKLDYFIKQIRAYMDGKVPVATVS-NK-TS-----ASSNTVKKPIAGANQVNSYGT	395
Lys_SP157588	VKLPTKDRAKEKVK-----QVAAKVT-KKKPT-----PANNTSKP-KTEWANK----	391
Lys_SP22L	VKLPTKDRAKEKVK-----QVAAKVT-KKKPT-----PANNTSKP-KTEWANK----	391
	** : : : : : : : : : : : : : *	
Lys_SPT99F3	WYKAEMASFTVTASEGII TRYKGPWT--GHPQAGVLQKGQTIKYDEVQKFDGHVWVSWET	458
Lys_vB_SPs5	WYKAEMASFTVTAPKGI TRYKGPWT--GHPQAGVLQKGQTIKYDEVQKFDGHVWVSWET	458
Lys_phISP15-1	WYKAEMASFTVTASEGII TRYKGPWT--GHPQAGVLQKGQTIKYDEVQKFDGHVWVSWET	458
Lys_phISP119-1	WYKTEHASFTVTASEGII TRYKGPWT--GHPQAGVLQKGQTIKYDEVQKFDGHVWVSWET	458
Lys_phISP38-1	YYMKESATFVCG-NKPIITRTVGPFT--TCPEGYHFPQGGWCEYDEVMQLQGHVWVSWET	452
Lys_SP157588	---GQFTTFASN-TQPIVVRRAVGLNAAKVDVNSWIYPNQWPFDRLIKKGQYHWRIFEY	447
Lys_SP22L	---GQFTTFASN-TQPIVVRRAVGLNAAKVDVNSWIYPNQWPFDRLIKKGQYHWRIFEY	447
	: : : * : : * : : : : : : : : * : : * : : :	
Lys_SPT99F3	FE---GETVYMPVRTWDAKT---GKVGKLGWGIK-----	486
Lys_vB_SPs5	FE---GETVYMPVRTWDAKT---GKVGKLGWGIK-----	486
Lys_phISP15-1	FE---GETVYMPVRTWDAKT---GKVGKLGWGIK-----	486
Lys_phISP119-1	FE---GETVYMPVRTWDAKT---GKVGKLGWGIK-----	486
Lys_phISP38-1	QG---QRYYPPIRKWNGVAPPNGQLDGLWGIK-----	482
Lys_SP157588	PTNPSAGKFYMPIGKIGTKG-KVKDKTLWGLTDIKSYG	485
Lys_SP22L	PTNPSAGKFYMPIGKIGTKG-KVKDKTLWGLTDIKSYG	485
	* : : : : * : : : : * : : : *	

[illegible]

Figure 4.4 Protein sequence alignment of putative endolysin proteins from three amino acid groups. (A) Alignment of 251 amino acid endolysins. (B) Alignment of 486 amino acid endolysins. (C) Alignment of 629 amino acid endolysins. The amino acid sequence of the nine putative endolysin proteins were uploaded in FASTA format Clustal Omega. **Consensus Symbols:** The following symbols denote the degree of residue conservation. ‘*’ (asterisk’s) indicates positions which have a single, fully conserved residue. ‘:’ (colon) indicates conservation between groups of strongly similar properties. ‘.’ (period) indicates conservation between groups of weakly similar properties. **Red:** hydrophobic amino acids, **Blue:** Acidic amino acids, **Magenta:** Basic amino acids, **Green:** Hydroxly + sulfhydryl + amine, **Grey/other:** Unusual amino/imino acids

4.3.3 Selection and characterisation of candidate putative endolysins

The protein alignment of the endolysins retrieved from *S. pseudintermedius* phages showed that the majority of the 26 endolysin proteins were highly similar or identical. As such, a representative endolysin from each group of similar endolysin proteins was selected, as well as any endolysins that showed low sequence alignment with others, with a total of 6 unique endolysins selected for further analysis (**Table 4.3**). Alignment of the six selected endolysins showed low amino acid identity (7.02 – 29.96%), demonstrating their unique sequences (**Table 4.2** and **Figure 4.13**). Using ScienceGateway Protein Molecular Weight Calculator, the predicted size of the six selected endolysins was shown to vary in size from 31.5 kDa to 73.9 kDa. The endolysins’ were labelled as ‘Lys’ for endolysin, followed by the simple name of the phage host that the endolysin protein was identified from (**Table 4.3**).

Table 4.2 Pairwise (%) identity of six endolysins selected. Pairwise (%) identity was determined using pairwise analysis through Clustal Omega

	Lys_SPT5	Lys_SN13	Lys_T99F3	Lys_119-2	Lys_38-1	Lys_22L
Lys_SPT5		27.98%	17.10%	7.02%	22.60%	28.72%
Lys_SN13	27.98%		18.95%	13.28%	21.78%	19.32%
Lys_T99F3	17.10%	18.95%		17.49%	29.88%	16.98%
Lys_119-2	7.02%	13.28%	17.49%		19.03%	29.96%
Lys_38-1	22.60%	21.78%	29.88%	19.03%		34.43%
Lys_22L	28.72%	19.32%	16.98%	29.96%	34.43%	

Table 4.3 Six novel candidate endolysin selected for characterisation. Six putative endolysins were selected based on their unique amino acid sequence within their given amino acid group.

Endolysin name	Amino acid length	Predicted size (kDa)
Lys_SPT5	251	31.5
Lys_SN13	629	73.9
Lys_T99F3	486	57.9
Lys_38-1	486	56.7
Lys_22L	486	56.9
Lys_119-2	315	38.2

There is still a lack of understanding of the required functional domains for endolysins to work efficiently against specific bacterial species, therefore, the six selected endolysins were subjected to protein domain analysis using InterProScan. The analysis revealed that four out of the six endolysins contained a cysteine, histidine-dependent amidohydrolases/peptidases (CHAP) domain (IPR007921) at their N-terminus; a functional enzymatic domain involved in the cleavage of N-acetylmuramic acid and l-alanine in the bacterial cell wall ⁷⁴. (**Figure 4.5A, B, D and E**). Two out of the six endolysins contained cell wall binding domains (CBD), the functional domain involved in adherence to the bacterial cell wall ⁷⁴ (**Figure 4.5C and D**). In addition, four out of the six endolysins contained an amidase-domain, which is known as the peptidoglycan cleavage domain (PCD), similarly involved in the cleavage of peptidoglycan bond structures (**Figure 4.5C, D, E and F**). Other domains identified included a peptidase and a glucosaminidase domain (**Figure 4.5B and C**). To gain a better understanding of the functional ability of these endolysins to restrict *S. pseudintermedius* growth, all six selected endolysin sequences were chemically synthesised and cloned into a pET28 expression vector (**Figure 4.5G**) for recombinant protein expression (see **Section 2.7** Expression and purification of endolysins).

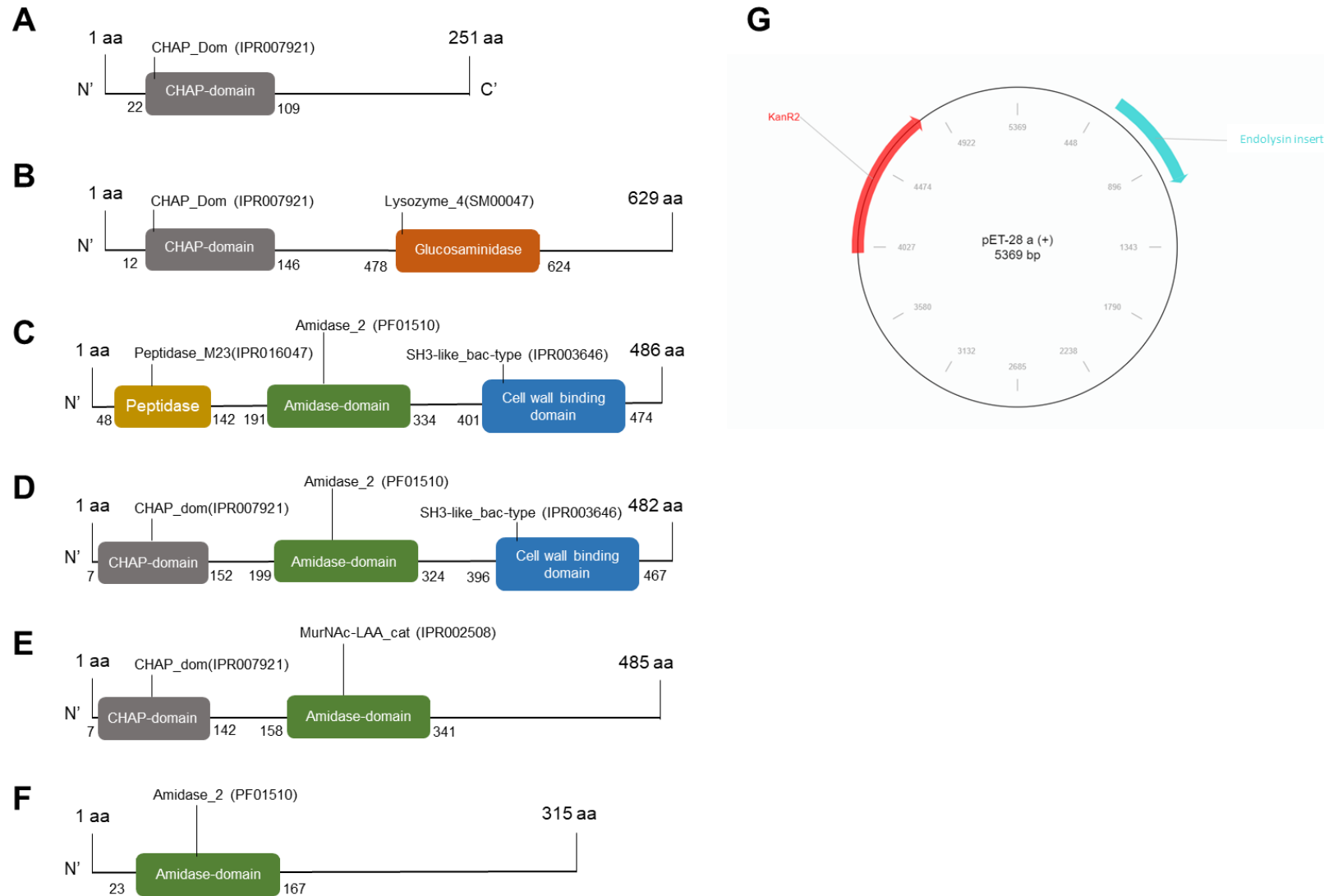


Figure 4.5 Domain organisation of six *S. pseudintermedius* endolysins. Domains were identified using InterProScan. Schematic representative of (A) Lys_SPT5, (B) SN13, (C) Lys_SPT99F3, (D) Lys_38-1, (E) Lys_22L, (F) Lys_119-2. Identified domains include CHAP domain (grey), amidase domain (green), cell wall binding domain (blue), peptidase (yellow) and glycosaminidase (orange). The numbers next to the domains indicated the residue location of the domains. (G) Schematic map of pET28a, vector used to clone selected endolysin genes into, for subsequent expression.

Following cloning of the six endolysin constructs, the expression vector was transformed into *E. coli* cells and protein expression was induced by IPTG at 21 °C (**Figure 4.6**). Expressed endolysins were subjected to metal-affinity purification, however, the expression protocol required optimisation for each endolysin due to low quantity of eluted endolysin on initial attempts (**Figure 4.14A**). Optimisation protocols involved varying the temperatures for endolysin expression from 18° C to 21°C for each endolysin and varying the cell lysis sonication processes from 3 x 30-second sonication at 60% capacity to 6 x 30-second sonication at 40% capacity (**Figure 4.14B**). Following optimisation of the expression protocols for all six endolysins, the purification protocols also required optimisation. For purification optimisation, various imidazole concentrations of the elution buffer were tested (between 250 mM to 400 mM). This optimisation led to the discovery that each endolysin needed slightly different requirements for optimal endolysin purification (See **Section 2.7 Expression and purification of endolysins**), with the successful purification of all six endolysins shown in **Figure 4.7B, C, D, E, F and G**.

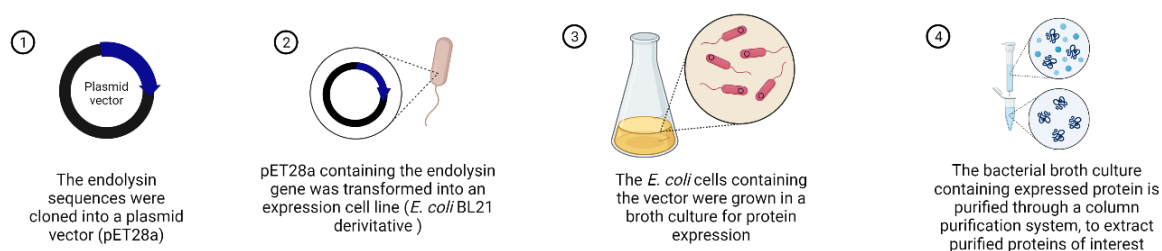


Figure 4.6 Workflow for cloning, transformation, expression, and purification of endolysins for therapeutic testing. (1) The six selected endolysin sequences were cloned into a plasmid vector before the vector was (2) transformed into an expression cell line. (3) The *E. coli* cells are then grown in broth culture and protein expression was induced. (4) Using a column purification method, the protein of interest was purified for further testing.

The efficiency of endolysin purification was variable for each of the six endolysin proteins. The purity of the respective endolysins was evaluated by SDS-PAGE, with each of the endolysins showing high purity due to the lack of unspecific banding in the elution fraction (marked with asterisks to highlight the band at the expected protein size) (**Figure 4.7**). The estimated yield of the eluted endolysins in **Figure 4.7** varied from 8 µg/µL for Lys_SPT99F3 to 0.5 µg/µL for Lys_SPT5, based on protein standards, with the minimum amount of endolysin required to move forward estimated to be 0.5 µg/µL based on required downstream experiments.

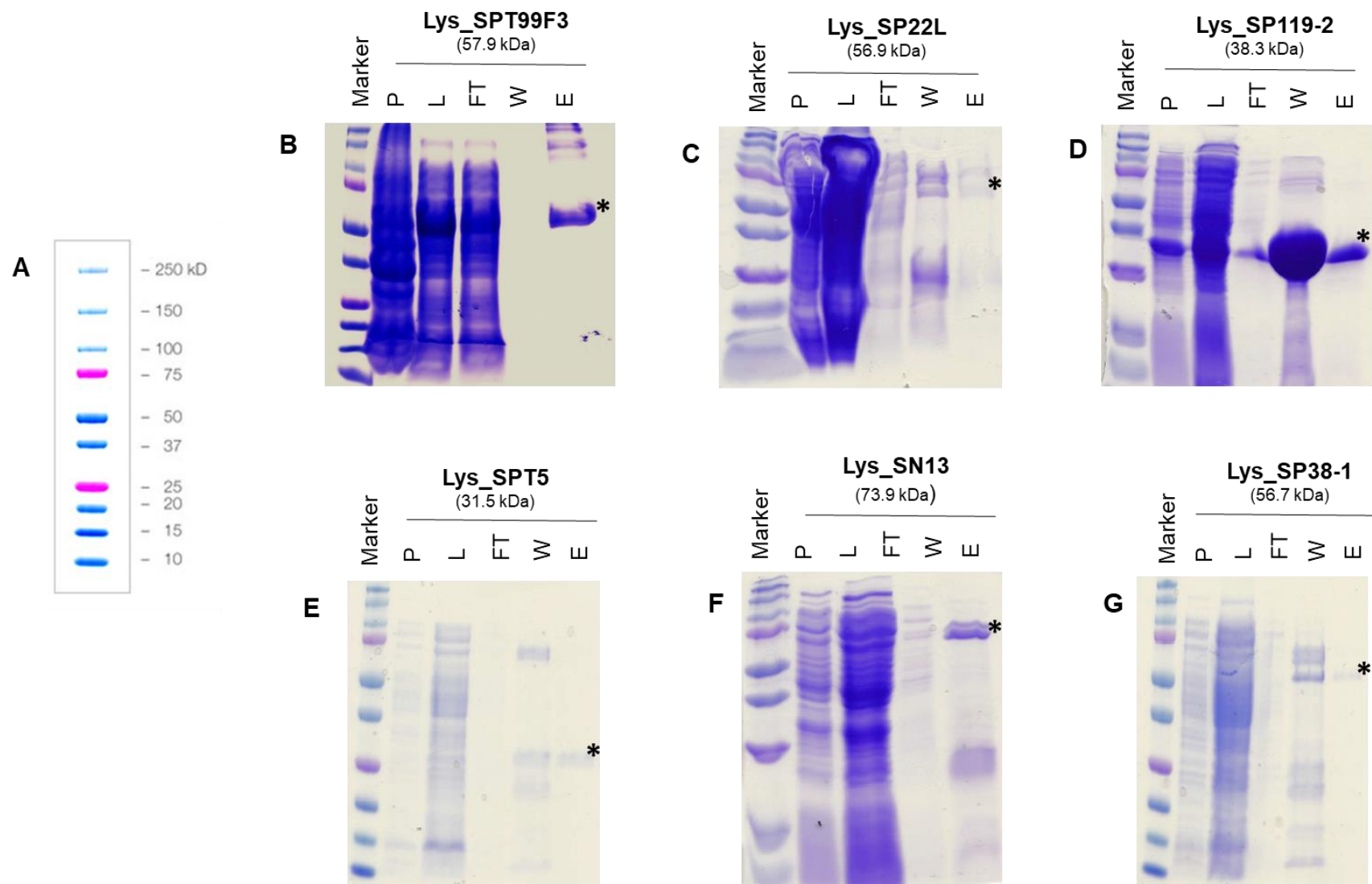


Figure 4.7 SDS-PAGE images of six purified endolysins.(A) Precision Plus Protein Dual Colour Standards (BioRad) marker used for SDS-PAGE gels. Protein purification of (B) Lys_SPT99F3, (C) Lys_SP22L, (D) Lys_SP119-2, (E) Lys_SPT5, (F) Lys_SN13, (G) Lys_SP38-1. Protein purification process observed on gels; **P** = cell pellet, **L** = lysate, **FT** = flow through, **W** = wash, **E** = elution. Successful purification of each endolysin at correct molecular weight is noted by the asterisk's (*).

Following successful purification, the six endolysins were spotted onto 60 *S. pseudintermedius* clinical isolates to test their lytic ability (see **Section 2.4.3** Host range analysis). The lytic ability of the six endolysins was measured based on the zones of clearing produced after spotting of 10 μ L of the endolysin (2 μ g/ μ L) on the bacterial host lawn and incubating at 37 °C overnight. The lytic ability was scored as follows: '+' = weak lysis, '++' = moderate lysis, or '+++' = strong lysis (**Figure 4.8**). This lysis scoring method was used to determine the lytic ability and the host range of all six endolysins.

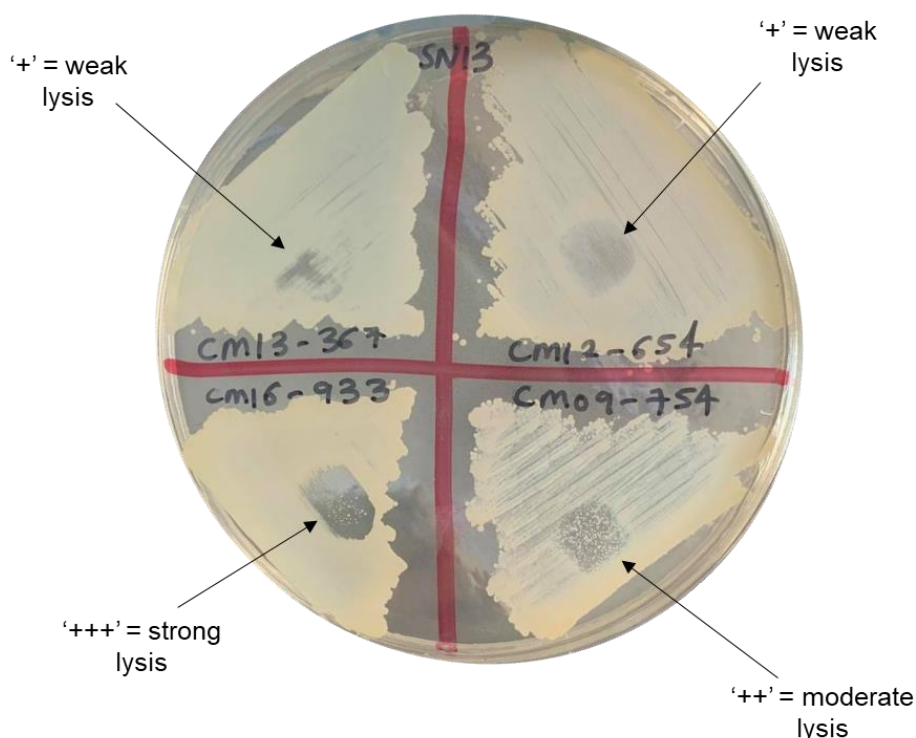


Figure 4.8 Scoring of endolysin lytic ability on *S. pseudintermedius* clinical isolates. Representative plate of lytic ability of Lys_SN13 (2 mg/mL) when spotted (10 μ L) on a bacterial lawn of 4 different *S. pseudintermedius* clinical strains and incubated the plates overnight at 37 °C. The different levels of lysis from the basis of scoring method to determine the host range ability of the selected endolysins.

Surprisingly, only 3 (Lys_SN13, Lys_SPT5 and Lys_SP22L) out of the six endolysins successfully lysed any of the *S. pseudintermedius* clinical isolates (**Table 4.4**). When comparing the host range of these endolysins, each had slightly different host spectra, with Lys_SN13 possessing the broadest host range able to lyse 60% of the total *S. pseudintermedius* isolates tested, followed by Lys_SPT5

and Lys_SP22L, able to lyse 36% and 10% of the total *S. pseudintermedius* isolates tested, respectively (**Figure 4.9A**). Interestingly, these were also three out of the four proteins that contained a CHAP domain. As shown in **Figure 4.9A**, at least one of the three endolysins were able to lyse isolates from all infection sites tested, with Lys_SN13 able to lyse over half of the isolates collected from the skin, urinary, respiratory, reproductive, and musculoskeletal infections. However, Lys_SN13 only lysed 33% of the isolates from ear infections; whereas Lys_SPT5 showed preferential lysis of isolates from ear infections, able to lyse 66% of isolates. The lytic ability of the three endolysins also showed that all three were able to lyse antibiotic sensitive *S. pseudintermedius* isolates (sensitive to all seven antibiotics tested). In contrast, only Lys_SN13 and Lys_SPT5 lysed low-resistant isolates (resistant to 1-2 antibiotics) (**Figure 4.9B**). Importantly, all three endolysins lysed a high percentage of multidrug resistant *S. pseudintermedius* isolates (resistant to 3 or more antibiotics simultaneously), with Lys_SN13 able to lyse 47% of MDR isolates within our collection, followed by Lys_SPT5 and Lys_SP22L able to lyse 40% and 18% of MDR strains, respectively (**Figure 4.9B**). Due to the broad host range and ease in purification, Lys_SN13 was selected as the lead candidate for further experiments.

Table 4.4 Host range analysis of six purified endolysin on 60 *S. pseudintermedius* clinical strains. Antibiotics tested included Pen = Penicillin, Amc = Ampicillin, CL = Cephalexin, SF = Sulfafurazole, W = Trimethoprim, Te = Tetracycline, Enr = Enrofloxacin, with the resistance profiles (R: Resistant, S: Sensitive) tested at Melbourne University. Lysis scoring of the phages were as follows; ; ‘-’ = no lysis, ‘+’ = weak lysis, ‘++’ = moderate lysis, or ‘+++’ = strong lysis. Spot testing was performed in triplicate.

Strain	Antibiotics tested							Source	Lytic activity of the selected endolysins					
	Pen	Amc	CL	SF	W	Te	Enr		Lys_SN13	Lys_SPT5	Lys_SP38-1	Lys_SPT99F ₃	Lys_SP22L	Lys_119-2
CM2017-0410	R	R	R	R	R	R	R	Skin	++	-	-	-	-	-
CM2016-0933	R	R	R	S	R	R	R	Musco-skeletal	+++	-	-	-	-	-
CM2012-0529	R	R	R	S	R	S	R	Musco-skeletal	++	-	-	-	-	-
CM2012-0654	R	R	R	S	R	S	R	Skin	+	-	-	-	+	-
CM2012-0745	R	R	R	S	R	S	R	Respiratory	+++	-	-	-	-	-
CM2013-0059	R	R	R	S	R	S	R	Respiratory	+++	++	-	-	+	-
CM2016-0920	R	R	R	S	R	S	R	Ear	++	-	-	-	-	-
CM2017-0272	R	R	R	S	R	S	R	Musco-skeletal	+++	-	-	-	-	-
CM2017-0292	R	R	R	S	R	S	R	Skin	-	-	-	-	-	-
CM2016-0889	R	S	R	S	R	R	R	Skin	-	+	-	-	-	-
CM2016-0917	R	S	R	S	R	R	R	Urinary	-	-	-	-	-	-
CM2015-0460	R	S	R	S	R	R	S	Urinary	+++	+++	-	-	+	-
CM2016-0471	R	S	S	R	R	R	R	Ear	-	-	-	-	-	-

CM2009-0471	R	S	S	R	R	R	S	Musco-skeletal	+++	+++	-	-	-	-
CM2012-0093	R	S	S	R	R	R	S	Ear	-	+++	-	-	-	-
CM2017-0973	R	S	S	R	R	R	S	Urinary	+++	-	-	-	++	-
CM2009-0886	R	S	S	R	S	R	S	Urinary	++	+	-	-	-	-
CM2015-0031	R	S	S	R	S	R	S	Musco-skeletal	-	-	-	-	-	-
CM2015-0597	R	S	S	R	S	R	S	Ear	-	++	-	-	-	-
CM2013-0255	R	S	S	S	R	R	S	Skin	+++	+	-	-	-	-
CM2013-0910	R	S	S	S	R	R	S	Urinary	+	-	-	-	-	-
CM2015-0965	R	S	S	S	R	R	S	Urinary	-	+	-	-	-	-
CM2015-1096	R	S	S	S	R	R	S	Musco-skeletal	++	++	-	-	+	-
CM2016-0937	R	S	S	S	R	S	R	Urinary	+++	-	-	-	-	-
CM2016-1008	R	S	S	S	R	S	R	Urinary	+	+	-	-	-	-
CM2011-0112	S	S	S	R	R	R	S	Urinary	-	-	-	-	-	-
CM2013-0351	S	S	S	R	R	R	S	Urinary	-	-	-	-	-	-
CM2011-0195	S	S	S	S	R	S	S	Respiratory	++	-	-	-	-	-
CM2012-0247	S	S	S	S	R	S	S	Urinary	-	-	-	-	-	-
CM2014-0677	S	S	S	S	R	S	S	Urinary	-	-	-	-	-	-

CM2017-0713	S	S	S	S	R	S	S	Urinary	+++	+++	-	-	-	-
CM2009-0754	S	S	S	S	S	S	S	Urinary	++	-	-	-	-	-
CM2009-0925	S	S	S	S	S	S	S	Skin	+++	++	-	-	-	-
CM2011-0079	S	S	S	S	S	S	S	Respiratory	-	-	-	-	-	-
CM2011-0097	S	S	S	S	S	S	S	Skin	-	++	-	-	-	-
CM2011-0132	S	S	S	S	S	S	S	Skin	-	-	-	-	-	-
CM2011-0460	S	S	S	S	S	S	S	Skin	++	-	-	-	-	-
CM2011-0653	S	S	S	S	S	S	S	Skin	-	+	-	-	-	-
CM2011-0669	S	S	S	S	S	S	S	Ear	-	++	-	-	-	-
CM2011-0671	S	S	S	S	S	S	S	Skin	++	-	-	-	-	-
CM2012-0111	S	S	S	S	S	S	S	Skin	+++	+	-	-	-	-
CM2012-0169	S	S	S	S	S	S	S	Urinary	+++	-	-	-	-	-
CM2012-0193	S	S	S	S	S	S	S	Reproductive	+++	-	-	-	-	-
CM2012-0201	S	S	S	S	S	S	S	Urinary	+++	-	-	-	-	-
CM2012-0405	S	S	S	S	S	S	S	Skin	-	-	-	-	-	-
CM2012-0503	S	S	S	S	S	S	S	Skin	+	-	-	-	-	-
CM2012-0550	S	S	S	S	S	S	S	Skin	+++	+	-	-	-	-

CM2013-0140	S	S	S	S	S	S	S	Skin	++	-	-	-	-	-
CM2013-0320	S	S	S	S	S	S	S	Skin	-	-	-	-	-	-
CM2013-0367	S	S	S	S	S	S	S	Skin	+	-	-	-	-	-
CM2013-0596	S	S	S	S	S	S	S	Urinary	-	-	-	-	-	-
CM2015-0358	S	S	S	S	S	S	S	Urinary	+++	++	-	-	+	-
CM2016-0216	S	S	S	S	S	S	S	Skin	-	-	-	-	-	-
CM2016-0262	S	S	S	S	S	S	S	Urinary	+	-	-	-	-	-
CM2016-0568	S	S	S	S	S	S	S	Urinary	-	-	-	-	-	-
CM2016-0674	S	S	S	S	S	S	S	Skin	-	+++	-	-	-	-
CM2016-0689	S	S	S	S	S	S	S	Skin	+++	-	-	-	-	-
CM2016-1113	S	S	S	S	S	S	S	Skin	-	+	-	-	-	-
CM2017-0472	S	S	S	S	S	S	S	Ear	+++	+	-	-	-	-
CM2017-0580	S	S	S	S	S	S	S	Urinary	+++	-	-	-	-	-

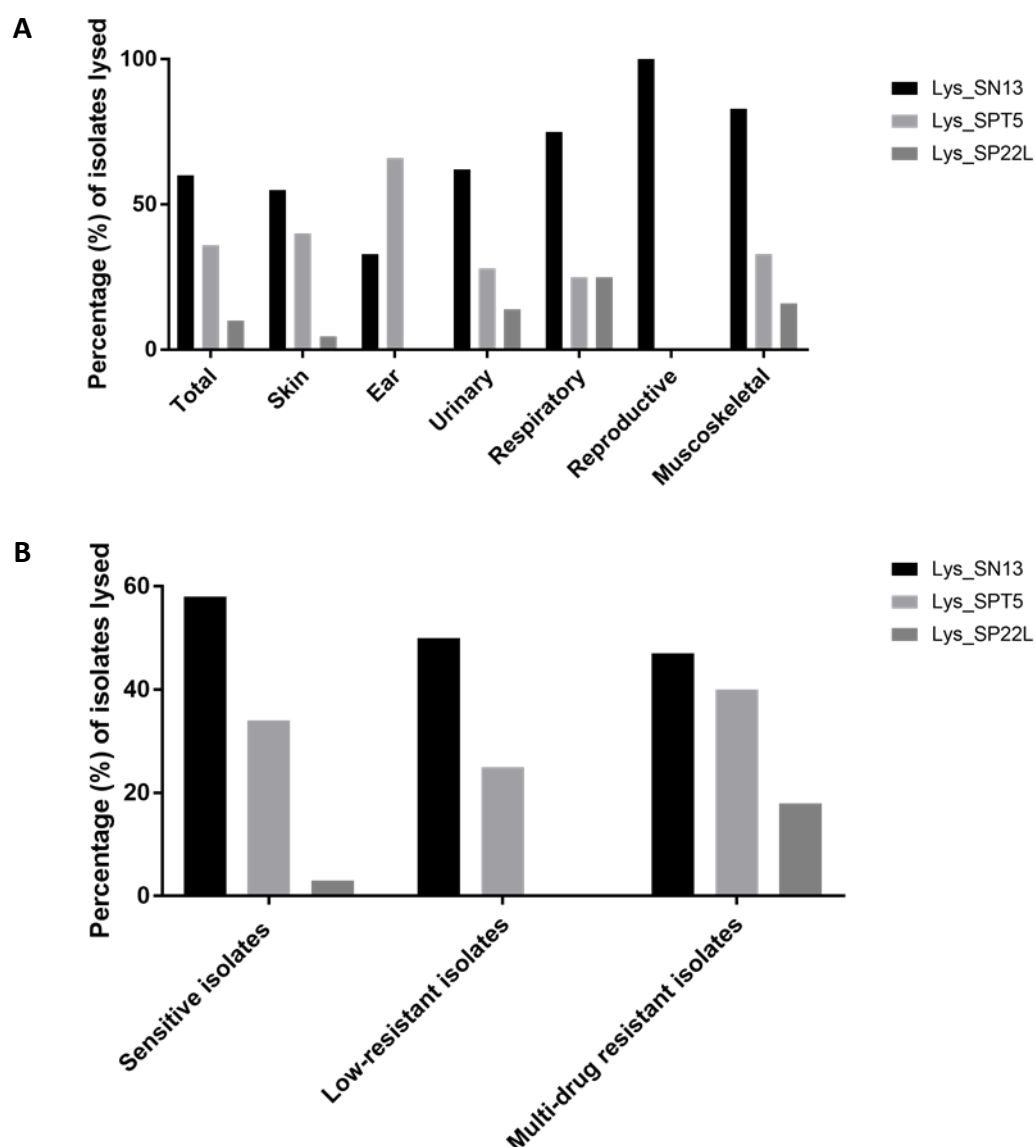


Figure 4.9 Lytic spectrum of three endolysins. (A) Lysis profile of Lys_SN13, Lys_SPT5, Lys_22L against *S. pseudintermedius* isolates from various canine infection sites. (B) Lysis profile of Lys_SN13, Lys_SPT5, Lys_22L against *S. pseudintermedius* of varying antibiotic-resistance categories. Sensitive isolates = sensitive to all seven antibiotics tested, Low-resistant isolates = resistant to one or two of the seven antibiotics tested, multi-drug resistant (MDR) isolates = resistant to three or more of the seven antibiotics tested.

With Lys_SN13 identified as the lead candidate, *in silico* analysis was used to model the tertiary structure of Lys_SN13 with other proteins in the Protein Data Bank (PDB), to gain a better understanding of the endolysin structural model and to assist in the identification of potential critical binding sites related to functional activity. The structural model of the CHAP domain from our candidate endolysin, Lys_SN13, is highly similar to the CHAP domain from the previously

characterised endolysin, LysGH15 derived from a *Staphylococcal* phage. However, Lys_SN13 only shows a 34.27% identity to the LysGH15 protein sequence¹⁰⁵ (**Figure 4.10A,B**). When comparing the active site between Lys_SN13 and LysGH15, the catalytic residues are highly conserved, suggesting a similar mode of catalysis (**Figure 4.10C,D**). In addition, it is evident that the critical residues involved in calcium-binding are highly conserved between LysGH15 and Lys_SN13 (**Figure 4.10D**).

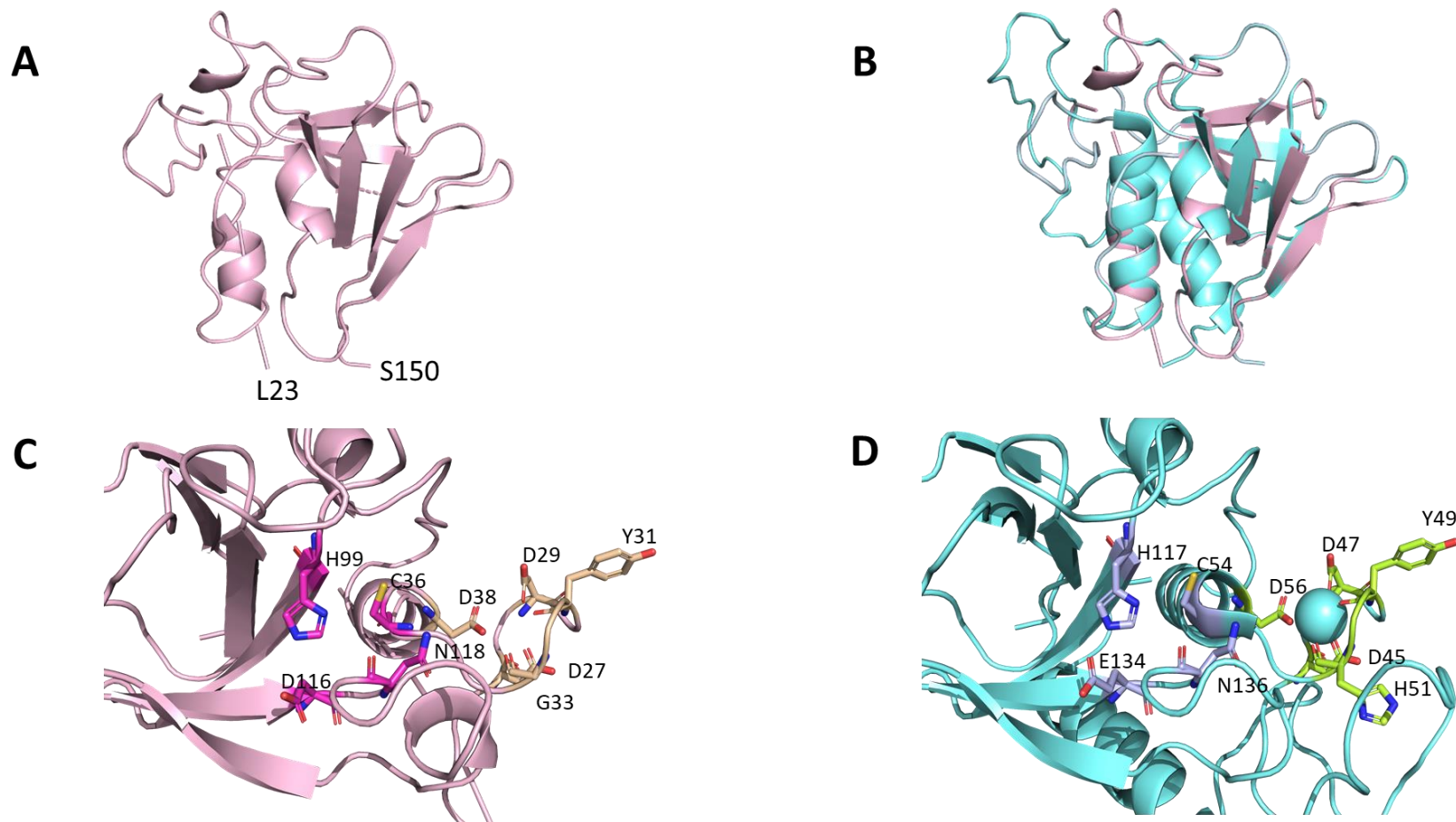


Figure 4.10 Structural analysis of CHAP domain and catalytic residues in Lys_SN13 and LysGH15. (A) Overall structural model of Lys_SN13 CHAP domain (B) Overall structural model of the CHAP domain of Lys_SN13 (pink) overlayed with CHAP domain of LysGH15 (cyan). (C) A detailed view of the CHAP domain of Lys_SN13 with catalytic site (bright pink) and calcium-binding site (wheat). (D) A detailed view of the CHAP domain of LysGH15 with catalytic site (dark blue) and calcium-binding site (green). Calcium molecule shown as cyan sphere. PyMOL was used to visualise the structural models.

To determine whether the lytic activity of Lys_SN13 was indeed dependant on calcium, EDTA was added to the elution buffer during the final protein purification step. EDTA chelates metal ions such as calcium thus would demonstrate whether the lack of available calcium would affect the lytic activity against *S. pseudintermedius*. When no EDTA was present within the elution buffer, Lys_SN13 had a strong lytic effect against *S. pseudintermedius*. However, the lytic activity diminished with the addition of 2mM of EDTA in the elution buffer (**Figure 4.11**). These results suggest that the lytic activity of Lys_SN13 was dependant on calcium, validating the findings shown for the homologous protein, LysGH15. The calcium dependency for the lytic activity for Lys_SN13 was therefore taken into consideration in further experiments.

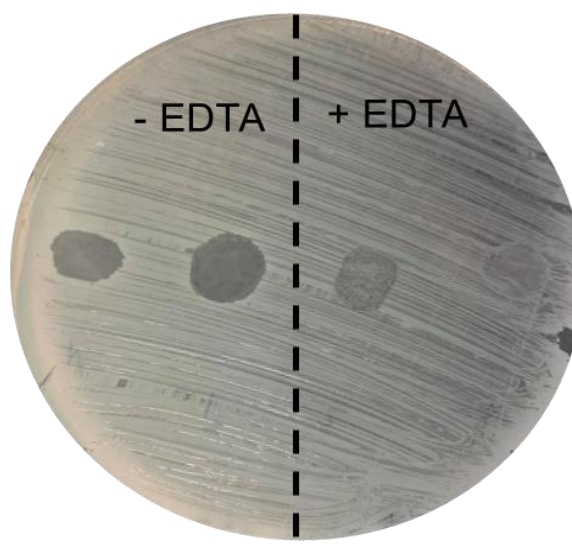


Figure 4.11 The effect of EDTA in elution buffer on the lytic ability of Lys_SN13. The lytic ability of SN13 was tested by spotting an elution of Lys_SN13 in PBS (right side) in comparison to Lys_SN13 in buffer containing 2mM EDTA.

We have demonstrated that Lys_SN13 can lyse clinical isolates of *S. pseudintermedius* and that the lytic ability appears to be dependent on calcium; however, our experiments only tested the proteins' lytic ability on a static bacterial lawn. To explore the lytic activity of Lys_SN13 in a more physiological context, we utilised a turbidity reduction assay in liquid broth culture. The *S. pseudintermedius* strain, CM16-0689, displayed normal growth kinetics when grown alone (closed circles). A significant growth disruption occurred with the addition of 1.25 µg and 5 µg of Lys_SN13 (closed squares and inverted triangles, respectively) (**Figure 4.12**). However, more

promisingly, the growth of *S. pseudintermedius* was significantly inhibited with concentrations of endolysin reaching 20 µg and 100 µg (open circles and triangles, respectively), with the OD₆₀₀ reaching 0.0 at 600 minutes with the highest dose of Lys_SN13. There were no obvious differences in bacterial inhibition between 20 µg and 100 µg of Lys_SN13. Overall, and this preliminary turbidity reduction assay demonstrated that low amounts of Lys_SN13 have little effect on *S. pseudintermedius*, however, higher amounts of Lys_SN13 can completely inhibit the growth of *S. pseudintermedius* within 10 hours. However, this experiment would need to be repeated to validate these findings

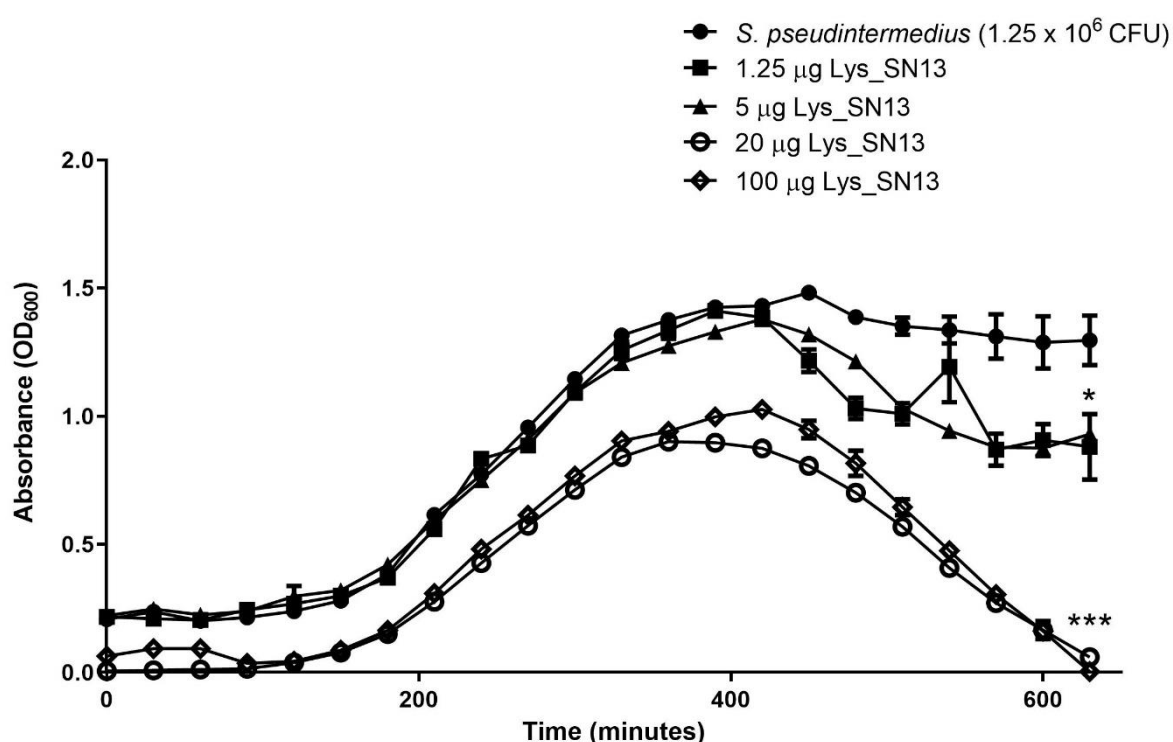


Figure 4.12 Turbidity reduction assay of Lys_SN13 at various concentrations against *S. pseudintermedius* CM16-0689. Absorbance (OD₆₀₀) of was measured every 5 minutes, with the absorbance plotted every hour. Error bars represent mean values ± SEM, P-values were determined by an ordinary one-way ANOVA post-hoc pairwise comparisons with Dunnett correction for multiple comparisons (n=2 biological replicates) comparing the *S.pseudintermedius* with various concentrations of lyse_SN13; 1.25 µg p= 0.0279 and 5 µg p= 0.0450 (represented as *) and 20 µg p= 0.0002 and 100 µg p= 0.0002 (represented as ***).

4.4 Discussion

S. pseudintermedius is a highly pathogenic bacterium within the veterinary sector, involved in numerous canine infections¹³. Due to the high levels of antibiotic resistance of *S. pseudintermedius*, recent research has focused on phage therapy as an alternative treatment option. However, to date,

all phages isolated against *S. pseudintermedius* contain a lysogeny module ^{16,17} (have the ability to integrate within the bacterial genome); therefore, they are deemed unfavourable from a therapeutic point of view ¹⁰⁶. To combat this issue, this chapter explores the use of phage-encoded endolysins, which are enzymes that have been shown to lyse bacteria by degrading the peptidoglycan layer ^{78,86–93,107,108}. Additionally, endolysins generally have a broader host range, less bacterial resistance and the dose is easily controlled ⁹⁸. Therefore, this chapter focused on identifying and purifying phage-encoded endolysins from *S. pseudintermedius* phages for the first time and exploring their efficacy in reducing *S. pseudintermedius* growth *in vitro*.

All phages contain a lytic cassette comprised of a holin and endolysin gene; hence endolysins are termed 'phage-encoded enzymes'. ¹⁰⁹. This genomic origin and organisation of endolysins has been regarded as an advantage in their identification, as endolysins can be mined either from the genome sequence of isolated phages or from whole bacterial genome sequences within the prophage genome ^{110–113}. Using such computational techniques can identify thousands of novel endolysins derived from isolated temperate phages or phages integrated within the bacterial genome (prophage), sequenced but not yet physically isolated or characterised. Our study utilised a collection of publicly available *S. pseudintermedius* phages (both isolated and prophages within the *S. pseudintermedius* bacterial genome) to mine their whole genome sequence for endolysin genes, leading to the successful identification of 26 endolysin-like genes (**Table 4.1**). Although not described previously, the majority of the 26 endolysins from *S. pseudintermedius* phages matched CHAP-domain containing proteins within *S. pseudintermedius* bacterial strains (**Table 4.1**). This finding was an indication that the endolysin-like proteins we identified were likely functional endolysins, as the CHAP-domain is present within other endolysins that show lytic activity against a range of bacteria including other *Staphylococcal spp.*, ^{114–117}. However, other domains are also important in the activity of endolysins, such as amidases and muramidase's ¹¹⁸. Such endolysins generally have a modular design and particularly target gram-positive bacteria ¹¹⁸, therefore further work is required to determine which domains show optimal activity against *S. pseudintermedius*. In general, endolysins typically possess the same enzymatic function, irrespective of the species of phage they were derived from, as all endolysins act to recognise and hydrolyse specific

peptidoglycan bonds of the bacterial surface, ultimately leading to bacterial lysis ¹¹⁸. However, despite this functional homology, the 26 endolysin-like proteins we identified were classified into distinct groups based on amino acid identity (**Figure 4.3** and **Figure 4.4**). The variation in amino acid sequence between endolysins from the same phage family has been shown previously in *Bacillus anthracis* endolysins; however, despite the differences, the endolysins were still able to lyse the target bacterial strain ⁸⁶.

Following the identification of endolysins, subsequent protein expression is crucial in understanding the efficacy of the enzymes in lysing the target bacterium. Generally, *E. coli*, a gram-negative bacterium, is used as the expression cell-line as they have a high transformation efficiency, high expression yield, a fast growth rate and a well-characterised genome ⁹⁸. Although the *E. coli* expression system has been used successfully in several studies, hurdles in protein expression remain ⁹⁸. Most notably, as the endolysins act to degrade the peptidoglycan layer from within the bacterial cell (**Figure 4.1**), if the endolysin being expressed can target *E. coli* peptidoglycan, then the expression of such endolysin within *E. coli* may disrupt the proteins post-translational folding due to premature cell lysis ^{119,120}. Additional protein expression challenges highlighted within this study included the individual requirements of each endolysin selected. For example, our results show that Lys_SN13 required calcium for its enzymatic activity (**Figure 4.10** and **Figure 4.11**); therefore, optimised buffers and reagents are required for successful purification (**Figure 4.7**). Although expression and purification protocols were successfully optimised for the purification of our six endolysins (**Figure 4.7**), given the time constraints, further optimisation was not performed. However, further optimisation to obtain a better yield of protein would include; (i) optimising the upscaling and expression of protein with the use of a bioreactor, (ii) optimising the protein purification and storage buffers with the addition of salts or metal ions (e.g., Mg^{2+} or CaCl), and (iii) trialling downstream purification techniques such as size-exclusive chromatography (SEC).

Following expression, to test the lytic ability of the endolysins, the six endolysin elutions were spotted onto the lawn of 60 *S. pseudintermedius* clinical isolates from various canine infections. Results showed that only three out the six endolysins showed any lytic activity on the *S. pseudintermedius* strain, with Lys_SN13 identified as the endolysin with the broadest host range,

able to lyse 60% of the strains tested (**Table 4.4**). Notably, at least one of the three endolysins were able to lyse strains from all infection sites, with Lys_SPT5 showing preferential lysis on *S. pseudintermedius* isolates collected from ear infections **Figure 4.9A**. It is evident from our findings that endolysins may be better suited for specific infections (**Table 4.4**), however, it would be interesting to add all three endolysins within a ‘cocktail’ and test whether we could achieve a broader host range, greater than 60%. The lytic spot test also revealed that the three endolysins lysed *S. pseudintermedius* strains of varying antibiotic-resistance profiles, with all three endolysins able to lyse multiple MDR *S. pseudintermedius* strains (**Figure 4.9B**). Additionally, preliminary results show that our candidate endolysin, Lys_SN13, significantly reduced the growth of *S. pseudintermedius* within 10 hours of administration (**Figure 4.12**). Interestingly, it appears that Lys_SN13 was most efficient at reducing the growth of *S. pseudintermedius* once the bacterial had reached the stationary phase of growth. However, due to time restraints caused by COVID-19 lockdowns, these experiments were only performed in duplicate. Therefore, future work is required to validate these findings. Future experiment should aim to optimise the activity variations of this endolysin (e.g., temperature and pH) and repeat this growth kinetic experiment to determine the lytic ability of Lys_SN13 under optimal conditions. Additionally, future experiments should aim to test the optimal lytic activity of Lys_SN13 against *S. pseudintermedius* at different growth stages. Although these are preliminary findings, this corroboration of results highlights the strong potential of endolysins as a novel therapeutic for antibiotic-resistant *S. pseudintermedius* infections.

The results from this study are promising; however, the endolysin field is still developing and there are many avenues for further research. This study found that the endolysins able to lyse *S. pseudintermedius* contained a CHAP-domain. Interestingly, the endolysins, which lacked a CHAP-domain, did not lyse the bacterial strains, with one exception of an endolysin that contained a CHAP domain but could not lyse *S. pseudintermedius* (**Figure 4.5**). These findings are supported by a previous study which showed that the CHAP-domain alone is necessary and sufficient for lysis of *S. aureus*, perhaps indicating that this domain is critical for lysis of *Staphylococcus spp.*, bacteria^{114–117}. To support this, result from this thesis found that the addition of EDTA to Lys_SN13 resulted in a decrease in lytic activity (**Figure 4.11**). This decrease in lytic activity is likely due to the

chelation of calcium needed to stabilize the active site of the CHAP domain as modeled against the LysGH15 structure (**Figure 4.10**). However, it should be noted that despite the decrease in activity, there was still a modest lytic activity, suggesting that other catalytic domains of Lys_SN13, such as the glucosaminidase domain possess additive or synergistic activity with the CHAP-domain. However, further work following this study should assess the lytic ability of each domain individually (e.g., CHAP-domain, glucosaminidase domain), compared to the full-length construct, to elucidate this hypothesis further. The advantage of using individual domains compared to the full-length construct may provide downstream protein purification benefits. Additionally, future research involving endolysins identified within this study characterise their stability in response to different parameters, including temperature and pH, to determine which endolysins would be best within certain infection niches. A greater understanding of the stability of endolysins would provide a baseline for formulation optimisation, which would be essential from a clinical point of view in developing highly effective, safe, and stable treatment options for *S. pseudintermedius* infections in canines.

4.5 Conclusions

The field of bacteriophage endolysins as novel therapeutics for bacterial infections is still very much in its infancy, with limited description and purification of endolysins to date. This chapter provides the field with six novel endolysins identified from *S. pseudintermedius* phages (isolated and prophages within the bacterial genome). The expression and characterisation of these endolysins led to the discovery that three of these novel endolysins were able to lyse *S. pseudintermedius* strains from numerous infection niches and of varying antibiotic-resistance levels. Lys_SN13 was identified as a potential lead candidate endolysin due to its broad host range and optimised expression conditions. The field of using endolysins, particularly within animal models, is still in its infancy; therefore, there is a plethora of avenues that require further research. However, the findings within this study portray the potential of using endolysins and set the groundwork for their use as a novel therapeutic for *S. pseudintermedius* infections in canines moving forward.

4.6 Appendix

Table 4.5 Pairwise (%) identity of nine putative endolysins from the 251 amino acid group.
Pairwise (%) identity was determined using pairwise analysis through Clustal Omega.

	SP120-	SP197-1	SP276-1	SPT5	SP152	SP252	phiSP44	phiSP119	vB_SpsM
1									
SP120-1		97.2%	98.0%	100%	100%	100%	97.6%	99.6%	100%
SP197-1	97.2%		99.2%	97.2%	97.2%	97.2%	99.6%	97.6%	97.2%
SP276-1	98.0%	99.2%		98.0%	98.0%	98.0%	98.8%	98.4%	98.0%
SPT5	100%	97.2%	98.0%		100%	100%	97.6%	99.6%	100%
SP152	100%	97.2%	98.0%	100%		100%	97.6%	99.6%	100%
SP252	100%	97.2%	98.0%	100%	100%		97.6%	99.6%	100%
phiSP44	97.6%	99.6%	98.8%	97.6%	97.6%	97.6%		98.0%	97.6%
phiSP119	99.6%	97.6%	98.4%	99.6%	99.6%	99.6%	98.0%		99.6%
vB_SpsM	100%	97.2%	98.0%	100%	100%	100%	97.6%	99.6%	

Table 4.6 Pairwise (%) identity of nine putative endolysins from the 486 amino acid group.
Pairwise (%) identity was determined using pairwise analysis through Clustal Omega.

	SPT99F3	vB_SPsS	phiSP15-1	phiSP119-1	phiSP38-1	SP_157588	SP22L
SPT99F3		98.97%	96.71%	96.30%	29.91%	16.75%	16.75%
vB_SPsS	98.97%		96.09%	95.68%	30.14%	17.01%	17.01%
phiSP15-1	96.71%	96.09%		97.33%	29.45%	16.75%	16.75%
phiSP119-1	96.30%	95.68%	97.33%		30.14%	16.50%	16.50%
phiSP38-1	29.91%	30.14%	29.45%	30.14%		34.43%	34.43%
SP_157588	16.75%	17.01%	16.75%	16.50%	34.43%		100.00%
SP22L	16.75%	17.01%	16.75%	16.50%	34.43%	100.00%	

Table 4.7 Pairwise (%) identity of nine putative endolysins from the 629 amino acid group.
Pairwise (%) identity was determined using pairwise analysis through Clustal Omega.

	SP120-2	SP197-2	SP276-2	SN13	SN11	SN10	SN8	phiSP44- 1	phiSP119- 3-1
SP120-2		99.0%	98.9%	99.0%	99.0%	99.0%	99.0%	99.2%	99.2%
SP197-2	99.0%		99.5%	99.4%	99.4%	99.4%	99.4%	98.6%	98.6%
SP276-2	98.9%	99.5%		99.4%	99.4%	99.4%	99.4%	98.6%	98.6%
SN13	99.0%	99.4%	99.4%		100%	100%	100%	98.9%	98.9%
SN11	99.0%	99.4%	99.4%	100%		100%	100%	98.9%	98.9%
SN10	99.0%	99.4%	99.4%	100%	100%		100%	98.9%	98.9%
SN8	99.0%	99.4%	99.4%	100%	100%	100%		98.9%	98.9%
phiSP44-1	99.2%	98.6%	98.6%	98.9%	98.9%	98.9%	98.9%		99.0%
phiSP119-3-1	99.2%	98.6%	98.6%	98.9%	98.9%	98.9%	98.9%	99.0%	

Lys_SPT5	---MKTYSEARSRLR---YVGRYIDFGYHAYQCIDLAVDYIYLLDIRMMGNAKDAI	53
Lys_SNI3	MALPKTGKPTAKQVVDMAINLIGSGVDVGYGRQCHDLPHYIFNRVYGFKTPGNARDMA	60
Lys_SPT99F3	---MLTAIDYLTGRGKISSDPRT---YDGY---P---KNVGRNYIENG-----I	39
Lys_SP119-2	-----	0
Lys_SP38-1	---MVASLSKKKFIISFLKSSGKQFNEDGNYGYQCDFANTGMLKLFGLHMLGAKDI	56
Lys_SP22L	---MAPSKTKQEAINYALSLEGGLDFDNFAGWQCFDVANYWNHIFGHGLGEGAKDI	56
Lys_SPT5	NN-----DFKNMATIVEPTSPVFPQ-VGDVAVFRNGIY--KQYGHIGIVYNSGNTNQFL	104
Lys_SNI3	WY-----RYPAGFKIYKNTTNFVPK-PGDMAIWTGGVYNNWTWHTGIVVGPSTKDYFY	113
Lys_SPT99F3	NYDEFCG-GYHRAFVYSNATNDVPAVTSGTVEANDYG---NFGGTF-VIR-----D	87
Lys_SP119-2	-----	0
Lys_SP38-1	PFNSINKNYFKTEAKVYSNTPEFLAE-AGDMVVFGENYV--GGYGHVAVNIE-ATLDYIV	112
Lys_SP22L	PNPRWN--DLTQEAIVPNTPEFLAE-AGDLAIFSSRFG--GGYGHVGVIE-ATLDYIV	110
Lys_SPT5	ILEQNFQGN---ANTP-----ASLRWDNYYG---CTHFIRPHYKSENT	141
Lys_SNI3	SVDQNNNNANSYVGSF-----AAKIKHSYFG---VTHFVRPAYKSEPK	153
Lys_SPT99F3	ANDNDNIYGLQRGSMRFVVGDKVNGQDIVGLQNSNYDNPHMSAHLHIQLRPKDALKDE	147
Lys_SP119-2	-----	0
Lys_SP38-1	VLEQNNLGGGTDGIEQPSSGNE-----SVTRRKHAYDFPMW-----FIRPNFK--SE	158
Lys_SP22L	LLEQNNLGGGITKT-----E-----VTTRRKHNVEYDMI-----FVRPKYK--KE	148
Lys_SPT5	TSKIANKISPPSHKAAGNAA-----SKIVSGSRAPYNLKSKGAYFNAKVDGLG	190
Lys_SNI3	PTPIPPENKPIKDPETK-----KPESINKPIYKVTKILFTTARIELVK	198
Lys_SPT99F3	KSQV-----CSGLAMEKYDITNLNKKQDKSKNGSVKELKHISYNNH-----KGNK	192
Lys_SP119-2	-----MAKEKIG-----TWNQVP-----VYTD	17
Lys_SP38-1	TTLLSAQSVTKQSKQPAKKPKKLN-----YIRDEI-----KGYN	193
Lys_SP22L	GSGRLPKKKI-----LLVAGHGLG-----YWSNDS-----G	174
Lys_SPT5	ATSATRYG-----DSRANYRFDVGQAE-----YV	214
Lys_SNI3	ANRFVHYITKSDNNHKNPKIVIKNANTALS-----TNDIVKYRDDLNDE-----I	245
Lys_SPT99F3	I-----TAPKPSIQGVVINDY-----GSMTPSQ-----VL	218
Lys_SP119-2	F-----LPIGTRRSQRQLVSGMPKFAVFD-TGN--RDSTAQNNDYVRNTYNI	63
Lys_SP38-1	M-----DKRGYKPRGTVLHNDL-----GSAGATAEAYHKGLNADYNRLKGV	236
Lys_SP22L	A-----AANGYNERDFIRKNIIVPNVAKHLKAGHDVHLVGGETMNDQ-----	216
Lys_SPT5	PG-----TLIYVFEIID-----GW-CRIYNN-----HNE--	238
Lys_SNI3	PH-----FFVDRLS-----VWACRPIES-----VQGYN	269
Lys_SPT99F3	PHLYARENNGTHVNGHASVYANREVLVYHPDYYVHHCNGQNA-----NANLIG	268
Lys_SP119-2	DHAYTA-----SAHVFDOKECIICIPVTEKAHVLYDTPIDNNHYGDDANDIAFG	114
Lys_SP38-1	AHSYVS-----GSTV-----YQALPEGKIAHVANRIG-----NRDYVG	270
Lys_SP22L	-----L-----FQDTRY-----GEMVG-----NYSDYG	234
Lys_SPT5	-----MIWHERLIVKEVF-----	251
Lys_SNI3	NAIVLSITEARTAVSDNFKMNEIECLSLAKLLLEANGKKMNTSSIVIDKSSWRTFKLHT-	328
Lys_SPT99F3	FEVCES-YPGRISD-ALFLENEEATLKVAADVMKSYGLPVNRNTVRLHNEFFGT	320
Lys_SP119-2	LEACYF--SDRDRT--LKSLDNACRVHMGALCASMDIN-	147
Lys_SP38-1	IEICQS--VGATD--KQFLANEQSFAQEAAAMLKKWGLPANRNTVRLHVEFYNT	320
Lys_SP22L	MYWVAR--QGFDSV-TEFHLDAAGAQASGGHVIIGMLSPDIDKAIQNTIYHFIGTIRN	291
Lys_SPT5	-----	251
Lys_SNI3	--GKDSLKS-----SSFTSKDYQKAVNELIKLFNDKDKLLNNKPKDVVEKIRIT	376
Lys_SPT99F3	SCPHRSW-----ELHVGKGAPYT-TANI-----	342
Lys_SP119-2	--PRNEM-----PGHQDTQFDKQDPGNI-----	168
Lys_SP38-1	ACPHR-----SMLLHTGFDPYK-----GIP-----	341
Lys_SP22L	IDPRDNLNVNNAKNGVNYRLAELGFTISVKDPMNININLESYTRGIAEDIHG----	345
Lys_SPT5	-----	251
Lys_SNI3	VVKENTKVPSELKPSNNIKDKQSKIDRIISNYSLKQALDIQFS-----LN	423
Lys_SPT99F3	-----NRMKDY--FIKKIK-HYVDGGLKLEVSKEATIKQSDVKQEVKKQ	382
Lys_SP119-2	--LEAAGY--GRSDMI--IDDLVV-KYMGDAPAPKVAKTVSQ-----	205
Lys_SP38-1	-----PQAMQL-KL-KDY--FIKQIR-AYMDGKVPVATVSNK-TSA-----S	377
Lys_SP22L	-----GKLEPVKL--PT--KDR--AKEVKV-----QAAKVTKKPTP-----A	378
Lys_SPT5	-----	251
Lys_SNI3	PKPQTSNGVTHYASLNQTRAAMDNKKIFNNNVQVYQFLKNQYQGISVDKLNKLLVGGK	483
Lys_SPT99F3	EAKQVVKATDMKQ-----	395
Lys_SP119-2	PKQSKPPKTVMAH-----	218
Lys_SP38-1	SNTVKPIAGAHQV-----	390
Lys_SP22L	NNTSKP-KTEMAH-----	390
Lys_SPT5	-----	251
Lys_SNI3	TLQNGQAFADGCKKYGVNEIYLIAHAFLESANGTSFFASGRITGVYNYFGIGAFDNNPN	543
Lys_SPT99F3	-----NKDGINYKAEHASFVTASE	415
Lys_SP119-2	-----H-----GIFTASDGN-DD	230
Lys_SP38-1	-----NSYGTYYMKESATFVCG-NK	409
Lys_SP22L	-----K-----GQFTTFASN-TQ	402
Lys_SPT5	-----	251
Lys_SNI3	AMEFARSHGNTS-----PAK-----AIIGGAEFVGKGYFDVGN-----TLY-	580
Lys_SPT99F3	GIITRYKGPWT--GHPQAGVLQKGGTIKYDEVQK--FDGHVWVSWETFE-----GETVYM	466
Lys_SP119-2	AIVVRRAFGMDAEEVDSGSIYPGEYVAFDQVIKDVKNKMMIRFKYQADGANKDNFYM	290
Lys_SP38-1	PITTRTVGFFT--TCPEGYMFQGGKCEYDEVML--QDGHVWIGVDWQG-----QRYYL	459
Lys_SP22L	PIVVRRAVGLNAAKVDVNSWYPMQWVPFDRLIK--KDGVMIRFEYPTNP--SAGKFYM	458
Lys_SPT5	-----	251
Lys_SNI3	-RMRWNPKKPGTHQVATDISHAKVQAKMISTMYKEIGLKGVEFYDQYVK	629
Lys_SPT99F3	PVRTNDAXTG-----KVGKLWGEIK-----	486
Lys_SP119-2	PIGKITDKDGK--LLKEKALHGKLEVN-----	315
Lys_SP38-1	PIRKNGVAPP--NQGLGDLHGTIK-----	482
Lys_SP22L	PIGKITGKTK--VKVDKTLNGTLDIKSYG-----	485

Figure 4.13 Protein sequence alignment of putative endolysin proteins from three amino acid groups. (A) Alignment of 251 amino acid endolysins. **(B)** Alignment of 486 amino acid endolysins. **(C)** Alignment of 629 amino acid endolysins. The amino acid sequence of the nine putative endolysin proteins were uploaded in FASTA format Clustal Omega. **Consensus Symbols:** The following symbols denote the degree of residue conservation. '*' (asterisk's) indicates positions which have a single, fully conserved residue. ':' (colon) indicates conservation between groups of strongly similar properties. '.' (period) indicates conservation between groups of weakly similar properties. **Red:** hydrophobic amino acids, **Blue:** Acidic amino acids, **Magenta:** Basic amino acids, **Green:** Hydroxly + sulfhydryl + amine, **Grey/other:** Unusual amino/imino acids

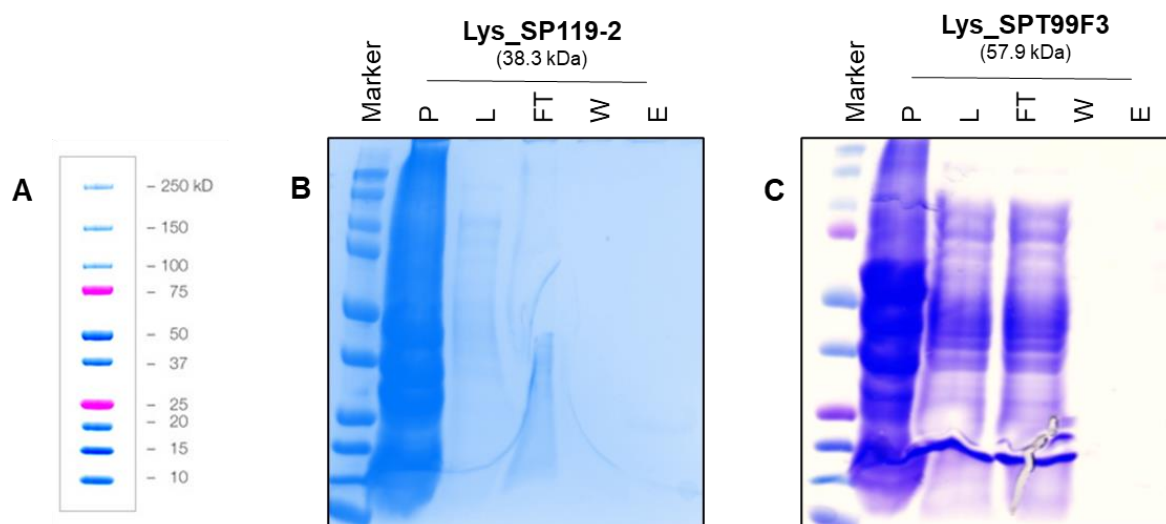


Figure 4.14 Representative SDS-PAGE images of protein purification optimisation. (A) Precision Plus Protein Dual Colour Standards (BioRad) marker used for SDS-PAGE gels. (B) Initial protein purification without optimisation of expression or purification. (C) Protein purification with the optimisation of expression protocols.

Chapter 5

Development and optimisation of a silkworm larvae (*Bombyx mori*) model for *Staphylococcus pseudintermedius* infections and treatment trials

5.1 Summary

Staphylococcus pseudintermedius is an opportunistic pathogen of canines, resulting in multi-drug resistant (MDR) infections, such as canine pyoderma, a moderate to severe skin infection in dogs. Due to the rise in antibiotic resistance, research surrounding phage and endolysin therapy has expanded; however, phage therapy trials are essential to progress their use in veterinary medicine. Previously, the silkworm larvae model has been used as an alternative model for phage therapy trials; therefore, in this chapter, we developed and optimised a silkworm larvae model to explore the efficacy of phage therapy against *S. pseudintermedius* infections. Silkworm haemolymph did not inhibit the growth of *S. pseudintermedius* or the lytic activity of phage related products. Instead, there was a proliferation of *S. pseudintermedius* following injection within the silkworm larvae. Injection of various concentrations of *S. pseudintermedius* resulted in dose-dependent mortality of the silkworm larvae, with 1.25×10^6 CFU observed as the LD50 concentration, used as a baseline survival for phage therapy trials. Administration of Phage SP_157588 or Lys_SN13 following the injection of the LD50 concentration resulted in higher mortality rates than *S. pseudintermedius* alone. Overall, these results suggest that the silkworm larvae model is a good model for *S. pseudintermedius* infections; however, more research is required to understand the pharmacokinetics of the host response to the application of phage therapy.

5.2 Introduction

Phage therapy represents an opportunity to combat methicillin-resistant *Staphylococcus pseudintermedius* (MRSP)¹³. In order to translate phage therapy from the laboratory into human or animal medicine, model organisms are essential^{121,122}. Higher vertebrate models such as chickens, rabbits, hamsters, and mice are frequently used to test the safety and efficacy of phage therapy with great success^{121,122}, with the recent development of a murine model for *S. pseudintermedius* cutaneous infections¹²³. Although this model was developed to understand skin disease pathogenesis, it provides an opportunity for *in vivo* trials of alternate treatment options of *S. pseudintermedius*¹²³. However, there are multiple issues associated with the use of high vertebrate models. In particular, ethical concerns, costs, training requirements, and housing facilities¹²⁴. To address these concerns, recent research has focused on the development and optimisation of invertebrate or lower vertebrate models for phage therapy trials^{121,122}. Such models include nematodes (*Caenorhabditis elegans*)^{125–127}, common fruit flies (*Drosophila melanogaster*)^{128–130}, wax moths (*Galleria mellonella*)^{131–135}, silkworm larvae (*Bombyx mori*), and zebrafish (*Danio rerio*)^{136,137}. Invertebrate models provide several advantages as they are inexpensive to maintain, have low handling requirements, generally have a short lifecycle for the rapid generation of results, and usually do not require ethics approval for use^{121,122}. Importantly, such invertebrate models have proven to be successful in phage therapy trials, as they display infection kinetics similar to higher-order species and show that phages can effectively reduce the bacterial counts within the model organism^{121,122}.

As mentioned, silkworm larvae (*Bombyx mori*) are a model of interest for phage therapy¹³⁸. Silkworm larvae have been used for silk production for thousands of years¹³⁹, and in Australia, they are predominantly reared as live feed for reptiles and fish^{140,141}. More recently, silkworm larvae have been successfully used in numerous research avenues including, bacterial, fungal, and viral infection and pathogenesis, as well as antimicrobial drug screening, demonstrating their potential as a model organism^{142–152}. Research into invertebrates as a model organism has favoured silkworm larvae, showing numerous benefits, as displayed in **Figure 5.1**. For example, silkworm larvae do not require ethics committee approval, as they are classed as a lower order species. Additionally,

silkworm larvae are also relatively cheap to purchase and maintain, the housing and rearing systems are relatively well-established, and larvae have an appropriate body size for handling¹³⁸.

Lastly, due to their extensive use in silk production, their lifecycle is well-characterised, which is important for their use in the laboratory (**Figure 5.2**). As highlighted in **Figure 5.2**, the 5th instar stage of the larvae life cycle was found to be the preferred stage to use silkworm larvae as a model organism, as its body size is optimal for handling¹³⁸. The 5th instar stage has also been successfully used in previous literature and provides a good body size for handling¹³⁸.

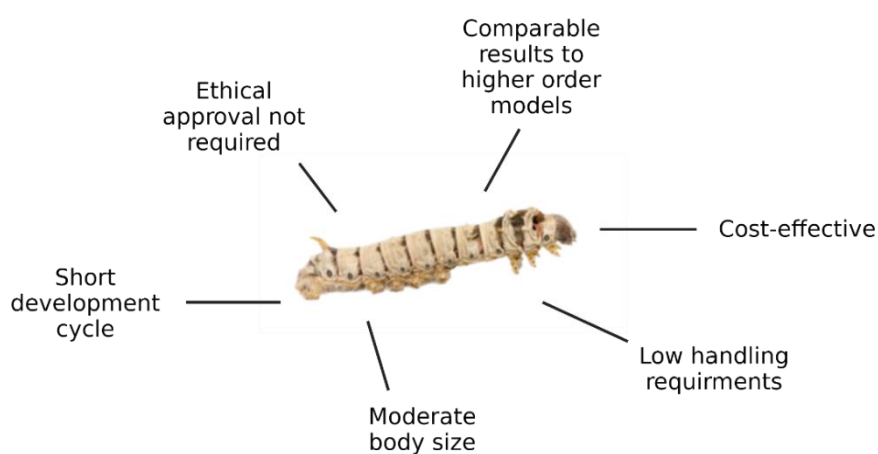


Figure 5.1 Benefits of silkworm (*Bombyx mori*) larvae as a model organism for research

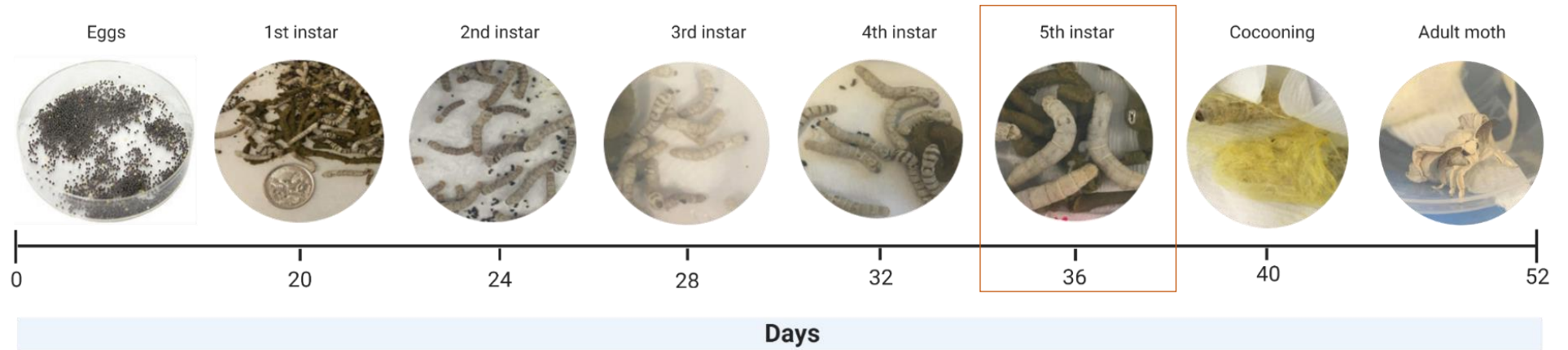


Figure 5.2 Life Cycle of Silkworm (*Bombyx mori*) larvae. The average days of each life cycle stage are displayed along the horizontal axis as environmental parameters such as light, temperature, and humidity influence silkworm growth. The 5th instar stage of the larvae life cycle is highlighted as this is the preferred stage for use as a model organism.

Previous research has highlighted the numerous benefits of invertebrates as an alternate model for vertebrate species, and silkworms appear to be an attractive alternative to mammalian models for phage research ¹³⁸. However, only one study has published the development and use of silkworms in phage therapy trials ¹³⁸. Within this study, silkworm larvae were experimentally infected with *S. aureus*, followed by administration of two phages. The phage alone had no adverse effect on the silkworm, and the phages were able to kill *S. aureus*, and thus increasing the silkworm larvae survival rate ¹³⁸. Importantly, the results obtained using the silkworm larvae model were comparable to those using the phage against *S. aureus* infections in mice ¹³⁸.

This chapter aims to develop and optimise the silkworm larvae model for *S. pseudintermedius* infection. This work aimed to test the safety and efficacy of candidate phage(s) and endolysin(s) from chapters 3 and 4, and their ability to reduce *S. pseudintermedius* CFU *in vivo*.

5.3 Results

5.3.1 Development of silkworm larvae (*Bombyx mori*) model

Due to the extensive use of silkworms in the silk production industry, the husbandry of silkworm larvae is well established. However, as this is the first instance of using silkworm larvae in our laboratory, housing requirements such as temperature, humidity and storage required optimisation. As shown in **Figure 5.3**, silkworm larvae were housed in groups of 10 or less in plastic containers with ventilation holes, lined with paper towel, as advised by the silkworm supplier. In addition, mulberry chow supplied by the supplier was lined onto the paper towel. The paper towel and food were removed and replaced every 24 hrs to reduce mould contamination. In the laboratory, silkworm larvae were housed either in a 28 °C incubator with 75% humidity, in a 28 °C CRT room or at 21 °C on the laboratory bench. The 28 °C incubator with humidity-controlled conditions resulted in optimal silkworm growth and survival and demonstrated less variation in temperature conditions than the other temperature-controlled environments (See **Figure 5.II**) and was utilised throughout the rest of this chapter.

Temperature	Humidity
25 – 28 °C	75%

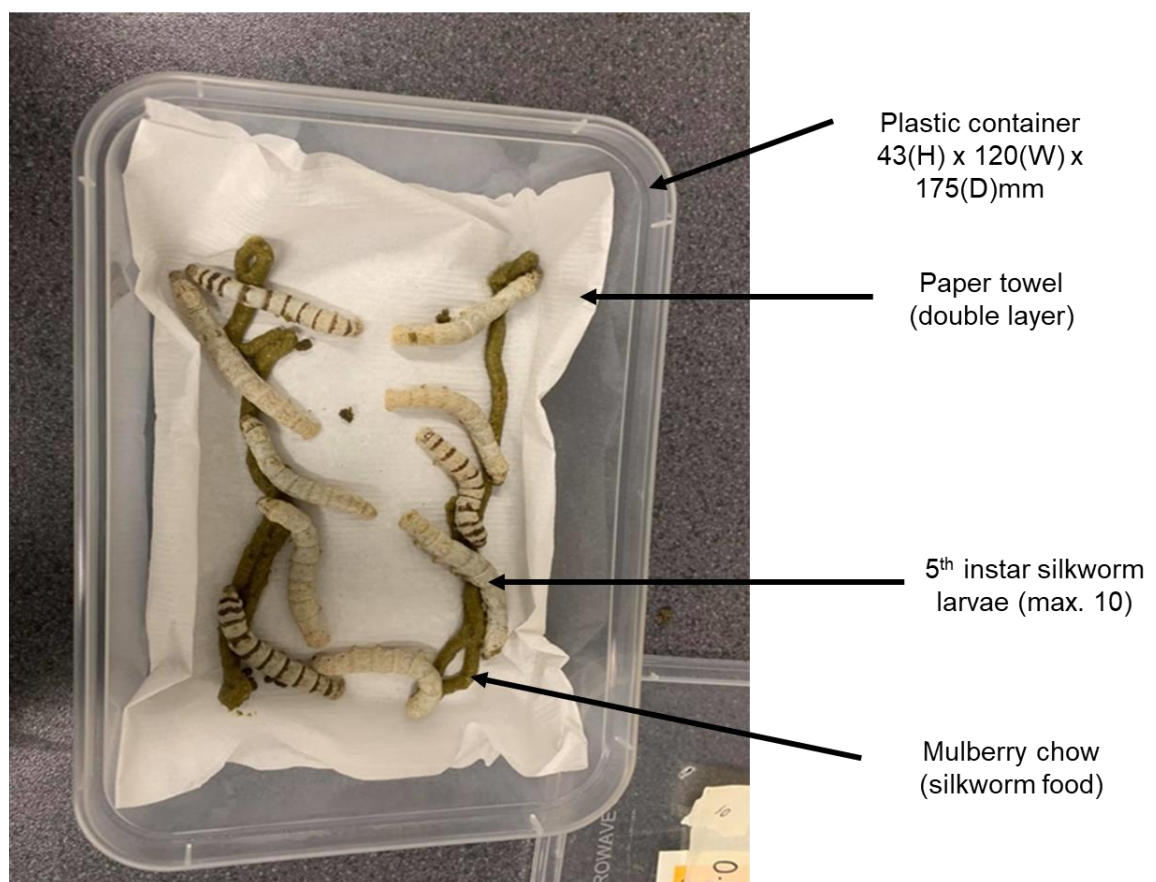


Figure 5.3 Silk worm husbandry conditions. Silkworm larvae were housed in groups of 10 or less, in plastic containers lined with paper towel. The silkworm were fed mulberry chow prior to experiments, supplied by Everything Silkworms©

The change in silkworm larvae weight throughout their lifecycle is well understood ¹⁵³, however, it is unknown whether this weight change across lifecycles is consistent across a group of silkworms. To avoid any bias in weight variability, we next wanted to understand if individual silkworm weight was consistent within a sample group to determine whether larvae weight would need to be standardised across treatment groups. We also wanted to know whether the silkworm weight could be used to indicate the silkworm instar stage (**Figure 5.2**). This was also carried out due to Australian suppliers' unreliable supply of worms of different growth stages. To address this, silkworm larvae were weighed over a 5-day period. As seen in the graph and the representative images (**Figure 5.4A and B**), the weight of silkworms significantly increased over the 5-day period, however, this change in weight was not consistent across all silkworms within the group, as can be seen on day 3 where there is a large variation between larvae weights **Figure 5.4**. Therefore, the

weight of the silkworms would need to be standardized across treatment groups in subsequent experiments.

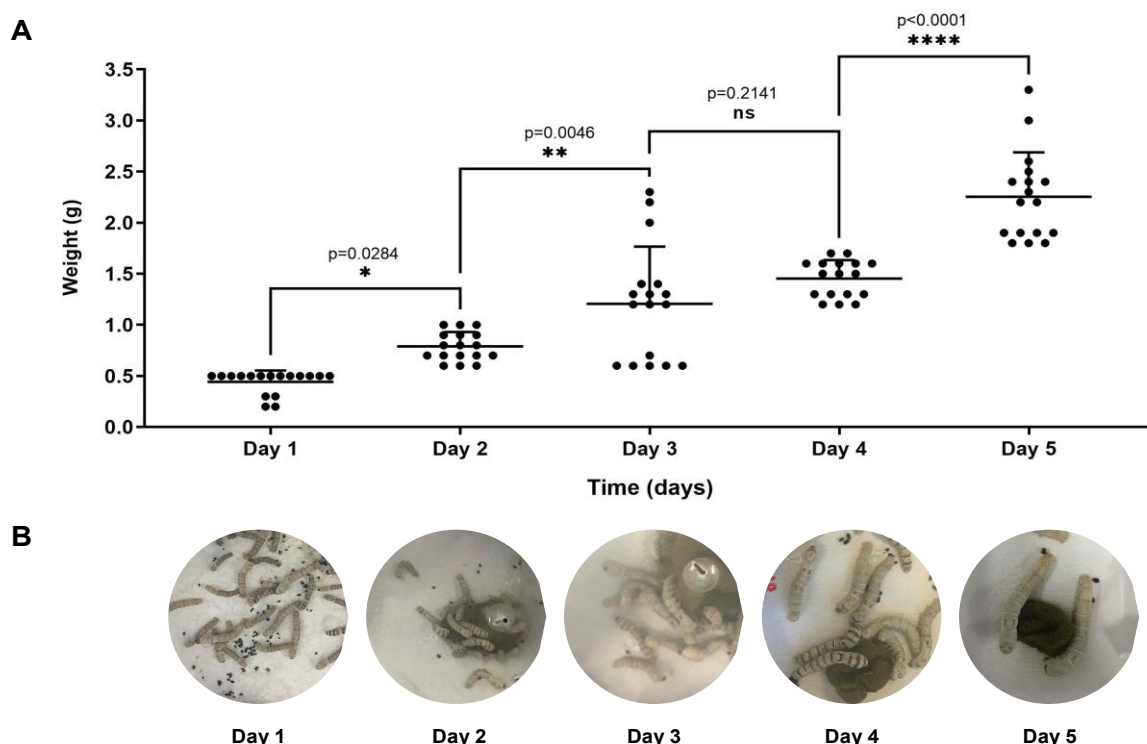


Figure 5.4 Silkworm growth over five consecutive days. (A) The body weight of 17 silkworm larvae increases over five consecutive days. (B) Representative images of silkworm larvae each day. Error bars represent mean values \pm SEM, P-values were determined by an ordinary one-way ANOVA post-hoc pairwise comparisons with Tukey correction for multiple comparisons (n=3 biological replicates).

Following optimisation of silkworm larvae housing conditions and growth over time, the extraction of silkworm haemolymph (blood equivalent in most invertebrates) also required optimisation. Extraction of haemolymph was required to assess the growth of *S. pseudintermedius* and phage lytic ability in the presence of haemolymph. Extraction methods from the literature were trialled on a minimum of 5 worms per group (Table 5.1). The extraction method was considered successful if we could consistently collect $\geq 20 \mu\text{L}$ from each worm, as this was appropriate for downstream experiments. The successful method for haemolymph extraction involved puncturing silkworm larvae with a 20-gauge needle in the lower abdomen and pipetting $>20 \mu\text{L}$ of haemolymph into an Eppendorf tube for further use (Table 5.1). The optimised extraction points are labelled in Figure 5.5, along with the injection points used from previously described methods¹⁵⁴. The injection point was used to administer bacteria, control buffers, endolysins or phages. If a double injection (e.g.,

bacteria followed by phage/endolysin) was performed, the first injection was performed on the right-hand side, followed by the second injection on the left-hand side. The extraction points were used to collect haemolymph, to quantify bacterial CFU and phage PFU in subsequent experiments.

Table 5.1 Silkworm larvae haemolymph extraction methods. Haemolymph extraction methods were trialled from previous literature, with the collection of 20 μL of haemolymph classed as a successful extraction.

Haemolymph extraction method ($n \geq 5$)	$\geq 20 \mu\text{L}$ haemolymph consistently collected? (Yes/No)	Citation
Harvesting hemolymph from cutting off the forelegs of silkworm	No	145,155,156
Harvesting haemolymph from cutting off the head of silkworm	No (contaminated with non-haemolymph material)	157
Creating a puncture wound and pipetting pooled haemolymph	Yes	138,158–161
Using a needle to syringe haemolymph from the circulatory system	No	162

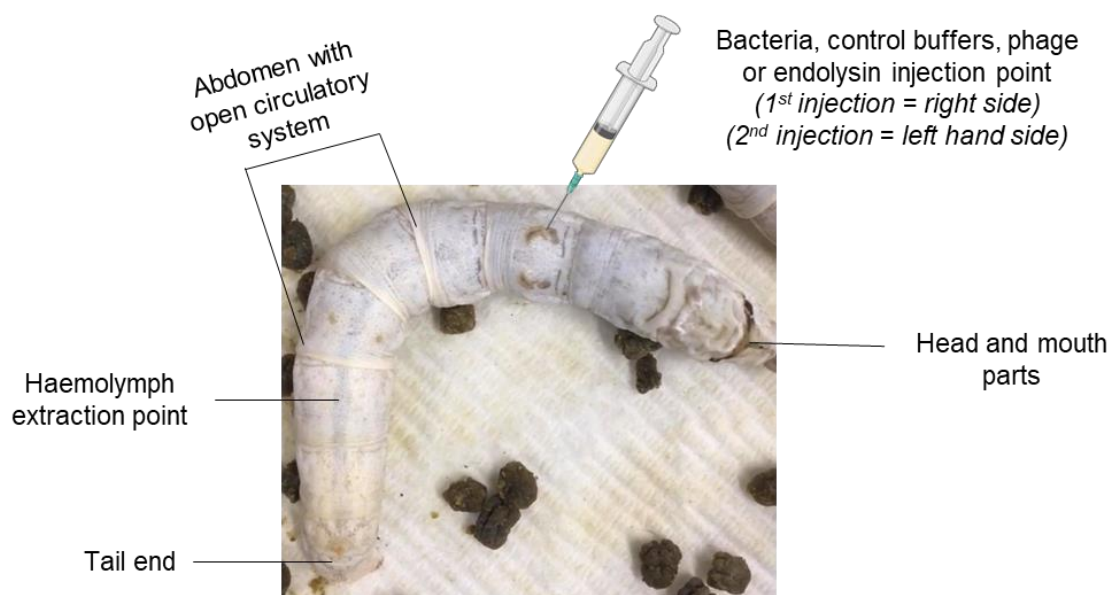


Figure 5.5 Diagram of silkworm larvae with injection and extraction points labelled. Injection points were used to administer bacteria, control buffers, phage and/or endolysins. The extraction point was used to extract haemolymph, to quantify bacterial CFU and phage PFU.

5.3.2 Suitability assessment of silkworm model for phage and *S. pseudintermedius* administration

While previous research has documented that phages are still able to kill bacteria in the presence of silkworm haemolymph¹³⁸, each phage is unique. Therefore, before moving forward with phage therapy infection trials, we first wanted to ensure that the silkworm haemolymph would not inhibit various components of the phage lifecycle (e.g., phage and/or secreted enzymes). To assess this, haemolymph was extracted from healthy silkworm larvae, and various haemolymph concentrations were mixed with a known titre of phage (**Figure 5.6A**). In this and all experiments moving forward, the isolated bacteriophage SP_157588 was utilised. The phage titre was not changed when mixed with silkworm haemolymph (**Figure 5.6B**). This was supported by the findings that the phage was still able to produce a zone of clearing on the host bacterial strain even in the presence of high haemolymph concentrations (**Figure 5.6C**). With the results that our phage was still able to lyse the bacterial strain in the presence of haemolymph effectively, we were confident in continuing to use our phage in subsequent trials.

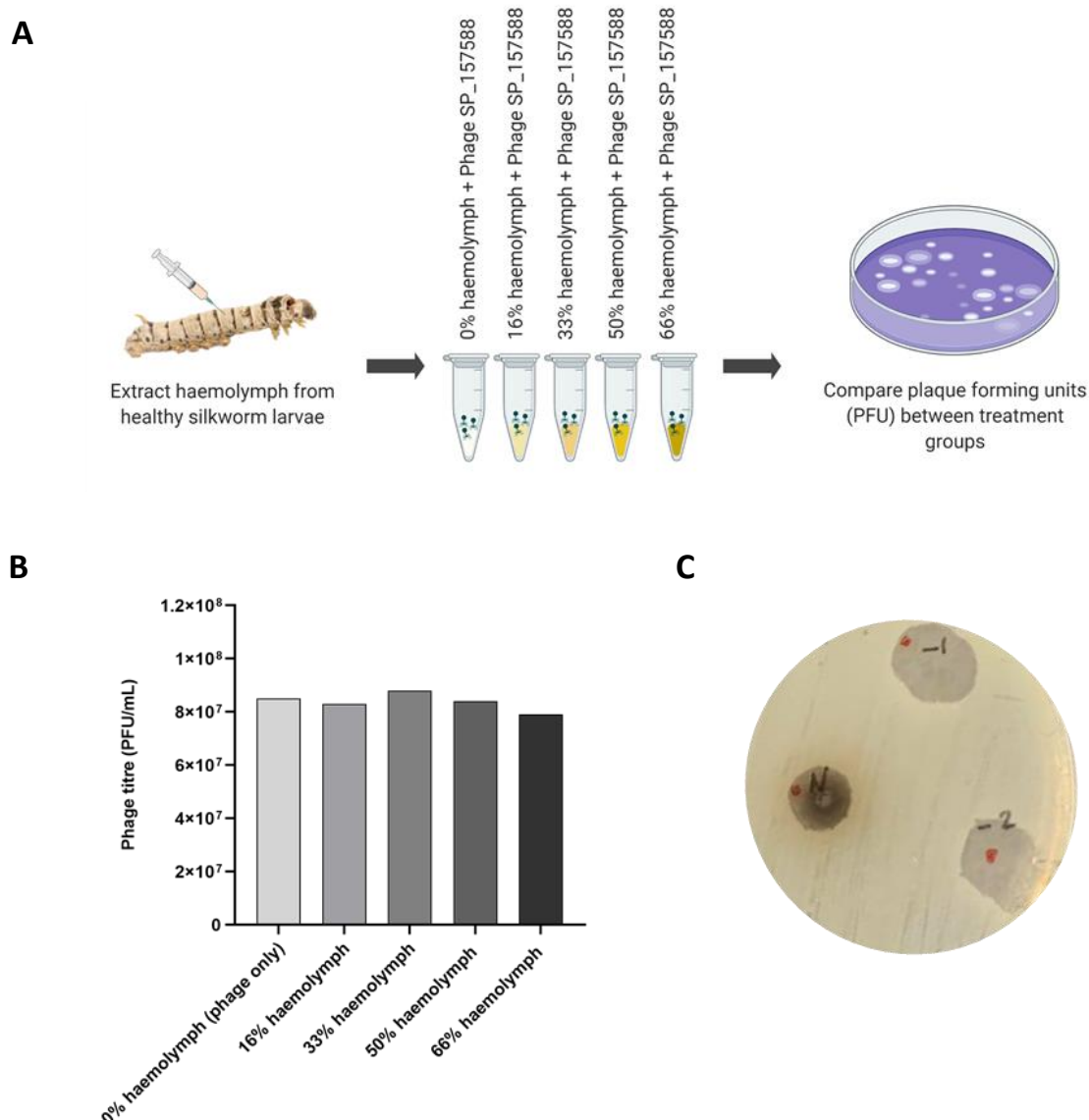


Figure 5.6 Phage lytic ability is not inhibited by silkworm larvae hemolymph. (A) Experimental design for lytic ability in the presence of silkworm haemolymph. (B) Phage Sp_{10s} plaque-forming units (CFU) after co-incubation with 0, 16, 33, 50 and 66% haemolymph. (C) Phage spotted onto *S. pseudintermedius* CM16-0689 lawn shows retained lytic ability in the presence of haemolymph.

Although the silkworm model has previously been used for various bacterial infections including, *S. aureus*, *Pseudomonas aeruginosa*, *Vibrio cholerae*, and *Escherichia coli*, it has never been used for *S. pseudintermedius* infections¹⁵². To ensure *S. pseudintermedius* was not going to be inhibited naturally by the silkworm's immune system, *ex vivo* and *in vivo* experiments were performed to ensure the silkworm hemolymph would not inhibit the growth of *S. pseudintermedius*. Haemolymph was extracted from healthy silkworm larvae, and various haemolymph concentrations were mixed with a known amount of *S. pseudintermedius* (Figure 5.7A). As shown in Figure 5.7B,

the addition of haemolymph to a known amount of *S. pseudintermedius* did not significantly affect the *in vitro* survival of *S. pseudintermedius*.

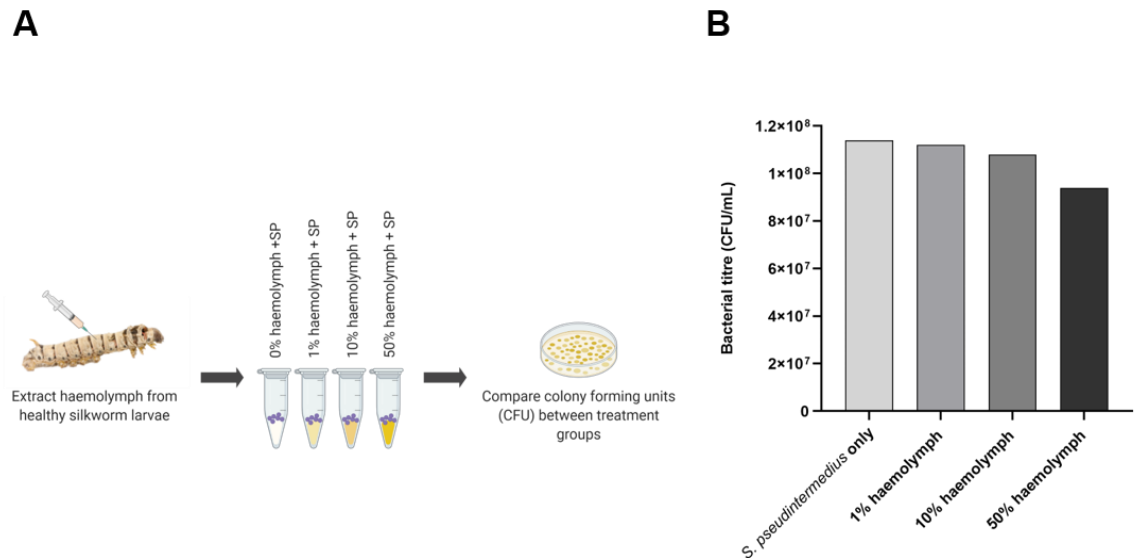


Figure 5.7 Cell viability of *S. pseudintermedius* is not inhibited by silkworm larvae hemolymph. (A) Experimental design for cell viability in the presence of silkworm haemolymph. (B) *S. pseudintermedius* strain CM16-0689 CFU after co-incubation with 0, 1, 10, and 50% haemolymph.

While *S. pseudintermedius* survived in the presence of up to 50% silkworm haemolymph *ex vivo*, we next wanted to assess whether *S. pseudintermedius* could survive and replicate when injected into silkworm larvae directly. To determine this, 5th instar silkworm larvae were injected with 50 µL of *S. pseudintermedius* at 1 × 10⁷ CFU. *S. pseudintermedius* was administered into the injection points labelled in **Figure 5.7**, which led to bacterial delivery to the open circulatory system. Infected silkworms were maintained in their normal housing conditions for 18 hrs and then their haemolymph was extracted for bacterial quantification. Quantification of *S. pseudintermedius* in the haemolymph following infection showed a 3-fold increase compared to the concentration of *S. pseudintermedius* injected, demonstrating that the silkworm model shows true infection kinetics and is an appropriate infection model moving forward (**Figure 5.8**).

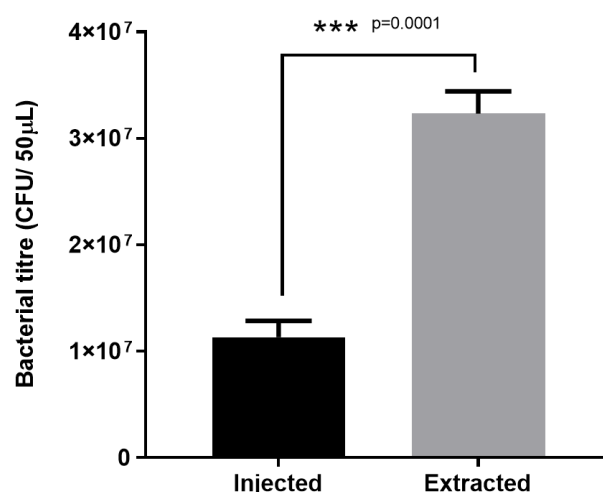


Figure 5.8 Proliferation of *S. pseudintermedius* CM16-0689 in the haemolymph. Silkworm larvae were injected with 1×10^7 CFU of *S. pseudintermedius*, and haemolymph was collected 18 hrs post-infection using a 20-gauge syringe. Extracted haemolymph was plated onto Nutrient Agar to quantify bacterial counts. This experiment was performed in triplicate. Error bars are represented as mean values \pm SEM, P values were determined by unpaired two-tailed Student's t test (n=4).

5.3.3 Safety trials of selected phage and endolysins

For the silkworm to be a successful model for phage trials, we next had to examine the safety of our control solutions (PBS or TSB) and the purified endolysin/phage formulations within the silkworm larvae. PBS was used as a control for endolysins (as the endolysins were eluted into PBS), whereas TSB was used as a control for phages and bacteria (as the phages and the *S. pseudintermedius* strains were grown in TSB). To determine the safety of the control solutions, our candidate phage (1×10^8 CFU/mL) and our candidate endolysin (50 or 100 µg) were injected (50 µL) into a group of silkworm larvae and their survival was monitored over 72 hrs (**Table 5.2**). The survival rates of the silkworm larvae were not affected by the injection of either PBS or TSB control solutions, with the exception of one silkworm death in the TSB only control group (**Table 5.2**). There were also no deaths in phage or endolysins groups, with 100% of silkworms surviving 72 hrs post-infection (**Table 5.2**). Therefore, subsequent experiments could be performed assuming that these components do not affect silkworm survival.

Table 5.2 Survival of silkworms following injection of control solutions or *S. pseudintermedius* phages and endolysins. Survival was monitored for 72 hours. Phage concentration was 1×10^8 CFU/mL. LysSN13 was tested at concentrations of 100 μ g and 50 μ g.

Phage/Endolysin	Survival rate (%) [alive/total]		
	24 hrs	48 hrs	72hrs
Phage Sp_157588 (1×10^8 CFU/mL)	100% [3/3]	100% [3/3]	100% [3/3]
LysSN13 (~100 μ g)	100% [3/3]	100% [3/3]	100% [3/3]
LysSN13 (~50 μ g)	100% [3/3]	100% [3/3]	100% [3/3]
TSB only	100% [5/5]	100% [5/5]	94% [4/5]
PBS only	100% [5/5]	100% [5/5]	100% [5/5]

5.3.4 Infection trials of *S. pseudintermedius* in silkworm larvae

Since we were able to show that both administrations of the phage and endolysin were safe, we next wanted to examine the therapeutic use of phages and endolysins within the silkworm larvae. Prior to efficacy trials, we first needed to optimise the lethal dose 50 (LD50) of *S. pseudintermedius* resulting in 50% silkworm mortality after 72 hrs, which would be a baseline survival prior to treatment (phage/endolysin) administration. To determine the LD50, various concentrations of *S. pseudintermedius* were administered into the silkworm larvae haemolymph, and survival was monitored and recorded every 24 hrs. As highlighted in **Table 5.3**, the various concentrations of *S. pseudintermedius* injected into the silkworm larvae resulted in a dose-dependent kill curve. Importantly, a concentration of 1.25×10^6 CFU of *S. pseudintermedius* was identified as the LD50, as only 50% of the silkworms survived at 72 hrs. These results can be visualised in **Figure 5.9**, where we see a high mortality rate when a high concentration of *S. pseudintermedius* is injected, and a low mortality rate when a low concentration of *S. pseudintermedius* is injected. Group 5 is identified as the LD50 group, as only 50% of the silkworm larvae survived. Group 5 received 1.25×10^6 CFU of *S. pseudintermedius*, therefore, this concentration will be used in subsequent experiments.

Table 5.3 Silkworm survival following *S. pseudintermedius* infection. Survival was monitored for 72 hours as our LD50 endpoint was 72 hrs. The LD50 was determined with two independent experiments performed with ≥ 17 silkworms. Our optimised LD50 was found to be 1.25×10^6 CFU/50 μ L.

Group	Bacterial concentration per worm	Volume injected	Survival rate % [alive/total]		
			24 hrs	48 hrs	72hrs
Group 1	2×10^7	50 μ l	39% [7/18]	39% [7/18]	11% [2/18]
Group 2	1×10^7	50 μ l	22% [4/18]	17% [3/18]	0% [0/18]
Group 3	5×10^6	50 μ l	83% [15/18]	67% [12/18]	28% [5/18]
Group 4	2.5×10^6	50 μ l	94% [17/18]	61% [11/18]	39% [7/18]
Group 5	1.25×10^6	50 μ l	100% [18/18]	89% [16/18]	50% [9/18]
Group 6	6.25×10^5	50 μ l	100% [18/18]	89% [16/18]	67% [12/18]
Group 7	3.12×10^5	50 μ l	100% [17/17]	94% [16/17]	94% [16/17]
Control	0	50 μ l	100% [17/17]	100% [17/17]	94% [16/17]
Handling control	0 (no injection)	0	100% [10/10]	100% [10/10]	100% [10/10]

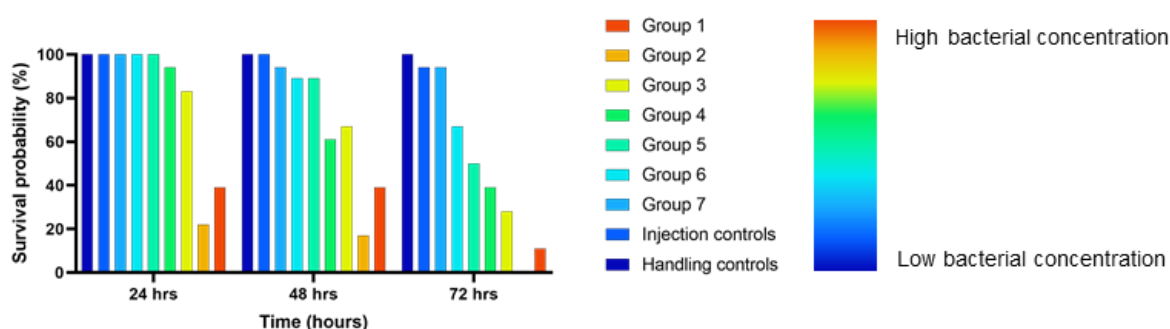


Figure 5.9 Visual representation of silkworm survival following *S. pseudintermedius* infection. Groups of silkworm larvae were injected with various concentrations of *S. pseudintermedius* and silkworm survival was measured over 72 hrs. Data is represented as survival percentage of a silkworm group (n = 10-18 worms). Colour of bar correlates to the concentration of *S. pseudintermedius* received, with blue indicating low bacterial concentration through to red indicating high bacterial concentration. Experiment was performed in duplicate.

5.4.5 Efficacy trials of phage and/or endolysins in silkworm larvae

Following the optimisation of the phage and endolysin treatment formulations along with the LD50 concentration of *S. pseudintermedius* in the silkworm, we next wanted to test the efficacy of phage or endolysin to reduce *S. pseudintermedius* *in vivo* and thus increase the survival rate. Efficacy trials were undertaken using the workflow developed in **Figure 5.10**. Briefly, the optimised LD50 concentration of *S. pseudintermedius* was administered to a group of silkworm larvae, immediately followed by the injection of 50 μ L of phage or endolysin at doses deemed safe in previous experiments (**Table 5.1**). The survival of the silkworm in response to the treatments were monitored and recorded over 72 hrs. As shown in **Table 5.4**, the double injection control of PBS or the injection of 100 μ g of LysSN13 did not alter silkworm survival. As expected, the group that received the LD50 concentration of *S. pseudintermedius* showed a 50% survival at 72 hrs (**Table 5.4**). Interestingly, groups that received the LD50 concentration of *S. pseudintermedius*, followed by a treatment of either Phage MOI 1, 10, 100 μ g of SN13 or 50 μ g of SN13 showed low levels of survival of 38%, 0%, 0% or 25%, respectively (**Table 5.4**). Perhaps indicating that this methodology requires further optimisation or that the administration of endolysin or phage following infection may elicit either a lethal immune response or release a bacterial toxin lethal to the worm.



Figure 5.10 Workflow of phage or endolysin efficacy trials in silkworm larvae.

Table 5.4 Efficacy of phage or endolysin following *S. pseudintermedius* infection. Survival was monitored for 72 hours (n = 10).

Group	Bacteria/Endolysin concentration per worm	Volume injected	Survival rate % [alive/total]		
			24 hrs	48 hrs	72hrs
Injection control (Double injection)	0 (PBS only)	50 µl x 2 = 100 µl	100% [5/5]	100% [5/5]	100% [5/5]
Endolysin only	100 µg	50µl	100% [5/5]	100% [5/5]	100% [5/5]
LD50 only	1.25 x 10 ⁶	50µl	100% [8/8]	100% [8/8]	50% [4/8]
LD50 + endolysin (100 µg)	1.25 x 10 ⁶ + 100 µg	100µl	100% [8/8]	75% [6/8]	0% [0/8]
LD50 + endolysin (50 µg)	1.25 x 10 ⁶ + 50 µg	100µl	100% [8/8]	75% [6/8]	25% [2/8]
LD50 + Phage SP_157588 (MOI 10)	1.25 x 10 ⁶ CFU + 1.25 x 10 ⁷ PFU	50µl	100% [9/9]	45% [4/9]	0% [0/9]
LD50 + Phage SP_157588 (MOI 1)	1.25 x 10 ⁶ CFU + 1.25 x 10 ⁶ PFU	50µl	100% [8/8]	88% [7/8]	38% [3/8]

5.4 Discussion

The use of phage therapy as a treatment option against MRSP infections in canines is an area of significant research interest¹³. However, more rapid *in vivo* models are required for safety and efficacy testing to progress the use of phages and endolysins¹²¹. In this chapter, we demonstrated that the silkworm model is a suitable reduction model to examine phage therapy against *S. pseudintermedius* infections.

To investigate the usefulness of the silkworm model as an *in vivo* option for phage treatment solutions moving forward, the hemolymph of 5th instar stage larvae was tested for its ability to support both bacteria and phage/endolysin treatments. Silkworm hemolymph did not inhibit *S. pseudintermedius* growth or the lytic activity of phage related components (**Figure 5.6**). *S. pseudintermedius* increased in CFU once injected into the silkworm after 18 hours, implying bacterial replication, thus showing true infection kinetics (**Figure 5.8**). The silkworm model successfully examined the use of phage or endolysin against such *S. pseudintermedius* infections, with variable results (**Table 5.4**), demonstrating the potential of the silkworm as a good model for bacterial infections and treatment trials. However, numerous challenges arose in developing this model.

As mentioned previously, in Australia, silkworm larvae are predominately reared as live feed for reptiles; therefore, the silkworms used in this study were purchased from live food or reptile companies or aquariums and pet shops. However, throughout this study, the main challenge was sourcing a constant supply of silkworm larvae. The unreliability in suppliers meant that factors such as weight, food supply and housing conditions (**Figure 5.3**) had to be controlled to limit variability between batches and improve the repeatability of experiments involving silkworm larvae from various sources. Moving forward, to maximise the efficiency of this model, setting up a silkworm rearing system from eggs would enable greater uniformity in both supply and health of silkworm larvae for continuous experiments. Additionally, there was significant variation in silkworm larvae weight over a 5-day period within the same batch of silkworms (**Figure 5.4**), which we overcame by sorting larvae into weight categories that were evenly divided across the treatment groups, to limit silkworm larvae weight as a confounding factor. This challenge could also be addressed by

rearing silkworm larvae in-house in excess and hand-picking larvae that fit within a given weight range for less variation within groups.

Throughout the development of the silkworm model, we faced challenges in extracting consistent and usable quantities of larvae haemolymph. Numerous methods have previously been used to successfully extract haemolymph from various insect models; however, few had been trialled on silkworm larvae specifically (**Table 5.1**)^{138,158–161,145,155,156}. We found that of the four methods trialled, only one method resulted in successful routine collection of usable haemolymph ($\geq 20 \mu\text{L}$), which involved piercing the dorsal tail-end (**Figure 5.5**) of silkworm larvae with a 20-gauge needle and pipetting the pooled haemolymph from the puncture site (**Table 5.1**). Utilising this optimised technique, we demonstrated that haemolymph collected from healthy silkworms did not inhibit *S. pseudintermedius* growth or the lytic activity of phage related components (**Figure 5.6** and **Figure 5.7**). Therefore, proving that the silkworm model was appropriate for further use with our specific bacteria, phage and endolysin candidates. With the successful development of our silkworm model, we were able to show a proliferation in *S. pseudintermedius* growth within the silkworm larvae 18 hrs after injection (**Figure 5.8**). This proliferation in bacterial growth resulted in a dose-dependent survival rate of the silkworm in response to *S. pseudintermedius* infection (**Figure 5.9**). Interestingly, previous studies have also shown that *Staphylococcus spp.* replicate within the silkworm larvae and affect survival rate in a dose-dependent manner¹³⁸. While research has begun trialling bacterial species other than *Staphylococcus* within the silkworm model, such as *Pseudomonas aeruginosa*, *Vibrio cholerae* and *Escherichia coli*, further work is required to determine the dose-dependent effect of such species and their suitability for phage therapy trials within the silkworm model¹⁵⁰. As such, we optimised the LD50 of *S. pseudintermedius* (1.25×10^6 CFU), which was used as the baseline survival prior to administration of phage and/or endolysins for subsequent experiments. Despite the technical challenges involved in developing the silkworm model, several protocols were optimised, demonstrating that silkworm larvae are viable for *S. pseudintermedius* infections. However, moving forward, numerous experimental factors should be considered when developing this model for alternate bacterial species. For example, future studies should examine the potential anti-bacterial effects of haemolymph on numerous

bacterial genus, as well as the bacteria's ability to proliferate in the silkworm larvae, to assess the use of the silkworm as an *in vivo* model for future phage efficacy trials.

With the successful development of the silkworm model, phage and/or endolysins were tested for their safety and efficacy against *S. pseudintermedius* infections. One prior study has shown that phages are not toxic to silkworm larvae, with as much as 4×10^9 PFU of purified phage remaining non-toxic to silkworms ¹³⁸. Similarly, our results demonstrated that both our phage and endolysin preparations were safe in this *in vivo* model, as injection of high concentrations of phage (1×10^8 CFU/mL) and endolysins (50-100 µg) did not affect silkworm survival when delivered in isolation (**Table 5.2**). To test the ability of our phage or endolysin preparations in reducing *S. pseudintermedius* viability to increase silkworm survival rate, the LD50 concentration of *S. pseudintermedius* was injected into silkworm larvae, followed by the injection of phage (1.25×10^7 or 1.25×10^6 PFU) or endolysin (50 or 100 µg), and survival was monitored over 72 hrs. Control groups injected with PBS only, phage only or endolysin only showed no change in survival, with 100% survival after 72 hrs, however, silkworm larvae injected with the bacterial LD50 concentration followed by phage or endolysins, showed very low survival rate between 0% and 38%. Interestingly, the groups that had a 0% survival rate after 72 hrs received the higher doses of phage or endolysin (MOI 10 of phage or 100 µg of endolysin), whereas the groups that had a slightly higher survival rate of 25% and 38% received lower doses of phage (MOI 1) or endolysin (50 µg), respectively (**Table 5.4**). These findings show that the LD50 concentration of *S. pseudintermedius* followed by administration of phage or endolysins unexpectedly resulted in higher mortality rates than the LD50 alone. Conversely, previous studies have shown that a lethal dose of *S. aureus* injected into silkworm larvae resulted in 0% survival, however, high titres of phage increased larvae survival rate to 100% ¹³⁸. Unfortunately, due to COVID-19 related time limitations, further experiments to describe the underlying pathology resulting in this unexpected finding were unable to be performed. One potential explanation is that phage or endolysin driven lysis of the *S. pseudintermedius in vivo*, resulted in an exaggerated inflammatory response due to release of bacterial components recognised by the immune system (such as lipopolysaccharides (LPS)) ^{163,164}, or alternatively, the release of toxin related bacterial products ¹⁶⁵. It has been well described that

S. pseudintermedius contains various virulence factors, including toxins released upon cell death¹⁶⁶. However, the involvement of such toxins in *S. pseudintermedius* pathogenesis is not well known, particularly in the case of phage or endolysin-induced bacterial lysis. To better understand the results observed in this chapter, further experiments are required to compare the survival rate of larvae injected with either live *S. pseudintermedius*, or a preparation of *S. pseudintermedius* lysed *in vitro* by phage/endolysin. This experiment would indicate whether the survival rates we observed in our initial studies were due to the liberation of toxins released during cell lysis. In parallel, *in vivo* measurement of key anti-bacterial mediators, such as members of the antimicrobial peptide family should be evaluated to see if the lysis of *S. pseudintermedius* by phage/endolysins does indeed trigger an exaggerated immune response¹⁶⁷. A better understanding of the host-response to phage/endolysin-induced *S. pseudintermedius* lysis is crucial in further developing treatment options for *S. pseudintermedius* infections. It would also be valuable to observe if the same phenomena concurs in higher order models. However, it should also be noted that the predominant concern of *S. pseudintermedius* infections in canines is canine pyoderma, a topical infection, rather than a systemic infection, therefore, an alternative model for skin infections may be more appropriate. As mentioned previously, there is currently a murine skin infection model developed, however, due to ethical concerns, the use of an *in vitro* skin model could be explored for use in topical phage therapy trials¹⁶⁸.

5.5 Conclusions

Throughout this chapter, we successfully developed a silkworm larvae model to explore phage therapy trials against *S. pseudintermedius* infections, for the first time. Although the silkworm was found suitable for the growth of *S. pseudintermedius* administered systemically, administration of phage/endolysin following *S. pseudintermedius* infection resulted in higher mortality rates than *S. pseudintermedius* alone. This result highlights the need for further development of *in vivo* models for *S. pseudintermedius* infections and the rapid growth of phage therapy research moving forward. Overall, this work highlights that the silkworm model is an ethical model that can

be used to reduce the use of high order models by only progressing with lead phage/endolysins that show exceptional safety and efficacy testing results.

5.6 Appendix

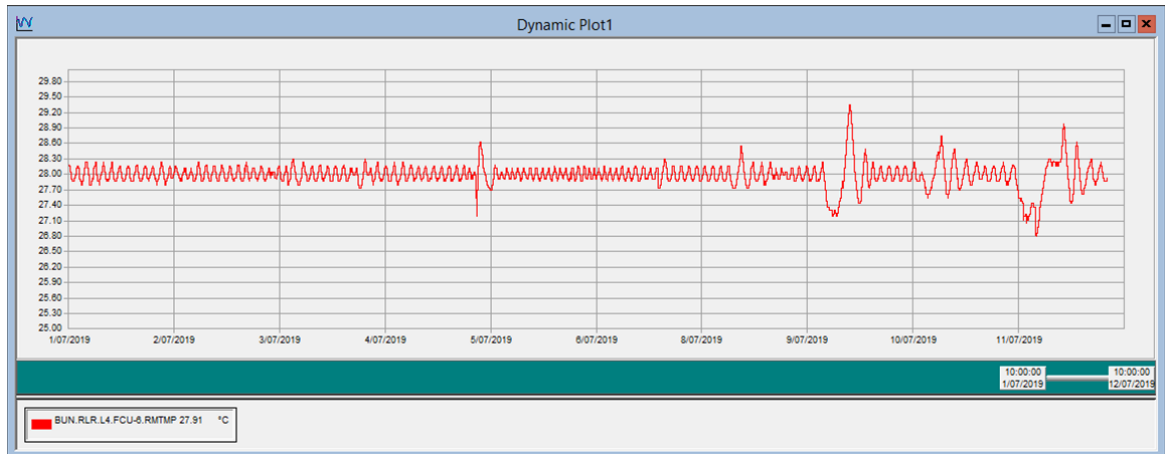


Figure 5.11 Temperate variation of 28 °C constant temperature room.

Chapter 6

Thesis discussion

6.1 Introduction

Due to the increase in incurable bacterial infections and the substantial economic burden caused by the rise in antibiotic resistance, there is a global demand for alternative therapeutics¹⁶⁹. One alternative treatment option that has received recent attention is the use of phage therapy, the therapeutic application of phages (viruses that infect and potentially kill bacteria) and their derived products such as endolysins (enzymes that degrade the peptidoglycan layer causing bacterial lysis)⁷². Although phages were first described in 1915, the production of antibiotics, termed the “silver-bullet”, resulted in the diminishment of phage research in western medicine¹⁷⁰. However, with the rise in antibiotic resistance, there has been a resurged interest in phage therapy.

Currently, in western medicine, phage therapy is only used for emergency cases where all other treatment options have been exhausted. These phages, administered as a last resort, are known as “compassionate use”¹⁷¹. Globally, there have been numerous compassionate cases of phage therapy, many of which have had successful outcomes due to reductions in bacterial load, improved clinical symptoms and in some cases, the avoidance of subsequent medical interventions such as amputation¹⁷¹. However, phage therapy has been more extensively trialled in animals, mainly in agricultural livestock, focusing on enteric pathogens such as *Campylobacter jejuni*, *Escherichia coli* and *Salmonella enterica*, particularly in chickens¹⁷². Numerous pre-clinical phage therapy trials have also been conducted in animal models such as mice and rats¹²²; however, there have only been a small handful of trials of phage therapy in companion animals such as rabbits and cats¹⁷³, with only one study examining the efficacy of phage therapy in canines¹⁷⁴. While this collection of work represents the success of phage therapy against a few bacterial pathogens, numerous bacterial species also require alternative therapeutics, for example, *Staphylococcus spp.*, a genus of gram-positive bacteria involved in both various humans and animal infections¹⁷⁵.

S. pseudintermedius is a severe threat in veterinary medicine as it is involved in numerous canine infections. Studies have shown that up to 97.8% of isolates are resistant to three or more antibiotics routinely used in veterinary medicine (**Chapter 1**,¹³). The work presented in this thesis explored phage therapy as a novel therapeutic for *S. pseudintermedius* infections in canines. We firstly isolated and characterised novel phages that lysed clinical isolates of *S. pseudintermedius* (**Chapter**

3). However, these phages were unfavourable for further use as they contained lysogeny modules and thus had the ability to integrate within the bacterial genome rather than lyse the bacteria. Therefore, to overcome this, we mined the genomes of all available bacteriophages, from this study and those found integrated into *S. pseudintermedius* bacterial genomes to identify and manufacture novel endolysins as an alternate treatment. Three of these endolysins were successful in lysing *S. pseudintermedius* clinical isolates (**Chapter 4**). Taken together, **Chapter 3 and Chapter 4** provide further knowledge to the field of phage therapy and its promising potential as an alternative treatment option for antibiotic-resistant bacterial infections. To test the safety and efficacy of the candidate phages and endolysins identified in **Chapter 3 and Chapter 4**, we developed a silkworm model to test whether this was an appropriate model for phage therapy trials against *S. pseudintermedius* infections (**Chapter 5**). In this final chapter, the findings from this thesis will be discussed within the context of the most current literature, with insights into where this work may influence future research in this field.

6.2 Phage therapy as a novel therapeutic for antibiotic-resistant infections

Although the field has shifted to phage therapy as an alternative to antibiotics, and there have been examples of multiple promising outcomes, there are still multiple gaps in our knowledge and hurdles that we need to overcome to progress phage therapy as a therapeutic. Such hurdles include, (i) the isolation of temperate phages, (ii) the lack of understanding of prophages' role, and (iii) the need for standardised animal models to assess the safety and efficacy of phage therapy.

Temperate phages are highly abundant and possess the ability to integrate within the bacterial genome, passed to daughter cells via bacterial replication¹⁷⁶. Although temperate phages are still able to lyse bacteria, due to their innate ability to remain dormant in the bacterial genome and their role in transferring genes between bacteria (such as antibiotic-resistant genes and their unpredictable nature), temperate phages are unfavourable for phage therapy¹⁷⁶. Temperate phages are more abundant than lytic phages¹⁷⁶; therefore, it is not surprising that in **Chapter 3**, we isolated four novel temperate phages, all of which were able to lyse multiple clinical strains of *S. pseudintermedius* isolates from canine infections. Unfortunately, all known phages isolated

against *S. pseudintermedius* are temperate phages ^{16,17}, which could be explained by the overall high abundance of temperate phages in nature or the fact that there is a high prevalence of prophages within the genome of *S. pseudintermedius* clinical isolates, which we identified for the first time in **Chapter 3**. Prophages are phages integrated within the bacterial genome, and when they excise from the genome, they can be isolated as temperate phages ¹⁷⁶. This high prevalence of prophages within the genome of *S. pseudintermedius* isolates is a novel finding and highlights a potential reason for isolating purely temperate phages against *S. pseudintermedius* to date. The role of these prophages in response to phage therapy is yet to be elucidated in the field but is essential knowledge from a clinical point of view as to whether the excision of prophages from the *S. pseudintermedius* genome hinders or improves therapeutic outcomes. Despite the phages against *S. pseudintermedius* being temperate, some have shown promising results, able to preferentially lyse MRSP stains ¹⁶, possess anti-biofilm effects ¹⁸, and show complete bacterial clearance within 75 minutes of phage administration *in vitro* (**Chapter 3**). With this, multiple studies focus on opportunities to use temperate phages, including mutating temperate phages to remove lysogeny modules by random mutagenesis or engineered methods ^{49,177–180}, using temperate phages within a cocktail ^{176,181,182} or isolating lytic proteins such as endolysins derived from the lysogenic phages ^{75,183–185}.

The ability to genetically modify temperate phages, especially the genes associated with lysogeny, have shown to result in phages with improved efficacy, broader host range and, importantly, phages that are no longer capable of lysogeny ^{180,186,187}. In addition, a patent exists to obtain *vir* mutants (virulent phage mutants) through random mutagenesis ¹⁸⁸; however, unfortunately, random mutagenesis protocols for *S. pseudintermedius* temperate phages have been unsuccessful ⁴⁹. These unsuccessful attempts demonstrate that further research is required to optimise site-specific modifications to remove the lysogeny modules or find an alternative use for temperate phages. On the other hand, a handful of studies have used temperate phages in animal models where there is a lack of lytic phages against particular bacterial species, such as *Clostridium difficile* ^{189,190}. While findings from these studies showed that the cocktail of temperate phages completely eradicated the *C. difficile* infection, preventing the emergence of phage resistant variants, further research is

required as to whether these findings would be validated in other bacterial species, such as *S. pseudintermedius*.

With the isolation of several temperate phages against *S. pseudintermedius*, with no success in creating *vir* mutants, we explored the use of phage-encoded endolysins as an alternate solution (**Chapter 4**). Endolysins have received significant attention in recent literature for their role in degrading the bacterial peptidoglycan layer, causing cell lysis. In comparison to phages, endolysins have many favourable characteristics¹⁹¹. Endolysins generally possess a broader host range, show less bacterial resistance, and therapeutic administration allows for a more controlled dosing strategy, as they do not replicate within the bacterial strain, unlike phages^{74,98}. Endolysins are also an attractive option for bacterial strains (including *S. pseudintermedius*) that contain prophages within their genome and in situations where only temperate phages have been isolated¹⁹². With the use of rapid advancements in sequencing technologies, it is now possible to mine and identify thousands of endolysin genes available across all prophages within bacterial genomes or from isolated temperate or lytic phages. Using a computational approach, we mined the genome of all currently available *S. pseudintermedius* bacterial sequences, as well as known phages against these (**Chapter 3 and Chapter 4**), to identify six novel endolysins. To our knowledge, this is the first time that a mass-endolysin screening has been performed, and the first endolysins derived from *S. pseudintermedius* phages. Importantly, following manufacture and protein purification of these novel enzyme's, three were able to lyse up to 60% of our library of clinical isolates of *S. pseudintermedius*, therefore, showing a broader host range than our isolated phages (**Chapter 3**). These findings are supported by a recent study conducted where it was found that the endolysin, Lys-phiSA012, possessed a broader host range against *Staphylococcal* isolates than the *S. aureus* phage it was derived from, phi-SA012⁹⁷. Alongside this, several studies have shown very promising results for the use of endolysins administered against numerous *Staphylococcus spp.* in animal models such as mice and rats, as well as trials in cows, monkeys, and humans^{193–202}. From these *in vivo* studies, it has been shown that endolysins were effective at reducing the bacterial burden and thus improving survival rates in animal models, with them being safe when administered through various routes such as intraperitoneal, topical, intramammary, intravenous and intranasal²⁰³.

Translational results from a recent case report demonstrated that the endolysin, Staphitekt SA.100 (derived from an *S. aureus* bacteriophage), was successful at treating chronic and recurrent dermatoses in 3 patients when applied topically²⁰⁴. However, a follow up randomised clinical trial found that in 50 patients', topical application of Staphitekt SA.100 over a 12-week period showed no effect on *S. aureus*²⁰⁵. While preliminary findings in animal models show promising results of endolysins as a therapeutic agent against *Staphylococcus spp.*, it is important to highlight that the use of endolysins is still a novel yet expanding field, thus further research is required to optimise their use in human and animal medicine. Challenges identified within the field include, (i) the need for high throughput protein optimisation, (ii) research into the protein domains essential for enzymatic activity, and (iii) the need for rapid and ethical pre-clinical models for endolysin safety and efficacy screening.

As highlighted throughout this thesis, the expression and storage of the six selected endolysins proved challenging (**Chapter 4**). We found that each protein required different expression and purification parameters (e.g. expression temperature, elution buffers, addition of metal ions), which has also been identified as a potential hurdle in other studies surrounding endolysin formulations²⁰⁶. Therefore, to progress with a pool of endolysins (such as the six identified within this thesis), high throughput and standardised screening tests should be developed to assess the protein expression and subsequent protein stability under various parameters. This workflow would allow for the rapid identification of optimal conditions required for each individual protein and progress their use in further testing. Such a screening method would also be favourable in individually testing the enzymatic activity of each endolysin domain in isolation to develop the most efficient protein for bacterial lysis. We have shown, along with numerous other studies, that endolysins contain several different domains that may be required for their lytic activity (**Chapter 4**), with one of these being the cysteine, histidine-dependent amidohydrolase/peptidase (CHAP) domain^{207–210}. The CHAP domain is an amidase domain responsible for cleaving amide bonds within the peptidoglycan and there is substantial evidence to show that the CHAP domain alone is sufficient to kill *Staphylococcal* cells^{207–210}. Importantly, of the six endolysins identified throughout this thesis, four contained a CHAP domain, three of which showed lysis on clinical isolates of *S. pseudintermedius*.

Therefore, further work should aim to isolate and express each individual domain from these endolysins, to test whether the CHAP domain alone is sufficient for *S. pseudintermedius* lysis. If results show that the CHAP domain does suffice, the field could shift to identifying CHAP domains encoded within *Staphylococcal* bacterial strains or phages as an anti-staphylococcal agent.

Throughout this thesis, we demonstrated that many *S. pseudintermedius* bacterial strains contain prophages within their genome. These prophages may excise as temperate phages due to phage-induced bacterial lysis during the normal bacterial life cycle. However, this phenomenon is yet to be elucidated in response to endolysin-induced bacterial lysis. Thus, again, research into whether prophages are induced following the administration of endolysins is essential. Furthermore, it is currently unknown whether the excision of prophages will assist therapeutic outcomes by further lysing pathogenic strains or hinder the outcome, as prophages may carry antibiotic-resistance genes that can be spread to bacteria infected by the prophage. Such research is essential for progressing endolysins forward as alternative therapeutics; thus, high throughput and rapid *in vivo* models are crucial in determining the safety and efficacy of both phage and endolysin candidates prior to their subsequent use in humans and animal medicine.

6.3 The need for ethical animal models for the progression of phage therapy

Phage therapy trials in animal models have provided insights into the safety and efficacy of phages and endolysins prior to their therapeutic use in humans and animals ^{121,122}. Currently, higher-order models such as mice are predominantly used ^{121,122}. However, issues surrounding their use include high cost, training requirements and housing facilities, as well as ethical concerns. Therefore, recent research has focused on alternative models for phage therapy research, with one possible solution including the development of ‘organ-on-a-chip’ which are fluidic devices that aim to replicate the physiological functions and responses of entire organs ²¹¹. Additionally, multiple studies have aimed to develop alternate animal models that show similar results to high order models, for example, nematodes (*Caenorhabditis elegans*), common fruit flies (*Drosophila melanogaster*), wax moths (*Galleria mellonella*), silkworm larvae (*Bombyx mori*), and zebrafish (*Danio rerio*) ¹²².

In **Chapter 5** we developed and optimised the silkworm larvae model as an ethical model for rapid and high throughput phage therapy trials. While numerous studies have successfully used silkworm larvae for bacterial infections and drug screening, to date, only one study has utilised the silkworm model for phage therapy trials^{138,150,152,212–215}. This study found that *S. aureus* infection was lethal to silkworm larvae, which was rescued by administration of *S. aureus* phages, and importantly, these findings were validated in a mouse model run in parallel¹³⁸. Therefore, we felt that the silkworm model was appropriate for *S. pseudintermedius* infection and subsequent phage therapy trials using our candidate phage and endolysin identified in **Chapter 3** and **Chapter 4**. Furthermore, while the silkworm larvae showed dose-dependent mortality to *S. pseudintermedius* infection, subsequent administration of our phage and endolysin resulted in higher mortality than the bacteria alone (**Chapter 5**). These findings were unexpected as our *in vitro* studies suggested that the administration of phage or endolysin would kill the *S. pseudintermedius* within the silkworm larvae, thus increasing the silkworm survival rate (**Chapter 5**). As this was only the second study using the silkworm model for phage therapy, and the first study optimising the silkworm model for *S. pseudintermedius* infections, there is a lack of information to address these findings. This further highlights the need for more significant research into reduction models for phage therapy applications and their analysis alongside higher-order animal models such as mice. Such research would fast track models such as silkworms to expedite **in vivo** analysis of candidate phage treatments. While significant research has focused on developing alternative animal models, such as nematodes (*Caenorhabditis elegans*), common fruit flies (*Drosophila melanogaster*), wax moths (*Galleria mellonella*), and zebrafish (*Danio rerio*), the silkworm model possesses many benefits over other models. For instance, the silkworm model has a moderate body size for ease in handling, has uncomplicated housing requirements, is low cost to purchase and maintain, and does not require ethics¹⁵⁴.

The numerous benefits of the silkworm model facilitate rapid and high throughput testing of phages and endolysins, allowing only the top candidates to progress to subsequent experiments. Overall, this thesis highlights a sufficient pipeline for phage and endolysin screening, isolation, and characterisation, which allows us to identify and move forward with only the best candidates within

our silkworm model. The pre-clinical end of our pipeline uses the silkworm larvae model to rapidly trial various phage/endolysin formulations and doses to determine the safety and efficacy of our phage therapy applications prior to their use in clinical trials.

6.4 Final reflections and conclusions

Throughout this thesis, we isolated novel phages and endolysins that showed strong lytic activity against multiple clinical isolates of *S. pseudintermedius*, which adds new candidates to the field of antimicrobial agents (**Chapter 3 and Chapter 4**). We also elucidated the high prevalence of prophages within the *S. pseudintermedius* genome for the first time, which has important implications in future therapeutic options (**Chapter 3**). Finally, we developed and optimised a silkworm model to rapidly test candidate endolysins and phages' safety and efficacy to progress their use in treatment options for *S. pseudintermedius* infections in canines (**Chapter 5**). Overall, the results obtained throughout this thesis contribute a further understanding of the phage therapy field and identify and highlight the hurdles for developing phage and endolysins as novel therapeutics against numerous bacterial infections. This work is directly relevant to the global antibiotic resistance crisis, as a statistic released by the Review on Antimicrobial Resistance stated that antibiotic-microbial resistant (AMR) infections contribute to 700,000 deaths annually ²¹⁶. However, without effective interventions, AMR infections are projected to cause 10 million deaths and a global economic loss of \$100 trillion by 2050, surpassing cancer as the leading cause of mortality worldwide ²¹⁶. Many factors have been identified that contribute to the rise in antibiotic-resistance, with the interactions between humans, domestic animals, wildlife, and agriculture ultimately spreading antibiotic resistance around the globe, as depicted in **Figure 6.1** ²¹⁷.

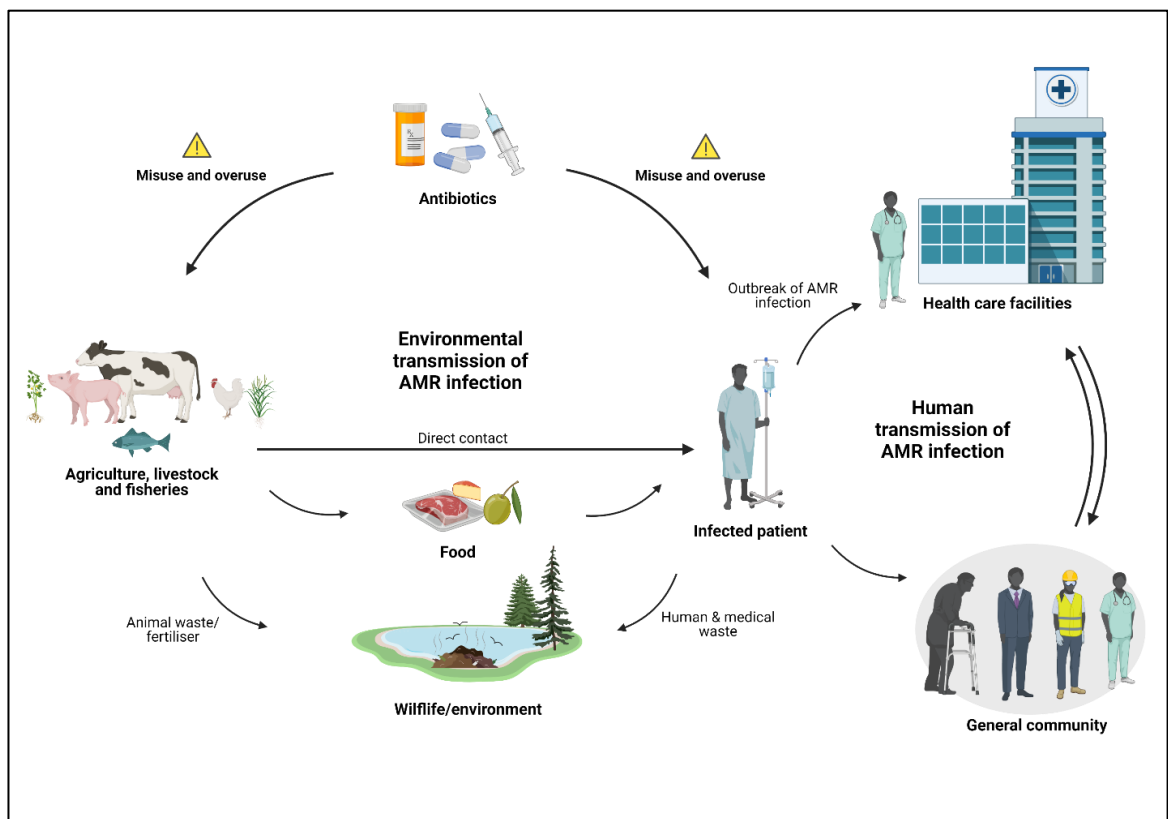


Figure 6.1 Global transmission of antibiotic resistance. Antibiotic resistant bacteria are derived from numerous sources and can be transmitted through the interactions of humans and animals, within the environment. This figure was adapted from the National Institute of Health (NIH) and aims to summarise the global threat to antimicrobial resistance.

With the high dissemination and the devastating impacts of antibiotic resistance, the Centre's for Disease Control and Prevention (CDC) has released a list of antibiotic-resistant bacteria of urgent, serious, or concerning risk to human and animal health, which includes *Staphylococcus spp.*²¹⁸. Traditionally, *S. pseudintermedius* is considered a canine pathogen; however, due to the interactions between humans and canine companions, this bacterium has also been reported to causes infections in humans^{219–225}. Numerous bacterial species cause disease within both humans and animals, transmitted in a continuous cycle; therefore, there has been a significant focus on a One Health approach to antibiotic-resistance. Phage therapy is a promising option to combat antibiotic resistant bacteria, as highlighted throughout this thesis. However, the development of phage therapy is a complex approach as there are multiple arms within the development of phage therapy including, research & development (R&D), clinical diagnostics, administration and monitoring of phage therapy, and manufacturing and product marketing. The development of phage therapy requires expertise in numerous fields, including microbial ecology, phage biology, genetics,

bioinformatics, host responses, infection kinetics from veterinarians and clinicians, biochemistry, and marketing. Therefore, companies and collaborations such as ‘AusPhageNetwork’, ‘Phage Australia’ and ‘Phage Directory’ are essential in creating an “ecosystem” of expertise to allow more efficient exploration of phage therapy from bench to patient and tackle the ever-growing antibiotic resistance crisis ²²⁶.

Chapter 7

Thesis references

7.1 Reference list

1. Lee, W.-B. *et al.* A microfluidic device for antimicrobial susceptibility testing based on a broth dilution method. *Biosens. Bioelectron.* **87**, 669–678 (2017).
2. Hyman, P. Phages for phage therapy: Isolation, characterization, and host range breadth. *Pharmaceuticals (Basel)* **12**, 35 (2019).
3. Van Twest, R. & Kropinski, A. M. Bacteriophage enrichment from water and soil. *Methods Mol. Biol.* **501**, 15–21 (2009).
4. Göller, P. C., Haro-Moreno, J. M., Rodriguez-Valera, F., Loessner, M. J. & Gómez-Sanz, E. Uncovering a hidden diversity: optimized protocols for the extraction of dsDNA bacteriophages from soil. *Microbiome* **8**, 17 (2020).
5. Calendar, R. Bacteriophages: Biology and Applications. Edited by Elizabeth Kutter and, Alexander Sulakvelidze. Boca Raton (Florida): CRC Press. \$129.95. xvi + 510 p; ill.; index. ISBN: 0-8493-1336-8. 2005. *Q. Rev. Biol.* **81**, 280–281 (2006).
6. Bankevich, A. *et al.* SPAdes: a new genome assembly algorithm and its applications to single-cell sequencing. *J. Comput. Biol.* **19**, 455–477 (2012).
7. Altschul, S. F., Gish, W., Miller, W., Myers, E. W. & Lipman, D. J. Basic local alignment search tool. *J. Mol. Biol.* **215**, 403–410 (1990).
8. Delcher, A. L., Bratke, K. A., Powers, E. C. & Salzberg, S. L. Identifying bacterial genes and endosymbiont DNA with Glimmer. *Bioinformatics* **23**, 673–679 (2007).
9. Sievers, F. *et al.* Fast, scalable generation of high-quality protein multiple sequence alignments using Clustal Omega. *Mol. Syst. Biol.* **7**, 539 (2011).
10. Jones, P. *et al.* InterProScan 5: genome-scale protein function classification. *Bioinformatics* **30**, 1236–1240 (2014).
11. Kelley, L. A., Mezulis, S., Yates, C. M., Wass, M. N. & Sternberg, M. J. E. The Phyre2 web portal for protein modeling, prediction and analysis. *Nat. Protoc.* **10**, 845–858 (2015).
12. PyMOL. <http://www.pymol.org/pymol>.
13. Lynch, S. A. & Helbig, K. J. The complex diseases of *Staphylococcus pseudintermedius* in canines: Where to next? *Vet. Sci.* **8**, 11 (2021).
14. Hartantyo, S. H. P. *et al.* Sick pets as potential reservoirs of antibiotic-resistant bacteria in Singapore. *Antimicrob. Resist. Infect. Control* **7**, 106 (2018).
15. Lin, D. M., Koskella, B. & Lin, H. C. Phage therapy: An alternative to antibiotics in the age of multi-drug resistance. *World J. Gastrointest. Pharmacol. Ther.* **8**, 162–173 (2017).
16. Moodley, A. *et al.* Isolation and characterization of bacteriophages active against methicillin-resistant *Staphylococcus pseudintermedius*. *Research in Veterinary Science* vol. 122 81–85 (2019).
17. Zeman, M. *et al.* New Genus Fibralongavirus in Siphoviridae Phages of *Staphylococcus pseudintermedius*. *Viruses* **11**, (2019).
18. Kim, S. G. *et al.* Two novel bacteriophages control multidrug- and methicillin-resistant *Staphylococcus pseudintermedius* biofilm. *Front. Med. (Lausanne)* **8**, 524059 (2021).
19. Nanda, A. M., Thormann, K. & Frunzke, J. Impact of spontaneous prophage induction on the fitness of bacterial populations and host-microbe interactions. *J. Bacteriol.* **197**, 410–419 (2015).

20. Waldor, M. K. & Mekalanos, J. J. Lysogenic conversion by a filamentous phage encoding cholera toxin. *Science (New York, N.Y.)* vol. 272 1910–1914 (1996).
21. Bertani, G. Studies on lysogenesis. I. The mode of phage liberation by lysogenic *Escherichia coli*. *J. Bacteriol.* **62**, 293–300 (1951).
22. Twort, F. W. An investigation on the nature of ultra-microscopic viruses. *Lancet* **186**, 1241–1243 (1915).
23. Jamal, M. *et al.* Bacteriophages: an overview of the control strategies against multiple bacterial infections in different fields. *J. Basic Microbiol.* **59**, 123–133 (2019).
24. Gill, J. J. & Hyman, P. Phage choice, isolation, and preparation for phage therapy. *Curr. Pharm. Biotechnol.* **11**, 2–14 (2010).
25. Kim, J. H., Gomez, D. K., Nakai, T. & Park, S. C. Isolation and identification of bacteriophages infecting ayu *Plecoglossus altivelis altivelis* specific *Flavobacterium psychrophilum*. *Vet. Microbiol.* **140**, 109–115 (2010).
26. Crosse, J. E. & Hingorani, M. K. A Method for isolating *Pseudomonas mors-prunorum* Phages from the Soil. *Nature* **181**, 60–61 (1958).
27. Rabiey, M. *et al.* Phage biocontrol to combat *Pseudomonas syringae* pathogens causing disease in cherry. *Microb. Biotechnol.* **13**, 1428–1445 (2020).
28. Yuan, X. *et al.* Isolation and characterization of a novel *Escherichia coli* Kayfunavirus phage DY1. *Virus Res.* **293**, 198274 (2021).
29. Batinovic, S. *et al.* Bacteriophages in natural and artificial environments. *Pathogens* **8**, 100 (2019).
30. Taylor, S. *et al.* Isolation and characterization of bacteriophage NTR1 infectious for *Nocardia transvalensis* and other *Nocardia* species. *Virus Genes* **55**, 257–265 (2019).
31. Chan, H. T. *et al.* Characterization of novel lytic bacteriophages of *Achromobacter marplantensis* isolated from a pneumonia patient. *Viruses* **12**, 1138 (2020).
32. d’Humières, C. *et al.* A simple, reproducible and cost-effective procedure to analyse gut phageome: from phage isolation to bioinformatic approach. *Sci. Rep.* **9**, 11331 (2019).
33. Cross, T. *et al.* An optimized enrichment technique for the isolation of *Arthrobacter* bacteriophage species from soil sample isolates. *J. Vis. Exp.* (2015) doi:10.3791/52781.
34. Dyson, Z. A., Tucci, J., Seviour, R. J. & Petrovski, S. Isolation and characterization of bacteriophage SPI1, which infects the activated-sludge-foaming bacterium *Skermania piniformis*. *Arch. Virol.* **161**, 149–158 (2016).
35. Ross, A., Ward, S. & Hyman, P. More Is Better: Selecting for Broad Host Range Bacteriophages. *Front. Microbiol.* **7**, 1352 (2016).
36. Gibson, S. B. *et al.* Constructing and characterizing bacteriophage libraries for phage therapy of human infections. *Front. Microbiol.* **10**, 2537 (2019).
37. al., J. et. (12) United States Patent. <https://patentimages.storage.googleapis.com/4f/c1/00/c3049582db1f54/US8821855.pdf>.
38. Guerin, E. *et al.* Isolation and characterisation of Φ crAss002, a crAss-like phage from the human gut that infects *Bacteroides xylanisolvens*. *Microbiome* **9**, 89 (2021).
39. James, S. L., Rabiey, M., Neuman, B. W., Percival, G. & Jackson, R. W. Isolation, Characterisation and Experimental Evolution of Phage that Infect the Horse Chestnut Tree Pathogen, *Pseudomonas syringae* pv. *aesculi*. *Curr. Microbiol.* **77**, 1438–1447 (2020).

40. Tan, C. Y., Ong, J. H. M. & Bifani, J. P. Screening and characterisation of novel environmental phages. in *IRC-SET 2020* 327–334 (Springer Singapore, 2021).
41. Viazis, S., Akhtar, M., Feirtag, J., Brabban, A. D. & Diez-Gonzalez, F. Isolation and characterization of lytic bacteriophages against enterohaemorrhagic *Escherichia coli*. *J. Appl. Microbiol.* **110**, 1323–1331 (2011).
42. VetBact. <http://www.vetbact.org/species/135>.
43. Guignard, B., Entenza, J. M. & Moreillon, P. Beta-lactams against methicillin-resistant *Staphylococcus aureus*. *Curr. Opin. Pharmacol.* **5**, 479–489 (2005).
44. Santos, T. M. A., Ledbetter, E. C., Caixeta, L. S., Bicalho, M. L. S. & Bicalho, R. C. Isolation and characterization of two bacteriophages with strong in vitro antimicrobial activity against *Pseudomonas aeruginosa* isolated from dogs with ocular infections. *Am. J. Vet. Res.* **72**, 1079–1086 (2011).
45. Hoff, J. C. & Drake, C. H. Simplified method for isolation and purification of bacteriophages. *J. Bacteriol.* **83**, 924–926 (1962).
46. Mullan, D. M. Isolation and purification of bacteriophages. <https://www.dairyscience.info/index.php/isolation-and-purification-of-bacteriophages.html>.
47. Kerek, Á., Sterczar, Á., Somogyi, Z., Kovács, D. & Jerzsele, Á. Investigation of the environmental presence of multidrug-resistant bacteria at small animal hospitals in Hungary. *Acta Vet. Hung.* **68**, 387–392 (2021).
48. Silva, V. *et al.* Clonal diversity and antimicrobial resistance of methicillin-resistant *Staphylococcus pseudintermedius* isolated from canine pyoderma. *Microorganisms* **9**, 482 (2021).
49. Breteau, M. Study of *Staphylococcus pseudintermedius* phages : towards the development of phage therapy. (University of Warwick, 2016).
50. Gallet, R., Kannoly, S. & Wang, I.-N. Effects of bacteriophage traits on plaque formation. *BMC Microbiol.* **11**, 181 (2011).
51. Doermann, A. H. & Hill, M. B. Genetic structure of bacteriophage T4 as described by recombination studies of factors influencing plaque morphology. *Genetics* **38**, 79–90 (1953).
52. Abedon, S. T. Phage therapy: eco-physiological pharmacology. *Scientifica (Cairo)* **2014**, 581639 (2014).
53. Weinbauer, M. G. & Suttle, C. A. Lysogeny and prophage induction in coastal and offshore bacterial communities. *Aquat. Microb. Ecol.* **18**, 217–225 (1999).
54. Edgar, R. & Qimron, U. The *Escherichia coli* CRISPR system protects from λ lysogenization, lysogens, and prophage induction. *J. Bacteriol.* **192**, 6291–6294 (2010).
55. Little, J. W. Lysogeny, Prophage Induction, and Lysogenic Conversion. in *Phages* 37–54 (ASM Press, 2014).
56. Cochran, P. K., Kellogg, C. A. & Paul, J. H. Prophage induction of indigenous marine lysogenic bacteria by environmental pollutants. *Mar. Ecol. Prog. Ser.* **164**, 125–133 (1998).
57. Banks, D. J., Lei, B. & Musser, J. M. Prophage induction and expression of prophage-encoded virulence factors in group A *Streptococcus* serotype M3 strain MGAS315. *Infect. Immun.* **71**, 7079–7086 (2003).
58. Jiang, S. C. & Paul, J. H. Occurrence of lysogenic bacteria in marine microbial communities as determined by prophage induction. *Mar. Ecol. Prog. Ser.* **142**, 27–38 (1996).
59. Rohde, C. *et al.* Expert opinion on three phage therapy related topics: Bacterial phage resistance, phage training and prophages in bacterial production strains. *Viruses* **10**, 178 (2018).

60. Brooks, M. R. *et al.* Prophage-Mediated Disruption of Genetic Competence in *Staphylococcus pseudintermedius*. *mSystems* **5**, (2020).
61. Wipf, J. R. K., Deutsch, D. R., Westblade, L. F. & Fischetti, V. A. Genome sequences of six prophages isolated from *Staphylococcus pseudintermedius* strains recovered from human and animal clinical specimens. *Microbiol. Resour. Announc.* **8**, (2019).
62. Phumthanakorn, N. *et al.* Genomic insights into methicillin-resistant *Staphylococcus pseudintermedius* isolates from dogs and humans of the same sequence types reveals diversity in prophages and pathogenicity islands. *PLoS One* **16**, e0254382 (2021).
63. Baliga, P., Shekar, M. & Kallappa, G. S. Genome-wide identification and analysis of chromosomally integrated putative prophages associated with clinical *Klebsiella pneumoniae* strains. *Curr. Microbiol.* **78**, 2015–2024 (2021).
64. Pei, Z. *et al.* Comprehensive scanning of prophages in *Lactobacillus*: Distribution, diversity, antibiotic resistance genes, and linkages with CRISPR-Cas systems. *mSystems* **6**, e0121120 (2021).
65. Crispim, J. S. *et al.* Screening and characterization of prophages in *Desulfovibrio* genomes. *Sci. Rep.* **8**, 9273 (2018).
66. Kleinheinz, K. A., Joensen, K. G. & Larsen, M. V. Applying the ResFinder and VirulenceFinder web-services for easy identification of acquired antibiotic resistance and *E. coli* virulence genes in bacteriophage and prophage nucleotide sequences. *Bacteriophage* **4**, e27943 (2014).
67. Serra-Moreno, R., Acosta, S., Hernalsteens, J. P., Jofre, J. & Muniesa, M. Use of the lambda Red recombinase system to produce recombinant prophages carrying antibiotic resistance genes. *BMC Mol. Biol.* **7**, 31 (2006).
68. López-Leal, G., Santamaria, R. I., Cevallos, M. Á., Gonzalez, V. & Castillo-Ramírez, S. Letter to the editor: Prophages encode antibiotic resistance genes in *Acinetobacter baumannii*. *Microb. Drug Resist.* **26**, 1275–1277 (2020).
69. Wang, M. *et al.* Role of enterotoxigenic *Escherichia coli* prophage in spreading antibiotic resistance in a porcine-derived environment. *Environ. Microbiol.* **22**, 4974–4984 (2020).
70. Zukancic, A. *et al.* Staphylococcal protein A (spa) locus is a Hot Spot for recombination and horizontal gene transfer in *Staphylococcus pseudintermedius*. *mSphere* **5**, (2020).
71. Frank, L. A. & Loeffler, A. Methicillin-resistant *Staphylococcus pseudintermedius*: clinical challenge and treatment options. *Vet. Dermatol.* **23**, 283–91, e56 (2012).
72. Gordillo Altamirano, F. L. & Barr, J. J. Phage therapy in the postantibiotic era. *Clin. Microbiol. Rev.* **32**, (2019).
73. Low, L. Y., Yang, C., Perego, M., Osterman, A. & Liddington, R. C. Structure and Lytic Activity of a *Bacillus anthracis* Prophage Endolysin. *J. Biol. Chem.* **280**, 35433–35439 (2005).
74. Abdelrahman, F. *et al.* Phage-encoded endolysins. *Antibiotics (Basel)* **10**, 124 (2021).
75. Mondal, S. I., Draper, L. A., Ross, R. P. & Hill, C. Bacteriophage endolysins as a potential weapon to combat *Clostridioides difficile* infection. *Gut Microbes* **12**, 1813533 (2020).
76. Sass, P. & Bierbaum, G. Lytic activity of recombinant bacteriophage phi11 and phi12 endolysins on whole cells and biofilms of *Staphylococcus aureus*. *Appl. Environ. Microbiol.* **73**, 347–352 (2007).
77. Briers, Y. *et al.* Muralytic activity and modular structure of the endolysins of *Pseudomonas aeruginosa* bacteriophages phiKZ and EL. *Mol. Microbiol.* **65**, 1334–1344 (2007).

78. Vander Elst, N. *et al.* Characterization of the bacteriophage-derived endolysins PlySs2 and PlySs9 with in vitro lytic activity against bovine mastitis *Streptococcus uberis*. *Antibiotics (Basel)* **9**, (2020).
79. Pohane, A. A. & Jain, V. Insights into the regulation of bacteriophage endolysin: multiple means to the same end. *Microbiology* **161**, 2269–2276 (2015).
80. Fischetti, V. A. Bacteriophage endolysins: a novel anti-infective to control Gram-positive pathogens. *Int. J. Med. Microbiol.* **300**, 357–362 (2010).
81. Gervasi, T. *et al.* Expression and delivery of an endolysin to combat *Clostridium perfringens*. *Appl. Microbiol. Biotechnol.* **98**, 2495–2505 (2014).
82. Mayer, M. J., Payne, J., Gasson, M. J. & Narbad, A. Genomic sequence and characterization of the virulent bacteriophage phiCTP1 from *Clostridium tyrobutyricum* and heterologous expression of its endolysin. *Appl. Environ. Microbiol.* **76**, 5415–5422 (2010).
83. Boizet, B., Lahbib-Mansais, Y., Dupont, L., Ritzenthaler, P. & Mata, M. Cloning, expression and sequence analysis of an endolysin-encoding gene of *Lactobacillus bulgaricus* bacteriophage mv1. *Gene* **94**, 61–67 (1990).
84. Tham, H. Y., Song, A. A.-L., Yusoff, K. & Tan, G. H. Effect of different cloning strategies in pET-28a on solubility and functionality of a staphylococcal phage endolysin. *Biotechniques* **69**, 161–170 (2020).
85. Gondil, V. S., Harjai, K. & Chhibber, S. Endolysins as emerging alternative therapeutic agents to counter drug-resistant infections. *Int. J. Antimicrob. Agents* **55**, 105844 (2020).
86. Park, S. *et al.* Characterisation of the antibacterial properties of the recombinant phage endolysins AP50-31 and LysB4 as potent bactericidal agents against *Bacillus anthracis*. *Sci. Rep.* **8**, 18 (2018).
87. Son, B. *et al.* Characterization of LysB4, an endolysin from the *Bacillus cereus*-infecting bacteriophage B4. *BMC Microbiol.* **12**, 33 (2012).
88. Oliveira, H. *et al.* Structural and enzymatic characterization of ABgp46, a novel phage endolysin with broad anti-Gram-negative bacterial activity. *Front. Microbiol.* **7**, 208 (2016).
89. Silva, M. D., Oliveira, H., Faustino, A. & Sillankorva, S. Characterization of MSlys, the endolysin of *Streptococcus pneumoniae* phage MS1. *Biotechnol. Rep. (Amst.)* **28**, e00547 (2020).
90. Leprince, A., Nuytten, M., Gillis, A. & Mahillon, J. Characterization of PlyB221 and PlyP32, two novel endolysins encoded by phages preying on the *Bacillus cereus* group. *Viruses* **12**, 1052 (2020).
91. Blasco, L. *et al.* In vitro and in vivo efficacy of combinations of colistin and different endolysins against clinical strains of multi-drug resistant pathogens. *Sci. Rep.* **10**, 7163 (2020).
92. Landlinger, C. *et al.* Engineered phage endolysin eliminates *Gardnerella* biofilm without damaging beneficial bacteria in bacterial vaginosis ex vivo. *Pathogens* **10**, 54 (2021).
93. Fursov, M. V. *et al.* Antibiofilm activity of a broad-range recombinant endolysin LysECD7: In vitro and in vivo study. *Viruses* **12**, 545 (2020).
94. Gu, J. *et al.* LysGH15, a novel bacteriophage lysin, protects a murine bacteremia model efficiently against lethal methicillin-resistant *Staphylococcus aureus* infection. *J. Clin. Microbiol.* **49**, 111–117 (2011).
95. Cho, J.-H., Kwon, J.-G., O'Sullivan, D. J., Ryu, S. & Lee, J.-H. Development of an endolysin enzyme and its cell wall-binding domain protein and their applications for biocontrol and rapid detection of *Clostridium perfringens* in food. *Food Chem.* **345**, 128562 (2021).

96. Yuan, Y. *et al.* The endolysin of the *Acinetobacter baumannii* phage vB_AbaP_D2 shows broad antibacterial activity. *Microb. Biotechnol.* **14**, 403–418 (2021).
97. Nakamura, T. *et al.* Lytic activity of polyvalent staphylococcal bacteriophage PhiSA012 and its endolysin Lys-PhiSA012 against antibiotic-resistant staphylococcal clinical isolates from canine skin infection sites. *Front. Med. (Lausanne)* **7**, 234 (2020).
98. Murray, E., Draper, L. A., Ross, R. P. & Hill, C. The advantages and challenges of using endolysins in a clinical setting. *Viruses* **13**, 680 (2021).
99. Sinha, S. Bacteriophage and phage-therapy: An alternative to antibiotics. <https://elifepress.com/wp-content/uploads/2020/08/21-27-Review-Article-eLifePress.pdf>.
100. Regulski, K., Champion-Arnaud, P. & Gabard, J. Bacteriophage manufacturing: From early twentieth-century processes to current GMP. in *Bacteriophages* 699–729 (Springer International Publishing, 2021).
101. Pirnay, J.-P. *et al.* Quality and safety requirements for sustainable phage therapy products. *Pharm. Res.* **32**, 2173–2179 (2015).
102. Ingmer, H., Gerlach, D. & Wolz, C. Temperate phages of *Staphylococcus aureus*. *Microbiol. Spectr.* **7**, (2019).
103. Junjappa, R. P. *et al.* Efficacy of anti-staphylococcal protein P128 for the treatment of canine pyoderma: potential applications. *Vet. Res. Commun.* **37**, 217–228 (2013).
104. Briers, Y., Peeters, L. M., Volckaert, G. & Lavigne, R. The lysis cassette of bacteriophage ϕ KMV encodes a signal-arrest-release endolysin and a pinholin. *Bacteriophage* **1**, 25–30 (2011).
105. Gu, J. *et al.* Structural and biochemical characterization reveals LysGH15 as an unprecedented “EF-hand-like” calcium-binding phage lysin. *PLoS Pathog.* **10**, e1004109 (2014).
106. Górski, A. *et al.* Phage therapy: Current status and perspectives. *Med. Res. Rev.* **40**, 459–463 (2020).
107. Legotsky, S. A. *et al.* Peptidoglycan degrading activity of the broad-range *Salmonella* bacteriophage S-394 recombinant endolysin. *Biochimie* **107 Pt B**, 293–299 (2014).
108. Briers, Y. *et al.* The high-affinity peptidoglycan binding domain of *Pseudomonas* phage endolysin KZ144. *Biochem. Biophys. Res. Commun.* **383**, 187–191 (2009).
109. Pohane, A. A., Joshi, H. & Jain, V. Molecular dissection of phage endolysin. *J. Biol. Chem.* **289**, 12085–12095 (2014).
110. Lai, M.-J. *et al.* Identification and characterisation of the putative phage-related endolysins through full genome sequence analysis in *Acinetobacter baumannii* ATCC 17978. *Int. J. Antimicrob. Agents* **42**, 141–148 (2013).
111. Vidová, B., Šramková, Z., Tišáková, L., Oravkinová, M. & Godány, A. Bioinformatics analysis of bacteriophage and prophage endolysin domains. *Biologia (Bratisl.)* **69**, 541–556 (2014).
112. Zink, R., Loessner, M. J. & Scherer, S. Characterization of cryptic prophages (monocins) in *Listeria* and sequence analysis of a holin/endolysin gene. *Microbiology* **141** (Pt 10), 2577–2584 (1995).
113. Fernández-Ruiz, I., Coutinho, F. H. & Rodríguez-Valera, F. Thousands of novel endolysins discovered in uncultured phage genomes. *Front. Microbiol.* **9**, (2018).
114. Horgan, M. *et al.* Phage lysin LysK can be truncated to its CHAP domain and retain lytic activity against live antibiotic-resistant staphylococci. *Appl. Environ. Microbiol.* **75**, 872–874 (2009).

115. Navarre, W. W., Ton-That, H., Faull, K. F. & Schneewind, O. Multiple enzymatic activities of the murein hydrolase from staphylococcal phage phi11. Identification of a D-alanyl-glycine endopeptidase activity. *J. Biol. Chem.* **274**, 15847–15856 (1999).
116. Becker, S. C. *et al.* Lytic activity of the staphylocytic Twort phage endolysin CHAP domain is enhanced by the SH3b cell wall binding domain. *FEMS Microbiol. Lett.* **362**, 1–8 (2015).
117. Becker, S. C. *et al.* LysK CHAP endopeptidase domain is required for lysis of live staphylococcal cells. *FEMS Microbiol. Lett.* **294**, 52–60 (2009).
118. Schmelcher, M., Donovan, D. M. & Loessner, M. J. Bacteriophage endolysins as novel antimicrobials. *Future Microbiol.* **7**, 1147–1171 (2012).
119. Zha, J. *et al.* Endolysin-based autolytic E. coli system for facile recovery of recombinant proteins. *J. Agric. Food Chem.* **69**, 3134–3143 (2021).
120. Yan, G. *et al.* External lysis of Escherichia coli by a bacteriophage endolysin modified with hydrophobic amino acids. *AMB Express* **9**, 106 (2019).
121. Brix, A., Cafora, M., Aureli, M. & Pistocchi, A. Animal models to translate phage therapy to human medicine. *Int. J. Mol. Sci.* **21**, 3715 (2020).
122. Penziner, S., Schooley, R. T. & Pride, D. T. Animal models of phage therapy. *Front. Microbiol.* **12**, 631794 (2021).
123. Richards, A. C. *et al.* Staphylococcus pseudintermedius surface protein L (SpsL) is required for abscess formation in a Murine model of cutaneous infection. *Infect. Immun.* **86**, (2018).
124. Andersen, M. L. & Winter, L. M. F. Animal models in biological and biomedical research - experimental and ethical concerns. *An. Acad. Bras. Cienc.* **91**, e20170238 (2019).
125. Augustine, J., Gopalakrishnan, M. V. & Bhat, S. G. Application of ΦSP-1 and ΦSP-3 as a therapeutic strategy against Salmonella Enteritidis infection using Caenorhabditis elegans as model organism. *FEMS Microbiol. Lett.* **356**, 113–117 (2014).
126. Santander, J. & Robeson, J. Bacteriophage prophylaxis against Salmonella enteritidis and Salmonella pullorum using Caenorhabditis elegans as an assay system. *Electron. J. Biotechnol.* **7**, 206–209 (2004).
127. Głowacka-Rutkowska, A. *et al.* The ability of lytic staphylococcal podovirus vB_SauP_phiAGO1. 3 to coexist in equilibrium with its host facilitates the selection of host mutants of attenuated virulence but does not preclude the phage antistaphylococcal activity in a nematode infection model. *Front. Microbiol.* **9**, 3227 (2019).
128. Heo, Y.-J. *et al.* Antibacterial efficacy of phages against Pseudomonas aeruginosa infections in mice and Drosophila melanogaster. *Antimicrob. Agents Chemother.* **53**, 2469–2474 (2009).
129. Lindberg, H. M., McKean, K. A. & Wang, I.-N. Phage fitness may help predict phage therapy efficacy. *Bacteriophage* **4**, e964081 (2014).
130. Jang, H.-J., Bae, H.-W. & Cho, Y.-H. Exploitation of Drosophila infection models to evaluate antibacterial efficacy of phages. *Methods Mol. Biol.* **1898**, 183–190 (2019).
131. Jeon, J., Park, J.-H. & Yong, D. Efficacy of bacteriophage treatment against carbapenem-resistant Acinetobacter baumannii in Galleria mellonella larvae and a mouse model of acute pneumonia. *BMC Microbiol.* **19**, 70 (2019).
132. Seed, K. D. & Dennis, J. J. Experimental bacteriophage therapy increases survival of Galleria mellonella larvae infected with clinically relevant strains of the Burkholderia cepacia complex. *Antimicrob. Agents Chemother.* **53**, 2205–2208 (2009).
133. Nale, J. Y., Chutia, M., Carr, P., Hickenbotham, P. T. & Clokie, M. R. J. “get in early”; Biofilm and wax moth (Galleria mellonella) models reveal new insights into the therapeutic potential of Clostridium difficile bacteriophages. *Front. Microbiol.* **7**, 1383 (2016).

134. Manohar, P., Nachimuthu, R. & Lopes, B. S. The therapeutic potential of bacteriophages targeting gram-negative bacteria using *Galleria mellonella* infection model. *BMC Microbiol.* **18**, 97 (2018).
135. Forti, F. *et al.* Design of a broad-range bacteriophage cocktail that reduces *Pseudomonas aeruginosa* biofilms and treats acute infections in two animal models. *Antimicrob. Agents Chemother.* **62**, (2018).
136. Cafora, M. *et al.* Phage therapy against *Pseudomonas aeruginosa* infections in a cystic fibrosis zebrafish model. *Sci. Rep.* **9**, 1527 (2019).
137. Al-Zubidi, M. *et al.* Identification of novel bacteriophages with therapeutic potential that target *Enterococcus faecalis*. *Infect. Immun.* **87**, (2019).
138. Takemura-Uchiyama, I. *et al.* Evaluating efficacy of bacteriophage therapy against *Staphylococcus aureus* infections using a silkworm larval infection model. *FEMS Microbiol. Lett.* **347**, 52–60 (2013).
139. Xiang, H. *et al.* The evolutionary road from wild moth to domestic silkworm. *Nat. Ecol. Evol.* **2**, 1268–1279 (2018).
140. Putra, D. F., Nur, F., Rahimi, S. A. E. & Othman, N. Effects of different live feed on growth and survival rate of clown loach, *Cromobotia macracantus*. *IOP Conf. Ser. Earth Environ. Sci.* **348**, 012099 (2019).
141. Silkworms as a Pet-Feeder. <https://everythingsilkworms.com.au/silkworms/silkworms-as-a-pet-feeder/> (2016).
142. Miyazaki, S., Matsumoto, Y., Sekimizu, K. & Kaito, C. Evaluation of *Staphylococcus aureus* virulence factors using a silkworm model. *FEMS Microbiol. Lett.* **326**, 116–124 (2012).
143. Paudel, A., Furuta, Y. & Higashi, H. Silkworm model for *Bacillus anthracis* infection and virulence determination. *bioRxiv* (2021) doi:10.1101/2021.06.12.448172.
144. Mikami, K. *et al.* Evaluation of pathogenicity and therapeutic effectiveness of antibiotics using silkworm *Nocardia* infection model. *Drug Discov. Ther.* **15**, 73–77 (2021).
145. Montali, A. *et al.* A silkworm infection model for in vivo study of glycopeptide antibiotics. *Antibiotics (Basel)* **9**, 300 (2020).
146. Paudel, A., Hamamoto, H., Panthee, S., Matsumoto, Y. & Sekimizu, K. Large-scale screening and identification of novel pathogenic *Staphylococcus aureus* genes using a silkworm infection model. *J. Infect. Dis.* **221**, 1795–1804 (2020).
147. Vishaka, G. V., Rathore, M. S., Chandrashekharaiyah, M., Nadaf, H. A. & Sinha, R. B. The silkworm (*Bombyx mori* L.)—A model for the production of beauvericin, a bioactive fungal metabolite. in *New and Future Developments in Microbial Biotechnology and Bioengineering* 99–104 (Elsevier, 2020).
148. Abdelli, N., Peng, L. & Keping, C. Silkworm, *Bombyx mori*, as an alternative model organism in toxicological research. *Environ. Sci. Pollut. Res. Int.* **25**, 35048–35054 (2018).
149. Umoto, D. I. S., Pambudi, S., Sjatha, F., Kato, T. & Park, E. Y. Dengue virus-like particles serotype-3 production in silkworm larvae and its capability eliciting a humoral immune response in mice model. *Research Square* (2020) doi:10.21203/rs.3.rs-36383/v1.
150. Kaito, C., Akimitsu, N., Watanabe, H. & Sekimizu, K. Silkworm larvae as an animal model of bacterial infection pathogenic to humans. *Microb. Pathog.* **32**, 183–190 (2002).
151. Ishii, M., Matsumoto, Y., Nakamura, I. & Sekimizu, K. Silkworm fungal infection model for identification of virulence genes in pathogenic fungus and screening of novel antifungal drugs. *Drug Discov. Ther.* **11**, 1–5 (2017).

152. Kaito, C. & Sekimizu, K. A silkworm model of pathogenic bacterial infection. *Drug Discov. Ther.* **1**, 89–93 (2007).
153. Hsueh, T. Y. & Tang, P. S. Physiology of the silkworm. I. growth and respiration of Bombyx Mori during its entire life-cycle. *Physiol. Zool.* **17**, 71–78 (1944).
154. Uchiyama, J., Takemura-Uchiyama, I. & Matsuzaki, S. Use of a silkworm larva model in phage therapy experiments. *Methods Mol. Biol.* **1898**, 173–181 (2019).
155. Reddy A, H. & C, S. A Critical Assessment of Bombyx mori Haemolymph Extract on Staphylococcus aureus an In vitro and In silico Approach. *J. Proteomics Bioinform.* **9**, 1–6 (2016).
156. Asami, Y., Horie, R., Hamamoto, H. & Sekimizu, K. Use of silkworms for identification of drug candidates having appropriate pharmacokinetics from plant sources. *BMC Pharmacol.* **10**, 7 (2010).
157. Isolation and purification of novel anti-fungal peptides from hemolymph of immunized larvae of housefly, Musca domestica. *Saengmyeong Gwahag Hoeji* **16**, 387–395 (2006).
158. Tabunoki, H., Dittmer, N. T., Gorman, M. J. & Kanost, M. R. Development of a new method for collecting hemolymph and measuring phenoloxidase activity in Tribolium castaneum. *BMC Res. Notes* **12**, 7 (2019).
159. Butolo, N. P. *et al.* A high quality method for hemolymph collection from honeybee larvae. *PLoS One* **15**, e0234637 (2020).
160. Borsuk, G. *et al.* A new method for quick and easy hemolymph collection from Apidae adults. *PLoS One* **12**, e0170487 (2017).
161. Tomiotto-Pellissier, F. *et al.* Galleria mellonella hemocytes: A novel phagocytic assay for Leishmania (Viannia) braziliensis. *J. Microbiol. Methods* **131**, 45–50 (2016).
162. Shields, J. D. Collection techniques for the analyses of pathogens in crustaceans. *J. Crustacean Biol.* **37**, 753–763 (2017).
163. Van Belleghem, J. D., Clement, F., Merabishvili, M., Lavigne, R. & Vaneechoutte, M. Pro- and anti-inflammatory responses of peripheral blood mononuclear cells induced by Staphylococcus aureus and Pseudomonas aeruginosa phages. *Sci. Rep.* **7**, 8004 (2017).
164. Zychlinsky, A. & Sansonetti, P. J. Apoptosis as a proinflammatory event: what can we learn from bacteria-induced cell death? *Trends Microbiol.* **5**, 201–204 (1997).
165. Heumann, D. & Roger, T. Initial responses to endotoxins and Gram-negative bacteria. *Clin. Chim. Acta* **323**, 59–72 (2002).
166. Yoon, J. W. *et al.* Prevalence of genes for enterotoxins, toxic shock syndrome toxin 1 and exfoliative toxin among clinical isolates of Staphylococcus pseudintermedius from canine origin. *Vet. Dermatol.* **21**, 484–489 (2010).
167. Romoli, O. *et al.* Differential sensitivity to infections and antimicrobial peptide-mediated immune response in four silkworm strains with different geographical origin. *Sci. Rep.* **7**, 1048 (2017).
168. Lee, S. *et al.* Construction of 3D multicellular microfluidic chip for an in vitro skin model. *Biomed. Microdevices* **19**, 22 (2017).
169. Fauconnier, A. *et al.* The unique role that WHO could play in implementing phage therapy to combat the global antibiotic resistance crisis. *Front. Microbiol.* **11**, (2020).
170. Summers, W. C. The strange history of phage therapy. *Bacteriophage* **2**, 130–133 (2012).
171. McCallin, S., Sacher, J. C., Zheng, J. & Chan, B. K. Current state of compassionate phage therapy. *Viruses* **11**, 343 (2019).

172. Loponte, R., Pagnini, U., Iovane, G. & Pisanelli, G. Phage therapy in veterinary medicine. *Antibiotics (Basel)* **10**, 421 (2021).
173. Ferriol-González, C. & Domingo-Calap, P. Phage therapy in livestock and companion animals. *Antibiotics (Basel)* **10**, 559 (2021).
174. Hawkins, C., Harper, D., Burch, D., Anggård, E. & Soothill, J. Topical treatment of *Pseudomonas aeruginosa* otitis of dogs with a bacteriophage mixture: a before/after clinical trial. *Vet. Microbiol.* **146**, 309–313 (2010).
175. Pantosti, A. Methicillin-resistant staphylococcus aureus associated with animals and its relevance to human health. *Front. Microbiol.* **3**, 127 (2012).
176. Monteiro, R., Pires, D. P., Costa, A. R. & Azeredo, J. Phage therapy: Going temperate? *Trends Microbiol.* **27**, 368–378 (2018).
177. Chang, Y., Bai, J., Lee, J.-H. & Ryu, S. Mutation of a *Staphylococcus aureus* temperate bacteriophage to a virulent one and evaluation of its application. *Food Microbiol.* **82**, 523–532 (2019).
178. Garcia, P., Madera, C., Martinez, B. & A. Rodriguez Biocontrol of *Staphylococcus aureus* in curd manufacturing processes using bacteriophages. *Int. Dairy J* **17**, 1232–1239 (2007).
179. Zhang, H., Fouts, D. E., DePew, J. & Stevens, R. H. Genetic modifications to temperate *Enterococcus faecalis* phage Ef11 that abolish the establishment of lysogeny and sensitivity to repressor, and increase host range and productivity of lytic infection. *Microbiology* **159**, 1023–1035 (2013).
180. Kilcher, S., Studer, P., Muessner, C., Klumpp, J. & Loessner, M. J. Cross-genus rebooting of custom-made, synthetic bacteriophage genomes in L-form bacteria. *Proc. Natl. Acad. Sci. U. S. A.* **115**, 567–572 (2018).
181. Meader, E., Mayer, M. J., Steverding, D., Carding, S. R. & Narbad, A. Evaluation of bacteriophage therapy to control *Clostridium difficile* and toxin production in an in vitro human colon model system. *Anaerobe* **22**, 25–30 (2013).
182. Zegans, M. E. *et al.* Interaction between bacteriophage DMS3 and host CRISPR region inhibits group behaviors of *Pseudomonas aeruginosa*. *J. Bacteriol.* **191**, 210–219 (2009).
183. Keary, R. *et al.* Genome analysis of the staphylococcal temperate phage DW2 and functional studies on the endolysin and tail hydrolase. *Bacteriophage* **4**, e28451 (2014).
184. Mayer, M. J., Narbad, A. & Gasson, M. J. Molecular characterization of a *Clostridium difficile* bacteriophage and its cloned biologically active endolysin. *J. Bacteriol.* **190**, 6734–6740 (2008).
185. Deutsch, S.-M., Guezenec, S., Piot, M., Foster, S. & Lortal, S. Mur-LH, the Broad-Spectrum Endolysin of *Lactobacillus helveticus* Temperate Bacteriophage ϕ -0303. *Appl. Environ. Microbiol.* **70**, 96–103 (2004).
186. Bourkal'tseva, M. V. *et al.* Bacteriophage phi297, a new species of *Pseudomonas aeruginosa* temperate phages with a mosaic genome: Potential use in phage therapy. *Russ. J. Genet.* **47**, 794–798 (2011).
187. Zhang, H. Genetic modifications to temperate *Enterococcus faecalis* phage fEf11 that abolish the establishment of lysogeny and sensitivity to repressor, and increase host range and productivity of lytic infection. *Microbiology* **159**, 1023–1035 (2013).
188. Rapson, M. E., Burden, F. A., Glancey, L. P., Hodgson, D. A. & Mann, N. H. Anti-bacterial agents. *US Patent* (2008).
189. Nale, J. Y. *et al.* Bacteriophage combinations significantly reduce *Clostridium difficile* growth in vitro and proliferation in vivo. *Antimicrob. Agents Chemother.* **60**, 968–981 (2016).

190. Nale, J. Y., Redgwell, T. A., Millard, A. & Clokie, M. R. J. Efficacy of an optimised bacteriophage cocktail to clear *Clostridium difficile* in a batch fermentation model. *Antibiotics (Basel)* **7**, (2018).
191. Nelson, D. C. *et al.* Endolysins as antimicrobials. *Adv. Virus Res.* **83**, 299–365 (2012).
192. Schuch, R., Fischetti, V. A. & Nelson, D. C. A genetic screen to identify bacteriophage lysins. *Methods Mol. Biol.* **502**, 307–319 (2009).
193. Gilmer, D. B., Schmitz, J. E., Euler, C. W. & Fischetti, V. A. Novel bacteriophage lysin with broad lytic activity protects against mixed infection by *Streptococcus pyogenes* and methicillin-resistant *Staphylococcus aureus*. *Antimicrob Agents Chemother* **57**, 02526–12 (2013).
194. Gilmer, D. B., Schmitz, J. E., Thandar, M., Euler, C. W. & Fischetti, V. A. The phage lysin PlySs2 decolonizes *Streptococcus suis* from murine intranasal mucosa. *PLoS One* **12**:e0169180, 0169180 (2017).
195. Lood, R., Raz, A., Molina, H., Euler, C. W. & Fischetti, V. A. A highly active and negatively charged *Streptococcus pyogenes* lysin with a rare d-alanyl-l-alanine endopeptidase activity protects mice against streptococcal bacteremia. *Antimicrob Agents Chemother* **58**, 00115–14 (2014).
196. Entenza, J. M., Loeffler, J. M., Grandgirard, D., Fischetti, V. A. & Moreillon, P. Therapeutic effects of bacteriophage Cpl-1 lysin against *Streptococcus pneumoniae* endocarditis in rats. *Antimicrob. Agents Chemother.* **49**, 4789–4792 (2005).
197. Jun, S. Y. *et al.* Preclinical safety evaluation of intravenously administered SAL200 containing the recombinant phage endolysin SAL-1 as a pharmaceutical ingredient. *Antimicrob. Agents Chemother.* **58**, 2084–2088 (2014).
198. Jun, S. Y. *et al.* Pharmacokinetics of the phage endolysin-based candidate drug SAL200 in monkeys and its appropriate intravenous dosing period. *Clin. Exp. Pharmacol. Physiol.* **43**, 1013–1016 (2016).
199. Jun, S. Y. *et al.* Pharmacokinetics and tolerance of the phage endolysin-based candidate drug SAL200 after a single intravenous administration among healthy volunteers. *Antimicrob Agents Chemother* **61**:e02629–16, 02629–16 (2017).
200. Fan, J. *et al.* Preliminary treatment of bovine mastitis caused by *Staphylococcus aureus*, with trx-SA1, recombinant endolysin of *S. aureus* bacteriophage IME-SA1. *Vet Microbiol* **191**, 001 (2016).
201. Nelson, D., Loomis, L. & Fischetti, V. A. Prevention and elimination of upper respiratory colonization of mice by group A streptococci by using a bacteriophage lytic enzyme. *Proc. Natl. Acad. Sci. U. S. A.* **98**, 4107–4112 (2001).
202. Cheng, Q., Nelson, D., Zhu, S. & Fischetti, V. A. Removal of group B streptococci colonizing the vagina and oropharynx of mice with a bacteriophage lytic enzyme. *Antimicrob. Agents Chemother.* **49**, 111–117 (2005).
203. Haddad Kashani, H., Schmelcher, M., Sabzalipoor, H., Seyed Hosseini, E. & Moniri, R. Recombinant endolysins as potential therapeutics against antibiotic-resistant *Staphylococcus aureus*: Current status of research and novel delivery strategies. *Clin. Microbiol. Rev.* **31**, (2018).
204. Totté, J. E. E., van Doorn, M. B. & Pasmans, S. G. M. A. Successful treatment of chronic *Staphylococcus aureus*-related dermatoses with the topical endolysin Staphfect SA.100: A report of 3 cases. *Case Rep. Dermatol.* **9**, 19–25 (2017).
205. Totté, J. *et al.* Targeted anti-staphylococcal therapy with endolysins in atopic dermatitis and the effect on steroid use, disease severity and the microbiome: study protocol for a randomized controlled trial (MAAS trial). *Trials* **18**, (2017).

- 206.Oliveira, H., São-José, C. & Azeredo, J. Phage-derived peptidoglycan degrading enzymes: Challenges and future prospects for in vivo therapy. *Viruses* **10**, 292 (2018).
- 207.Zou, Y. & Hou, C. Systematic analysis of an amidase domain CHAP in 12 *Staphylococcus aureus* genomes and 44 staphylococcal phage genomes. *Comput. Biol. Chem.* **34**, 251–257 (2010).
- 208.Donovan, D. M., Lardeo, M. & Foster-Frey, J. Lysis of staphylococcal mastitis pathogens by bacteriophage phi11 endolysin. *FEMS Microbiol. Lett.* **265**, 133–139 (2006).
- 209.O, N. W. W. T.-T. H. F. K. F. S. Multiple enzymatic activities of the murein hydrolase from staphylococcal phage phi11. Identification of a D-alanyl-glycine endopeptidase activity. *J Biol* 15847–15856 (1999).
- 210.K, Y. K. J. K. N. U. M. S. K. S. M. K. K. N. S. T. A. K. The two-component cell lysis genes holWMY and lysWMY of the *Staphylococcus warneri* M phage var phiWMY: cloning, sequencing, expression, and mutational analysis in *Escherichia coli*. vol. *Gene* 351 97–108 (2005).
- 211.Chin, W. H. & Barr, J. J. Phage research in ‘organ-on-chip’ devices. *Microbiol. Aust.* **40**, 28 (2019).
- 212.Hamamoto, H., Tonoike, A., Narushima, K., Horie, R. & Sekimizu, K. Silkworm as a model animal to evaluate drug candidate toxicity and metabolism. *Comp. Biochem. Physiol. C. Toxicol. Pharmacol.* **149**, 334–339 (2009).
- 213.Nwibo, D. D., Hamamoto, H., Matsumoto, Y., Kaito, C. & Sekimizu, K. Current use of silkworm larvae (*Bombyx mori*) as an animal model in pharmaco-medical research. *Drug Discov. Ther.* **9**, 133–135 (2015).
- 214.Kaito, C. *et al.* Silkworm pathogenic bacteria infection model for identification of novel virulence genes. *Mol. Microbiol.* **56**, 934–944 (2005).
- 215.Kurokawa, K., Kaito, C. & Sekimizu, K. Two-component signaling in the virulence of *Staphylococcus aureus*: a silkworm larvae-pathogenic agent infection model of virulence. *Methods Enzymol.* **422**, 233–244 (2007).
- 216.Manesh, A., Varghese, G. M. & CENDRIC Investigators and Collaborators. Rising antimicrobial resistance: an evolving epidemic in a pandemic. *Lancet Microbe* (2021) doi:10.1016/S2666-5247(21)00173-7.
- 217.McEwen, S. A. & Collignon, P. J. Antimicrobial resistance: A One Health perspective. *Microbiol. Spectr.* **6**, (2018).
- 218.CDC. Biggest Threats and Data. <https://www.cdc.gov/drugresistance/biggest-threats.html> (2021).
- 219.Lozano, C. *et al.* *Staphylococcus pseudintermedius* human infection cases in Spain: Dog-to-human transmission. *Vector Borne Zoonotic Dis.* **17**, 268–270 (2017).
- 220.van Duijkeren, E. *et al.* Transmission of methicillin-resistant *Staphylococcus pseudintermedius* between infected dogs and cats and contact pets, humans and the environment in households and veterinary clinics. *Vet. Microbiol.* **150**, 338–343 (2011).
- 221.Somayaji, R., Priyantha, M. A. R., Rubin, J. E. & Church, D. Human infections due to *Staphylococcus pseudintermedius*, an emerging zoonosis of canine origin: report of 24 cases. *Diagn. Microbiol. Infect. Dis.* **85**, 471–476 (2016).
- 222.Laarhoven, L. M. *et al.* Longitudinal study on methicillin-resistant *Staphylococcus pseudintermedius* in households. *PLoS One* **6**, e27788 (2011).

223. Börjesson, S., Gómez-Sanz, E., Ekström, K., Torres, C. & Grönlund, U. *Staphylococcus pseudintermedius* can be misdiagnosed as *Staphylococcus aureus* in humans with dog bite wounds. *Eur. J. Clin. Microbiol. Infect. Dis.* **34**, 839–844 (2015).
224. Paul, N. C., Moodley, A., Ghibaud, G. & Guardabassi, L. Carriage of methicillin-resistant *Staphylococcus pseudintermedius* in small animal veterinarians: indirect evidence of zoonotic transmission. *Zoonoses Public Health* **58**, 533–539 (2011).
225. Sasaki, T. *et al.* Methicillin-resistant *Staphylococcus pseudintermedius* in a veterinary teaching hospital. *J. Clin. Microbiol.* **45**, 1118–1125 (2007).
226. Lin, R. C. Y. Australian Phage Network. *Springer Nature* <http://naturemicrobiologycommunity.nature.com/posts/australian-phage-network> (2020).